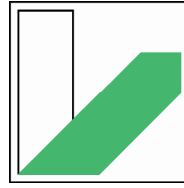




Universität Bayreuth
Lehrstuhl für Hydrologie



UNIVERSITÄT
BAYREUTH

University of Bayreuth
Department of Hydrology

Dissertation

**Development of a novel sizing approach for passive mine
water treatment systems based on iron removal kinetics**

Dissertation submitted on 03 April 2023 in partial fulfilment of the requirements for the academic degree Doctor of Science (Dr. rer. Nat.) at the Bayreuth Graduate School of Mathematical and Natural Sciences (BayNAT), University of Bayreuth

Submitted by Joscha Opitz,
born in Hemer, Germany

Bayreuth, April 2023

This doctoral thesis was prepared at the Department of Hydrology at the University of Bayreuth from August 2017 until March 2023 and was supervised by Prof. Dr. Stefan Peiffer.

This is a full reprint of the thesis submitted to obtain the academic degree of Doctor of Natural Sciences (Dr. rer. nat.) and approved by the Bayreuth Graduate School of Mathematical and Natural Sciences (BayNAT) of the University of Bayreuth.

Date of thesis submission: 03.04.2023

Admission by the executive board: 10.05.2023

Date of thesis defense: 05.02.2024

Acting director: Prof. Dr. Jürgen Köhler

Doctoral committee:

- | | |
|-------------------------------------|--------------------|
| ▪ Prof. Dr. Stefan Peiffer | Thesis reviewer 1 |
| ▪ Prof. Dr. Britta Planer-Friedrich | Thesis reviewer 2 |
| ▪ Prof. Dr. Martin Obst | Committee chairman |
| ▪ Prof. Dr. Jan Fleckenstein | |

(additional thesis reviewer: Prof. Dr. Gregory Druschel)

Preface

The dissertation consists of five main chapters: **Chapter 1** is a summary of the environmental problem covered in this thesis, the current state of science, and the study objectives to provide the reader with both the basic knowledge on the field of research and the overall research goal. **Chapter 2** contains a detailed description of the Westfield study site in the former lignite district of Upper Palatinate in eastern Bavaria (southeast Germany) and the innovative pilot plant that was implemented at the Westfield legacy site to conduct research on sustainable, passive mine water treatment systems. **Chapter 3** outlines the materials and methods of the research project, covering the comprehensive fieldwork at the Westfield site and associated laboratory analyses as well as the extensive laboratory studies conducted in the Hydrology Laboratory at the University of Bayreuth. **Chapter 4** summarises the results and findings of the research project that were previously published in several journal articles as detailed below. Finally, **chapter 5** provides a synoptic summary of the study results, implications, and conclusions as well as engineering profiles for the three passive treatment stages assessed in this research project with recommendations for their designing and sizing for simple application by scientists and engineers alike.

The results reported in this thesis were previously published in peer-reviewed journal articles between 2020 and 2023. Accordingly, the following five journal articles are the first instance of publication in chronological order:

- Opitz J, Alte M, Bauer M, Peiffer S (2020) Quantifying iron removal efficiency of a passive mine water treatment system using turbidity as a proxy for (particulate) iron. *Appl. Geochem.* 122: 104731. <https://doi.org/10.1016/j.apgeochem.2020.104731>
- Opitz J, Alte M, Bauer M, Peiffer S (2021) The role of macrophytes in constructed surface-flow wetlands for mine water treatment: A review. *Mine Water Environ.* 40(3): 587-605. <https://doi.org/10.1007/s10230-021-00779-x>
- Opitz J, Bauer M, Eckert J, Peiffer S, Alte M, (2022) Optimising operational reliability and performance in aerobic passive mine water treatment: The multistage Westfield pilot plant. *Water Air Soil Pollut.* 233: 66. <https://doi.org/10.1007/s11270-022-05538-4>
- Opitz J, Bauer M, Alte M, Schmidtman J, Peiffer S (2022) Sedimentation kinetics of hydrous ferric oxides in ferruginous, circumneutral mine water. *Environ. Sci. Technol.* 56(10): 6360-6368. <https://doi.org/10.1021/acs.est.1c07640>
- Opitz J, Alte M, Bauer M, Peiffer S (2023) Development of a novel sizing approach for passive mine water treatment systems based on ferric iron sedimentation kinetics. *Water Res.* 233: 119770. <https://doi.org/10.1016/j.watres.2023.119770>

Excerpts and/or text passages from these manuscripts were paraphrased, adapted, or adopted in the thesis at hand, either in the general sense or at times even word-by-word. In this context, it is important to note that individual self-citations at the respective passages or at the beginning of respective chapters were explicitly omitted with reference to the preface information at hand and the original, published articles listed above to make the overall thesis more readable. Where figures or tables were adopted from the above-noted publications, either unchanged or modified, the respective article is cited in the figure caption. Permissions were obtained from the publisher(s) where not explicitly stated or given in the publishing agreement.

Abstract

The contamination of ground- and surface water by mining activities is one of the greatest and most costly environmental problems worldwide. Most notably, oxidation of ubiquitous sulphide minerals such as pyrite results in the release of iron, acidity, and sulphate as well as associated metal(loid)s in harmful concentrations (“acid mine drainage”). Subsequent progressive dilution and neutralisation of acidic mine water leads to precipitation of hydrous ferric oxides (“ochre” or “yellow boy”) and thus to extensive pollution of water resources and degradation of aquatic ecosystems. The overall objective of the research project at hand was to introduce, advance, and optimise a sustainable and environmentally friendly (passive-biological) technology for treatment of ferruginous, circumneutral mine water. The advantage of passive compared to conventional treatment is the complete elimination of energy and chemicals input to minimise the environmental footprint. The primary focus of the project was on the natural, i.e. physical and biogeochemical immobilisation of iron as primary, omnipresent contaminant in mine water.

A three-stage pilot plant was implemented at a former open pit in the historic lignite district of Upper Palatinate in southeast Germany for treatment of the ferruginous, yet circumneutral seepage water. Progressing iron removal throughout the innovative pilot plant is achieved in increasingly efficient passive treatment stages with settling ponds for pre-treatment, surface-flow wetlands for polishing, and sediment filters for purification. The consecutive treatment stages were built as identical, parallel triplicates such that hydraulic variation in the three lines generated a comprehensive, previously missing database for evaluation of iron removal performance and kinetics. The overall objective of the field study was to demonstrate operational reliability of the pilot system, and to determine and parameterise the mechanisms governing passive iron removal. Additional laboratory column studies were conducted to quantify sedimentation kinetics of particulate hydrous ferric oxides in ferruginous mine water.

Results of the systematic laboratory experiments showed that settling of hydrous ferric oxides is governed by two interrelated regimes, a rapid second-order aggregation-driven step (r_1) at high iron levels followed by a slower first-order settling step (r_2) at lower iron levels. A mixed first-/second-order model was found to adequately describe the process $\frac{-d[Fe]}{dt} = k_{r2}[Fe] + k_{r1}[Fe]^2$ with coefficients k_{r1} and k_{r2} determined as $9.4 \times 10^{-3} \text{ m}^3/\text{g}/\text{h}$ and $5.4 \times 10^{-3} \text{ h}^{-1}$. Moreover, in-depth evaluation demonstrated that the removal of particulate hydrous ferric oxides at moderate iron levels ($< 10 \text{ mg/L}$) may be reasonably well approximated by a simplified first-order model $\frac{-d[Fe]}{dt} = k_{sed}[Fe]$ with $k_{sed} = 2.4(\pm 0.4) \times 10^{-2} \text{ h}^{-1}$, which agrees well with initial literature estimates.

The multistage pilot plant achieved excellent iron removal rates in the order of 98% with effluent concentrations averaging $0.21(\pm 0.07) \text{ mg/L}$, thus reliably meeting the strict site-specific effluent limit of 1 mg/L . Both treatment performance and operational reliability of the pilot system were comparable to the conventional plant currently operated on site and even surpassed the latter in terms of ammonia and manganese removal, thereby demonstrating that passive treatment is a suitable, more sustainable alternative for long-term seepage water treatment at the project site. By systematically varying flow rates (and thus residence time), it was demonstrated that sedimentation-driven removal of hydrous ferric oxides in the pilot-scale settling ponds may indeed be approximated by a simplified first-order approach for the low to moderate iron levels observed in the seepage water. The coefficient k_{sed} for the pilot-scale settling ponds was found in the order of $2.1(\pm 0.7) \times 10^{-2} \text{ h}^{-1}$, which corresponds well with the previous laboratory studies. The sedimentation kinetics may be readily combined with preceding ferrous iron oxidation kinetics to estimate the required residence time for pre-treatment of ferruginous mine water in settling ponds. In contrast, iron removal in surface-flow wetlands is more complex due to the phytologic component. Therefore, the established liner, area-adjusted iron removal approach was advanced by parameterising the underlying concentration-dependency for reliable

polishing of finely-dispersed, colloidal iron from pre-treated mine water $A = \frac{Q \times ([Fe]_{in} - [Fe]_{out})}{m \times [Fe]_{in}^n}$ with coefficients m and n empirically determined as 0.2 and 1.4, respectively.

Altogether, the qualitative understanding of the natural mechanisms governing iron transport, transformation, and removal throughout passive systems together with respective kinetics go far beyond the established state of science. Thus, insights and results from the pilot field study and associated laboratory experiments provide a novel technical and scientific basis for the customised sizing of both settling ponds and wetlands, demonstrating that strategically combining increasingly efficient passive treatment stages broadly following the Pareto principle may allow for optimisation of treatment performance and operational reliability whilst providing an opportunity to minimise land consumption, maintenance requirements, and overall costs. The advantages of passive eco-technologies for resource conservation are evident, especially for moderate pollutant and volume flows in the long-term aftercare of abandoned mining legacies. In this respect, the advancement and optimisation of a sustainable technology in this research project has the potential to make a substantial contribution to overcoming the environmental and socio-economic consequences of active, post-closure, and historic mining in Germany.

Zusammenfassung

Die Belastung von Grund- und Oberflächenwasser durch bergbauliche Aktivitäten ist eines der größten und kostspieligsten Umweltprobleme weltweit. Insbesondere die Oxidation ubiquitärer, sulfidischer Minerale wie Pyrit führt zur Freisetzung von Eisen, Säure und Sulfat sowie assoziierten Metall(oid)en in schädlichen Konzentrationen (sog. „Acid Mine Drainage“). Die konsekutive Verdünnung und Neutralisation von Grubenwasser in Gewässersystemen führt zur Ausfällung von Eisenhydroxiden (sog. „Verockerung“) und damit zu einer stark verminderten Nutzbarkeit von Wasserressourcen sowie einer teils vollständigen Zerstörung aquatischer Ökosysteme. Übergreifendes Ziel des vorliegenden Projektes war die Einführung, Weiterentwicklung und Optimierung eines nachhaltigen und umweltfreundlichen (passiv-biologischen) Verfahrens für die Aufbereitung eisenhaltigen, pH-neutralen Grubenwassers. Entscheidender Vorteil solcher passiven Systeme im Vergleich zur konventionellen Wasseraufbereitung ist der Verzicht auf den Einsatz von Energie, Chemikalien und weiteren Betriebsmitteln, womit der ökologische Fußabdruck deutlich verringert wird. Der primäre Fokus der vorliegenden Studie zur passiven Grubenwasseraufbereitung liegt auf der natürlichen physikalischen und biogeochemischen Immobilisierung des im Bergbau nahezu omnipräsenten Eisens.

An einem ehem. Tagebauabschnitt im Oberpfälzer Braunkohlerevier bei Wackersdorf (Bayern) wurde eine dreistufige, passive Pilotanlage zur Entfernung von Eisen aus dem am Tiefpunkt der ehem. Grube anfallenden Sickerwasser implementiert. Der Rückhalt von Eisen erfolgte in der Pilotanlage in zunehmend effizienten Anlagenstufen mit Absetzbecken zur Vorreinigung, Wetlands zur Feinreinigung und Sedimentfiltern zur Nachreinigung. Das innovative Konzept der Pilotanlage sah neben dem mehrstufigen Aufbau auch drei nahezu identische, parallele Züge vor, sodass durch gezielte Variation des Volumenstroms umfangreiche und bislang fehlende Vergleichsdatensätze zur Untersuchung der Reinigungsleistung und dem Rückhalt von Eisen zugrundeliegenden Mechanismen sowie zur Quantifizierung von deren Kinetik gewonnen wurden. Ergänzend wurden im Labor Säulenversuche durchgeführt, um die Sedimentation partikulärer Eisenhydroxide in eisenreichem, neutralem Grubenwasser zu quantifizieren.

Die Ergebnisse der systematischen Laborversuche zeigen, dass die Sedimentation von Eisenhydroxiden durch zwei verknüpfte Regime – einem schnellen, koagulationsbasierten Schritt zweiter Ordnung (r_1) bei hohen Eisengehalten und einem langsameren, absetzbasierten Schritt erster Ordnung (r_2) bei niedrigen Eisengehalten – bestimmt wird. Zur Beschreibung der Prozesskinetik wurde ein zusammengesetztes Modell erster-/zweiter Ordnung abgeleitet $\frac{-d[Fe]}{dt} = k_{r2}[Fe] + k_{r1}[Fe]^2$ und die Koeffizienten k_{r1} and k_{r2} mit $9,4 \times 10^{-3} \text{ m}^3/\text{g}/\text{h}$ und $5,4 \times 10^{-3} \text{ h}^{-1}$

ermittelt. Darüber hinaus konnte gezeigt werden, dass die Entfernung partikulärer Eisenhydroxide bei niedrigem bis moderatem Eisenniveau ($< 10 \text{ mg/L}$) hinreichend genau mit einem vereinfachten Ansatz erster Ordnung $\frac{-d[Fe]}{dt} = k_{sed}[Fe]$ abgeschätzt werden kann. Der Koeffizient erster Ordnung k_{sed} wurde mit $2,4(\pm 0,4) \times 10^{-2} \text{ h}^{-1}$ ermittelt, was gut mit ersten Abschätzungen aus der Literatur übereinstimmt.

Die Ergebnisse der Pilotstudie zeigen eine hervorragende Reinigungsleistung des mehrstufigen passiven Systems in der Größenordnung von 98% mit Eisenkonzentrationen im Ablauf der Pilotanlage von im Mittel $0,21(\pm 0,07) \text{ mg/L}$. Der außerordentlich strenge Grenzwert für Eisen am Projektstandort von 1 mg/L konnte durch die strategische Kombination zunehmend effizienter Komponenten über die gesamte Projektlaufzeit durchgehend eingehalten und somit der Nachweis für Eignung und Betriebssicherheit erbracht werden. Insofern ist die Pilotanlage mit der am Projektstandort betriebenen, konventionellen Anlage vergleichbar. Für sekundäre bergbautypische Schadstoffe wie Mangan und Ammonium konnte die Reinigungsleistung der konventionellen Anlage sogar deutlich übertroffen werden. Durch die systematische Variation des Volumenstroms (und damit der hydraulischen Retentionszeit) konnte gezeigt werden, dass der sedimentationsbasierte Rückhalt partikulärer Eisenhydroxide in den Absetzbecken tatsächlich durch einen vereinfachten Ansatz erster Ordnung abgeschätzt werden kann. Der Koeffizient k_{sed} wurde für die Absetzbecken in der Größenordnung von $2,1(\pm 0,7) \times 10^{-2} \text{ h}^{-1}$ ermittelt, was gut mit den o.a. Laborergebnissen übereinstimmt. Die Kinetik der Sedimentation kann insofern direkt mit der Kinetik der vorausgehenden Eisen(II)-Oxidation kombiniert werden, um die integrierte Verweilzeit zur Vorreinigung in Absetzbecken abzuschätzen. Demgegenüber wurde der Rückhalt von kolloidalem Eisen in den dicht bepflanzten Wetlands aufgrund der phytologischen Komponente als deutlich komplexer festgestellt. Infolgedessen wurde eine Weiterentwicklung des etablierten, flächenbasierten Ansatzes zur Feinreinigung in Wetlands vorgenommen, indem die zugrundeliegende Konzentrationsabhängigkeit der Filtration parametrisiert $A = \frac{Q \times ([Fe]_{in} - [Fe]_{out})}{m \times [Fe]_{in}^n}$ und die Koeffizienten m und n mit 0,2 und 1,4 ermittelt wurden.

Zusammenfassend wurde im Zusammenspiel von Pilotstudie und Laborversuchen ein anwendungsorientiertes Verständnis der natürlichen Mechanismen der Eisenentfernung und deren Kinetik entwickelt, und damit der Grundstein für die wissenschaftlich fundierte Konzipierung und Bemessung passiver Systeme gelegt. Die kinetischen Grundlagen erlauben eine in der Ingenieurökologie typische, näherungsweise Abschätzung der zur Grobreinigung in Absetzbecken und Feinreinigung in Wetlands erforderlichen Retentionszeit bzw. Anlagengröße und damit die maßgeschneiderte Bemessung mehrstufiger passiver Systeme. Besonderes Augenmerk lag hier auf strengen Grenzwertniveaus, da durch gezielte Kombination zunehmend effizienter Anlagenstufen in Anlehnung an das Pareto-Prinzip die Konzipierung passiver Systeme hinsichtlich der Reinigungsleistung und Betriebssicherheit optimiert werden kann. Dabei gehen die vorliegend abgeleiteten, qualitativen und quantitativen Erkenntnisse deutlich über den etablierten Stand der Wissenschaft und Technik hinaus. Die Vorteile ingenieurökologischer, passiver Technologien liegen v.a. für moderate Schadstoff- und Volumenströme bei der langfristigen Nachsorge bergbaulicher „Ewigkeitslasten“ für Klima- und Ressourcenschutz sowie zur Minimierung von Flächenverbrauch und Kosten auf der Hand. Nachhaltige Technologien gewinnen mit Blick auf die Umsetzung der EU-WRRRL für die langfristige Wasser- bzw. Gewässerbewirtschaftung massiv an Bedeutung. Somit konnte vorliegend durch Einführung und Weiterentwicklung einer nachhaltigen Technologie ein substanzieller Beitrag zu deren Etablierung sowie zur Bewältigung der umwelttechnischen und sozioökonomischen Folgen des aktiven und nachsorgenden Bergbaus geleistet werden.

Table of contents

Preface	I
Abstract.....	II
Zusammenfassung	III
Table of contents	V
List of Figures	VI
List of Tables	VII
1 Introduction	1
1.1 Environmental problem	1
1.2 Passive mine water treatment.....	2
1.3 Current state of science	3
1.4 Situation in Germany.....	8
1.5 Study objectives	9
2 Study site	10
2.1 The Westfield legacy site	10
2.2 Seepage water chemistry.....	11
2.3 Seepage water management.....	11
2.4 The Westfield pilot plant.....	12
3 Materials and methods	13
3.1 Pilot plant operation	13
3.2 Field data collection	14
3.3 Laboratory batch studies.....	16
3.4 Solids characterisation	18
4 Results and evaluation	19
4.1 Performance of the Westfield pilot plant (studies 1 and 3).....	19
4.2 Sedimentation of hydrous ferric oxides (study 4)	22
4.3 Development of a novel sizing approach (studies 2 and 5).....	23
5 Summary, implications, and conclusions	26
5.1 Iron removal	26
5.2 Implications	27
5.3 Conclusions and outlook.....	31
References	35
Abbreviations.....	43
Glossary.....	44
Acknowledgements	45
Appendix (publications).....	46
Study 1 – Appl. Geochem. 122: 104731	47
Study 2 – Mine Water Environ. 40: 587	57
Study 3 – Water Air Soil Pollut. 233: 66	77
Study 4 – Environ. Sci. Technol. 56: 6360	98
Study 5 – Water Res. 233: 119770	117

List of Figures

Fig. 1	Surface water pollution by (a) acid mine drainage and (b,c) ochre formation	1
Fig. 2	Study site: (a) lignite mining regions in Germany, (b) the historic Upper Palatine lignite district, and (c) the Westfield project site; from Opitz et al. (2022a)	10
Fig. 3	Layout of the trifurcated pilot plant with details of concrete sampling manholes (top) as well as settling ponds and wetlands (bottom); modified from Opitz et al. (2023)	12
Fig. 4	Experimental setup of the sedimentation column experiments during (a) preparation, (b) mixing and filling, and (c) sampling; modified from Opitz et al. (2022b)	16
Fig. 5	Discrete hydraulic loading and cumulative mass removal for iron mass balances with different time resolutions for the 452-day period; modified from Opitz et al. (2020b)....	19
Fig. 6	Contaminant development in the Westfield pilot plant as median concentrations for the 452-day period with arrows indicating trends; modified from Opitz et al. (2022a).....	20
Fig. 7	Removal efficiency of relevant contaminants for the conventional plant (2011-2021) and the Westfield pilot plant (2018-2019) based on median inflow-outflow levels with overall removal and sample number indicated below columns; from Opitz et al. (2022a).....	21
Fig. 8	Double-logarithmic plot of initial sedimentation rates $\Delta[Fe]/\Delta t$ vs. initial iron concentration $[Fe]_0$ for all 36 datasets of the basic series at different initial iron levels with dashed lines indicating slopes; modified from Opitz et al. (2022b)	22
Fig. 9	Correlation of iron removal rates $\Delta[Fe]/\Delta t$ and inflow iron concentration $[Fe]_{in}$ in settling ponds and wetlands with overall regressions as dashed lines; modified from Opitz et al. (2023).....	24
Fig. 10	Ratio of (pseudo) first-order ferrous iron oxidation and hydrous ferric oxide sedimentation coefficients k'_{ox} and k_{sed} as a semi-logarithmic function of pH at different temperature and oxygen saturation levels; modified from Opitz et al. (2023)	25
Fig. 11	Schematic illustration of mechanisms governing iron removal from neutral mine water	26
Fig. 12	Plug flow model approach for iron transformation and removal in passive systems.....	27
Fig. 13	Iron removal calculated via the established areal model and via the kinetics-based model with $k_{hom} \approx 2.1 \times 10^{-1} \text{ h}^{-1}$ in combination with different laboratory-derived values for k_{sed} as coloured lines, the detail showing corresponding $[Fe(OH)_3]$	28
Fig. 14	Iron removal calculated via the kinetics-based model with the field-derived $k_{sed} = 2.1 \times 10^{-2} \text{ h}^{-1}$ (Opitz et al. 2023) at 10 °C for (a) different pH levels at $P_{O_2} \approx 0.21 \text{ atm}$, and (b) different oxygen levels at $\text{pH} \approx 7$	28
Fig. 15	Hypothetical HRT to reach a discharge limit of 3 mg/L depending on initial iron level for the linear areal model (grey shading) and the kinetics-based model (graphs) at 10 °C, different pH levels, and low to moderate oxygen level.....	29
Fig. 16	Development of iron concentration throughout the Marchand settling ponds A to F as a function of nominal HRT with symbols as iron concentrations reported by Hedin (2013) and modelled lines (dotted lines); modified from Opitz et al. (2023).....	29
Fig. 17	Schematic flow chart for passive treatment of circumneutral, ferruginous mine water; loosely based on Hedin et al. (1994).....	30
Fig. 18	Schematic setup of multistage passive mine water treatment systems.....	31

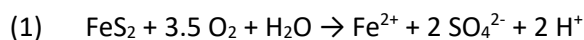
List of Tables

Tab. 1	Inflow water chemistry of the conventional treatment plant at the Westfield study site from 2011 to 2022 (n=145)	11
Tab. 2	Operation phases of the Westfield pilot plant with intended and actual ¹ flow rates [L/h] in the three parallel system lines 1 to 3	13
Tab. 3	Monitoring and sample collection at the Westfield pilot plant during the 452-day study period	14
Tab. 4	Impulse-response tracer tests conducted at the Westfield pilot plant.....	15
Tab. 5	Overview of the experimental sedimentation series; from Opitz et al. (2022b)	17
Tab. 6	Chemical, physical, and mineralogical characterisation of solids	18

1 Introduction

1.1 Environmental problem

Groundwater and seepage water flowing through underground rocks or sediments are naturally enriched with various ions through gradual leaching and dissolution of minerals. Solutes include not only easily soluble, mostly benign ions but also metals and metalloids present in the geological formation. In mining or post-mining landscapes, metal(loid) levels of the mineral deposits are usually considerably higher and the ensuing mobilisation processes are enhanced as excavation, resource extraction, and groundwater drawdown result in (temporal) aeration and displacement of the underground strata (Nordstrom & Alpers 1999; Plumlee et al. 1999). Moreover, dumping of excavated waste rock promotes oxygenation and percolation of the formerly anoxic materials. In an oxic environment, iron sulphide minerals such as pyrite or marcasite that are omnipresent in coal, lignite, and most metal ores are oxidised, releasing substantial amounts of acidity, iron, sulfate, and associated metal(loid)s into aquatic environments:



The phenomenon visually illustrated in Fig. 1a is widely known as “*acid mine drainage*” (AMD) (Evangelou & Zhang 1995). AMD is considered to be one of the most serious and costly environmental problems worldwide, with liabilities resulting from AMD legacies at the turn of the millennium estimated at several hundred billion US-\$ worldwide (Tremblay & Hogan 2001).

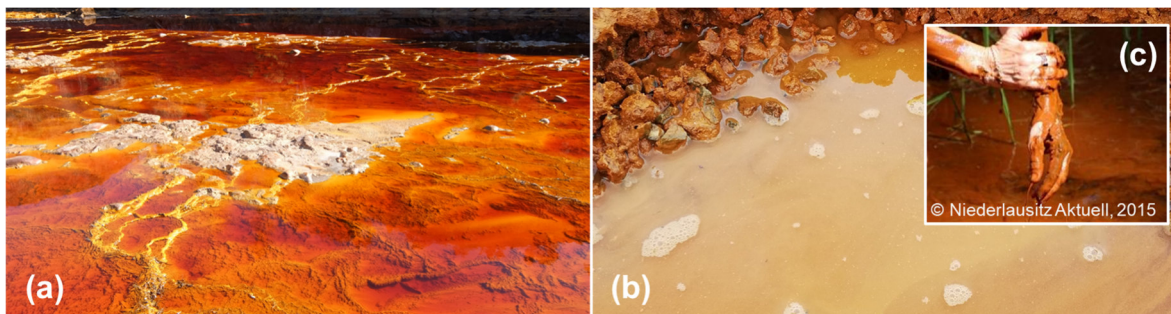
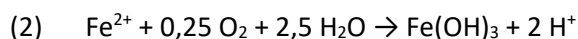


Fig. 1 Surface water pollution by (a) acid mine drainage and (b,c) ochre formation

Upon discharge into surface waters, AMD is subjected to dilution, neutralisation, and oxygenation. As a result of this critical change in hydrochemistry from acidic to circumneutral and from anoxic to oxic, various mineral phases are oversaturated, typically including aluminium, iron, and manganese (hydr)oxides (Banks et al. 1997; Gombert et al. 2019; Nordstrom 2011). In this project, we focus on iron as the primary and almost omnipresent contaminant in mining environments. In a circumneutral and oxic environment, dissolved ferrous iron readily oxidises to ferric iron, which in turn instantly precipitates as hydrous ferric oxides (Stumm & Morgan 1996). Such amorphous ferric solids cause the characteristic discoloration of mining-impacted waters known as “*yellow boy*” or “*ochre*” as illustrated in Fig. 1b/c:



Such colloidal hydrous ferric oxides are transported over great distances in mining-influenced watersheds until they either slowly settle to the bottom of the water body or until they are held back by submerged obstacles or hydrophytes (Yazbek et al. 2021). The increased turbidity impairs light transmission through the water, thus impairing visibility and photosynthesis for the aquatic fauna and flora, respectively. Moreover, sustained deposition of hydrous ferric oxides onto the sediment smothers the spawning, living, and feeding habitat of many aquatic and semi-aquatic organisms (insects, amphibians, fish, reptiles, birds), particularly in the vulnerable larval stage, thus severely damaging the benthic and aquatic biocenosis (e.g. Byrne et al. 2012; Cadmus et al. 2016, 2018; McKnight & Feder 1984). In summary, mine water causes extensive legacies of environmental degradation in aquatic environments.

1.2 Passive mine water treatment

To prevent or mitigate the pollution of aquatic environments by mining activities, different active and passive technologies were developed for treatment of contaminated mine waters (Younger et al. 2002). Active or “conventional” mine water treatment is typically achieved through addition of chemicals for oxygenation, alkalisation, flocculation, and settling in high-performance reactor systems. Such chemical treatment plants are both energy- and resource-intensive, which in turn results in comprehensive long-term costs considering that mining legacies often require mine water treatment in perpetuity. In contrast, passive mine water treatment is achieved by stimulating and enhancing natural, i.e. biogeochemical and physical processes in low-cost, eco-technological treatment systems (Skousen et al. 2017). In this project, we focus on the passive removal of iron from ferruginous, circumneutral mine water in well-established passive components such as settling ponds and constructed, surface-flow wetlands.

Passive technologies for mine water treatment were developed in the Anglo-American area in the 1980ties and 1990ties to reduce long-term costs for treatment of contaminated discharges from abandoned coal mines (Kleinmann et al. 2021). In the US, passive mine water treatment is listed as both Best Practicable Control Technology Currently Available (BPT) and Best Available Technology Economically Achievable (BAT) and thus found its way into the Clean Water Act (Hellier et al. 1994; US EPA 2013). Integrated systems for passive treatment of circumneutral, primarily ferruginous mine water typically consist of cascades for thorough aeration followed by bare settling ponds for pre-treatment and aerobic wetlands for polishing (Hedin et al. 1994). The sizing of settling ponds is commonly based on simple assignment of an overflow rate in the order of 100 m²/L/s or a hydraulic retention time (HRT) in the order of 8 to 48 h to facilitate complete ferrous iron oxidation and sedimentation of the bulk (particulate) iron load (e.g. PIRAMID Consortium 2003; Watzlaf et al. 2004; Younger et al. 2002). The sizing of wetlands is most often based on an area-adjusted removal rate, with the wetland surface area (A) calculated from inflow iron loading and an empirical, areal sizing coefficient (R_A):

$$(3) \quad A = \frac{Q \times ([Fe]_{in} - [Fe]_{out})}{R_A}$$

with Q as volumetric flow rate, $[Fe]_{in}$ as inflow iron concentration and $[Fe]_{out}$ as target effluent iron concentration or site-specific discharge limit. The areal coefficient R_A was derived from full-scale passive systems in the Appalachian coalfields treating highly ferruginous mine water (Hedin et al. 1994). The coefficient R_A was recommended by Hedin et al. (1994) with 10 g/m²/d for formal application procedures and 20 g/m²/d for basic water quality improvement at historic or abandoned legacy mine sites – the so-called “abandoned mined land criteria”.

All above-noted approaches for sizing of settling ponds and wetlands are experience-based rules of thumb, suggesting that the iron removal rate in passive systems is constant over time and independent of concentration. From a kinetics-based perspective, this corresponds to a linear or “zero-order” removal process. A brief review of the performance of passive systems shows that areal iron removal rates range from below 1 g/m²/d up to and above 50 g/m²/d, with most reports markedly below 10 g/m²/d (Opitz et al. 2023). Studies on passive systems in Great Britain showed that iron removal rates are governed by iron loading and, at AMD-sites, mine water pH (Mayes et al. 2009; Younger 2000). Altogether, most passive systems display satisfactory treatment performance, and the area-adjusted sizing approach is still considered relatively robust for typical ferruginous coal mine discharges. Nevertheless, there is general agreement that passive iron removal in settling ponds and wetlands is inadequately described by a linear relationship, and that better knowledge on the underlying multicausal mechanisms may lead to advanced and more customised designing and sizing of passive systems (e.g. Flanagan et al. 1994; Johnson and Hallberg 2002; Kruse et al. 2009; Mayes et al. 2009; Sapsford 2013; Stark and Williams 1995).

1.3 Current state of science

Passive removal of iron from circumneutral, ferruginous mine water basically requires two main processes to proceed to completion, namely (1) oxidation of dissolved ferrous ions to ferric iron which readily precipitates at neutral pH, and (2) sedimentation or filtration of the resultant hydrous ferric oxides in settling ponds and wetlands, respectively. The underlying mechanisms are briefly summarised in the following, with special focus on overall iron removal kinetics.

Step 1 – Transition of ferrous ions to particulate hydrous ferric oxides:

The mechanisms governing ferrous iron oxidation in aqueous solution are well understood, with homogeneous ferrous iron oxidation describing the basic (abiotic) transfer of ferrous to ferric ions with dissolved oxygen as oxidising agent. Progression of the oxidation sequence as detailed by the Haber-Weiss chain mechanism towards a thermodynamic equilibrium is controlled (and at times constrained) by oxidation kinetics (Stumm & Morgan 1996; Weiss 1935). The kinetics for homogeneous ferrous iron oxidation were determined by Stumm & Lee (1961), empirically describing an overall, laboratory-derived function between pH 5 and 8 with:

$$(4) \quad -\frac{d[Fe(II)]}{dt} = k_{ox}[Fe(II)]P_{O_2}\{OH^-\}^2$$

The rate constant k_{ox} was determined experimentally with $5.0(\pm 1.6) \times 10^{-14}$ mol/L/s at room temperature (Stumm & Morgan 1996). At solution-atmosphere equilibrium, oxygen partial pressure P_{O_2} and hydroxyl ion activity $\{OH^-\}$ may be substituted by dissolved oxygen concentration $[O_2]$ and proton activity $\{H^+\}$, respectively (Cravotta 2015). Application of the overall rate provided in equation (4) is generally considered sufficiently robust for ferruginous, circumneutral mine waters as demonstrated in various field studies (e.g. Dempsey et al. 2001; Geroni & Sapsford 2011; Kirby et al. 1999). The rate law is commonly simplified for atmospheric and acid-base equilibrium, i.e. excess oxygen close to saturation and stable pH, to a pseudo first-order rate law (Sung & Morgan 1980):

$$(5) \quad -\frac{d[Fe(II)]}{dt} = k'_{ox}[Fe(II)]$$

The reaction rate is proportional to the concentration of ferrous ions (or rather $Fe(OH)_2$) and increases hundredfold per pH unit due to the inversely second-order dependency on proton activity at neutral pH (Stumm & Lee 1961). The severe shift from $Fe(OH)_2$ to $Fe(OH)^+$ and Fe^{2+} at acidic pH < 4 results in pH-independent (abiotic) reaction rates and hence in persistent ferrous iron loads in acidic mine discharges along the further flow path (Davis et al. 2000; Nordstrom 2011). As opposed to this, ferrous iron oxidation at pH > 8 is extremely fast and thus limited by oxygen diffusion rather than oxidation kinetics (Singer & Stumm 1970), in further consequence resulting in precipitation of ferrous hydroxides and subsequent oxygenation to green rust or ferric oxyhydroxides (Schwertmann & Fechter 1994).

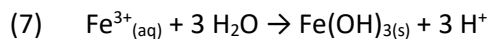
Homogeneous ferrous iron oxidation kinetics predominantly apply to low pH and nanomolar to low micromolar ferrous ion levels such as commonly found in laboratory experiments and freshwater environments. However, mining environments in general and passive mine water treatment systems in particular are characterised by the ubiquitous and copious presence of hydrous ferric oxides as well as ochreous coatings of submerged surfaces (Opitz et al. 2020b). Under such conditions, ferrous ions tend to sorb to (reactive) surfaces and oxidise considerably faster than discrete dissolved ferrous ions (Stumm & Sulzberger 1992; Wehrli et al. 1989). In particular, freshly precipitated hydrous ferric oxides were shown to further autocatalyze ferrous iron oxidation (Burke & Banwart 2002; Tamura et al. 1976; Tamura et al. 1980). Accordingly, heterogeneous ferrous iron oxidation is of critical importance for ferruginous mine waters, and a strong autocatalytic effect was demonstrated in field studies at various mine sites (e.g. Dempsey et al. 2001, 2002; Dietz & Dempsey 2017; Geroni & Sapsford 2011). A simplified empirical rate law for heterogeneous ferrous iron oxidation can be given as:

$$(6) \quad -\frac{d[Fe(II)]}{dt} = k_{het} \frac{[Fe(II)][Fe(III)][O_2]}{[H^+]} \approx k'_{het} [Fe(II)][Fe(III)]$$

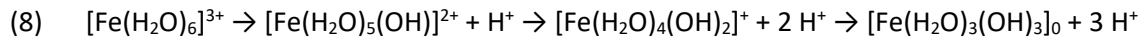
The heterogeneous rate constant k_{het} is usually estimated in the order of 1.6×10^{-6} L/mg/min at room temperature. However, as the autocatalytic mechanism intrinsically depends on sorption of ferrous ions to hydrous ferric oxides, it stands to reason that the reaction rate is not only governed by the concentration, but also by the specific physicochemical and mineralogical properties of the solids as noted by Tamura et al. (1976). By way of example, the specific surface area of ferric solids may range from few dozen m^2/g for crystalline oxyhydroxides up to several hundred m^2/g for freshly precipitated, amorphous hydrous ferric oxides (Hiemstra & van Riemsdijk 2009; Michel et al. 2010). As a consequence, amorphous hydrous ferric oxides such as ferrihydrite tend to display a much higher site density of singly coordinated surface oxygen functional groups relative to crystalline oxyhydroxides such as goethite (Bottero et al. 1993; Hiemstra 2013). Moreover, impurities in and non-monomer structures of hydrous ferric oxides may also impair adsorption rates (Baumgartner & Faivre 2015). Accordingly, the rate constant k_{het} may vary by as much as an order of magnitude, basically decreasing with increasing structure (Mettler et al. 2001; Park & Dempsey 2005). Nevertheless, the adsorption equilibrium is assumed to occur fairly rapid in ferruginous environments relative to oxidation due to the omnipresence of amorphous hydrous ferric oxides, especially at circumneutral pH and in association with high iron and sulfate levels (Jeon et al. 2001; van Beek et al. 2012). Therefore, equation (6) is considered an explicitly simplified, yet robust approximation for heterogeneous ferrous iron oxidation in mining environments (Dietz & Dempsey 2017).

For the sake of completeness, it should be noted that microbially driven (i.e. biotic) ferrous iron oxidation may be of importance at strongly acidic pH as well as low iron or oxygen levels (Kappler et al. 2021; Melton et al. 2014). However, biotic ferrous iron oxidation is generally considered of little importance for overall iron removal in mining environments with respective discharge criteria typically in the low micromolar order. The contribution of biotic oxidation in competition with favourable abiotic kinetics in circumneutral mine waters is yet to be demonstrated (and quantified) if applicable (Kirby et al. 1999).

Following ferrous iron oxidation, transition of freshly oxidised ferric iron from aqueous to solid phase proceeds via hydrolysis and precipitation. A simplified overall equation is given as:



Solubility of ferric ions is negligible at $pH > 3.5$, which is why the hexaaquo ferric iron rapidly hydrolyses driven by thermodynamic charge balancing through either stepwise loss of protons from polarised water molecules in the primary hydration shell or through replacement of water molecules by hydroxyl ions (Duan & Gregory 2003; Flynn 1984):



An equilibrium of different hydrolysed ferric species and ferric complexes of variable charge and structure (e.g. $FeCl_2^+$, $FeCl_2^+$, $Fe(SO_4)^+$, $Fe(CO_3)^+$) is reached corresponding to pH and solution composition (Grundl & Delwiche 1993; Schwarzenbach 1970). Hydrolysed ferric iron occurs predominantly as cationic and neutral mononuclear hydroxo-species $[Fe(H_2O)_4(OH)_2]^+$ and $[Fe(H_2O)_3(OH)_3]_0$ at circumneutral pH with amount-of-substance fraction ratios approx. 90:10, 50:50, and 10:85 at pH 6, 7, and 8, respectively. Some anionic $[Fe(H_2O)_2(OH)_4]^-$ may occur at alkaline $pH > 7.5$ as well. Additionally, polymerised dimers such as $[Fe_2(H_2O)_8(OH)_2]^{4+}$ and other polynuclear hydrolysis products are to be expected (Bottero et al. 1994; Flynn 1984). However, this theoretical equilibrium may be upset in mining environments due to elevated concentrations of coordinating anions, especially sulfate and chloride, that affect electrostatic proportions and increase hydrolyzation rates (Xiao et al. 2010). In addition, iron hydrolysis may be suppressed by organic substances (Karlsson & Persson 2012). A fourth-order relationship with pH was suggested for ferric iron hydrolysis at $pH < 3$ by Singer & Stumm (1969). In

circumneutral solution, the decreasing charge of the hydrolysed ion is associated with a substantial gain in entropy, whereby the hydrolytic reactions in equation (8) occur almost instantaneous (Grundl & Delwiche 1993).

The supersaturation-driven processes described above result in transitions of aqueous ferric species to amorphous hydrous ferric oxides (Das 2018). Such dispersed ferric phases are initially small enough to remain suspended for long time spans (Banfield et al. 2000) and thus cause the visually characteristic turbid or “ochreous” discoloration of ferruginous mine waters that goes hand in hand with the degradation of aquatic ecosystems (Filella & Buffle 1993; Matthies et al. 2012). The resultant sediment in passive systems largely consist of ochre, i.e. poorly ordered ferric phases that are metastable towards more crystalline oxyhydroxides. Overall, hydrolysis and precipitation of ferric iron in ferruginous, circumneutral mine waters are quasi-instantaneous (Jolivet et al. 2004) and the transition from aqueous to solid phase may thus be disregarded for overall iron removal in passive systems.

Step 2.1 – Sedimentation of particulate hydrous ferric oxides in the free water body:

In mining environments, passive iron removal is primarily focused on ferrous iron oxidation from AMD with a minor focus on subsequent removal of the resultant hydrous ferric oxides (Cravotta 2021; Kirby et al. 1999; Tarutis et al. 1999). While this is certainly applicable to acidic mine discharges due to slow ferrous iron oxidation kinetics, the transition from ferrous to ferric and aqueous to solid phase outlined above is only the first and not necessarily the rate-determining step for overall iron removal in passive systems (Chikanda et al. 2021; Sapsford 2013). For irreversible iron removal, the freshly precipitated ferric colloids need to increase in size through either adsorptive oxidation and precipitation, or interconnection of the dispersed colloids to form growing clusters (*aggregation*). The larger particles are effectively removed from solution through either gravitational settling (*sedimentation*) or physical interception on submerged obstacles or within a porous matrix (*filtration*). As opposed to the above-described ferrous iron oxidation, the formation, aggregation, and sedimentation kinetics of waterborne hydrous ferric oxides in mining environments are poorly understood.

Initially, the steady growth of dispersed ferric precursor phases occurs through adsorption, polymerisation, and surface complexation of dissolved ferrous and hydrolysed ferric aquo species and subsequent surface deposition as noted above (Grundl & Delwiche 1993; Hiemstra & van Riemsdijk 2007). After extensive ferrous iron oxidation, growth of aqueous ferric macromolecules and (nano)particles is increasingly governed by collision and attachment as well as enmeshment or bridging of the dispersed ferric solids. Aggregation is promoted by the thermodynamic disposition of freshly formed colloids to free surface energy reduction, with the formation of larger aggregates reducing the overall free energy and surface area (Baumgartner & Faivre 2015; Penn 2004). At relatively constant loading, the particle size distribution in passive systems is governed by an equilibrium between particle formation, aggregation, breakage, and settling (e.g. Braskerud 2003; Kim & Stolzenbach 2004; Matthies et al. 2012). Thus, the interaction of dispersed hydrous ferric oxides in a well-defined colloidal dispersion system may be reasonably well described using basic adsorption- and aggregation theory such as DLVO or Smoluchowski (e.g. Berka & Rice 2005; Buffle et al. 1998; González et al. 2004, Grant et al. 2001; Phenrat et al. 2007). This, however, is usually not the case and thus inapplicable for mining environments in general and in the initial, dynamics stages of passive mine water treatment systems in particular (Rand & Ranville 2019). Therefore, simplified (empirical) kinetic relationships or model approaches are commonly derived in eco-technological engineering sciences to estimate contaminant removal.

By way of example, a simplified first-order rate law was proposed by Sapsford & Watson (2011) to approximate sedimentation of dispersed hydrous ferric oxides subsequent to ferrous iron oxidation in passive mine water treatment systems:

$$(9) \quad -\frac{d[Fe]}{dt} = k_{sed}[Fe]$$

Although the first-order sedimentation coefficient k_{sed} depends on particle characteristics such as shape, density, impurities etc., (Dietrich 1982), such effects are expected to be masked by the high iron loads in mine waters and the variable water content of the solids. The range for k_{sed} as estimated from laboratory sedimentation and field studies was reported with 1.3×10^{-2} to $2.1 \times 10^{-1} \text{ h}^{-1}$ by Pizarro et al. (1999) and 9.6×10^{-3} to $3.2 \times 10^{-1} \text{ h}^{-1}$ by Sapsford (2013), although it should be noted that methodological and hydrochemical differences in the two studies may have distorted sedimentation rates. A targeted laboratory experiment with pre-oxygenated mine water containing only freshly precipitated hydrous ferric oxides by Sutton et al. (2015) yielded a coefficient k_{sed} in the order of $2.3 \times 10^{-2} \text{ h}^{-1}$ to reach a residual iron level of $< 1 \text{ mg/L}$ after approx. 135 h.

Alternatively, higher- or broken-order rate laws were suggested for sedimentation of particulate matter based on the assumption that particle settling rates are primarily a function of interaction rather than gravitation (Hunt & Pandya 1984; Gunnars et al. 2002). For example, second-order models were suggested to approximate binary particle collisions in dilute dispersions:

$$(10) \quad -\frac{d[Fe]}{dt} = k'_{sed}[Fe]^2$$

The coefficient k'_{sed} was reported in the range 2.3×10^{-3} to $9.3 \times 10^{-2} \text{ m}^3/\text{g/h}$, although it should be noted that respective experiments focused on iron removal in either estuarine or marine environments where both salinity and organic matter play a crucial role in (hetero)aggregation (e.g. Fox et al. 1983; Mayer 1982; Hunter et al. 1997). Based on sedimentation rates of goethite particles in seawater, Farley and Morel (1986) found k'_{sed} in the order of $7.3 \times 10^{-3} \text{ m}^3/\text{g/h}$ but noted that a mixed rate law would be required to adequately consider the interrelated aggregation- and settling-based regimes. Thus far, no systematic assessment was reported on sedimentation kinetics of hydrous ferric oxides at moderate to high micromolar levels typically observed in ferruginous mine water.

Freshly precipitated hydrous ferric oxides in mining environments were observed to display a natural tendency towards homoaggregation, which was attributed to favourable double-layer compression and surface charge neutralisation in circumneutral, ferruginous mine waters (Barnes et al. 2009; Dempsey et al. 2001). Progressing aggregation of hydrous ferric oxides results in continual particle enlargement towards a size that ensures effective gravitational settling (Banfield et al. 2000). The critical aggregate size where dispersed colloidal hydrous ferric oxides transition to settleable particles was estimated in the upper nanometre to lower micrometre range (Hunter et al. 1997), which is in accordance with both controlled laboratory experiments (e.g. Hove et al. 2008; Lo & Waite 2000; Xiao et al. 2010) and ferric sediments collected from mining environments (e.g. Dietz & Dempsey 2017; Fenton et al. 2009; Marcello et al. 2008; Matthies et al. 2012; Wang et al. 2020). Recently, Chikanda et al. (2021) reported effective sedimentation of ferric particles in a drain and pond system following a mine discharge after proceeding aggregation of ferric colloids to $> 300 \text{ nm}$. It is generally assumed that the aggregation-driven settling of waterborne particles may be approximated by simplified rate equations in due consideration of critical influencing factors (Grant et al. 2001). Unfortunately, there is as of yet no application-oriented, mixed or non-integer order model approach for the sedimentation of hydrous ferric oxides in circumneutral, ferruginous mine water.

Step 2.2 – Filtration of hydrous ferric oxides by macrophytes:

In natural or constructed surface-flow wetlands, the emergent macrophytes have a “filtering” effect by intercepting and trapping suspended particulate matter, thus accelerating the above-noted sedimentation step (e.g. Cotton et al. 2006; Horvath 2004; Pluntke & Kozerski 2003; Saiers et al. 2003). As described by Opitz et al. (2021), interception of waterborne hydrous ferric oxides by hydrophytes and other obstacles in constructed wetlands for mine water

treatment is usually visually apparent by ochreous coating of submerged rhizomes, stems, leaves, litter, and any technical structure. Particles of all sizes are affected by this “filtering” effect, although an increase in particle size naturally increases the likelihood to directly strike, stick to, or settle on submerged macrophytes (Cotton et al. 2006; Elliott 2000; Li et al. 2007). Nevertheless, even nanoscale colloids may be intercepted by submerged wetland hydrophytes (Pluntke & Kozerski 2003; Saiers et al. 2003). Generally, particle interception was observed to increase not only in vegetated compared to unvegetated ponds (Pluntke & Kozerski 2003), but also with an increase in vegetation cover in the flow path or cross-section (Saiers et al. 2003; Verschoren et al. 2017).

Details on improved particle removal by wetland macrophytes are extensively discussed by Batty & Younger (2002) and Opitz et al. (2021). To date, quantitative approaches to filtration in wetlands are predominantly based on modelling of macrophyte-colloid interaction that is further related to changes in ecological and hydrodynamic boundary conditions. The most important phytophysiological factors are plant species and macrophyte density, water depth, and vegetation development – which often vary both spatially and seasonally within one and the same wetland. Thus, numerical simulations are commonly limited to (site-)specific ecological conditions or assumptions with limited transferability. To our knowledge, no parameterisation for the removal of hydrous ferric oxides in mine water treatment wetlands is provided in the literature as of yet (Opitz et al. 2021).

Since filtering affects particles of all sizes, it may prove necessary and possible to estimate the share of macrophyte-based filtration in overall ferric iron removal or to develop a simplified, concentration-dependent filtration power law to account for increased iron removal in wetlands by macrophytes. For instance, filtration studies of dispersed micrometre and submicron colloids by Pluntke & Kozerski (2003) and Saiers et al. (2003), respectively, indicate that particle concentration is to be expected as the determining factor for interception of waterborne particles by hydrophytes. As filtration is not only governed by physicochemical, but also ecological factors, it is assumed that any quantitative approach to estimate filtration-based removal of hydrous ferric oxides in wetlands would either (1.) require consideration of different potentially critical (ecological) influencing factors, or (2.) warrant considerable simplification or generalisation. To date, evaluation of literature reports for areal iron removal in wetlands clearly showed that treatment performance of wetlands is very heterogeneous, highlighting our limited understanding of the underlying iron removal mechanisms and kinetics in densely vegetated wetlands (e.g. Batty & Younger 2002; Cravotta & Brady 2015; Opitz et al. 2021; Wieder 1989).

Research hypothesis:

- We hypothesise that it may be possible to approximate the kinetics for passive removal of particulate iron under low flow rates such as observed in bare settling ponds by identifying and parameterising the critical (i.e. rate-determining) physicochemical aggregation and/or sedimentation mechanisms.
- We hypothesise that it may be possible to approximate overall iron removal rates in densely vegetated, surface-flow wetlands either by identifying and parameterising the rate-determining processes and critical influencing factors, or by way of an empirical relationship for standardised constructed conditions (e.g. water depth, wetland vegetation).
- Such simplified relationships for removal of particulate hydrous ferric oxides may be utilised to develop engineering rather than scientific model approaches for approximation of the necessary size or hydraulic retention time of passive mine water treatment systems for iron removal from ferruginous, circumneutral mine water – especially settling ponds and surface-flow wetlands for pre-treatment and polishing, respectively.

1.4 Situation in Germany

Germany has a long history in metal, coal, and industrial minerals mining, remaining one of the world's biggest lignite producing countries to date. The environmental impacts in both historical and operational mining districts on the chemical and ecological status of ground- and surface water are of growing environmental concern from municipal up to federal levels, with environmental concerns highlighted by nationwide assessments according to the European Water Framework Directive (WFD). In the lignite districts of Middle Germany and Lusatia, the impacts on everyday life such as the sulfate loads threatening the drinking water supply of Berlin as well as the ochreous discoloration of the rivers Lusatian Neisse, Black Elster, and Spree, the latter also threatening the Spree Forest UNESCO biosphere reserve, have become a topic of public concern and debate (Kruspe et al. 2015). Therefore, considerable public funds are allocated to emergency and long-term measures in the former LMBV mining area for mitigation and remediation of ochre formation and dispersion, not only in numerous pit lakes but also in the Spree catchment upstream of the Spremberg dam (Benthaus et al. 2020).

Whereas passive treatment is a key driver in the successful mitigation of mine discharges in the Anglo-American area as outlined in chapter 1.2, passive technologies are non-existent in Germany. In an extensive review of the German mine water situation following the implementation of the WFD, Hasche-Berger & Wolkersdorfer (2005) noted that *“mine water in Germany is usually treated by conventional methods”*. In fact, no passive mine water treatment system is operational nationwide since the only large-scale passive system ever formally permitted and constructed at the former Pöhla mine site in southwestern Saxony was decommissioned in 2014 due to maintenance issues and difficulties in complying with specific pollutant limits. Other experimental field trials such as implemented at the Lehesten mine site in southern Thuringia or the Vetschau site in southeast Brandenburg were either abandoned or retrofitted with chemical alkalisation and dosing, or mechanical scraper systems due to insufficient operational efficiency or reliability (Bilek 2012).

In the early 2000s, the European Commission (EC) supported research on technologies for mine water management and on development of related policy (e.g. ERMITE Consortium 2004; PIRAMID Consortium 2003). Following this, passive technologies were included in the respective European reference BAT-document for “Management of Tailings and Waste-rock in Mining Activities“ (BREF 01.2009). However, although wetland systems were designated as a relatively new technology suitable for small flow rates, it was also noted that *“many specific mechanisms and maintenance requirements [are] not yet fully understood [and] optimum sizing and configuration criteria are still under study“* (EC 2009). This evaluation combined with the lack of standardised German guidelines and domestic showcases as well as the scale of mine water issues in extensive, long-time lignite districts are probably the main reason why passive technologies were approached with scepticism in Germany over the last decades.

According to a 2016 status report on German (fresh)waters under the European WFD that was published by the German Federal Environmental Agency, the water balance in waters affected by decades-long mining activities is often disturbed to such a degree that the timely improvement of the chemical and quantitative state is deemed impossible, specifically pointing out the economic costs of established improvement measures (UBA 2016). The post-operative challenge around former (lignite) mining districts may even be further exacerbated by climate change and the resultant pressure on clean water resources. Considering the contemporary developments around the WFD on the one hand and the intended lignite phase-out on the other hand, Germany will inevitably face an increasing demand for cost-effective, sustainable mine water treatment technologies in the years to come. Therefore, the timely adoption and advancement of passive treatment systems is considered an indispensable component for long-term and sustainable mitigation of mine water issues as well as for protection of receiving waters and aquatic ecosystems in Germany.

1.5 Study objectives

Conceptualisation and sizing of eco-technological, passive-biological systems for treatment of wastewater from various sectors (industry, landfills, runoff, sewage etc.) are typically based on empirical coefficients or rules of thumb for applied simplification of the complex kinetics of underlying biological, chemical, and physical contaminant removal processes. Technical guidelines generally recommend conservative approximation of the required size, volume, HRT, or overflow rate for water treatment to an acceptable level. Respective formulae are based on a simplified design parameters or coefficients such as pollutant load, volume flow, household number, or catchment area (e.g. DVGW 2005a,b; DWA 2005, 2006, 2013; Ekama et al. 2006; Kadlec & Wallace 2009; Kadlec et al. 2000; Wegelin 1996; Wildemann et al. 1993).

The critical sizing parameter for passive removal of (above all) dissolved and particulate iron from circumneutral, ferruginous mine water is the iron loading, which is in turn a function of iron concentration and flow rate. As noted in chapter 1.2, the established, area-adjusted sizing approach in equation (3) is basically a simplified rule of thumb that was initially derived from and developed for highly ferruginous mine waters with iron levels exceeding 25 mg/L that are associated with moderate discharge limits in the order of 2 to 5 mg/L. For lower iron loadings on the one hand and/or more stringent discharge criteria on the other hand, there is currently no adequate sizing approach for passive treatment systems.

Thus, the overall objective of this research project was to advance the established practice for the designing and sizing of aerobic, passive treatment systems for the removal of dissolved and especially particulate iron from circumneutral mine water. A respective sizing approach should be based on the underlying physical and/or biogeochemical processes, but should also be practicable for everyday engineering services and requirements – i.e. scientifically sound and application-oriented. To that end, the critical iron removal mechanisms were qualitatively and quantitatively investigated under both laboratory and field conditions to parameterise a corresponding engineering model approach.

Objectives of the partial studies:

- Proof of operational reliability for a multistage passive pilot plant for removal of iron as primary contaminant in ferruginous, circumneutral mine water in due consideration of the strict, site-specific discharge limit of only 1 mg/L at the Westfield study site;
- Proof of hydraulic reliability of a multistage passive mine water treatment system in due consideration of both winter operation and flow variability;
- Identification, assessment, and parameterisation of the critical mechanisms for removal of (particulate) iron from circumneutral mine water under controlled laboratory conditions;
- Comparison of iron removal kinetics derived from controlled laboratory batch studies on the one hand and field pilot plant results under “real” conditions on the other hand;
- Development of a well-founded and transferrable, yet still application-oriented sizing model approach for reliable, full-scale passive mine water treatment systems.

Based on the pilot study, it is explicitly envisaged to develop the technical basis of valuation for designing, sizing, and ecological engineering of a full-scale passive system for long-term seepage water treatment at the study site. In view of the German context as outlined in chapter 1.4, such a lighthouse project would advance the technology readiness level (TRL) of passive systems as per the EU-H2020 scale to at least 6 and 7 (i.e. technology and system prototype demonstration), which would in turn form the basis for nationwide use and spread of passive technologies, i.e. striving for TRL 8 and 9 (i.e. actual system proven in operational environment) (ESA 2008). In summary, the project should improve the state of scientific knowledge and technique, thus making a substantial contribution to overcome the drastic, long-lasting ecological and socio-economic consequences of mine water issues in Germany.

2 Study site

2.1 The Westfield legacy site

The Westfield study site is located near the town of Wackersdorf in the former lignite district of Upper Palatinate in Bavaria, southeast Germany (Fig. 2a). The Upper Palatinate lignite deposits were formed in a Tertiary trench system predominantly embedded in Triassic sandstones. Both lignite and associated waste rock in the former mining district contain sulphide minerals, predominantly pyrite and marcasite, as a natural consequence of the primordial formation during marine transgression and regression cycles (Evangelou & Zhang 1995). Opencast mining in the Wackersdorf area ceased in 1982 and the post-mining landscape is now in an advanced stage of rehabilitation. Progressing oxidation of sulphide minerals in the backfilled pits results in extensive AMD formation as is common for abandoned lignite districts.

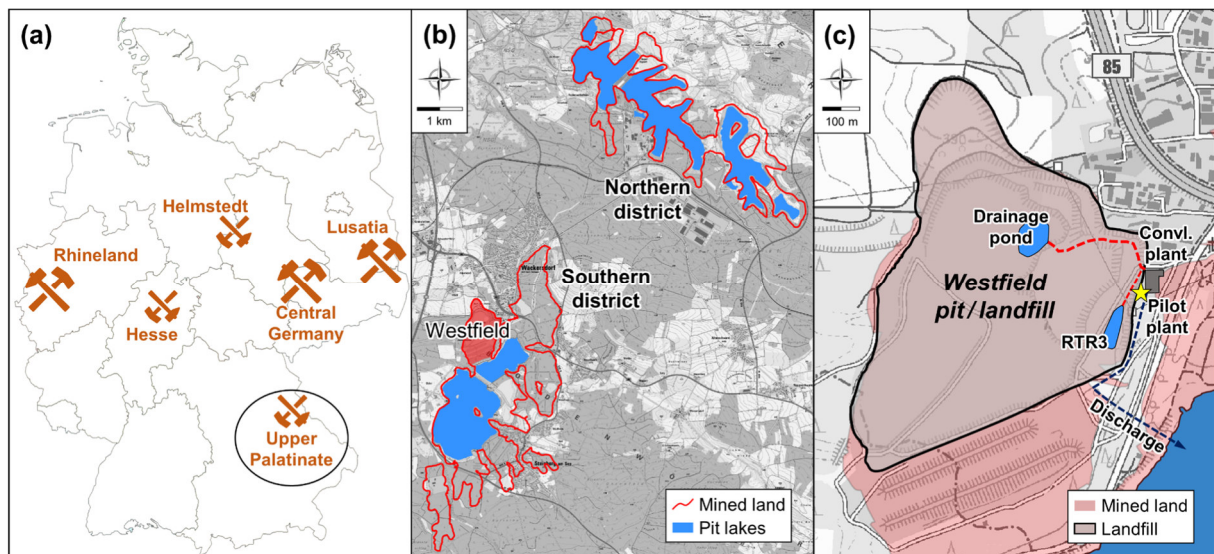


Fig. 2 Study site: (a) lignite mining regions in Germany, (b) the historic Upper Palatinate lignite district, and (c) the Westfield project site; from Opitz et al. (2022a)

As described by Opitz et al. (2022a), the Westfield is a former opencast segment in the southern Upper Palatinate district (Fig. 2b). Two major lignite seams were mined in the Westfield between 1941 and 1982, and parts of the pit were concurrently backfilled with waste rock and ashes from the nearby lignite power station in Schwandorf. Due south, the mined Westfield was separated from adjacent opencast segments by a broad, approx. 30 ha dam structure through dumping of waste rock from 1956 to 1958 and bottom ash from 1960 to 1982.

After the end of industrial-scale lignite mining in the Upper Palatinate district in 1982, the remaining 52 ha of the former Westfield segment were approved as a landfill for combustion residues under waste law in 1984 (Fig. 2c). An estimated 4×10^6 t (approx. 3.1×10^6 m³) power plant ash was deposited in the Westfield landfill until formal decommissioning in 2003. Nevertheless, dumping of bottom and electrostatic precipitator ash in the former Westfield pit still left a deep morphological depression behind and the artificial dewatering system of the Westfield landfill was maintained even after decommissioning because it was found that groundwater runoff from the landfill (that was commissioned without base sealing) would have affected aquifer systems due west and thus threatened regional drinking water resources in the long term. As a consequence, up to the present day and in the foreseeable future seepage water is continually pumped out from a so-called “*drainage pond*” at the lowest point of the former Westfield pit and waste disposal site (Fig. 2c). Artificial dewatering creates an extensive groundwater drawdown cone that collects contaminated seepage water from the surrounding mined land. With rehabilitation and recultivation completed in 2023, long-term seepage water management remains the only (perpetual) task for sustainable reclamation of the Westfield legacy.

2.2 Seepage water chemistry

Groundwater in the post-mining landscape around the Westfield site is strongly affected by decades of industrial-scale lignite mining, causing extensive formation of AMD. Furthermore, the ground- and seepage water converging in the Westfield drainage pond is mineralised through lixiviation of readily soluble compounds from the deposited ashes. As a consequence, the seepage water leaking in the drainage pond is contaminated with mining- and ash-typical solutes such as iron, manganese, ammonia, sulfate, chloride, and alkali(ne) earth metals. Due to the alkalisating character of the deposited ashes, the seepage water is circumneutral or even (negligibly) alkaline (Opitz et al. 2020b).¹

Tab. 1 Inflow water chemistry of the conventional treatment plant at the Westfield study site from 2011 to 2022 (n=145)

pH	EC	Fe ¹	Mn	NH ₄	Ca	Mg	Na	Cl ²	SO ₄
7.2-7.5	2.8 (±0.3) mS/cm	5.6 (±3.5) mg/L	1.3 (±0.3) mg/L	1.2 (±0.3) mg/L	576 (±61) mg/L	101 (±18) mg/L	142 (±32) mg/L	192 (±80) mg/L	1,824 (±290) mg/L

¹ Iron decreased after commissioning of the RTR3 in 2019 owing to intrinsic sedimentation in the basin.

² Chloride steadily dropped from 250 – 350 mg/L in 2011 to 100 – 150 mg/L since 2018 due to progressing lixiviation.

The levels of metal(loid)s other than iron or manganese in the seepage water are low despite considerable mobility in the surrounding mined land due to the high sorption capacity of the fine-grained electrostatic precipitator ashes deposited in the landfill (Mishra & Tripathi 2008) and to the circumneutral seepage water pH where solubility of most metals is low (Stumm & Morgan 1996). Groundwater seeping at the drainage pond is strongly ferruginous with (ferrous) iron levels far exceeding 100 mg/L. However, the temporary impoundment of seepage water results in thorough oxygenation, which is why ferrous iron is largely already oxidised. Hence, the remaining (particulate) ferric iron levels are reduced by an order of magnitude, averaging about 10 mg/L. Temporal heterogeneity in the inflow water chemistry in Tab. 1 is attributable to the varying mixing ratio of rainwater and seepage water in the drainage pond.

2.3 Seepage water management

A conventional (physicochemical) treatment plant was implemented at the Westfield site in 1995 for treatment of the ferruginous seepage water. The primary purpose of the conventional treatment plant is to remove dissolved and particulate iron as well as other suspended solids (TSS) to protect the receiving water from ochre depositions. Iron removal in the conventional treatment plant is achieved in a classical reactor system through addition of lime slurry for alkalisating and pH-stabilisation followed by the addition of flocculants, recycled sludge, and flocculant aids for iron removal. In 2019, the intermediate reservoir “RTR3” marked in Fig. 2c was commissioned as a retention/feeding pond for the discontinuously operated, conventional treatment plant. The seepage water collecting in the Westfield drainage pond is continuously pumped to the RTR3, from where it may be pumped to the treatment plant during operation. The treated water is discharged to the nearby pit lake Knappensee south of the Westfield site. As treatment and discharge of seepage water from the decommissioned Westfield landfill were permitted under (waste)water law rather than mining law, also representing about 25% of the pit lakes’ inflow, a site-specific discharge limit for total iron of 1 mg/L was set to protect the lake from dispersion and deposition of hydrous ferric oxides (Opitz et al. 2020a).

¹ Ashes deposited in the Westfield landfill as of 1974 were produced not only from local medium-sulphur lignite, but also from low-sulphur lignite imported from the coalfields in the North Bohemian Basin (Czech Republic). After depletion of the Upper Palatine deposits in 1982, operation of the Schwandorf power plant continued with imported Czech lignite. In addition, alkaline additives were admixed to the electrostatic precipitator ashes after modernisation of the flue-gas desulfurization system in the power plant.

2.4 The Westfield pilot plant

In 2017, the Westfield pilot plant was implemented next to the conventional treatment plant (see yellow star in Fig. 2c). The conceptual design for passive treatment of the ferruginous seepage water was a multistage pilot system for progressing iron removal broadly following Pareto's principle to comply with the strict discharge limit:

1. Pre-treatment in settling ponds;
2. Polishing in surface-flow wetlands;
3. Purification in sediment filters.

The innovative pilot plant was implemented with three parallel lines as illustrated in Fig. 3. Contrary to most multiline (pilot) systems that were installed to test different materials or setups (e.g. Cravotta & Trahan 1999; García et al. 2004; Nyquist & Greger 2009; Whitehead & Prior 2005), the trifurcated Westfield pilot plant was built with three almost identical, parallel lines to generate comprehensive comparison datasets for assessment of treatment performance and kinetic relationships as well as critical influencing factors for upscaling (Opitz et al. 2022b).

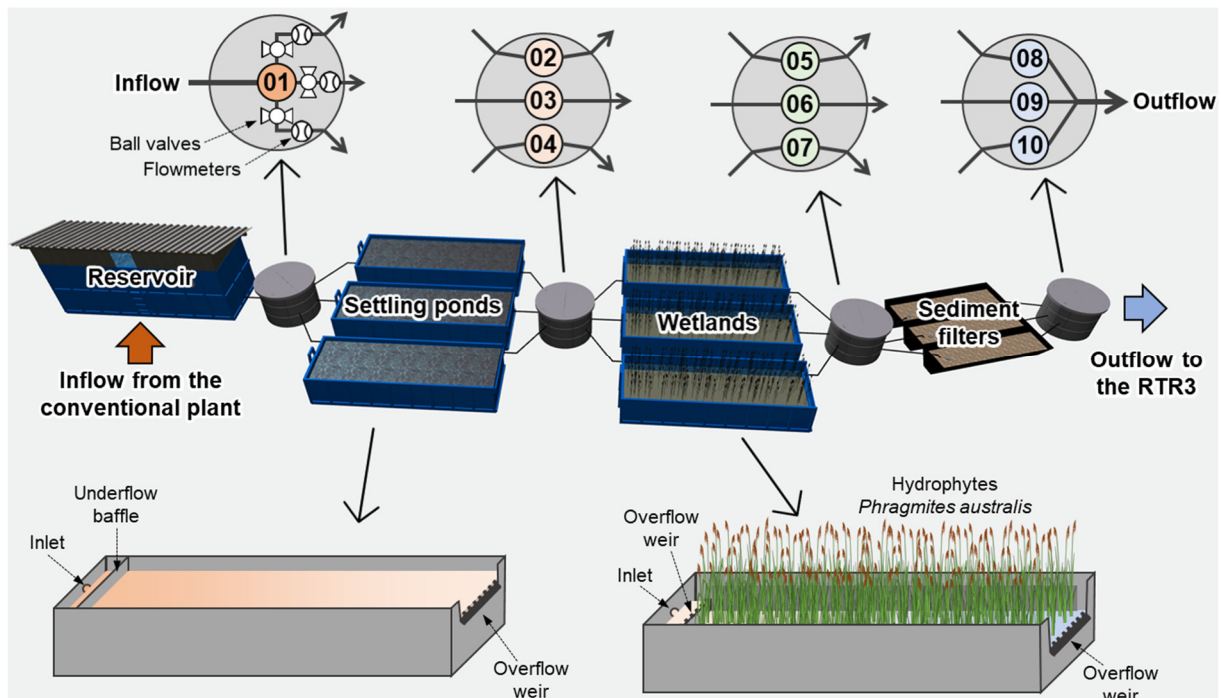


Fig. 3 Layout of the trifurcated pilot plant with details of concrete sampling manholes (top) as well as settling ponds and wetlands (bottom); modified from Opitz et al. (2023)

The Westfield pilot plant was constructed utilising commercial roll-off containers as reservoir (7,0 m x 2,35 m x 2,25 m), settling ponds and wetlands (7,0 m x 2,35 m x 1,25 m). The sediment filters were implemented as trenches with a semi-circular profile and sealed with a 2.5 mm high-density polyethylene liner (ca. 4,00 m x 0,20 m x 0,50 m). Concrete manholes DN2000 were set between the components as weatherproof housing for 10 flow-through cells that served as sampling- and monitoring points (MP01 to MP10), consecutively numbered 01 to 10 in the top details of Fig. 3. The trifurcated system lines remained separate until the system discharge, whereby the outflow of one component corresponded to the inflow of the subsequent one. The triplicate sediment filter outflows were merged and discharged back to the RTR3, thus preventing any emissions from the pilot plant. Altogether, the Westfield pilot plant was large enough to assess passive iron removal processes under real conditions and at a fairly large scale, thus avoiding scaling effects typically observed in small- or laboratory scale settings. Nevertheless, the pilot plant was small enough to be easily managed and maintained.

3 Materials and methods

3.1 Pilot plant operation

The preceding reservoir of the Westfield pilot plant was fed with seepage water split off from the inflow to the conventional treatment plant on site. The main purpose of the reservoir was to mitigate variations caused by discontinuous operation of the Westfield’s seepage water pump system. As the reservoir gravitationally drained to the pilot plant, the overall volumetric inflow rate to the pilot plant was governed by the reservoirs’ water level. As a consequence, the flow rate in (at least) one of the three system lines decreased upon progressing emptying of the reservoir, especially on weekends and holidays.

Flow rates in the three lines of the Westfield pilot plant were set with ball valves in the parallel inlet pipes branching off the first measuring and sampling point (MP01). The flow rates were continuously recorded by flowmeters (STÜBBE DFM200) at a 30-second interval. The overall flow rate of the Westfield pilot plant at normal operation averaged approx. 800 L/h with lower to upper quartiles of 746 to 851 L/h, which is about 4% of the average seepage water yield at the Westfield drainage pond. During weekends, episodic minimal flow rates were recorded as low as approx. 400 L/h. An overview of flow rates in the three system lines during the different project phases between November 2017 and December 2019 is compiled in Tab. 2:

Tab. 2 Operation phases of the Westfield pilot plant with intended and actual¹ flow rates [L/h] in the three parallel system lines 1 to 3

Project phase	System line 1	System line 2	System line 3
Test period (15.11.2017 – 22.07.2018)	<i>Flow rates before the study period were not recorded</i>		
Reference period (23.07.2018 – 12.11.2018)	270 <i>269 (±37,6)</i>	270 <i>277 (±8,0)</i>	270 <i>262 (±58,5)</i>
Variation period 1 (13.11.2019 – 05.03.2019)	170 <i>178 (±11,4)</i>	270 <i>276 (±14,3)</i>	370 <i>345 (±75,5)</i>
Variation period 2 (06.03.2019 – 26.06.2019)	190 <i>203 (±13,5)</i>	390 <i>394 (±30,7)</i>	230 <i>212 (±55,3)</i>
Maintenance break (27.06.2019 – 19.08.2019)	<i>Negligible or no flow following routine servicing of the pump system</i>		
Variation period 3 (20.08.2019 – 10.12.2019)	430 <i>424 (±112)</i>	160 <i>155 (±22,5)</i>	120 <i>139 (±20,4)</i>

¹ Actual flow rates in *grey italics* are integrated to illustrate the fluctuation of overall flow rates as average ± SD (n = 21,696).

The test period was conducted to develop, test, and debug operational procedures and most importantly to allow for vegetational development of dense reed stands in the wetlands. During the following 452-day study period, flow rates were adjusted in the inflow of the three system lines to vary both hydraulic loading and residence time for further evaluation of iron removal kinetics. In a first step, flow rates were adjusted as similar as possible at approx. 270 L/h in the three parallel system lines during the so-called “*reference period*” to validate comparability in the triplicate systems as suggested by Kuehn & Moore (1995). In a second step, flow rates in the three system lines were varied between approx. 150 and 450 L/h each during the so-called “*variation periods*” to generate a comprehensive dataset with variable iron loading and HRT for evaluation of system performance and iron removal rates as a function of hydraulic loading.

3.2 Field data collection

Basic hydrochemical parameters including temperature, pH, electrical conductivity, oxygen concentration and turbidity were continuously recorded at a 30-second interval by in-situ online sensors installed in the sampling and monitoring flow-through cells between the treatment stages and connected to a multi-parameter monitoring system (WTW IQ SENSOR NET). The middle system line (MP01, MP03, MP06, MP09) and wetland outflows (MP05, MP07) were equipped with all sensors, whilst the remaining monitoring points (MP02, MP04, MP08, MP10) were only equipped with turbidity sensors. As additional quality assurance measure, all basic water quality parameters except for turbidity were measured weekly using hand-held sensors and data loggers with additional redox potential measurements (WTW MULTI 3530 IDS).

The monitoring regime of the Westfield pilot plant is presented in Tab. 3. It is important to note that the analytical scope was constraint after the initial “test period” because some parameters (especially metals) were invariably close to or below the detection limits. This is in agreement with the long-lasting seepage water monitoring at the Westfield site.

Tab. 3 Monitoring and sample collection at the Westfield pilot plant during the 452-day study period

Monitoring schemes (<i>interval</i>)	Measurands and parameters	Measurement techniques
In-situ sensor monitoring ¹ (30-second interval logging)	<ul style="list-style-type: none"> ▪ Flow rate ▪ pH and temperature ▪ Electrical conductivity ▪ Oxygen concentration ▪ Turbidity 	<ul style="list-style-type: none"> ▪ STÜBBE DFM200 ▪ WTW SENSOLYT® 700 IQ/SET ▪ WTW TETRACON® 700 IQ ▪ WTW FDO® 700 IQ ▪ WTW VISOTURB® 700 IQ
Iron monitoring (semi-weekly sampling)	<ul style="list-style-type: none"> ▪ Total iron, Fe(tot) ▪ Particulate iron, Fe(III)_{part} ▪ Dissolved ferric iron, Fe(III)_{aq} ▪ Dissolved ferrous iron, Fe(II)_{aq} 	<ul style="list-style-type: none"> ▪ Spectrophotometry ▪ id. ▪ id. ▪ id.
Basic parameter monitoring (weekly manual measurement)	<ul style="list-style-type: none"> ▪ pH and temperature ▪ Electrical conductivity ▪ Oxygen concentration ▪ Redox potential 	<ul style="list-style-type: none"> ▪ WTW SENTIX® 940 ▪ WTW TETRACON® 925 ▪ WTW FDO® 925 ▪ WTW SENTIX® ORP-T 900
Multi-parameter monitoring ² (weekly sampling)	<ul style="list-style-type: none"> ▪ Al, Ba, Ca, Cr, Cu, K, Mg, Na, Ni, Pb, V, Zn ▪ Br, Cl, F, NO₂, NO₃, PO₄, SO₄ ▪ NH₄, PO₄, SO₄ ▪ DOC, TOC, TIC ▪ Mn 	<ul style="list-style-type: none"> ▪ ICP-OES ▪ Ion chromatography ▪ Photometry ▪ DOC-meter ▪ Graphite furnace AAS
Supplemental monitoring ² (monthly sampling)	<ul style="list-style-type: none"> ▪ Na, K ▪ As ▪ Flow rate 	<ul style="list-style-type: none"> ▪ Flame AAS ▪ Graphite furnace AAS ▪ Bucket-and-stopwatch

¹ The in-situ WTW sensors were connected to two dataloggers (WTW MULTI 3530 IDS) installed in a nearby depot building. The flowmeters were connected to a separate datalogger (JUMO LOGOSCREEN 600) mounted close to MP01.

² Parameters in grey were discontinued after the test phase (not detectable or matrix problems).

For multi-parameter analysis, three samples were collected weekly from sampling taps built into the flow-through cells at all 10 monitoring points indicated in the top details of Fig. 3. The first sample was filtered with a syringe filter at 0.45 µm, stabilised with 150 µL of 1 M hydrochloric acid and stored at 4 °C for cation analyses via ICP and AAS. The second sample was immediately frozen for anion analysis via ion chromatography and photometry. The third and last sample was stored at 4 °C for dissolved and total organic as well as total inorganic carbon measurements (DOC, TOC, TIC). Results from the weekly samplings were used to calculate the CO₂-corrected acidity broadly following Kirby & Cravotta (2005) and Peine (1998) using the software PHREEQC, version 3 (Parkhurst & Appelo 2013). Chemicals and materials used for calibration, stabilisation, and laboratory analyses as well as for sample or standard preparation were analytical grade.

Materials and methods

For semi-weekly iron analyses, two samples were collected twice weekly from the sampling taps at all 10 monitoring points. The first sample was filtered with a syringe filter at 0.45 μm , stabilised with 150 μL of 1 M hydrochloric acid and stored at 4 $^{\circ}\text{C}$ for spectrophotometric analysis of dissolved ferrous and ferric iron. The second, unfiltered sample was immediately spiked with 150 μL of 12 M hydrochloric acid and stored at 4 $^{\circ}\text{C}$ for at least 24 h to re-dissolve any particulate hydrous ferric oxides at $\text{pH} < 2$ before spectrophotometric analysis of total iron (Hedin 2008). Based on these analyses, dissolved iron was calculated as the sum of dissolved ferrous and ferric iron, and particulate iron was calculated by subtracting total dissolved from total iron (Butler et al. 2008; Matthies et al. 2012). Iron analyses were conducted using acetate buffer solution and 1,10-phenantroline at 512 nm (Tamura et al. 1974). Standards for calibration of the spectrophotometer (HACH DR 3800) were prepared with ferrous chloride solution dissolved in purified, degassed water and acidified with 1 M nitric acid (Opitz et al. 2020b).

Regarding the extensive iron monitoring, it is important to note that colloidal hydrous ferric oxides readily pass 0.45 μm syringe filters and are therefore excluded from the particulate iron fraction (Taillefert et al. 2000). Differentiating dissolved and particulate fractions at 0.45 μm has, however, become common practice in environmental monitoring of surface waters (Filella 2007). In the context of this project, the difference is considered negligible as submicron hydrous ferric oxides are metastable towards larger particles due to progressive aggregation of ferric solids in water samples (Baumgartner & Faivre 2015; Cornell et al. 1989). Nevertheless, the analysis of dissolved iron species as described above was used for quality control.

TSS levels in the later stages of the pilot plant such as wetlands and sediment filters were negligible throughout the 452-day study period, mostly falling close to or below the respective on-site TSS detection limit of 1 mg/L. For comparison with the long-term Westfield seepage water monitoring, daily averaged turbidity measurements were used as a high-resolution proxy for TSS (Opitz et al. 2020b; Pfannkuche & Schmidt 2003).

For hydraulic and hydrodynamic characterisation of the Westfield pilot plant, tracer tests were conducted in one component of the three treatment stages each (Stephenson & Sheridan 2021). To that end, a pulse injection of diluted Rhodamin WT (ACROS ORGANICS, 20%) was injected into the inlet of the treatment component and effluent fluorescence was measured in the flow-through cell behind the same treatment component. Fluorescence measurements were conducted with a submerged, in-situ fluorometer (TURNER DESIGNS CYCLOPS 7) and recorded at a 30-second interval by a mobile datalogger (ADAMCZEWSKI VARIOLOG). The tracer tests were conducted in the winter of 2020, i.e. the time of the year when thermal mixing in the pilot plant and hydrophyte density in wetlands are relatively low, thus providing a conservative approximation of actual residence time distributions (RTD) in the three pilot-scale treatment stages (Braskerud 2001). Tracer tests were terminated after reaching the basic fluorescent level, although it should be noted that slow tracer tests at lower flow rates in settling ponds and wetlands had to be discontinued after a maximum of approx. 192 h to prevent imminent dye re-cycling to the pilot plant via the RTR3. Fluorescence data was corrected for temperature and converted to tracer concentration following Smart & Laidlaw (1977) and Bodin et al. (2012), respectively. Key data of the tracer tests are compiled in the following Tab. 4:

Tab. 4 Impulse-response tracer tests conducted at the Westfield pilot plant

Tracer test data	Settling ponds	Wetlands	Sediment filters
Tracer injection point	MP01	MP02	MP06
Fluorescence recording	MP03	MP05	MP09
Number of tracer tests	5	8	8
Range of flow rates	162 – 519 L/h	172 – 500 L/h	167 – 515 L/h
Approx. test duration	> 200 h	100 – 240 h	3 – 5 h

3.3 Laboratory batch studies

The column experiments described in Opitz et al. (2022b) were conducted for identification and parameterisation of the physicochemical processes governing the sedimentation-based removal of particulate iron. To that end, large-scale plexiglass sedimentation columns were custom-made with a height of 200 cm and an internal diameter of 19.4 cm broadly following Sapsford (2013). The top was sealed with a plexiglass lid and fitted with a brazen hose barb, which was in turn connected to a vacuum pump (BROOK CROMPTON BS2212) via a rubber hose with a three-way valve. Two sampling ports for replicate sample collection were incorporated into the column one above the other at heights of 60 and 120 cm from the bottom and fitted with special airtight septa (RESTECK MININERT PRECISION SAMPLING VALVES). Each column was secured to a steel framework and brought into balance. Polyethylene reservoirs with a height of 35 cm and a diameter of 60 cm were placed below the columns as illustrated in Fig. 4a. Up to six columns were run parallel under controlled laboratory conditions at $20(\pm 2)$ °C.

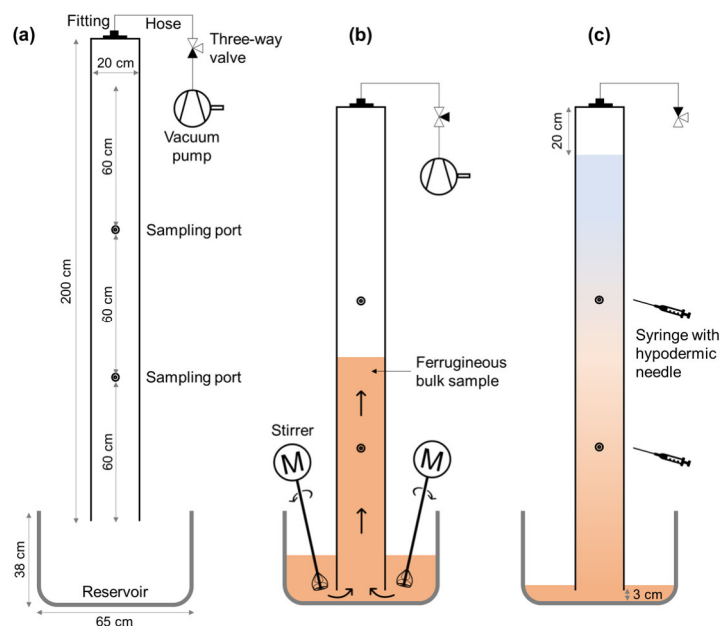


Fig. 4 Experimental setup of the sedimentation column experiments during (a) preparation, (b) mixing and filling, and (c) sampling; modified from Opitz et al. (2022b)

Ferruginous stock solutions for the sedimentation column experiments with 20 – 50 g/L of ferric solids were freshly prepared on the evening before and homogenised over night by a magnetic stirrer at 300 – 350 rpm. Incremental amounts of the ferruginous stock solution were added to 80 L of tap water in the reservoirs below the sedimentation columns, and the resultant bulk samples was thoroughly mixed with motor-operated basket stirrers (BOSCH SCINTILLA SA) for approx. 1 min to disperse solids and break up incipient aggregates. As illustrated in Fig. 4b, the empty columns were lowered into the reservoirs to 3 cm above the reservoir bottom and the bulk sample was pumped into the column in less than 1 min by the vacuum pump. After filling the columns to a height of 180 cm, the three-way valve was closed so the vacuum pump could be disconnected and relocated to the next column.

The first (replicate) sample was taken after filling of the column by opening the double-sealed safety interlock of a sampling port, piercing a 12 cm long stainless-steel hypodermic needle (B.BRAUN 0.8 MM STERICAN) through the air-tight seal, and collecting a 5 mL sample via a sterile syringe (B.BRAUN 5ML INJECT). This sampling procedure with samples collected from the centre of the column ensured minimal hydraulic, static, or temperature-related boundary effects. The replicate sampling then continued at a 4 h interval for 3 to 4 days to generate concentration-time profiles of the sedimentation process at different initial iron levels. The setup and experimental procedure of the column experiments is further detailed in Opitz et al. (2022b).

Materials and methods

Stock solutions for sedimentation column experiments were produced using both natural and synthetic hydrous ferric oxides. Natural “ochre” was collected at the Westfield project site by scooping the uppermost, freshest sediment layer from the pilot plant’s reservoir depicted in Fig. 3 with polypropylene buckets. The large ochre sample was homogenised and sieved with stainless-steel wire mesh sieves (RETSCH ANALYTICAL) at 1,000 and 100 µm mesh size to remove large aggregates and exogeneous, organic or siliciclastic material (leaves, insects etc.). Another two samples were collected at the Westfield site at higher ferrous iron levels, one under slightly acidic and one under acidic conditions with pH of 5 to 7 and 2 to 5, respectively. The additional samples were subjected to the same homogenisation and sieving procedure noted above, and all ochre samples were stored in a cold room at 4 °C in an aqueous state before usage for stock solutions.

Synthetic ferrihydrite and lepidocrocite were produced in the laboratory following the standard instructions by Schwertmann & Cornell (1991) as briefly summarised in the following:

- 6-line ferrihydrite was synthesised by bringing a 0.1 M ferric nitrate solution to pH 8 through dropwise addition of 1 M sodium hydroxide solution followed by ageing, dialysing, and freeze-drying of the resultant dispersion.
- Lepidocrocite was synthesised by mixing 0.2 M ferrous chloride and urotropine solutions to precipitate ferrous hydroxide, followed by addition of 1 M sodium nitrite solution for oxidation, followed by decanting, washing to < 20 µS/cm, and freeze-drying.

Several series were conducted during the sedimentation column experiments as compiled in Tab. 5 and briefly described below. In a first step, the basic series was conducted over a wide range of iron levels to investigate the underlying hydrous ferric oxide removal kinetics. In a second step, the pH, salinity, and solids’ series were conducted to assess potentially critical influencing factors of both bulk solution (mineralisation, pH) and ferric solids (e.g. mineralogy, composition, mass density, texture, charge) on aggregation and sedimentation dynamics as it was shown that these may affect collision and settling behaviour of waterborne ferric solids or particles (e.g. Mylon et al. 2004; Vikesland et al. 2016). The pH- and salinity series were both conducted at moderate (10 – 15 mg/L) and high (60 – 80 mg/L) initial iron levels as particle interaction is expected to be positively correlated with particle concentration. Lastly, the quality control or “real mine water series” was conducted to verify that results from tap water experiments are transferrable to mine waters as suggested by Wan et al. (2015). Data validation and quality control included outlier identification by rank-order-based outlier detection.

Tab. 5 Overview of the experimental sedimentation series; from Opitz et al. (2022b)

Series	Datasets	Ferric solids	Iron level	Bulk sample composition
Basic series	36	Natural ochre	3 – 240 mg/L	Tap water
pH series	24	Natural ochre	10 – 80 mg/L	Tap water (pH 5.5 – 8.0) ¹
Salinity series	22	Natural ochre	10 – 80 mg/L	Tap water (5 – 240 mS/cm) ²
Solids’ series	8	Syn. ferrihydrite	15 – 35 mg/L	Tap water
	4	Syn. Lepidocrocite	50 mg/L	
	8	Sl. acidic ochre	15 – 40 mg/L	
	6	Acidic ochre	10 – 30 mg/L	
Real mine water series	10	Natural ochre	10–175 mg/L	Real mine water ³

¹ pH of the bulk solution was varied in increments of 0.5 pH units (5.5, 6.0, 6.5, 7.0, 7.5, and 8.0) by careful buffering with 2 mM 3-(N-morpholino)propanesulfonic acid and adjusting pH through dropwise addition of 10 M NaOH or 12 M HCl.

² Electrical conductivity of the bulk solution was adjusted by addition of NaCl salt to approx. 5, 10, 50, 100, 150, and 250 mS/cm.

³ Approx. 400 L of “real” mine water with negligible iron were collected from the RTR3 and transported to the laboratory.

3.4 Solids characterisation

Settled solids were collected from the Westfield pilot plant after approx. one year from open sediment traps installed in the bottom of the 10 sampling- and monitoring flow-through cells indicated in the top details of Fig. 3. Following this, sediment samples from parallel cells were blended to produce four composite samples for inflow (MP01), settling ponds (MP02-MP04), wetlands (MP05-MP07), and sediment filters (MP08-MP10). The solids were sieved to < 2 mm for removal of larger depositions that are considered unrepresentative of particulate matter from the seepage water such as leaves or insects (Opitz et al. 2020b; Schaidler et al. 2014).

During the laboratory batch studies described in chapter 3.3, the different ferric solids compiled in Tab. 5 were also subjected to detailed chemical, physical, and mineralogical analyses. The characterisation of solids from both field and laboratory studies is briefly described below, with an overview of laboratory analyses given in Tab. 6:

- The pH was determined by pH sensor measurements (WTW SENTIX® 940);
- The elemental composition with a focus on iron and associated metals was determined by ICP-OES via aqua regia digestion of triplicate freeze-dried and washed subsamples;
- The z-average hydrodynamic diameter and zetapotential were examined by electrophoresis (MALVERN ZETASIZER NANO ZS) using folded capillary zeta cells (MALVERN DTS1070) broadly following Juang & Wu (2002);
- The isoelectric point (IEP) was obtained by measuring the electrophoretic mobility of several subsamples with pH adjusted between 4 and 8 broadly following Barnes et al. (2009);
- The mineralogy was determined by X-ray diffraction (XRD) with a cobalt X-ray source and LynxEye detector (BRUKER AXS D4 ENDEAVOR), diffractograms collected from 10° to 80° 2θ with a 2 second acquisition and 0.06° 2θ step size on dried and powdered subsamples.

Tab. 6 Chemical, physical, and mineralogical characterisation of solids

Samples	pH	Iron content	Diameter	IEP	Mineralogy
Solids samples from the Westfield pilot plant					
Inflow	✓	✓	n/a	n/a	✓
Settling ponds	✓	✓	n/a	n/a	✓
Wetlands	✓	✓	n/a	n/a	✓
Sediment filters	✓	✓	n/a	n/a	✓
Solids samples from the laboratory batch studies					
Natural ochre	✓	✓	✓	✓	✓
Slightly acidic ochre	✓	✓	n/a	n/a	✓
Acidic ochre	✓	✓	n/a	n/a	✓
Synthetic ferrihydrite	n/a	✓	✓	✓	✓
Synthetic lepidocrocite	n/a	✓	n/a	n/a	✓

After dismantling of the pilot plant, the accumulated sediment from settling ponds, the plants and sediment from wetlands, and the sediment filter matrix including solid depositions from the granite gravel were closely examined and documented. Selected samples were subjected to laboratory analyses with a focus on mineralogy (XRD) and elemental composition (ICP-OES). As there are only few geochemical and/or mineralogical studies on ferric solids or sediments from the southern Wackersdorf district, results of solids characterisations were compared to findings from the northern Rauberweiher district (e.g. Peine 1998; Regensburg et al. 2004) or the nearby Czech Sokolov basin (e.g. Murad & Rojik 2003, 2005).

4 Results and evaluation

The five studies described below refer to the individual manuscripts provided in the appendix.

4.1 Performance of the Westfield pilot plant (studies 1 and 3)

Studies 1 and 3 focused on the performance of the pilot plant that was operated and monitored at the Westfield study site between 2017 und 2020. Evaluation of the extensive datasets demonstrated the excellent performance of the Westfield pilot plant for year-round contaminant removal with a special focus on passive iron removal.

The **first study** (Opitz et al. 2020b) demonstrated application of a simple technique to monitor the transport of particulate iron as the primary contaminant in the seepage water throughout the multistage Westfield pilot plant. The data collected at all ten monitoring points by online turbidity sensors on the one hand and manually collected samples on the other hand provided a robust, near-monocausal basis for the development of an empirical, linear proxy-relationship between in-situ measured turbidity [$Turb.$] and the concentration of hydrous ferric oxides [$Fe(OH)_3$] in the seepage water ($R^2 = 0.86$) with:

$$(11) [Fe(OH)_3] = 0.092[Turb.] + 0.031$$

Stochastic and seasonal fluctuations as well as episodic disturbances such as rain events or bioturbation were averaged out in the comprehensive datasets. This surrogate relationship allowed approximation of particulate iron at a considerably higher resolution than may be achieved by manual sample collection, thereby reducing monitoring costs and efforts. The high-resolution dataset was used to validate sample analyses (i.e. for quality control) and to improve iron mass balance estimates for the passive system in due consideration of short-term variations in flow rates and/or inflow iron concentration.

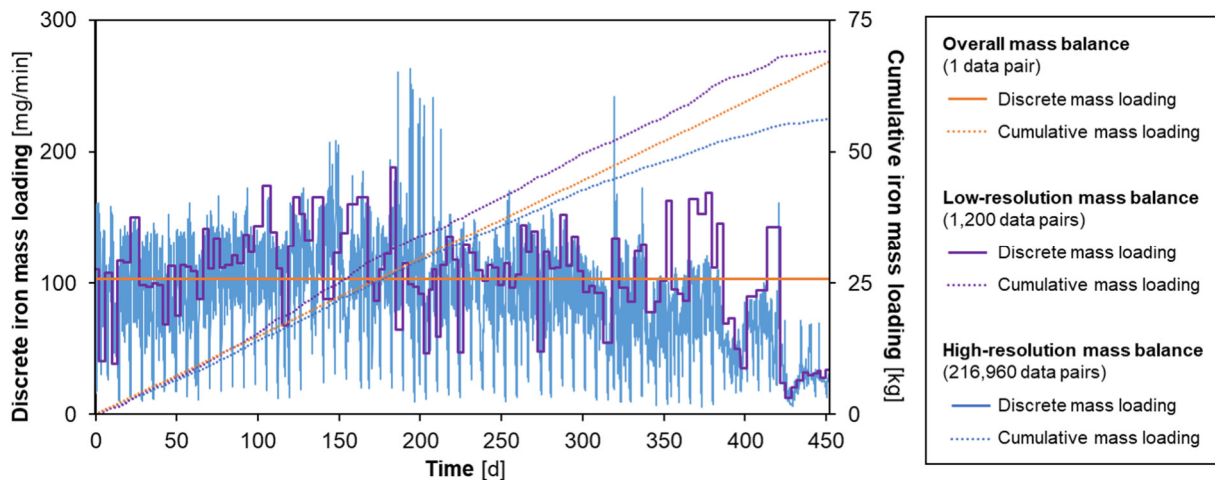


Fig. 5 Discrete hydraulic loading and cumulative mass removal for iron mass balances with different time resolutions for the 452-day period; modified from Opitz et al. (2020b)

By way of example, the iron mass inflow to, and outflow from, the pilot plant over the entire study period was estimated at 67.2 and 1.7 kg, respectively, based on flow recordings and iron analyses both averaged over the 452-day period. Similar results were obtained by way of a low-resolution mass balance based on semi-weekly iron analyses and accordingly averaged flow rates with 69.3 and 1.7 kg, respectively. In contrast, high-resolution estimates based on 30-min interval turbidity-iron-conversions and respectively averaged flow recordings were 56.3 and 1.2 kg, respectively. Lower mass flows obtained via the high-resolution mass balance are attributable to decreased hydraulic loading of the system during weekends when pump operation ceased, whereby the pilot plant was only fed from the (dwindling) reservoir as can be seen in Fig. 5. Such variations in mass flow are easily overlooked by routine monitoring efforts based on manual sample collection and analysis at any practical interval.

Results and evaluation

The **third study** (Opitz et al. 2022a) evaluated the results of the trifurcated Westfield pilot plant over the entire 452-day study period, not only for iron but also for secondary contaminants such as arsenic, manganese, ammonia, nitrate, and TSS/turbidity. In-depth evaluation of the pilot plant data revealed important benefits and limitations of the consecutive treatment stages for transport, transformation, and removal of particularly redox-sensitive compounds that are omnipresent in mining environments. Most importantly, iron, arsenic, and TSS were predominantly removed in the preceding settling ponds (63 – 77%), with only little removal in wetlands (20 – 31%) and sediment filters (4 – 6%) as indicated by concave arrows in the upper panels of Fig. 6. However, the discrete treatment efficiency of the consecutive treatment stages for the above contaminants was broadly similar or even increased in wetlands and/or sediment filters even though the latter stages received substantially lower loadings. By way of example, discrete median removal in settling ponds, wetlands, and sediment filters was 69, 73, and 72% for iron, 73, 69, and 44% for arsenic, and 62, 82, and 78% for TSS/turbidity, respectively.

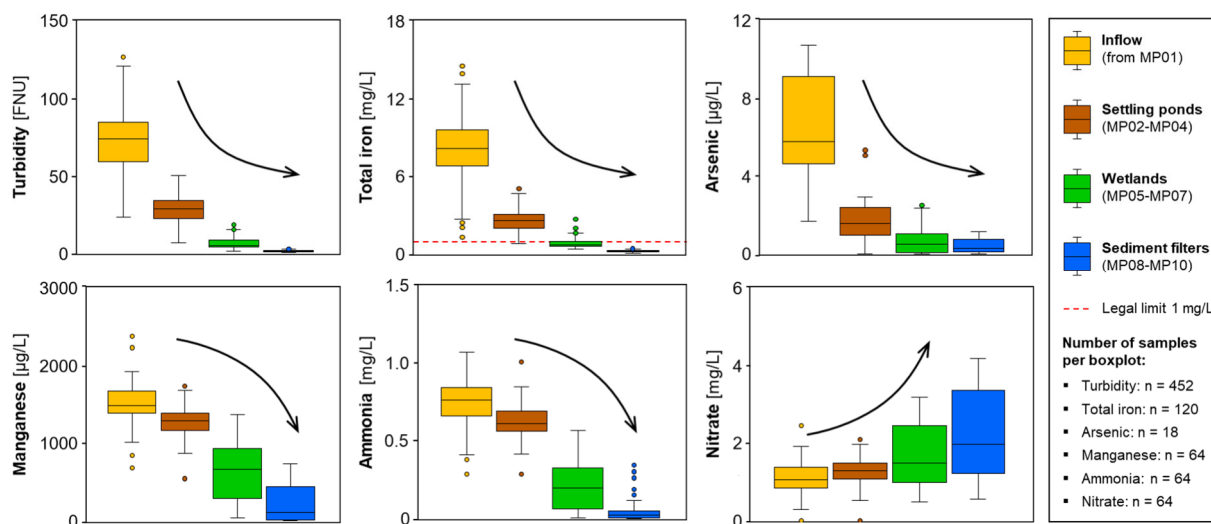


Fig. 6 Contaminant development in the Westfield pilot plant as median concentrations for the 452-day period with arrows indicating trends; modified from Opitz et al. (2022a)

In contrast, the removal of manganese and ammonia was rather low in the preceding settling ponds with 13 and 20%, respectively, but increased to 56 and 74% in wetlands and even up to 92 and 97% in sediment filters as indicated by convex arrows in the lower panels of Fig. 6. Discrete median removal in settling ponds, wetlands, and sediment filters was 13, 49, and 83% for manganese and 20, 68, and 90% for ammonia, respectively. There is good reason to assume that oxidation of bivalent manganese was catalysed by adapted microbial communities closely linked with reactive surfaces in wetlands and especially in the sediment filter matrix (Luan et al. 2012; Neculita & Rosa 2019). This was substantiated by visual observation and chemical analyses of extensive black coatings on plant litter in wetlands, the pipework succeeding wetland outflows, and especially the granite gravel in the sediment filters.

Beyond that, the pilot study highlighted the importance of the densely vegetated, near-natural environment of the surface-flow constructed wetlands for nitrification. It stands to reason that ammonia removal caused a concomitant increase in nitrate levels with a median of 85% over the study period. In this context, it is interesting to note that data showed year-round ammonia removal, whereas nitrate generation was apparently considerably higher in autumn and winter (i.e. September to April). Hence, there is good reason to assume that nitrification was stable year-round, but that a significant nitrogen fraction was fixed in plants, litter, and sediment as a result of primary production (algae, macrophytes) and/or lost to the atmosphere by way of denitrification in the sediment, especially during spring and summer. Notably, the Westfield pilot plant showed an overall net-negative nitrogen budget of approx. 178 mol or approx. 36% of inflow ammonia/nitrate-nitrogen over the study period. Median ammonia-nitrogen removal

rates in the surface-flow wetlands were estimated at up to 8.8 mmol/m²/d, which corresponds well with literature reports on pilot- and full-scale wetlands in the order of 1 to 20 mmol/m²/d by Dzakpasu et al. (2014) and Mitsch & Gosselink (2000).

Comparison of aggregated median concentration developments for relevant parameters from the passive pilot plant to the full-scale conventional treatment plant operated at the Westfield site are illustrated in Fig. 7. Monitoring data from the conventional treatment plant operated at the Westfield site was provided by courtesy of the plant operator, comprising monthly chemical analyses of inflow and outflow water as of the last major overhaul of the treatment plant in 2010. A comparability analysis for the datasets from the conventional plant (2011 to 2021) and the Westfield pilot plant (2018 to 2019) is provided in Opitz et al. (2022a), showing that the hydrochemistry of the seepage water from the Westfield drainage pond remained stable over the years, which is why the two aggregated datasets are considered broadly comparable.

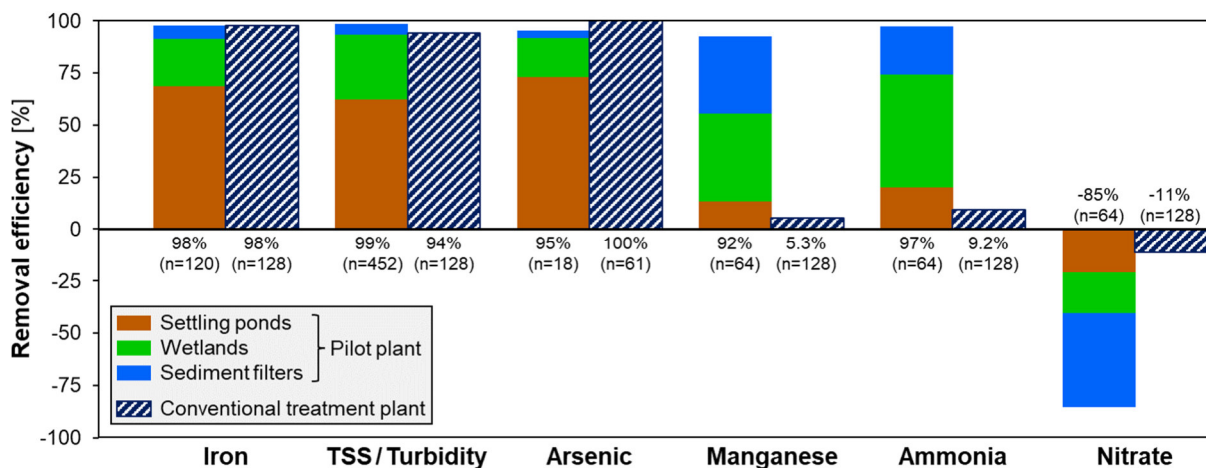


Fig. 7 Removal efficiency of relevant contaminants for the conventional plant (2011-2021) and the Westfield pilot plant (2018-2019) based on median inflow-outflow levels with overall removal and sample number indicated below columns; from Opitz et al. (2022a)

Direct juxtaposition as described in Opitz et al. (2022a) shows that the two treatment plants are comparable in terms of iron removal, reliably meeting the strict regulatory requirements. The same applies to secondary contaminants such as arsenic and TSS/turbidity. Beyond that, it is worth noting that both manganese and ammonia mostly pass the conventional treatment plant as clearly discernible in Fig. 7 with overall median removal in the order of 5 to 10%, rarely exceeding 20%. This goes to show that the biogeochemical processes stimulated in the passive system, especially in wetlands and sediment filters, provide a distinct technological benefit regarding overall water quality amelioration.

In summary, the results from long-term operation of the Westfield pilot plant provide a much better understanding of spatiotemporal trends, cycles, and developments on the migration and removal of particulate iron (and other contaminants) throughout the three different, consecutive passive treatment stages. Iron, TSS, and arsenic removal followed the designated removal pattern according to Pareto’s principle, with broadly similar discrete removal efficiencies in the three consecutive treatment stages of 60 to 80%. Thus, the settling ponds effectively protect the following, more delicate wetlands and sediment filters from clogging, whereas the latter ensure reliable polishing despite lower loading. Wetlands and sediment filters were found to reliably polish particulate and redox-sensitive compounds such as ammonia, arsenic, iron, manganese, and TSS even at residual levels whilst concomitantly mitigating spatiotemporal fluctuations that inevitably arise in open systems. Altogether, the studies noted above highlight the importance of the multistage passive setup of the pilot plant in ensuring full operational reliability even for particularly strict environmental regulations or discharge limits such as set at the Westfield legacy site.

4.2 Sedimentation of hydrous ferric oxides (study 4)

The overall objective of the **fourth study** (Opitz et al. 2022b) was to develop a kinetics-based model approach for sedimentation of particulate hydrous ferric oxides in circumneutral and ferruginous mine water. By subjecting both real ochre from the Westfield study site and several synthetic ferric (hydr)oxides to large-scale sedimentation column experiments under different hydrochemical and mineralogical conditions, the laboratory study provided novel insights into the interrelation of particle interaction (aggregation) and gravitational settling (sedimentation) of waterborne hydrous ferric solids. The datasets with initial iron levels ranging from < 5 mg/L up to approx. 250 mg/L showed a fast, aggregation-driven step (r2) at high iron levels followed by a slower, sedimentation-driven step (r1) at lower iron levels as illustrated in Fig. 8. The two regimes could be reasonably well described by a mixed first- and second-order model:

$$(12) \quad -\frac{d[Fe]}{dt} = k_{r2}[Fe] + k_{r1}[Fe]^2$$

The large-scale column experiments allowed for parameterisation of the respective coefficients with $k_{r1} = 9.4 \times 10^{-3} \text{ m}^3/\text{g}/\text{h}$ and $k_{r2} = 5.4 \times 10^{-3} \text{ h}^{-1}$. The mixed model and coefficients allowed good reproduction of the experiments. Accordingly, statistical analysis of the overall regression yielded a process standard deviation of 1.1 mg/L and a confidence interval of $\pm 1.7\%$.

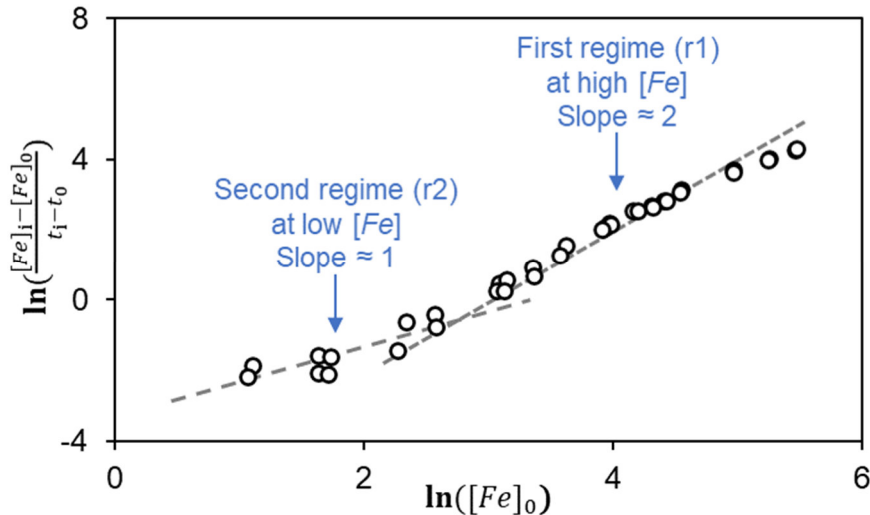


Fig. 8 Double-logarithmic plot of initial sedimentation rates $\Delta[Fe]/\Delta t$ vs. initial iron concentration $[Fe]_0$ for all 36 datasets of the basic series at different initial iron levels with dashed lines indicating slopes; modified from Opitz et al. (2022b)

Notably, it was found that sedimentation of particulate hydrous ferric oxides at low to moderate iron levels (i.e. < 10 mg/L) could be approximated by a simplified first-order model following equation (9). The first-order coefficient k_{sed} was found with $2.4(\pm 0.4) \times 10^{-2} \text{ h}^{-1}$, which is in line with incipient estimates from the literature compiled in chapter 1.3. It is, however, important to note that the simplified first-order relationship tends to progressively underestimate sedimentation towards higher iron levels where aggregation plays a major role, and to overestimate sedimentation toward residual iron levels < 1 mg/L where the finely dispersed ferric colloids remain suspended. Nevertheless, the first-order coefficient k_{sed} noted above corresponds to a “half-life” or time requirement in the order of 28 h to remove 50% of initial ferric solids, which is in agreement with the retention time recommended for the design or sizing settling ponds in passive mine water treatment systems in the order of 12 to 48 h (Opitz et al. 2022b).

Variation of potentially critical hydrochemical boundary conditions such as pH or salinity as well as the mineralogy of the ferric solids showed only minor effects on kinetic parameters, indicating that sedimentation of waterborne hydrous ferric oxides in mine waters are broadly transferrable among different mine sites. This corresponds well with previous studies on the

behaviour of hydrous ferric oxides naturally precipitated in circumneutral or even acidic mine waters, which are neigh-on universally dominated by sulfate ions and typically facilitate rapid oxidation, precipitation, and aggregation of ferric solids upon oxygenation and neutralisation with emergence from mines or pits (e.g. Barnes et al. 2009; Dempsey et al. 2001).

In summary, the results of the laboratory study provide a consistent, quantitative approach and parametrisation for the two-step aggregation/settling-based removal of hydrous ferric oxides in circumneutral mine water. In an application-oriented context, the results also confirm the hypothesis of Sapsford & Watson (2011) that sedimentation may be approximated by a simple first-order model – at least for moderate iron levels. The conservative value for k_{sed} suggested above ensures that iron removal is underestimated rather than overestimated in the relevant concentration range of approx. 1 to 10 mg/L as is common practice in engineering sciences. These findings could considerably improve our (quantitative) understanding of iron transport and removal in mining environments. Moreover, the relationships noted above may readily be integrated into transport models or used for the calculation of temporal iron removal profiles in passive mine water treatment systems to determine the optimal application range of settling ponds for pre-treatment. In the overall context of the research project, the kinetic parameters provide the basis for evaluation of iron removal kinetics in the Westfield pilot plant.

4.3 Development of a novel sizing approach (studies 2 and 5)

Finally, studies 2 and 5 focused on the development of novel sizing approaches for both bare settling ponds and densely vegetated, surface-flow wetlands for pre-treatment and polishing of circumneutral, ferruginous mine water, respectively.

The **second study** (Opitz et al. 2021) was a comprehensive literature review to gain insights into the intrinsic mechanisms that govern superior iron removal efficacy observed in densely vegetated wetlands relative to (unvegetated) settling ponds. The general literature review on surface-flow wetlands for passive treatment of either waste- or mine water provided a basic understanding of the physicochemical, biological, and hydraulic effects of wetland vegetation with a focus on the removal of particulate matter and other contaminants that are relevant in both waste- and mine water settings. The most critical effects of the emergent macrophyte vegetation in surface-flow wetlands for iron removal as identified in Opitz et al. (2021) were:

- Enhanced biogeochemical ferrous iron oxidation and precipitation due to catalytic reactions and bacterial activity on immersed macrophyte surfaces;
- Physical filtration of colloidal hydrous ferric oxides that are unlikely to gravitationally settle within a given residence time by the submerged parts of the dense wetland vegetation;
- Scavenging and heteroaggregation of dissolved and colloidal iron, respectively, by clastic sediments or plant-derived natural organic matter;
- Improved hydrodynamics and hydraulic efficiency of densely vegetated, surface-flow wetlands, considerably augmenting retention and exposure time.

Thus, it stands to reason that (particulate) iron removal in wetlands is a multicausal process where iron removal rates are expected to vary depending on ecological and constructional factors such as water depth, macrophyte species, plant density, and vegetation development. These findings indicate that the sizing of wetlands for passive treatment of ferruginous mine water must necessarily be based on a simplified engineering model approach rather than an overall kinetic approximation of the complex iron removal mechanisms in due consideration of various potentially critical influencing factors. In addition, the literature review helped to identify phytologic, hydrodynamic, seasonal, and meteorologic effects that may affect both treatment performance and data quality in open passive systems. In the overall context of the research project at hand, study 2 thus provided a qualitative basis for the quantitative assessment of field data from the pilot-scale wetlands at the Westfield pilot plant.

The overall objective of the **fifth study** (Opitz et al. 2023) was to develop and propose novel sizing approaches for integrated passive mine water treatment systems based on actual field results from the Westfield pilot plant. To that end, study 5 combined the fundamental insights into passive iron removal mechanisms in a free body of water as outlined in study 4 and in densely vegetated wetlands as outlined in study 2 with the field data collected from pilot-scale settling ponds and wetlands at the Westfield pilot plant. The results were then used to advance the designing and sizing of integrated passive mine water treatment systems in due consideration of the concentration-dependency governing passive iron removal.

Firstly, evaluation of datasets from the pilot-scale settling ponds of the Westfield pilot plant confirmed that sedimentation-driven removal of particulate hydrous ferric oxides in free surface settling ponds may indeed be approximated by the simplified first-order model approach at low to moderate iron levels as highlighted in study 4 (Opitz et al. 2022b). The respective first-order coefficient k_{sed} for the pilot-scale settling ponds was found in the order of $2.1(\pm 0.7) \times 10^{-2} \text{ h}^{-1}$, which corresponds well with both initial literature reports noted in chapter 1.3 and systematic sedimentation experiments outlined in chapter 4.2.

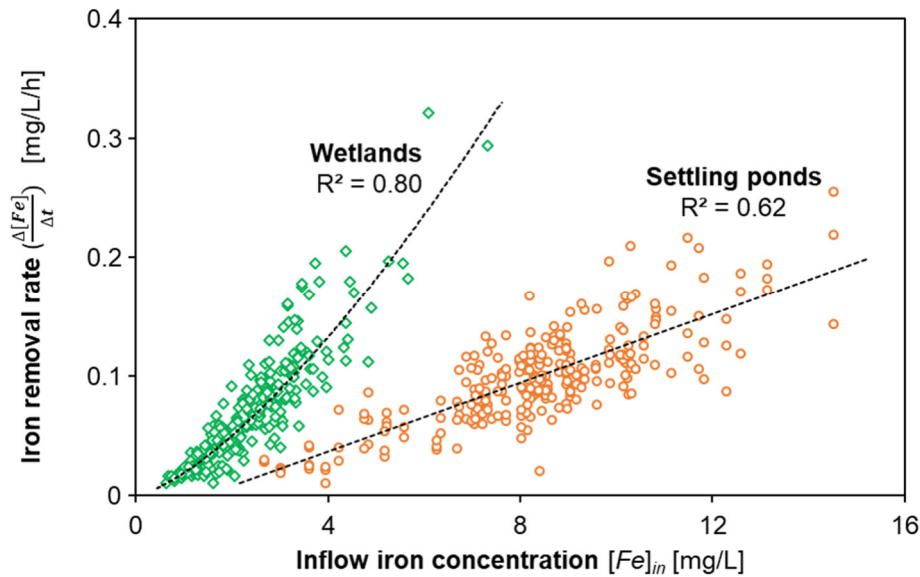


Fig. 9 Correlation of iron removal rates $\Delta[Fe]/\Delta t$ and inflow iron concentration $[Fe]_{in}$ in settling ponds and wetlands with overall regressions as dashed lines; modified from Opitz et al. (2023)

Secondly, iron removal in surface-flow wetlands was found to be more efficient relative to the unvegetated settling ponds as illustrated in Fig. 9, but also more complex due to the phytologic component as noted in study 2 (Opitz et al. 2021). As iron removal in the pilot-scale wetlands could not be adequately described by a simple model or kinetic relationship, the established area-adjusted iron removal approach initially proposed by Hedin et al. (1994) was advanced by parameterising the underlying concentration-dependency for polishing of pre-treated mine water. By converting the superlinear regression of iron removal rates in wetlands from Fig. 9 to areal iron removal as per equation (3), the concentration-dependency of the area-adjusted removal rate R_A was fitted as $R_A = m \times [Fe]_{in}^n$ with $m = 0.2$ and $n = 1.4$. Thus, the quantitative results of the pilot-scale wetlands provide a novel approach for customised sizing of integrated passive systems.

Altogether, the findings of the pilot study highlight that passive iron removal is predominantly controlled by two driving processes, namely transfer from dissolved ferrous ions to dispersed hydrous ferric oxides via oxidation on the one hand, and sedimentation of resultant hydrous ferric oxides via aggregation and settling (or filtration) on the other hand. This is in accordance with observations from several full-scale passive mine water treatment systems reported by Chikanda et al. (2021), Matthies et al. (2012), and Hedin (2008), showing that overall iron

Results and evaluation

removal along the flow path was associated with a progressing shift from ferrous to ferric and colloidal to particulate iron. Notably, the particulate fraction did not accumulate along the flow path but was concomitantly removed through aggregation from higher nanometre to lower micrometre fractions and, finally, sedimentation. Ferrous iron oxidation and hydrous ferric oxide sedimentation as the two potentially rate determining processes in a free water body may both be approximated by (pseudo) first-order rate equations as outlined above. Assuming stable pH and oxygen levels, total iron $[Fe(tot)]$ profiles in settling ponds may thus be estimated by coupling and integration of equations (5) and (9) with:

$$(13) \quad [Fe(tot)]_t = [Fe(II)]_0 \times e^{k'_{ox} \times t} + \frac{k'_{ox}[Fe(II)]_0(e^{-k'_{ox}t} - e^{-k_{sed}t})}{k_{sed} - k'_{ox}} + [Fe(OH)_3]_0 \times e^{-k_{sed} \times t}$$

The rate-determining of the two processes can now be identified by direct comparison of the first-order coefficients as outlined by Espenson (1981). The sedimentation coefficient k_{sed} was found to be broadly independent of mine water chemistry in study 4 (Opitz et al., 2022b), whereas the pseudo first-order oxidation coefficient k'_{ox} is in turn a first- and second-order function of oxygen concentration and proton activity, respectively (Stumm & Morgan 1996). According to equation (4), k'_{ox} decreases hundredfold with a decrease in pH by one unit. Hence, ferrous iron oxidation is rate-determining at acidic pH < 6, whilst hydrous ferric oxide sedimentation is rate-determining at neutral to alkaline pH > 7. The ratio of the two coefficients k_{sed} and k'_{ox} converges between pH 6 and 7 as illustrated in Fig. 10, which is why the two processes proceed at similar rates, with small variations in the hydrochemistry (pH, oxygen level, temperature) inordinately affecting ferrous iron oxidation.

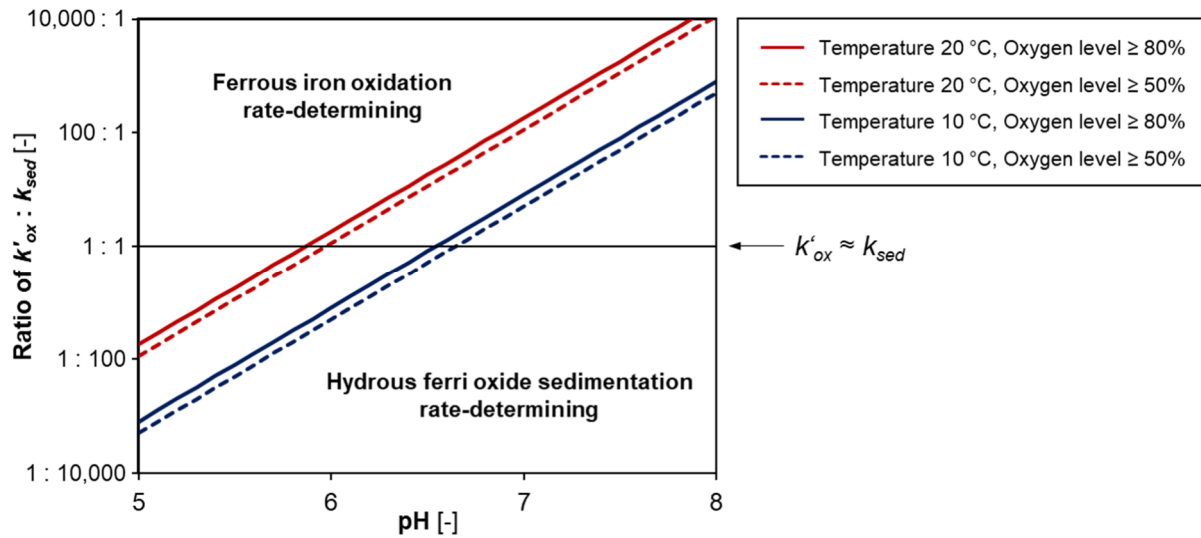


Fig. 10 Ratio of (pseudo) first-order ferrous iron oxidation and hydrous ferric oxide sedimentation coefficients k'_{ox} and k_{sed} as a semi-logarithmic function of pH at different temperature and oxygen saturation levels; modified from Opitz et al. (2023)

In summary, the results of the research project show that the established areal, concentration-independent sizing approach is unlikely to adequately reflect passive iron removal kinetics. The relationships outlined above explain the extreme range in areal removal rates observed in passive mine water treatment systems worldwide as compiled in the SI to study 5. We therefore conclude that the established areal sizing approach is likely a suitable rule of thumb for “typical” (coal) mine discharges, yet with increasing tendency to overestimate and underestimate iron removal dynamics towards high and residual iron levels, respectively. In such cases, overall iron removal rates may readily deviate up to orders of magnitude from the established linear approach. The results of this study now provide a robust basis for kinetics-based deliberations on overall iron removal in passive treatment systems, thus ultimately increasing confidence in sustainable mine water treatment technologies as further detailed in the concluding chapter 5.

5 Summary, implications, and conclusions

5.1 Iron removal

Several interrelated physical and biogeochemical processes contribute to passive transport, transformation, and removal of iron in ferruginous, circumneutral mine water as schematically illustrated in Fig. 11. Transition from ferrous to ferric iron by way of oxidation was investigated intensively in the past decades and respective kinetics are well-described in the literature as briefly outlined in chapter 1.3. Field and laboratory ferrous iron oxidation rates are broadly in accordance – and also applicable to circumneutral, oxic mine waters, although more research is needed on heterogeneous oxidation in ferruginous mine waters. Ferric iron transition from aqueous to solid phase in circumneutral environments by way of hydrolysis and precipitation is extremely fast (i.e. almost instantaneous) relative to oxidation and sedimentation and can thus be disregarded in the context of overall iron removal.

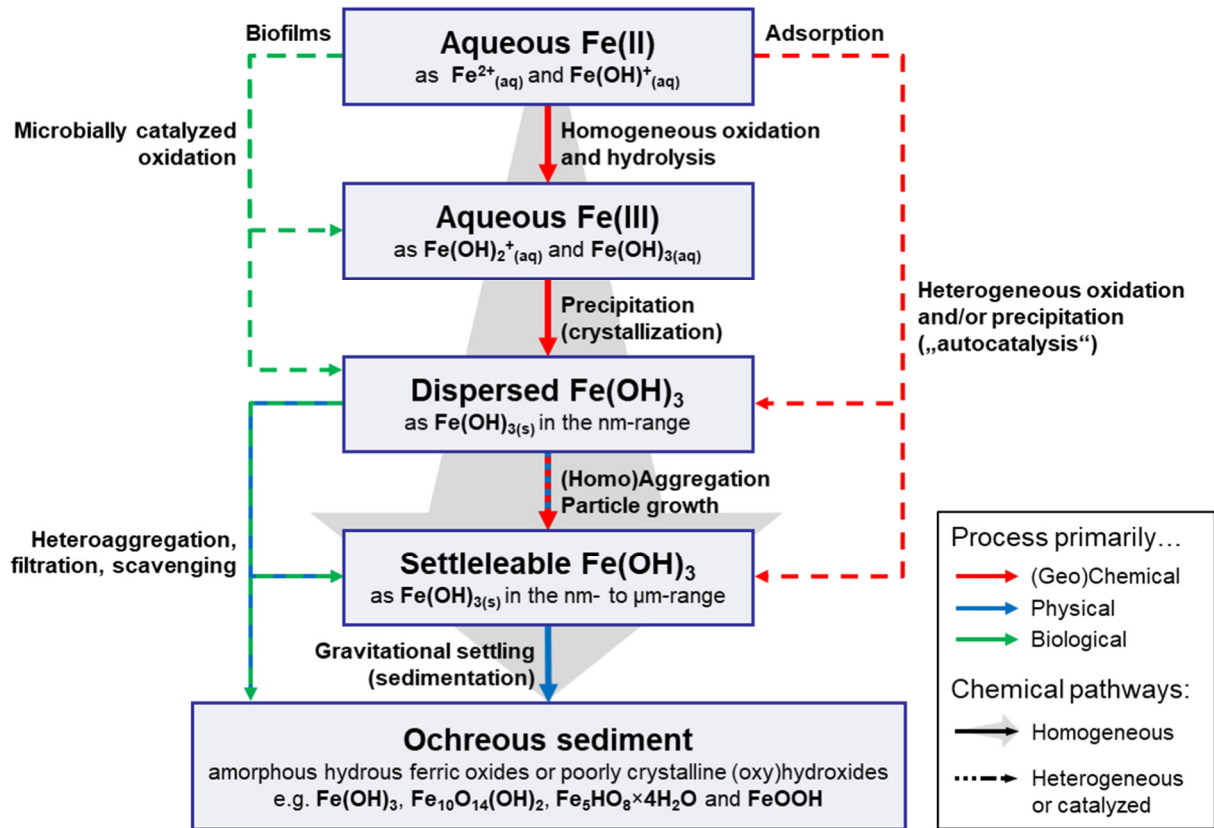


Fig. 11 Schematic illustration of mechanisms governing iron removal from neutral mine water

Sedimentation of hydrous ferric oxides is promoted by rapid homoaggregation at higher iron levels and slower gravitational settling at lower iron levels. In this project, it was shown that the overall process can be reasonably well described by a mixed first-/second-order relationship. What is more, sedimentation of hydrous ferric oxides at low to moderate iron levels may be approximated by a simplified first-order model. In surface-flow wetlands, residual colloidal iron is removed not only by sedimentation, but also by filtration in the dense vegetation as well as heteroaggregation and scavenging in combination with natural organic matter (NOM) or clastic compounds. The underlying mechanism(s) as well as their relevance and kinetics are poorly studied thus far and further research will be necessary to fathom potential model approaches for colloidal iron filtration in vegetated compared to unvegetated ponds. The processes are, however, inevitably related to the ecological and phytophysiological wetland layout. Therefore, an empirical model approach was derived based on the results of pilot-scale wetlands densely planted with common reed (*Phragmites australis*) at a water depth of approx. 0.4 to 0.5 m.

5.2 Implications

Proceeding from the simplified two-step iron removal model outlined above, only three iron “fractions” are ultimately relevant in passive mine water treatment systems, namely:

1. dissolved ferrous iron $[Fe(II)]$ as reactant,
2. dispersed hydrous ferric oxides $[Fe(OH)_3]$ as both reactant and intermediate, and
3. settled ochre $[Ochre]$ as accumulating sediment as overall product.

Other iron transformation species are insignificant in circumneutral environments as outlined in chapter 1.3. Thus, the transport, transformation, and removal of these three iron fractions in passive systems may be described for (relatively) stable inflow rates and iron concentrations by a differential equation system. In good approximation of a plug flow reactor, it is assumed that volumetric inflow equals outflow, and that the time any water molecule, solute, or colloid spends in the pond or wetland approximately equals the nominal HRT². The resulting model approach is illustrated in Fig. 12 with two consecutive process stages, no reverse reactions, and filtration only applicable to vegetated wetlands:

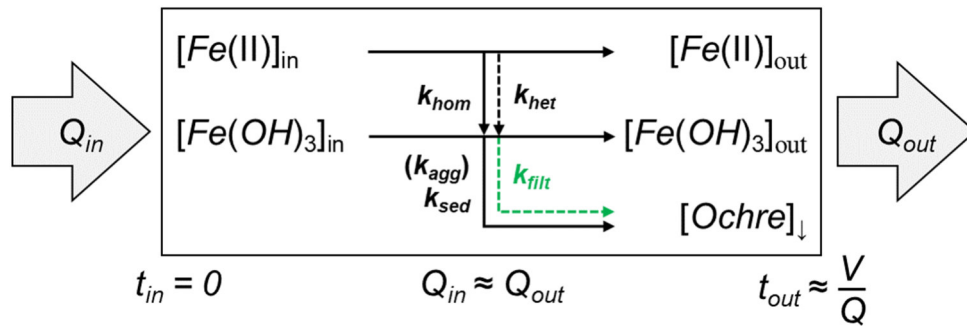


Fig. 12 Plug flow model approach for iron transformation and removal in passive systems

Only dissolved ferrous iron and dispersed hydrous ferric oxides can be present in the inflow mine water. In the further course, the total amount of iron in the system is described by the sum of all three fractions at any point in time (t) according to the overall mass balance:

$$(14) \quad [Fe(tot)] = [Fe(II)]_{in} + [Fe(OH)_3]_{in} = [Fe(II)]_t + [Fe(OH)_3]_t + [Ochre]_t$$

Rearrangement of equation (14) allows calculation of all relevant iron fractions in inflow (t_{in}) and outflow (t_{out}) as per the following equations:

$$(15) \quad [Fe(II)]_{out} = [Fe(II)]_{in} + [Fe(OH)_3]_{in} - [Fe(OH)_3]_{out} - [Ochre]_{\downarrow}$$

$$(16) \quad [Fe(OH)_3]_{out} = [Fe(OH)_3]_{in} + [Fe(II)]_{in} - [Fe(II)]_{out} - [Ochre]_{\downarrow}$$

$$(17) \quad [Ochre]_{\downarrow} = [Fe(II)]_{in} + [Fe(OH)_3]_{in} - [Fe(II)]_{out} - [Fe(OH)_3]_{out}$$

In the following, the differences between the established area-adjusted model approach by Hedin et al. (1994) describing zero-order iron removal and the kinetics-based model approach of a two-step iron removal process as per equation (13) are graphically illustrated and detailed. To allow juxtaposition, the established linear iron removal model is converted to a volumetric rather than areal removal approach (with $R_v = 10$ to 20 g/m³/d) assuming a standardised water depth of 1 m, which may be readily integrated to:

$$(18) \quad [Ochre]_{\downarrow} = [Fe(tot)]_{in} - t \times R_v$$

A hypothetical discharge limit of 3 mg/L relating to the visual ochre threshold often mandated for (abandoned) mine sites is displayed in the following figures as red line for orientation.

² Deviation from plug flow is, to a certain extent, accounted for by conservative engineering models. From an academic perspective, hydraulic and hydrodynamic effects on temporal contaminant removal may be numerically considered (Guo & Cui 2021; Sheridan et al. 2014; von Sperling 2002).

Firstly, Fig. 13 gives a basic overview of the different *laboratory* derived first-order sedimentation coefficients k_{sed} from Opitz et al. (2022b), Sapsford (2013), and Sutton et al. (2015). The four intrinsically different column trials initially reported by Sapsford (2013) cover a wide range that is, obviously, inadequate for sizing purposes. As opposed to this, column results from Opitz et al. (2022b) and Sutton et al. (2015) are in accordance, and broadly corresponding to the linear areal approach – at least until moderate iron levels are reached, whereupon the exponential decay curve becomes conspicuous. Whilst small variations in k_{sed} are to be expected due to hydrochemical and/or mineralogical differences between mine sites, results of the systematic experimental series from Tab. 5 reported by Opitz et al. (2022b) indicate that sedimentation rates are mainly a function of particle interaction and size, and thus primarily governed by iron concentration. Therefore, the results obtained for k_{sed} in both laboratory and field experiments are expected to be broadly transferrable to different mine sites.

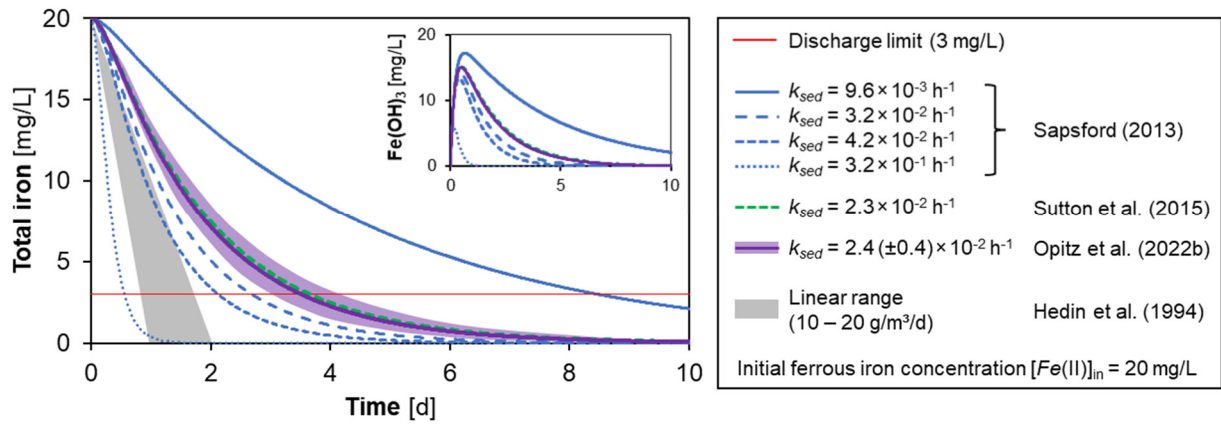


Fig. 13 Iron removal calculated via the established areal model and via the kinetics-based model with $k'_{ox} \approx 2.1 \times 10^{-1} \text{ h}^{-1}$ in combination with different laboratory-derived values for k_{sed} as coloured lines, the detail showing corresponding $[\text{Fe(OH)}_3]$

The effect of pH and oxygen concentration as critical factors for ferrous iron oxidation are illustrated in Fig. 14a and b, respectively. The graphs confirm the rate-limiting effect of acidic pH < 7 on overall iron removal as outlined in chapter 5.1. This is all the more important as the established linear sizing approach presupposes equal iron removal over time – irrespective of known, critical influencing factors such as pH or oxygen level, whilst the kinetics-based model considers overall iron removal dynamics more realistically. Nonetheless, it is important to note that the kinetics-based model disregards (auto)catalytic effects that may play a crucial role in ferruginous mine waters as outlined in chapter 5.1 and further discussed below.

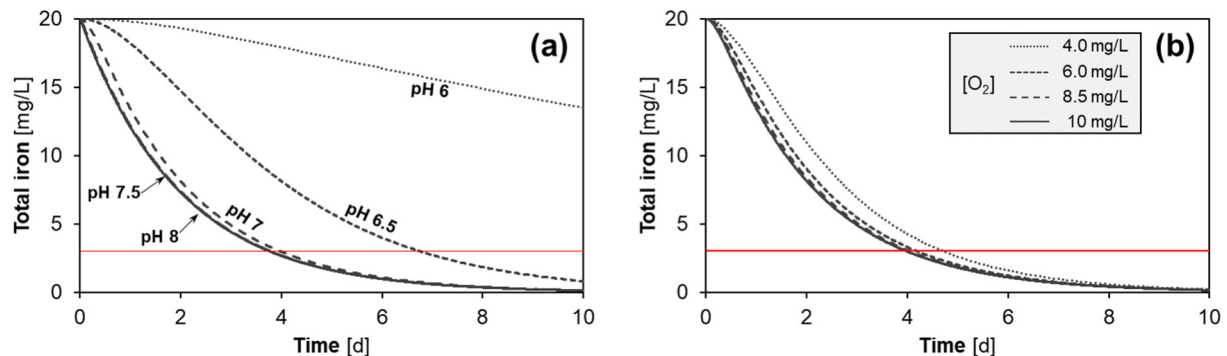


Fig. 14 Iron removal calculated via the kinetics-based model with the field-derived $k_{sed} = 2.1 \times 10^{-2} \text{ h}^{-1}$ (Opitz et al. 2023) at 10 °C for (a) different pH levels at $P_{O_2} \approx 0.21 \text{ atm}$, and (b) different oxygen levels at $\text{pH} \approx 7$

The difference between linear and kinetics-based iron removal is highlighted in Fig. 15. The hypothetical juxtaposition shows fragility of linear sizing for unfavourable conditions such as acidic pH and low iron loading as pointed out by Hedin et al. (1994) themselves. Specifically,

the hypothetical scenario indicates that the linear approach tends to undersizing for low initial iron levels and acidic pH, but eventually possibly also oversizing for high iron loading at neutral pH. Again, it is important to note that the kinetics-based model approach is considerably simplified regarding (auto)catalytic effects that accelerate both ferrous iron oxidation and hydrous ferric oxide sedimentation as outlined in chapter 5.1, wherefore the curves should be expected to correspond better with the areal range when properly adapted to higher iron levels.

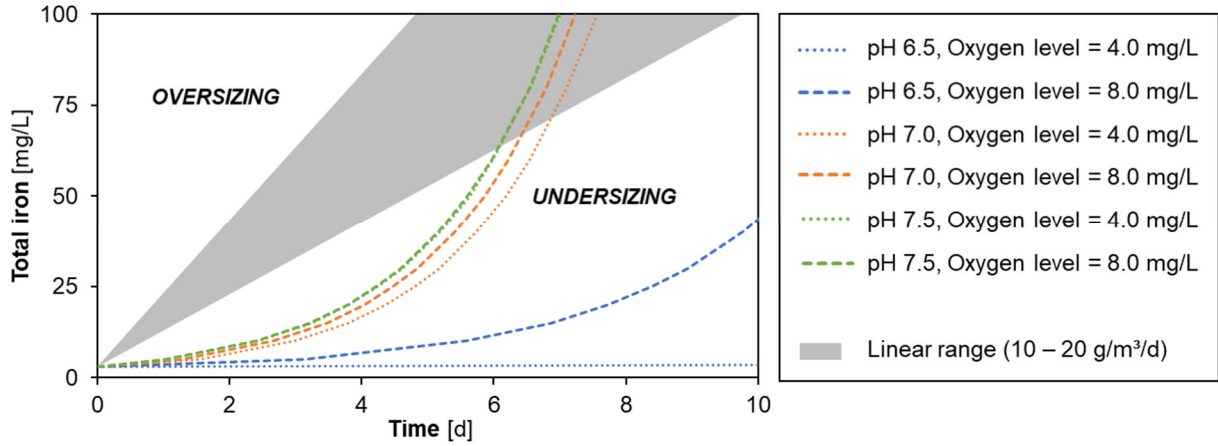


Fig. 15 Hypothetical HRT to reach a discharge limit of 3 mg/L depending on initial iron level for the linear areal model (grey shading) and the kinetics-based model (graphs) at 10 °C, different pH levels, and low to moderate oxygen level

Coupling of contaminant removal and (residence) time is increasingly used to model iron transport in mining-impacted waters (e.g. Baken et al. 2015; Cravotta 2021; Garcia-Rios et al. 2021; Yazbek et al. 2021). However, in-depth evaluation of passive iron removal in full-scale treatment systems is usually limited because only inflow and outflow data is available. Having said that, the Marchand passive system in Pennsylvania described by Hedin (2008, 2013) is one of the largest and best-characterised mine water treatment systems worldwide, consisting of six consecutive settling ponds (A – F) with a total surface area of approx. 2.5 ha followed by a 2.9 ha wetland. According to long-term monitoring data from 2007 to 2012, the circumneutral and ferruginous discharge from the abandoned Marchand coal mine is estimated at an average 426 m³/h with an inflow iron level of approx. 72 mg/L that is successfully lowered below the discharge limit of 3 mg/L (Hedin 2013). The intermediate sampling points of the six settling ponds provide a rare opportunity to model the underlying iron removal kinetics by relative least-square fitting of iron concentration development along the flow path as shown in Fig. 16.

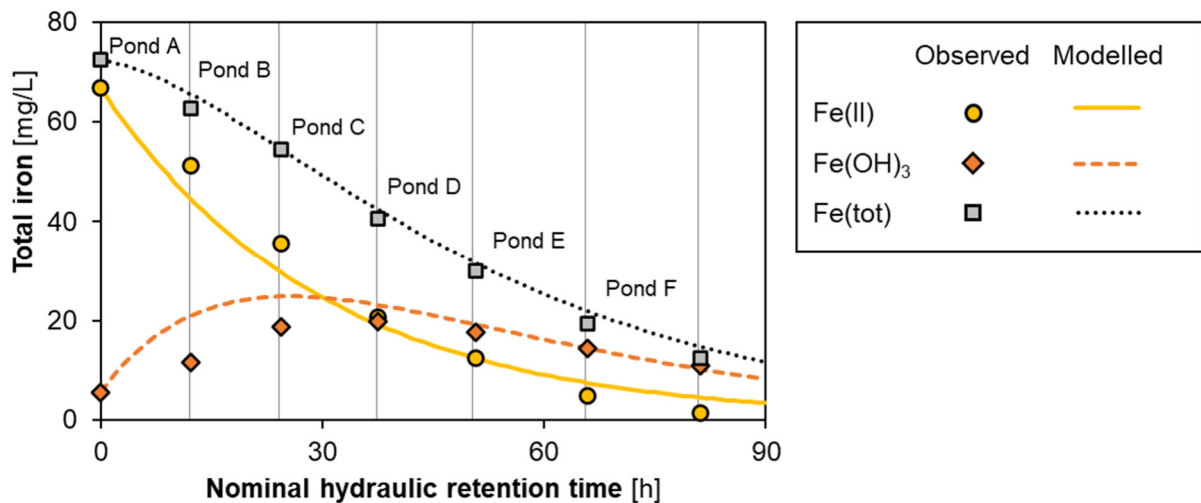


Fig. 16 Development of iron concentration throughout the Marchand settling ponds A to F as a function of nominal HRT with symbols as iron concentrations reported by Hedin (2013) and modelled lines (dotted lines); modified from Opitz et al. (2023).

Summary, implications, and conclusions

Based on the nominal HRT of the settling ponds and assuming approx. 80% oxygen saturation as well as a moderate (median) temperature of approx. 10 °C, the oxidation coefficient k'_{ox} was fitted at $3.3 \times 10^{-2} \text{ h}^{-1}$, which corresponds to a pH of approx. 6.7. This assorts well with the water pH (range 6.3 to 7.1) and temperature (annual average 13 to 14 °C) reported by Hedin (2008). The sedimentation coefficient k_{sed} was fitted at $3.8 \times 10^{-2} \text{ h}^{-1}$, exceeding estimates from study 4 or 5, and thus substantiating the above-noted assumption that well-known heterogeneous and/or (auto)catalytic effects on both ferrous iron oxidation and hydrous ferric oxide settling discussed in chapters 1.3 and 5.1 are broadly disregarded in equation (13). Notwithstanding this, the kinetics-based model approach works reasonably well to reproduce the observed iron development through the Marchand system, particularly considering the fluctuations of critical parameters (flow rate, inflow iron level, HRT etc.) reported by Hedin (2008, 2013).

With regard to catalytic effects, the simplified kinetics-based model approach is expected to underestimate overall iron removal rates, especially at higher iron concentrations. This is to a certain extent imperative and intentional as noted by Opitz et al. (2023), not only to simplify respective sizing approaches but also because engineering models are intrinsically expected to underestimate rather than overestimate system performance to minimise overall failure risks (e.g. Doorn & Hansson 2011; Elishakoff & Chamis 2001). More specifically, the engineering model approaches proposed in the following chapter 5.3 provide an explicitly conservative basis for sizing of settling ponds and wetlands in multistage mine water treatment systems, with special focus on (1.) operational reliability for strict discharge limits, and (2.) low to moderate iron levels that are ultimately relevant for environmentally acceptable discharge to receiving surface waters following established design schemes such as provided in Fig. 17.

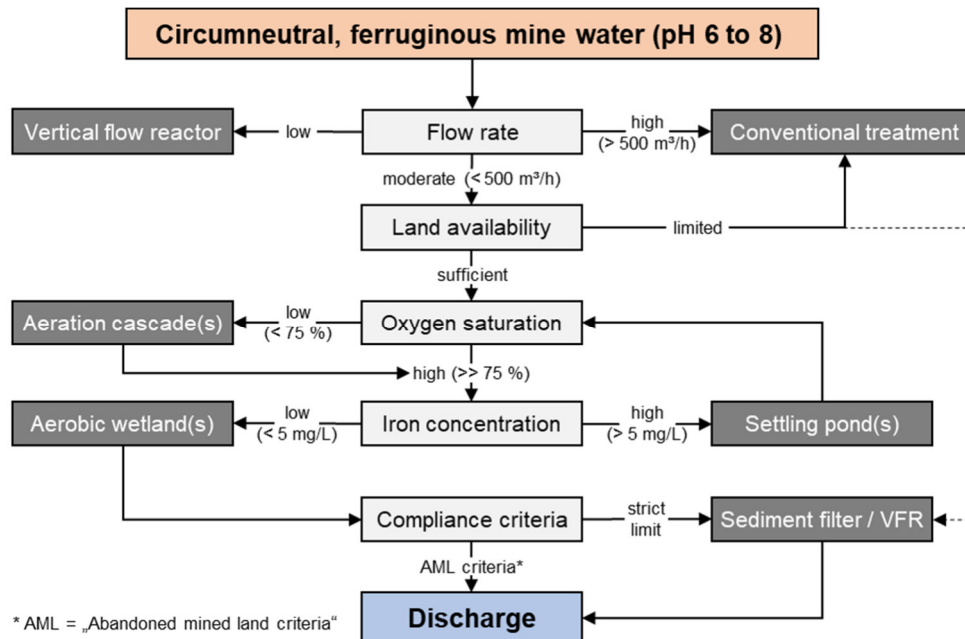


Fig. 17 Schematic flow chart for passive treatment of circumneutral, ferruginous mine water; loosely based on Hedin et al. (1994)

In conclusion, kinetics-based estimation of temporal iron removal may be readily utilised for (1.) initial assessments of site-specific passive treatment options, and (2.) customised sizing of passive systems. Although kinetics-based sizing may neither be infallible nor resolve the intrinsic trade-off between operational reliability on the one hand, and economic construction and land use on the other hand, it may very well provide a well-founded basis of assessment to, by way of example, balance operational reliability, land consumption, and building costs with respect to site-specific issues such as fluctuating flow rates or iron levels as well as land area limitations. Thus, more customised sizing of passive systems may ultimately lead to increasing confidence in sustainable passive mine water treatment technologies.

5.3 Conclusions and outlook

The results of the research project at hand provide new insights into the (natural) transport and removal of iron in mining environments, particularly in integrated passive treatment systems. Our findings help to understand the kinetics governing iron removal in bare settling ponds and densely vegetated, surface flow wetlands – which were poorly understood thus far despite the existence of numerous full-scale passive mine water treatment systems worldwide. Briefly abstracted, the removal of iron from mine water is not a complex mechanism, but rather a concatenation of several simple processes in complex interrelationships.

As a final note on the iron removal processes outlined in chapter 5.1, it is worth noting that the size of both settling ponds and wetlands is linearly correlated with the flow rate, while iron removal per square metre increases exponentially with increasing iron concentration. As a consequence, it stands to reason that mine water treatment facilities should be implemented as close as possible to the mine discharge or pollutant source to optimally benefit from catalytic processes such as heterogeneous ferrous iron oxidation and homoaggregation of ferric solids. Whilst dilution of mine water with surface water reduces the iron concentration, the mixing adversely affects passive iron removal dynamics and thus results in extensive iron transport and deposition along the flow path, smothering and degrading freshwater environments. In conclusion, dilution is not recommended as solution for pollution.

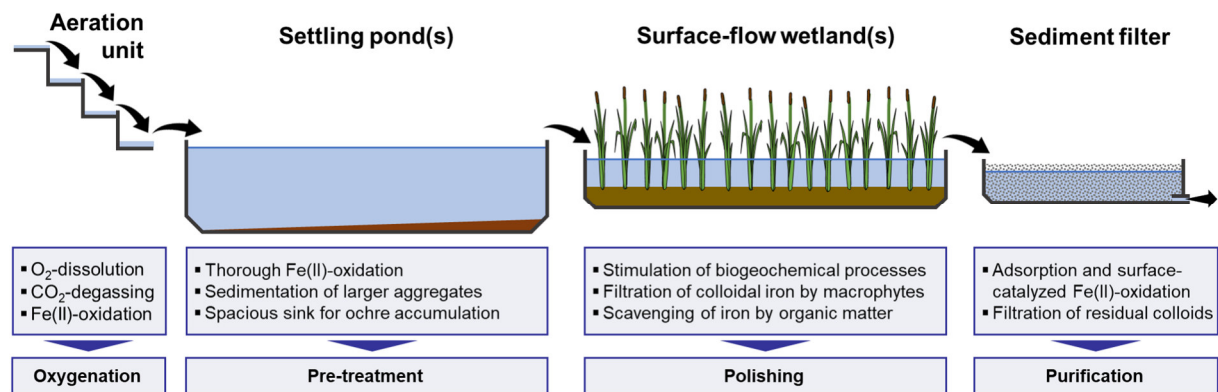


Fig. 18 Schematic setup of multistage passive mine water treatment systems

Combining settling ponds and aerobic wetlands for pre-treatment and polishing, respectively, is generally tested and applied in mine water management (e.g. PIRAMID Consortium 1999; Sapsford & Watson 2011; Skousen et al. 1994). Additional integration of downstream sediment filters as tested in the Westfield pilot plant considerably increases overall treatment efficiency and operational reliability, not only for iron but also for other contaminants and particularly redox-sensitive compounds (Opitz et al. 2022a). The qualitative and quantitative results of this research project now allow the customised designing and sizing of integrated passive systems for reliable treatment of ferruginous, circumneutral mine water in consecutive treatment stages broadly following Pareto's principle as illustrated in Fig. 18. Hence, strategically combining increasingly efficient passive treatment stages provides considerable potential to optimise treatment performance whilst minimising land consumption and investment costs (Opitz et al. 2022a). Moreover, designing and sizing the consecutive treatment stages in integrated mine water treatment systems according to the kinetic optimum of the underlying physicochemical processes will go a long way towards construction of more efficient, reliable passive systems and thus protection of receiving surface waters from mine water pollution worldwide. Thus, the designing and sizing of settling ponds, surface-flow wetlands, and sediment filters is briefly summarised in the following three individual profiles for simple application by scientists and engineers alike:

Settling ponds	
Main Function	<p>Pre-treatment</p> <ul style="list-style-type: none"> ▪ Ferrous iron oxidation ▪ Homoaggregation of hydrous ferric oxides ▪ Gravitational settling of particulate (ferric) solids ▪ Continuous oxygen dissolution and carbon dioxide degassing
Design configuration	<p>Design, construction, layout, and geometry are well-established. Briefly summarised, settling ponds are bare basins with impermeable base sealing and a high length-to-width / depth ratio. The ponds should include spacious storage capacity for ochre accumulation (e.g. DWA 2005c, 2013; Ekama et al. 2006; NCB 1982).</p>
Operational cycles	<p>The sediment chamber of settling ponds should provide adequate capacity for de-sludging cycles in the order of at least several years depending on iron loading.</p>
Waste	<p>Non-hazardous ochre may be processed and utilised for commercial purposes such as gas cleaning and water treatment or as low-grade additives or colorants in construction materials (e.g. Dobbie et al. 2009; Hedin 2003; Sahoo et al. 2014; Srivastava et al. 2022).</p>
Design	<p>Settling ponds should provide sufficient HRT for thorough ferrous iron oxidation and subsequent sedimentation of the bulk (particulate) iron load. To protect subsequent, more delicate components such as wetlands or sediment filters from overloading, iron concentration should be decreased to an innocuous level in the order of 3 – 10 mg/L.</p>
Sizing	<p>We recommend application of a kinetics-based model approach for sizing of settling ponds for pre-treatment of ferruginous mine water. For thoroughly oxygenised mine discharges, the necessary HRT and thus surface area may be approximated based on basic parameters (inflow iron level, flow rate, pH) and general assumptions (steady pH, ambient temperature) as well as technical constraints (e.g. pre-oxygenation, sound hydraulic design):</p> $(19) \quad A = \frac{Q \times (\ln [Fe]_{out} - \ln [Fe]_{in})}{-k_{sed} \times h}$ <p>The coefficient k_{sed} of $2, 1(\pm 0,7) \times 10^{-2} \text{ h}^{-1}$ as derived from the Westfield pilot plant is in good agreement with previous laboratory studies (e.g. Opitz et al. 2022b; Sapsford 2013; Sutton et al. 2015). With regards to the “half-live”, the coefficient corresponds to a HRT of about one day to remove 50% of the initial hydrous ferric oxides, which agrees well with the flat HRT recommended for sizing of settling ponds as noted in chapter 1.2. For highly ferrous mine waters, the necessary HRT for oxidation may be considered following equation (13).</p>
Advantages	<p>Robust in operation; inexpensive in construction; free gas transfer; ample HRT; simple maintenance and periodic de-sludging; relatively pure ochre for recycling or disposal.</p>
Limitations	<p>Poor hydraulic efficiency; freezing in winter; iron removal inherently limited at low levels with residual, dispersed colloids unlikely to settle within reasonable HRT; large areal footprint; susceptible to mixing.</p>

Constructed, surface-flow wetlands	
Main Function	<p>Polishing</p> <ul style="list-style-type: none"> ▪ Filtration of ferric colloids by macrophytes ▪ Scavenging and heteroaggregation of dissolved or colloidal iron ▪ Stimulation of biogeochemical (treatment) processes ▪ (Ad)Sorption of metals and other pollutants on sediment and litter ▪ Removal of secondary contaminants (Mn, NH₄, PO₄ etc.)
Design configuration	<p>Design, construction, vegetation, and geometry are well-established. Briefly summarised, horizontal “aerobic” wetlands are shallow basins with a shallow rooting substrate planted with tall-growing hydrophytes emerging from a free water body with a water depth of 15 to 50 cm (e.g. DWA 2006; Hedin et al. 1994; Kadlec & Wallace 2009; Kadlec et al. 2000; PIRAMID Consortium 1999; Wildemann et al. 1993).</p>
Operational cycles	<p>Constructed wetlands should be refurbished in the order of decades to minimise costs and allow for ecological development.</p>
Waste	<p>Heterogeneous mixture of soil, ochre, and (decomposing) plant litter that may be difficult to dispose of due to the organic fraction.</p>
Design	<p>Wetlands should provide ample HRT and slow flow velocity through the dense vegetation for effective removal of residual dissolved and colloidal iron, with submerged macrophytes considerably augmenting effective retention and exposure times. Effluent iron levels should be reduced to the site-specific legal discharge limit, typically in the order of 1 – 3 mg/L, to protect final sediment filters or the receiving surface water from overloading.</p>
Sizing	<p>We recommend application of the advanced areal approach for sizing of wetlands for polishing of pre-treated, ferruginous mine water. By incorporating the empirical relationship as parameterised in the study at hand, the concentration-dependency of iron removal in densely vegetated wetlands is adequately reflected. The simplified approach allows approximation of the necessary wetland area:</p> $(20) \quad A = \frac{Q \times ([Fe]_{in} - [Fe]_{out})}{m \times [Fe]_{in}^n}$ <p>The empirical coefficients $m = 0.2$ and $n = 1.4$ were determined for polishing of residual (colloidal) iron levels < 5 mg/L in reed-planted wetlands with a water depth of approx. 40 to 50 cm. The conservative approach provides a more reliable estimate of the necessary wetland size as compared to the established linear, area-adjusted approach, especially at low iron levels and/or strict discharge criteria.</p>
Advantages	<p>Good hydrodynamics and hydraulic efficiency; omnipresent catalytic surfaces (periphyton); self-sustaining (nutrient) cycles; habitat value; aesthetic value; high treatment performance and reliability at low, moderate, and even high iron loading.</p>
Limitations	<p>Biotic oxygen consumption; diurnal and seasonal variability (redox potential, pH, oxygen etc.); small ochre storage capacity; complex waste disposal; start-up phase of 1-2 years; moderate areal footprint.</p>

Horizontal-flow sediment filters	
Main Function	<p>Purification</p> <ul style="list-style-type: none"> ▪ Physical filtration of residual colloids ▪ Adsorption of dissolved metals and other contaminants ▪ Degradation of redox-sensitive compounds ▪ Stabilisation of basic hydrochemical parameters
Design configuration	<p>Design, construction, filling, and geometry are well-established. Briefly summarised, sediment filters are elongated basins filled with inert gravel, preferably in multichambered filter with consecutive grain-size fractions decreasing towards the outflow to prevent matrix clogging (e.g. Blanco et al. 2018; DVGW 2005, 2017; DWA 2019; Sapsford & Williams 2009; Sapsford et al. 2007; Wegelin 1996).</p>
Operational cycles	<p>The filter matrix tends to progressing colmatation and thus requires regular refurbishment in the order of several month, preferably years.</p>
Waste	<p>Filter gravel with plaque layers of predominantly iron and manganese (oxyhyd)oxides as well as organic residues and fine sediments.</p>
Design	<p>The basic principles for so-called “horizontal flow roughing filters” were established by Wegelin (1996), with usually three consecutive filter chambers with a 1:2:2 ratio of decreasing grain size fractions (medium to coarse gravel; 6.3 – 63 mm) to facilitate an overall filter velocity in the order of 0.3 – 1.5 m/h. Filter depth is typically in the order of 1.5 m with additional freeboard to allow for headloss. The sediment filter should be designed to reliably reduce effluent iron levels below the site-specific discharge limit, with additional removal of secondary contaminants considered if required.</p>
Sizing	<p>We recommend sizing of sediment filters according to established principles noted above, particularly Wegelin (1996). The volume and porosity of the filter matrix should be estimated such that filter velocity (v_F) and effective HRT for the three-tiered sediment filter are within the recommended target dimensions noted above with:</p> $(21) \quad v_F = \frac{Q}{A_F}$ $(22) \quad t = \frac{\sum_1^3 V \times P}{Q} \times (1 - SF)$ <p>The porosity (P) of each filter tier may be considered individually. A safety factor (SF) of about 15 – 25% is recommended to account for clogged pore space. For the sediment filters of the Westfield pilot plant, excellent results were obtained for a coarse granite gravel filter matrix (8 – 16 mm) despite a relatively high filter velocity in the order of 1.8 – 6.1 m/h and a low HRT in the order of 0.5 – 1.0 h.</p>
Advantages	<p>Robust and low maintenance; optimal hydrodynamics and hydraulic efficiency; intensive biotic and abiotic (catalytic) reactions in the filter matrix; small areal footprint; excellent operational reliability.</p>
Limitations	<p>Low particulate loading required to minimise progressive colmatation; small ochre storage capacity; short(er) refurbishment cycles; start-up phase of up to 1 year.</p>

References

- Baken S, Salaets P, Desmet N, Seuntjens P, Vanlierde E, Smolders E (2015) Oxidation of iron causes removal of phosphorus and arsenic from stream water in groundwater-fed lowland catchments. *Environ. Sci. Technol.* 49: 2886-2894. <https://doi.org/10.1021/es505834y>
- Banfield J, Welch S, Zhang H, Ebert T, Penn R (2000) Aggregation-based crystal growth and microstructure development in natural iron oxyhydroxide biomineralization products. *Science* 289: 751-754. <https://doi.org/10.1126/science.289.5480.751>
- Banks D, Younger P, Arnesen R, Iversen E, Banks S (1997) Mine-water chemistry: The good, the bad and the ugly. *Environ. Geol.* 32: 157-174. <https://doi.org/10.1007/s002540050204>
- Barnes A, Sapsford D, Dey M, Williams K (2009) Heterogeneous Fe(II) oxidation and zeta potential. *J. Geochem. Explor.* 100: 192-198. <https://doi.org/10.1016/j.gexplo.2008.06.001>
- Batty L, Younger P (2002) Critical role of macrophytes in achieving low iron concentrations in mine water treatment wetlands. *Environ. Sci. Technol.* 36(18): 3997-4002. <https://doi.org/10.1021/es020033>
- Baumgartner J, Faivre D (2015) Iron solubility, colloids and their impact on iron (oxyhydr)oxide formation from solution. *Earth Sci. Rev.* 150: 520-530. <https://doi.org/10.1016/j.earscirev.2015.09.003>
- Benthaus F, Totsche O, Luckner L (2020) In-lake neutralization of East German lignite pit lakes: Technical history and new approaches from LMBV. *Mine Water Environ.* 39: 603-617. <https://doi.org/10.1007/s10230-020-00707-5>
- Berka M, Rice J (2005) Relation between aggregation kinetics and the structure of kaolinite aggregates. *Langmuir* 21: 1223-1229. <http://doi.org/10.1021/la0478853>
- Bilek F (2012) Reinigungsverfahren von Grundwasser und Oberflächengewässern. Project VODAMIN, TP04, Saxon State Office for Environment, Agriculture and Geology (Eds.), Dresden, 79 pp
- Blanco I, Sapsford D, Trumm D, Pope J, Kruse N, Cheong Y, McLauchlann H, Sinclair E, Weber P, Olds W (2018) International trials of vertical flow reactors for coal mine water treatment. *Mine Water Environ.* 37: 4-17. <https://doi.org/10.1007/s10230-017-0491-z>
- Bodin H, Mietto A, Ehde P, Persson J, Weisner S (2012) Tracer behaviour and analysis of hydraulics in experimental free water surface wetlands. *Ecol. Eng.* 49: 201-211. <https://doi.org/10.1016/j.ecoleng.2012.07.009>
- Bottero J, Arnaud M, Villieras F, Michot L, de Donato P, François M (1993) Surface and textural heterogeneity of fresh hydrous ferric oxides in water and in the dry state. *J. Colloid Sci.* 159: 45-52. <https://doi.org/10.1006/jcis.1993.1295>
- Bottero J, Manceau A, Villieras F, Tchoubar D (1994) Structure and mechanisms of formation of iron oxide hydroxide (chloride) polymers. *Langmuir* 10: 316-319. <https://doi.org/10.1021/la00013a046>
- Braskerud B (2001) The influence of vegetation on sedimentation and resuspension of soil particles in small constructed wetlands. *J. Environ. Qual.* 30: 1447-1457. <http://doi.org/10.2134/jeq2001.3041447x>
- Braskerud B (2003) Clay particle retention in small constructed wetlands. *Water Res.* 37(16): 3793-3802. [https://doi.org/10.1016/S0043-1354\(02\)00484-0](https://doi.org/10.1016/S0043-1354(02)00484-0)
- Buffle J, Wilkinson K, Stoll S, Filella M, Zhang J (1998) A generalized description of aquatic colloidal interactions: The three colloidal component approach. *Environ. Sci. Technol.* 32: 2887-2899. <https://doi.org/10.1021/es980217h>
- Burke S, Banwart S (2002) A geochemical model for removal of iron(II)(aq) from mine water discharges. *Appl. Geochem.* 17: 431-443. [https://doi.org/10.1016/S0883-2927\(01\)00092-0](https://doi.org/10.1016/S0883-2927(01)00092-0)
- Butler B, Ranville J, Ross P (2008) Direct versus indirect determination of suspended sediment associated metals in a mining-influenced watershed. *Appl. Geochem.* 23: 1218-1231. <https://doi.org/10.1016/j.apgeochem.2007.11.021>
- Byrne P, Wood P, Reid I (2012) The impairment of river systems by metal mine contamination: A review including remediation Options. *Crit. Rev. Environ. Sci. Technol.* 42: 2017-2077. <https://doi.org/10.1080/10643389.2011.574103>
- Cadmus P, Clements W, Williamson J, Ranville J, Meyer J, Ginés M (2016) The use of field and mesocosm experiments to quantify effects of physical and chemical stressors in mining-contaminated streams. *Environ. Sci. Technol.* 50: 7825-7833. <https://doi.org/10.1021/acs.est.6b01911>
- Cadmus P, Brinkman SF, May MK (2018) Chronic toxicity of ferric iron for aquatic organisms: Derivation of a chronic water quality criterion using single species and mesocosm data. *Arch. Environ. Contam. Toxicol.* 74: 605-615. <https://doi.org/10.1007/s00244-018-0505-2>
- Chikanda F, Otake T, Koide A, Ito A, Sato T (2021) The formation of Fe colloids and layered double hydroxides as sequestration agents in the natural remediation of mine drainage. *Sci. Total Environ.* 774: 145183. <https://doi.org/10.1016/j.scitotenv.2021.145183>

References

- Cornell R, Giovanoli R, Schneider W (1989) Review of the hydrolysis of iron(III) and the crystallization of amorphous iron(III) hydroxide hydrate. *J. Chem. Technol. Biotechnol.* 46: 115-134. <https://doi.org/10.1002/jctb.280460204>
- Cotton J, Wharton G, Bass J, Heppell C, Wotton R (2006) The effects of seasonal changes to in-stream vegetation cover on patterns of flow and accumulation of sediment. *Geomorphology* 77: 320-334. <https://doi.org/10.1016/j.geomorph.2006.01.010>
- Cravotta C (2015) Monitoring, field experiments, and geochemical modeling of Fe(II) oxidation kinetics in a stream dominated by net-alkaline coal-mine drainage, Pennsylvania, USA. *Appl. Geochem.* 62: 96-107. <https://doi.org/10.1016/j.apgeochem.2015.02.009>
- Cravotta C (2021) Interactive PHREEQ-N-AMDTreat water-quality modeling tools to evaluate performance and design of treatment systems for acid mine drainage. *Appl. Geochem.* 126: 104845. <https://doi.org/10.1016/j.apgeochem.2020.104845>
- Cravotta C, Trahan M (1999) Limestone drains to increase pH and remove dissolved metals from acidic mine drainage. *Appl. Geochem.* 14: 581-606. [https://doi.org/10.1016/S0883-2927\(98\)00066-3](https://doi.org/10.1016/S0883-2927(98)00066-3)
- Cravotta C, Brady K (2015) Priority pollutants and associated constituents in untreated and treated discharges from coal mining or processing facilities in Pennsylvania, USA. *Appl. Geochem.* 62: 108-130. <https://doi.org/10.1016/j.apgeochem.2015.03.001>
- Das B (2018) Theoretical study of small iron-oxyhydroxide clusters and formation of ferrihydrite. *J. Phys. Chem. A* 122: 652-661. <https://doi.org/10.1021/acs.jpca.7b09470>
- Davis R, Welty A, Borrego J, Morales J, Pendon J, Ryan J (2000) Rio Tinto estuary (Spain): 5000 years of pollution. *Environ. Geol.* 39(10): 1107-1116. <https://doi.org/10.1007/s002549900096>
- Dempsey B, Roscoe H, Ames R, Hedin R, Jeon B (2001) Ferrous oxidation chemistry in passive abiotic systems for the treatment of mine drainage. *Geochem. Explor. Environ. Anal.* 1: 81-88. <https://doi.org/10.1144/geochem.1.1.81>
- Dempsey B, Dietz J, Jeon B, Roscoe H, Ames R (2002) Heterogeneous oxidation of ferrous iron for treatment of acid mine drainage. In: Proc. National Meeting ASMR, Vol. 1: 487-495. <http://doi.org/10.21000/JASMR02010487>
- Dietrich W (1982). Settling velocity of natural particles. *Water Resour. Res.* 18: 1615-1626. <https://doi.org/10.1029/WR018i006p01615>
- Dietz J, Dempsey B (2017) Heterogeneous oxidation of Fe(II) in AMD. *Appl. Geochem.* 81: 90-97. <https://doi.org/10.1016/j.apgeochem.2017.04.003>
- Dobbie K, Heal K, Aumonier J, Smith K, Johnston A, Younger P (2009) Evaluation of iron ochre from mine drainage treatment for removal of phosphorus from wastewater. *Chemosphere* 75: 795-800. <https://doi.org/10.1016/j.chemosphere.2008.12.049>
- Doorn N, Hansson S (2011) Should Probabilistic Design Replace Safety Factors? *Philos. Technol.* 24:151-168. <https://doi.org/10.1007/s13347-010-0003-6>
- Duan J, Gregory J (2003) Coagulation by hydrolysing metal salts. *Adv. Colloid Interface Sci.* 100-102: 475-502. [https://doi.org/10.1016/S0001-8686\(02\)00067-2](https://doi.org/10.1016/S0001-8686(02)00067-2)
- DVGW (2005) Technical Rule W 223 – Removal of Iron and Manganese for Drinking Water Purification (Part 1- 3). German Technical and Scientific Association for Gas and Water e.V., Bonn
- DVGW (2017) Technical Rule W 213 – Filtration Processes for Particle Removal (Part 1-9). German Technical and Scientific Association for Gas and Water e.V., Bonn
- DWA (2005) Technical Rule A 201: Grundsätze für Bemessung, Bau und Betrieb von Abwasserteichanlagen. German Association for Water, Wastewater and Waste e.V., Bad Hoennef
- DWA (2006) Technical Rule A 262: Grundsätze für Bemessung, Bau und Betrieb von Pflanzenkläranlagen mit bepflanzten Bodenfiltern zur biologischen Reinigung kommunalen Abwassers. German Association for Water, Wastewater and Waste e.V., Bad Hoennef
- DWA (2013) Technical Rule A 166: Bauwerke der zentralen Regenwasserbehandlung und -rückhaltung – Konstruktive Gestaltung und Ausrüstung. German Association for Water, Wastewater and Waste e.V., Bad Hoennef
- DWA (2019) Technical Rule A 166: Abwasserfiltration durch Raumfilter nach biologischer Reinigung. German Association for Water, Wastewater and Waste e.V., Bad Hoennef
- Dzakpasu M, Scholz M, McCarthy V, Jordan S (2014) Nitrogen transformations and mass balance in an integrated constructed wetland treating domestic wastewater. *Water Sci. Technol.* 70: 1496-1502. <https://doi.org/10.2166/wst.2014.402>
- Ekama G, Barnard J, Gunthert F, Krebs P, McCorquodale J, Parker D, Wahlberg E (2006) Secondary Settling Tanks: Theory, Modelling, Design and Operation. IWA Publishing, Report No. 6, London, 232 pp
- Elishakov I, Chamis C (2001) Interrelation Between Safety Factors and Reliability. NASA CR-2011-211309. 72 pp

References

- Elliott A (2000) Settling of fine sediment in a channel with emergent vegetation. *J. Hydraul. Eng.* 126: 570-577. [https://doi.org/10.1061/\(ASCE\)0733-9429\(2000\)126:8\(570\)](https://doi.org/10.1061/(ASCE)0733-9429(2000)126:8(570))
- ERMITE Consortium (2004) Environmental Regulation of Mine Waters in the European Union. EC 5th Framework RTD Project EVK1-CT-2000-00078
- Espenson J (1981) Chemical Kinetics and Reaction Mechanisms. McGraw-Hill Series in Advanced Chemistry, New York, 281 pp
- European Commission (2009) Reference Document on Best Available Techniques for Management of Tailings and Waste Rock in Mining Activities. European Integrated Pollution Prevention and Control Bureau, MTWR BREF 01.2009, 511 pp
- European Space Agency (2008) Technology Readiness Levels Handbook for Space Applications, Rev. 6. ESA TEC-SHS/5551/MG/ap, 60 pp
- Evangelou V, Zhang Y (1995) A review: Pyrite oxidation mechanisms and acid mine drainage prevention. *Crit. Rev. Environ. Sci. Technol.* 25: 141-199. <https://doi.org/10.1080/10643389509388477>
- Farley K, Morel F (1986) Role of coagulation in the kinetics of sedimentation. *Environ. Sci. Technol.* 20: 187-195. <https://doi.org/10.1021/es00144a014>
- Fenton O, Healy M, Rodgers M, O'Huallachain D (2009) Sitespecific P absorbency of ochre from acid mine drainage near an abandoned Cu-S mine in the Avoca-Avonmore catchment, Ireland. *Clay Miner.* 44: 113-123. <https://doi.org/10.1180/claymin.2009.044.1.113>
- Filella M (2007) Colloidal properties of submicron particles in natural waters. In: Wilkinson K, Lead J (Eds.), Environmental Colloids and Particles: Behaviour, Separation and Characterisation. IUPAC series on Analytical and Physical Chemistry of Environmental Systems. John Wiley & Sons, Chichester, 17-93
- Filella M, Buffle J (1993) Factors controlling the stability of submicron colloids in natural waters. *Colloids and Surf. A* 73: 255-273. [https://doi.org/10.1016/0927-7757\(93\)80020-F](https://doi.org/10.1016/0927-7757(93)80020-F)
- Flanagan N, Mitsch W, Beach K (1994) Predicting metal retention in a constructed mine drainage wetland. *Ecol. Eng.* 3: 135-159. [https://doi.org/10.1016/0925-8574\(94\)90042-6](https://doi.org/10.1016/0925-8574(94)90042-6)
- Flynn C (1984) Hydrolysis of inorganic iron(III) salts. *Chem. Rev.* 84: 31-41. <https://doi.org/10.1021/cr00059a0031984>
- Fox L, Wofsy S (1983) Kinetics of removal of iron colloids from estuaries. *Geochim. Cosmochim. Acta* 47: 211-216. [https://doi.org/10.1016/0016-7037\(83\)90134-5](https://doi.org/10.1016/0016-7037(83)90134-5)
- García J, Chiva J, Aguirre P, Álvarez E, Sierra J, Mujeriego R (2004) Hydraulic behaviour of horizontal subsurface flow constructed wetlands with different aspect ratio and granular medium size. *Ecol. Eng.* 23: 177-187. <https://doi.org/10.1016/j.ecoleng.2004.09.002>
- Garcia-Rios M, de Windt L, Luqot L, Cadiot C (2021) Modeling of microbial kinetics and mass transfer in bioreactors simulating the natural attenuation of arsenic and iron in acid mine drainage. *J. Hazard. Mater.* 405: 124133. <https://doi.org/10.1016/j.jhazmat.2020.124133>
- Geroni J, Sapsford D (2011) Kinetics of iron (II) oxidation determined in the field. *Appl. Geochem.* 26: 1452-1457. <https://doi.org/10.1016/j.apgeochem.2011.05.018>
- Gombert P, Sracek O, Koukouzas N, Gzyl G, Valladares S, Frączek R, Klinger C, Bauerek A, Areces J, Chamberlain S, Paw K, Pierzchała Ł (2019). An overview of priority pollutants in selected coal mine discharges in Europe. *Mine Water Environ.* 38, 16-23. <https://doi.org/10.1007/s10230-018-0547-8>
- González A, Odriozola G, Leone R (2004) Colloidal aggregation with sedimentation: Concentration effects. *Eur. Phys. J. E* 13: 165-178. <https://doi.org/10.1140/epje/e2004-00052-1>
- Grant S, Kim J, Poor C (2001) Kinetic theories for the coagulation and sedimentation of particles. *J. Colloid Sci.* 238: 238-250. <https://doi.org/10.1006/jcis.2001.7477>
- Grundl T, Delwiche J (1993) Kinetics of ferric oxyhydroxide precipitation. *J. Contam. Hydrol.* 14: 71-87. [https://doi.org/10.1016/0169-7722\(93\)90042-Q](https://doi.org/10.1016/0169-7722(93)90042-Q)
- Gunnars A, Blomqvist S, Johannson P, Andersson C (2002) Formation of Fe(III) oxyhydroxide colloids in freshwater and brackish seawater, with incorporation of phosphate and calcium. *Geochim. Cosmochim. Acta* 66: 745-758. [https://doi.org/10.1016/S0016-7037\(01\)00818-3](https://doi.org/10.1016/S0016-7037(01)00818-3)
- Guo C, Cui Y (2021) Improved solute transport and pollutant degradation model of free water surface constructed wetlands considering significant linear correlation between model parameters. *Bioresour. Technol.* 327: 124817. <https://doi.org/10.1016/j.biortech.2021.124817>
- Hasche-Berger A, Wolkersdorfer C (2005) Contemporary reviews of mine water studies in Europe: Part 1 – Germany. In: Wolkersdorfer C, Bowell R (Eds.) *Mine Water Environ.* 23: 162-182. <https://doi.org/10.1007/s10230-004-0060-0>

References

- Hedin R (2003) Recovery of marketable iron oxide from mine drainage in the USA. *Land Contam. Reclamat.* 11: 93-98. <https://doi.org/10.2462/09670513.802>
- Hedin R (2008) Iron removal by a passive system treating alkaline coal mine drainage. *Mine Water Environ.* 27: 200-209. <https://doi.org/10.1007/s10230-008-0041-9>
- Hedin R (2013) Temperature independent removal of iron in a passive mine water system. Proc. IMWA Conference 2013, 599-604.
- Hedin R, Narin R, Kleinmann R (1994) Passive treatment of coal mine drainage. US Bureau of Mines, Information Circular 9389, 35 pp
- Hellier W, Giovannetti E, Slack P (1994) Best professional judgement analysis for constructed wetlands as a best available technology for the treatment of post-mining groundwater seeps. In: Proc. International Land Reclamation and Mine Drainage Conference, Vol. 1: 60-69
- Hiemstra T (2013) Surface and mineral structure of ferrihydrite. *Geochim. Cosmochim. Acta* 105: 316-325. <https://doi.org/10.1016/j.gca.2012.12.002>
- Hiemstra T, van Riemsdijk W (2007) Adsorption and surface oxidation of Fe(II) on metal (hydr)oxides. *Geochim. Cosmochim. Acta* 71: 5913-5933. <https://doi.org/10.1016/j.gca.2007.09.030>
- Hiemstra T, van Riemsdijk W (2009) A surface structural model for ferrihydrite I: Sites related to primary charge, molar mass, and mass density. *Geochim. Cosmochim. Acta* 73: 4423-4436. <https://doi.org/10.1016/j.gca.2009.04.032>
- Horvath T (2004). Retention of particulate matter by macrophytes in a first-order stream. *Aquat. Bot.* 78: 27-36. <https://doi.org/10.1016/j.aquabot.2003.09.003>
- Hove M, van Hille R, Lewis A (2008) Mechanisms of formation of iron precipitates from ferrous solutions at high and low pH. *Chem. Eng. Sci.* 63: 1626-1635. <https://doi.org/10.1016/j.ces.2007.11.016>
- Hunt J, Pandya J (1984) Sewage sludge coagulation and settling in seawater. *Environ. Sci. Technol.* 18(2): 119-121. <https://doi.org/10.1021/es00120a015>
- Hunter K, Leonard M, Carpenter P, Smitz J (1997) Aggregation of iron colloids in estuaries: A heterogeneous kinetics study using continuous mixing of river and sea waters. *Colloids Surf. A* 120: 111-121. [https://doi.org/10.1016/S0927-7757\(96\)03719-3](https://doi.org/10.1016/S0927-7757(96)03719-3)
- Jeon B, Dempsey B, Burgos W, Royer R (2001) Reactions of ferrous iron with hematite. *Colloids Surf. A* 191: 41-55. [https://doi.org/10.1016/S0927-7757\(01\)00762-2](https://doi.org/10.1016/S0927-7757(01)00762-2)
- Johnson D, Hallberg K (2005) Pitfalls of passive mine water treatment. *Rev. Environ. Sci. Biotechnol.* 1: 335-343. <https://doi.org/10.1023/A:1023219300286>
- Jolivet J, Chanéac C, Tronc E (2004) Iron oxide chemistry – From molecular clusters to extended solid networks. *Chem. Commun.* 35: 481-483. <https://doi.org/10.1039/b304532n>
- Juang R, Wu W (2002) Adsorption of sulfate and copper(II) on goethite in relation to the changes of zeta potentials. *J. Colloid Sci.* 249: 22-29. <https://doi.org/10.1006/jcis.2002.8240>
- Kadlec R, Wallace S (2009) Treatment Wetlands (2nd Ed.). CRC Press. 1046 pp
- Kadlec R, Knight R, Vymazal J, Brix H, Copper P, Haberl R (2000) Constructed Wetlands for Pollution Control: Processes, Performance, Design and Operation. IWA Publishing, Report No. 8, London, 156 pp
- Kappler A, Bryce C, Mansor M, Lueder U, Byrne J, Swanner E (2021) An evolving view on biogeochemical cycling of iron. *Nat. Rev. Microbiol.* 19: 360-374. <https://doi.org/10.1038/s41579-020-00502-7>
- Karlsson T, Persson P (2012) Complexes with aquatic organic matter suppress hydrolysis and precipitation of Fe(III). *Chem. Geol.* 322: 19-27. <https://doi.org/10.1016/j.chemgeo.2012.06.003>
- Kim S, Stolzenbach K (2004) Aggregate formation and collision efficiency in differential settling. *J. Colloid Sci.* 271: 110-119. <https://doi.org/10.1016/j.jcis.2003.10.014>
- Kirby C, Cravotta C (2005) Net alkalinity and net acidity 1: Theoretical considerations. *Appl. Geochem.* 20: 1920-1940. <https://doi.org/10.1016/j.apgeochem.2005.07.002>
- Kirby C, Thomas H, Southam G, Donald R (1999) Relative contributions of abiotic and biological factors in Fe(II) oxidation in mine drainage. *Appl. Geochem.* 14: 511-530. [https://doi.org/10.1016/S0883-2927\(98\)00071-7](https://doi.org/10.1016/S0883-2927(98)00071-7)
- Kleinmann R, Skousen J, Wildemann T, Hedin R, Nairn R, Gusek J (2021) The early development of passive treatment systems for mining-influenced water: A north American perspective. *Mine Water Environ.* 40: 818-830. <https://doi.org/10.1007/s10230-021-00817-8>
- Kruse N, Gozzard E, Jarvis A (2009) Determination of hydraulic residence times in several UK mine water treatment systems and their relationship to iron removal. *Mine Water Environ.* 28: 115-123. <https://doi.org/10.1007/s10230-009-0068-6>

References

- Kruspe R, Neumann J, Opitz M, Theiss S, Uhlmann W, Zimmermann K (2014) Qualitative und quantitative Beeinflussungen von Fließgewässerorganismen durch Eisen am Beispiel der Lausitzer Braunkohlenfolgelandschaft. Saxon State Office for Environment, Agriculture and Geology (Eds.), Dresden, Vol. 35: 94 pp. <http://d-nb.info/107066362X>
- Kuehn E, Moore J (1995) Variability of treatment performance in constructed wetlands. *Water Sci. Technol.* 32: 241-250. [https://doi.org/10.1016/0273-1223\(95\)00625-7](https://doi.org/10.1016/0273-1223(95)00625-7)
- Li Y, Deletic A, Fletcher T (2007) Modelling wet weather sediment removal by stormwater constructed wetlands: Insights from a laboratory study. *J. Hydrol.* 338: 285-296. <https://doi.org/10.1016/j.jhydrol.2007.03.001>
- Lo B, Waite T (2000) Structure of hydrous ferric oxide aggregates. *J. Colloid Sci.* 222: 83-89. <https://doi.org/10.1006/jcis.1999.6599>
- Luan F, Santelli C, Hansel C, Burgos W (2012). Defining manganese(II) removal processes in passive coal mine drainage treatment systems through laboratory incubation experiments. *Appl. Geochem.* 27: 1567-1578. <https://doi.org/10.1016/j.apgeochem.2012.03.010>
- Marcello R, Galato S, Peterson M, Riella H, Bernardin A (2008) Inorganic pigments made from the recycling of coal mine drainage treatment sludge. *J. Environ. Manage.* 88: 1280-1284. <https://doi.org/10.1016/j.jenvman.2007.07.005>
- Matthies R, Aplin A, Horrocks B, Mudashiru L (2012) Occurrence and behaviour of dissolved, nano-particulate and micro-particulate iron in waste waters and treatment systems: New insights from electrochemical analysis. *J. Environ. Monit.* 14: 1174-1181. <https://doi.org/10.1039/c2em10846a>
- Mayer L (1982) Aggregation of colloidal iron during estuarine mixing: Kinetics, mechanism, and seasonality. *Geochim. Cosmochim. Acta* 46: 2527-2535. [https://doi.org/10.1016/0016-7037\(82\)90375-1](https://doi.org/10.1016/0016-7037(82)90375-1)
- Mayes W, Johnston D, Potter H, Jarvis A (2009) A national strategy for identification, prioritisation and management of pollution from abandoned non-coal mine sites in England and Wales. I. Methodology development and initial results. *Sci. Total Environ.* 407: 5435-5447. <https://doi.org/10.1016/j.scitotenv.2009.06.019>
- McKnight D, Feder G (1984) The ecological effect of acid conditions and precipitation of hydrous metal oxides in a Rocky Mountain stream. *Hydrobiologia* 199: 129-138. <https://doi.org/10.1007/BF00011952>
- Melton E, Swanner E, Behrens S, Schmidt C, Kappler A (2014) The interplay of microbially mediated and abiotic reactions in the biogeochemical Fe cycle. *Nat. Rev. Microbiol.* 12: 797-808. <https://doi.org/10.1038/nrmicro3347>
- Mettler S, Abdelmoula M, Hoehn E, Schönenberger R, Weidler P, von Gunten U (2001) Characterization of iron and manganese precipitates from an in situ ground water treatment plant. *Ground Water* 39: 921-930. <https://doi.org/10.1111/j.1745-6584.2001.tb02480.x>
- Michel F, Barrón V, Torrent J, Morales M, Serna C, Boily J, Liu Q, Ambrosini A, Cismasu A, Brown G (2010) Ordered ferrimagnetic form of ferrihydrite reveals links among structure, composition, and magnetism. *PNAS* 107: 2787-2792. <https://doi.org/10.1073/pnas.0910170107>
- Mishra A, Tripathi B (2008) Utilization of fly ash in adsorption of heavy metals from wastewater. *Toxicol. Environ. Chem.* 90: 1091-1097. <https://doi.org/10.1080/02772240801936786>
- Mitsch W, Gosselink J (2000) Wetlands (5th Ed.). John Wiley & Sons. 752 pp.
- Murad E, Rojik P (2003) Iron-rich precipitates in a mine drainage environment: Influence of pH on mineralogy. *Am. Mineral.* 88: 1915-1918, <https://doi.org/10.2138/am-2003-11-1234>
- Murad E, Rojik P (2005) Iron mineralogy of mine-drainage precipitates as environmental indicators: Review of current concepts and a case study from the Sokolov Basin, Czech Republic. *Clay Miner.* 40: 427-440. <https://doi.org/10.1180/0009855054040181>
- Mylon S, Chen K, Elimelech M (2004) Influence of natural organic matter and ionic composition on the kinetics and structure of hematite colloid aggregation: Implications to iron depletion in estuaries. *Langmuir* 20: 9000-9006. <https://doi.org/10.1021/la049153g>
- National Coal Board (1982) Technical Management of Water in the Coal Mining Industry. Westminster Press, London, 96 pp
- Neculita C, Rosa E (2019) A review of the implications and challenges of manganese removal from mine drainage. *Chemosphere* 214: 491-510. <https://doi.org/10.1016/j.chemosphere.2018.09.106>
- Nordstrom K (2011) Mine waters: Acidic to circumneutral. *Elements* 7: 393-398. <https://doi.org/10.2113/gselements.7.6.393>
- Nordstrom K, Alpers C (1999) Geochemistry of acid mine waters. In: Plumlee G, Logsdon M (Eds.) The Environmental Geochemistry of Mineral Deposits, *Rev. Econ. Geol.* 6A: 133-160. <https://pubs.er.usgs.gov/publication/70199480>

References

- Nyquist J, Greger M (2009) A field study of constructed wetlands for preventing and treating acid mine drainage. *Ecol. Eng.* 35: 630-642. <https://doi.org/10.1016/j.ecoleng.2008.10.018>
- Opitz J, Alte M, Bauer M, Schäfer W, Söll W (2020a) Estimation of self-neutralisation rates in a lignite pit lake. *Mine Water Environ.* 39: 556-571. <https://doi.org/10.1007/s10230-020-00692-9>
- Opitz J, Alte M, Bauer M, Peiffer S (2020b) Quantifying iron removal efficiency of a passive mine water treatment system using turbidity as a proxy for (particulate) iron. *Appl. Geochem.* 122: 104731. <https://doi.org/10.1016/j.apgeochem.2020.104731>
- Opitz J, Alte M, Bauer M, Peiffer S (2021) The role of macrophytes in constructed surface-flow wetlands for mine water treatment: A review. *Mine Water Environ.* 40: 587-605. <https://doi.org/10.1007/s10230-021-00779-x>
- Opitz J, Bauer M, Eckert J, Peiffer S, Alte M, (2022a) Optimising operational reliability and performance in aerobic passive mine water treatment: The multistage Westfield pilot plant. *Water Air Soil Pollut.* 233: 66. <https://doi.org/10.1007/s11270-022-05538-4>
- Opitz J, Bauer M, Alte M, Schmidtman J, Peiffer S (2022b) Sedimentation kinetics of hydrous ferric oxides in ferruginous, circumneutral mine water. *Environ. Sci. Technol.* 56: 6360-6368. <https://doi.org/10.1021/acs.est.1c07640>
- Opitz J, Alte M, Bauer M, Peiffer S (2023) Development of a novel sizing approach for passive mine water treatment systems based on ferric iron sedimentation kinetics. *Water Res.* 233: 119770. <https://doi.org/10.1016/j.watres.2023.119770>
- Park B, Dempsey B (2005). Heterogeneous oxidation of Fe(II) on ferric oxide at neutral pH and a low partial pressure of O₂. *Environ. Sci. Technol.* 39: 6494-6500. <https://doi.org/10.1021/es0501058>
- Parkhurst D, Appelo C (2013) Description of input and examples for PHREEQC version 3 – A computer program for speciation, batch-reaction, one-dimensional transport, and inverse geochemical calculations. USGS Techniques and Methods, Book 6(A43): 497 pp. <https://doi.org/10.3133/tm6A43>
- Peine A (1998) Acidic lignite pit lakes – Characterisation and quantification of biogeochemical processes and estimation of the importance of internal neutralisation. *Bayreuther Forum Ökologie* 62: 131 pp. <https://eref.uni-bayreuth.de/id/eprint/29202>
- Penn R (2004) Kinetics of oriented aggregation. *J. Phys. Chem. B* 108: 12707-12712. <https://doi.org/10.1021/jp036490>
- Pfannkuche J, Schmidt A (2003) Determination of suspended particulate matter concentration from turbidity measurements: Particle size effects and calibration procedures. *Hydrol. Process.* 17: 1951-1963. <https://doi.org/10.1002/hyp.1220>
- Phenrat T, Saleh N, Sirk K, Tilton R, Lowry G (2007) Aggregation and sedimentation of aqueous nanoscale zero-valent iron dispersions. *Environ. Sci. Technol.* 41: 284-290. <https://doi.org/10.1021/es061349a>
- PIRAMID Consortium (2003) Engineering Guidelines for the Passive Remediation of Acidic and/or Metalliferous Mine Drainage and Similar Wastewaters. EC 5th Framework RTD Project EVK1-CT-1999-000021, 166 pp. <https://eprints.ncl.ac.uk/19801>
- Pizarro J, Belzile N, Filella M, Leppard G, Negre J, Perret D, Buffle J (1995) Coagulation/sedimentation of submicron iron particles in a eutrophic lake. *Water Res.* 29: 617-632. [https://doi.org/10.1016/0043-1354\(94\)00167-6](https://doi.org/10.1016/0043-1354(94)00167-6)
- Plumlee G, Smith K, Montour M, Ficklin W, Mosier E (1999) Geologic controls on the composition of natural waters and mine waters draining diverse mineral-deposit types. In: Plumlee G, Logsdon M (Eds.) *The Environmental Geochemistry of Mineral Deposits, Rev. Econ. Geol.* 6B: 373-432. <https://pubs.er.usgs.gov/publication/70189454>
- Pluntke T, Kozerski H (2003) Particle trapping on leaves and on the bottom in simulated submerged plant stands. *Hydrobiologia* 506: 575-581. <https://doi.org/10.1023/B:HYDR.0000008569.29286.ec>
- Rand L, Ranville J (2019) Characteristics and stability of incidental iron oxide nanoparticles during remediation of a mining-impacted stream. *Environ. Sci. Technol.* 53: 11214-11222. <https://doi.org/10.1021/acs.est.9b03036>
- Regenspurg S, Brand A, Peiffer S (2004) Formation and stability of schwertmannite in acidic mining lakes. *Geochim. Cosmochim. Acta* 68: 1185-1197. <https://doi.org/10.1016/j.gca.2003.07.015>
- Sahoo H, Tripathy S, Equeenuddin S, Sahoo P (2014) Utilization of ochre as an adsorbent to remove Pb(II) and Cu(II) from contaminated aqueous media. *Environ. Earth Sci.* 72: 243-250. DOI: <https://doi.org/10.1007/s12665-013-2950-6>
- Saiers J, Harvey J, Mylon S (2003) Surface-water transport of suspended matter through wetland vegetation of the Florida everglades. *Geophys. Res. Lett.* 30: 1474-1479. <https://doi.org/10.1029/2003GL018132>
- Sapsford D (2013) New perspectives on the passive treatment of ferruginous circumneutral mine waters in the UK. *Environ. Sci. Pollut. Res.* 20: 7827-7836. <https://doi.org/10.1007/s11356-013-1737-3>

References

- Sapsford D, Watson I (2011) A process-orientated design and performance assessment methodology for passive mine water treatment systems. *Ecol. Eng.* 37: 970-975. <https://doi.org/10.1016/j.ecoleng.2010.12.010>
- Sapsford D, Williams K (2009) Sizing criteria for a low footprint passive mine water treatment system. *Water Res.* 43: 423-432. <https://doi.org/10.1016/j.watres.2008.10.043>
- Sapsford D, Barnes A, Dey M, Williams K, Jarvis A, Younger P (2007) Low footprint passive mine water treatment: Field demonstration and application. *Mine Water Environ* 26: 243-250. <https://doi.org/10.1007/s10230-007-0012-6>
- Schaider L, Senn D, Estes E, Brabander D, Shine J (2014) Sources and fates of heavy metals in a mining-impacted stream: Temporal variability and the role of iron oxides. *Sci. Total Environ.* 490: 456-466. <http://dx.doi.org/10.1016/j.scitotenv.2014.04.126>
- Schwarzenbach G (1970) Electrostatic and non-electrostatic contributions to ion association in solution. *Pure Appl. Chem.* 24: 307-334. <https://doi.org/10.1351/pac197024020307>
- Schwertmann U, Cornell R (1991) *Iron Oxides in the Laboratory: Preparation and Characterization* (2nd Ed.). Wiley-VCH, Weinheim, 188 pp. <https://doi.org/10.1002/9783527613229>
- Schwertmann U, Fechter H (1994) The formation of green rust and its transformation to lepidocrocite. *Clay Miner.* 29: 87-92. <https://doi.org/10.1180/claymin.1994.029.1.10>
- Sheridan C, Glasser D, Hildebrandt D (2014) Estimating rate constants of contaminant removal in constructed wetlands treating winery effluent: A comparison of three different methods. *Process Saf. Environ. Prot.* 92: 903-916. <https://doi.org/10.1016/j.psep.2013.09.004>
- Singer P, Stumm W (1969) Oxygenation of ferrous iron – The rate-determining step in the formation of acid mine drainage. *Water Pollution Control Research Series*, 215 pp.
- Singer P, Stumm W (1970) Acidic mine drainage: The rate-determining step. *Science* 167: 1121-1123. <https://doi.org/10.1126/science.167.3921.1121>
- Skousen J, Zipper C, Rose A, Ziemkiewicz P, Nairn R, McDonald L, Kleinmann R (2017) Review of passive systems for acid mine drainage treatment. *Mine Water Environ.* 36: 133-153. <https://doi.org/10.1007/s10230-016-0417-1>
- Smart P, Laidlaw I (1977) An evaluation of some fluorescent dyes for water tracing. *Water Resour. Res.* 13: 15-33. <https://doi.org/10.1029/WR013i001p00015>
- Srivastava P, Al-Obaidi S, Webster G, Weightman A, Sapsford D (2022) Towards passive bioremediation of dye-bearing effluents using hydrous ferric oxide wastes: Mechanisms, products and microbiology. *J. Environ. Manage.* 317: 115332. <https://doi.org/10.1016/j.jenvman.2022.115332>
- Stark L, Williams F (1995) Assessing the performance indices and design parameters of treatment wetlands for H⁺, Fe, and Mn retention. *Ecol. Eng.* 5: 433-444. [https://doi.org/10.1016/0925-8574\(95\)00008-9](https://doi.org/10.1016/0925-8574(95)00008-9)
- Stephenson R, Sheridan C (2021) Review of experimental procedures and modelling techniques for flow behaviour and their relation to residence time in constructed wetlands. *J. Water Process Eng.* 41: 102044. <https://doi.org/10.1016/j.jwpe.2021.102044>
- Stumm W, Lee G (1961) Oxygenation of ferrous iron. *Ind. Eng. Chem.* 53: 143-146. <https://doi.org/10.1021/ie50614a030>
- Stumm W, Morgan J (1996) *Aquatic Chemistry: Chemical Equilibria and Rates in Natural Waters* (3rd Ed.). Wiley VCH, 1040 pp.
- Stumm W, Sulzberger B (1992) The cycling of iron in natural environments: Considerations based on laboratory studies of heterogeneous redox processes. *Geochim. Cosmochim. Acta* 56: 3233-3257. [https://doi.org/10.1016/0016-7037\(92\)90301-X](https://doi.org/10.1016/0016-7037(92)90301-X)
- Sung W, Morgan J (1980) Kinetics and product of ferrous iron oxygenation in aqueous systems. *Environ. Sci. Technol.* 14: 561-568. <https://doi.org/10.1021/es60165a006>
- Sutton A, Sapsford D, Moorhouse A (2015) Mine water treatability studies for passive treatment of coal mine drainage. In: Proc. 10th ICARD & IMWA Conference, Vol. 1: 10 pp
- Taillefert M, Lienemann C, Gaillard J, Perret D (2000) Speciation, reactivity, and cycling of Fe and Pb in a meromictic lake. *Geochim. Cosmochim. Acta* 64: 169-183. [https://doi.org/10.1016/S0016-7037\(99\)00285-9](https://doi.org/10.1016/S0016-7037(99)00285-9)
- Tamura H, Goto K, Yotsuyanagi T, Nagayama M (1974) Spectrophotometric determination of iron(II) with 1,10-phenanthroline in the presence of large amounts of iron(III). *Talanta* 21: 314-318. [https://doi.org/10.1016/0039-9140\(74\)80012-3](https://doi.org/10.1016/0039-9140(74)80012-3)
- Tamura H, Goto K, Nagayama M (1976) The effect of ferric hydroxide on the oxygenation of ferrous ions in neutral solutions. *Corros. Sci.* 16: 197-207. [https://doi.org/10.1016/0010-938X\(76\)90046-9](https://doi.org/10.1016/0010-938X(76)90046-9)
- Tamura H, Kawamura S, Hagayama M. (1980). Acceleration of the oxidation of Fe²⁺ ions by Fe(III)-oxyhydroxides. *Corros. Sci.* 20: 963-971. [https://doi.org/10.1016/0010-938X\(80\)90077-3](https://doi.org/10.1016/0010-938X(80)90077-3)

References

- Tarutis W, Stark L, Williams F (1999) Sizing and performance estimation of coal mine drainage wetlands. *Ecol. Eng.* 12: 353-372. [https://doi.org/10.1016/S0925-8574\(98\)00114-1](https://doi.org/10.1016/S0925-8574(98)00114-1)
- Tremblay G, Hogan C (2001) Mine Environment Neutral Drainage Manual Vol. 4 – Prevention and Control. MEND Report 5.4.2d, Ottawa, 352 pp.
- Umweltbundesamt (2016) Die Wasserrahmenrichtlinie – Deutschlands Gewässer 2015. Federal Ministry for the Environment, Nature Conservation and Nuclear Safety (Eds.), Dessau, 144 pp
- United States Environmental Protection Agency (2014) Reference Guide to Treatment Technologies for Mining-Influenced Water. EPA 542-R-14-001, Washington, 94 pp
- van Beek C, Hiemstra T, Hofs B, Nederlof M, van Paassen J, Reijnen G (2012). Homogeneous, heterogeneous and biological oxidation of iron(II) in rapid sand filtration. *J. Water Supply Res. Technol.* 61: 1-13. <https://doi.org/10.2166/aqua.2012.033>
- Verschoren V, Schoelynck J, Cox T, Schoutens K, Temmerman S, Meire P (2017) Opposing effects of aquatic vegetation on hydraulic functioning and transport of dissolved and organic particulate matter in a lowland river: A field experiment. *Ecol. Eng.* 105: 221-230. <https://doi.org/10.1016/j.ecoleng.2017.04.064>
- Vikesland P, Rebodos R, Bottero J, Rose J, Masion A (2016) Aggregation and sedimentation of magnetite nanoparticle clusters. *Environ. Sci. Nano* 3: 567-577. <https://doi.org/10.1039/C5EN00155B>
- von Sperling M (2002) Relationship between first-order decay coefficients in ponds, for plug flow, CSTR and dispersed flow regimes. *Water Sci. Technol.* 45: 17-24. <https://doi.org/10.2166/wst.2002.0003>
- Wan Y, Wu H, Roelvink D, Gu F (2015) Experimental study on fall velocity of fine sediment in the Yangtze Estuary. *Ocean Eng.* 103: 180-187. <https://doi.org/10.1016/j.oceaneng.2015.04.076>
- Wang N, Deng N, Qiu Y, Su Z, Hunag C, Hu K, Wang J, Ma L, Xiao E, Xiao T (2020) Efficient removal of antimony with natural secondary iron minerals: Effect of structural properties and sorption mechanism. *Environ. Chem.* 17: 332-344. <https://doi.org/10.1071/EN20002>
- Watzlaf G, Schroeder K, Kleinmann R, Kairies C, Nairn R (2004) The Passive Treatment of Coal Mine Drainage. DOE/NETL-2004/1202, Pittsburgh, 72 pp
- Wegelin M (1996) Surface water treatment by roughing filters – A design, construction and operation manual. Swiss Centre for Development in Technology and Management, SANDEC Report 2/96, St. Gallen, 163 pp
- Wehrli B, Sulzberger B, Stumm W (1989) Redox processes catalyzed by hydrous oxide surfaces. *Chem. Geol.* 78: 167-179. [https://doi.org/10.1016/0009-2541\(89\)90056-9](https://doi.org/10.1016/0009-2541(89)90056-9)
- Weiss J (1935). Elektronenbergangsprozesse im Mechanismus von Oxydations- und Reduktionsreaktionen in Lösungen. *Sci. Nat.* 23: 64-69. <https://doi.org/10.1007/BF01497021>
- Whitehead P, Prior H (2005) Bioremediation of acid mine drainage: an introduction to the Wheal Jane wetlands project. *Sci. Total Environ.* 338: 15-21. <https://doi.org/10.1016/j.scitotenv.2004.09.016>
- Wieder R (1989) A survey of constructed wetlands for acid coal mine drainage treatment in the eastern United States. *Wetlands* 9: 299-315. <https://doi.org/10.1007/BF03160750>
- Wildemann T, Brodie G, Gusek J (1993) Wetland design for mining operations. BiTech Publishers, 230 pp.
- Xiao F, Yi P, Pan X, Zhang B, Lee C (2010) Comparative study of the effects of experimental variables on growth rates of aluminum and iron hydroxide flocs during coagulation and their structural characteristics. *Desalination* 250: 902-907. <https://doi.org/10.1016/j.desal.2008.12.050>
- Yazbek L, Cole K, Shedleski A, Singer D, Herndon E (2021) Hydrogeochemical processes limiting aqueous and colloidal Fe export in a headwater stream impaired by acid mine drainage. *ACS ES&T Water* 1: 68-78. <https://doi.org/10.1021/acsestwater.0c00002>
- Younger P (2000) The adoption and adaptation of passive treatment technologies for mine waters in the United Kingdom. *Mine Water Environ.* 19: 84-97. <https://doi.org/10.1007/BF02687257>
- Younger P, Banwart S, Hedin R (2002) Mine Water – Hydrology, Pollution, Remediation. Springer Science, 442 pp. <https://doi.org/10.1007/978-94-010-0610-1>

Abbreviations

AAS	Atomic absorption spectrometry (e.g. flame or graphite tube)
AMD	Acid mine drainage
AML	Abandoned mine land (criteria)
BAT	Best available technology economically achievable
BPT	Best practicable control technology currently available
DLVO-Theory	Theory by Derjaguin, Landau, Verwey and Overbeek
EC	European Commission
EPA	Environmental Protection Agency
ERMITE	Environmental Regulation of Mine Waters in the European Union
EU-H2020	European Union Horizon 2020 framework programme
HRT	Hydraulic retention time
ICP-OES	Inductively coupled plasma optical emission spectrometry
IEP	Isoelectric point
NCB	National Coal Board
NOM	Natural organic matter
PHREEQC	pH-redox-equilibrium code (<i>computer program</i>)
PIRAMID	Passive In-situ Remediation of Acidic Mine / Industrial Water
RTD	Residence time distribution
SI	Supporting information
TRL	Technology readiness level
TSS	Total suspended solids
VFR	Vertical flow reactor
WFD	Water framework directive (EU directive 2000/60/EC)
XRD	X-ray diffraction

Glossary

A	Surface area	m^2
A_F	Cross sectional filter area	m^2
h	Height or (water) depth	m
V	Volume	m^3
Q	Flow rate	m^3/h
v_F	Flow or filter velocity	m/h
P	Porosity	%
t	Time / Hydraulic retention time	h
$[Fe]$	Iron concentration	mg/L
$[Fe]_0$	Initial iron concentration (<i>in column experiments</i>)	mg/L
$[Fe]_i$	Iron concentration at t_i (<i>in column experiments</i>)	mg/L
$[Fe]_{in}$	Inflow iron concentration	mg/L
$[Fe]_{out}$	Outflow iron concentration	mg/L
$[Fe(II)]$	Ferrous iron concentration	mg/L
$[Fe(III)]$	Ferric iron concentration	mg/L
$[Fe(OH)_3]$	Concentration of hydrous ferric oxides	mg/L
$[Fe(tot)]$	Total iron concentration	mg/L
$[Ochre]$	Sedimented iron	mg/L
P_{O_2}	Oxygen partial pressure	atm
$[O_2]$	Dissolved oxygen concentration	mg/L
$\{OH^-\}$	Hydroxide ion activity	mol/L
$\{H^+\}$	Proton activity	mol/L
$[Turb.]$	Turbidity (<i>measured in-situ</i>)	FNU
R_A	Area-adjusted (iron) removal rate	$g/m^2/d$
R_V	Volume-adjusted (iron) removal rate	$g/m^3/d$
k_{ox}	Homogeneous ferrous iron oxidation coefficient	$mol/L/h$
k'_{ox}	Pseudo first-order ferrous iron oxidation coefficient	h^{-1}
k_{het}	Heterogeneous ferrous iron oxidation coefficient	$L/mg/h$
k_{sed}	Sedimentation coefficient	h^{-1}
k'_{sed}	Higher-order sedimentation coefficient	$m^3/g/h$
SF	Safety factor	-

Acknowledgements

Project-related acknowledgements

The research project was funded and supported by the German Environmental Foundation (project no. 33012/01-23). I am especially grateful for the constant support and encouragement by Franz-Peter Heidenreich, whose belief in the project allowed us to unlock our full potential.

The project was supported by Uniper Kraftwerke GmbH by providing administrative support and access to the Westfield study site. A special thanks goes to Hans Förner for his support of, and deep interest in, this research project from day one.

I am grateful for the support of the University of Bayreuth Graduate School that allowed me to continue my studies and to participate in national and international scientific conferences.

Finally, a sincere thanks goes to the members of the project advisory board, Jörg Frauenstein, Brigitte Freilinger, Franz-Peter Heidenreich, Günther Michler³, Jörn-Helge Möller, Martin Roth, Prof. Dr. Reinhard Niessner, Hans Förner and Dr. Wolfgang Schäfer for their constant interest, lively discussions, encouragement, and technical advice.

Personal acknowledgements

First, I would like to thank Matthias Alte, Stefan Peiffer, and Martin Bauer for their supervision and for making this integrated research project possible in the first place, sparing neither pains nor expenses to bring the project to a successful conclusion. The doctoral studies under their supervision were characterised by lively, fruitful discussions on the one hand and a high level of independence and self-responsibility on the other hand. I really got to appreciate both.

Thanks also to BASE TECHNOLOGIES GmbH and the entire team for constant support and advice throughout the “Wetland” project. A special thanks goes to Christian Böckl, David Dohle, and Michael Degner for invaluable assistance during the construction and operation phase of the Westfield pilot plant as well as to Stephanie Stief for the painstaking transformation of endless data loggings and laboratory records into a workable state.

Second, illimitable thanks go to Jutta Eckert as the one person who accompanied me every step of the way, both in the field and in the laboratory. Without her constant support, tireless dedication, cheerful and forbearing attitude as well as knowledge of every trick in the book, the workload would have been simply impossible. On top of that, she was somehow always able to acquire the necessary equipment and chemicals on short(est) notice, either by being remarkably flexible or by knowing whom to bribe on campus with a cake or a good turn. Thanks also to the technical staff of the Hydrology Department, Martina Rohr, Luisa Hopp, Silke Hammer, and Isolde Baumann for meticulous assistance with sample analyses. I am also grateful to my fellow PhD students and postdocs, especially Johanna, Jan-Pascal, Kerstin, and Karel for additional measurements, lively discussions, and access to special equipment.

Last but not least, I would like to thank all my family and friends who stood by me throughout the years despite limited time and erratic temper on my part. A very special thanks goes to those who unexpectedly came up with emotional support, food, or equipment during especially challenging (or cold) times – even at the “remote” project site or in the cellar lab in Bayreuth. To those who were always able to make me laugh or rest, irrespective of workload and time of day. Those who voluntarily spellchecked or revised early versions of manuscripts or this very thesis, irrespective of their own interest in the finer details of mine water geochemistry. Thanks first and foremost to Isabel and Denise, thanks also to my family, to Simon, Linda, Jens, Kathi, Matthias, Tom, Melli, Eva, Peter, Steffi, Lena, and all those who kept my head above water.

³ After the retirement of Günther Michler, the Water Authority Weiden was represented by Sonja Kraus and Daniela Schikora, whom I would also like to cordially thank for their readiness to step in.

Appendix (publications)

List of journal articles

- Opitz J, Alte M, Bauer M, Peiffer S (2020) Quantifying iron removal efficiency of a passive mine water treatment system using turbidity as a proxy for (particulate) iron. *Appl. Geochem.* 122: 104731. <https://doi.org/10.1016/j.apgeochem.2020.104731>
- Opitz J, Alte M, Bauer M, Peiffer S (2021) The role of macrophytes in constructed surface-flow wetlands for mine water treatment: A review. *Mine Water Environ* 40(3): 587-605. <https://doi.org/10.1007/s10230-021-00779-x>
- Opitz J, Bauer M, Eckert J, Peiffer S, Alte M, (2022) Optimising operational reliability and performance in aerobic passive mine water treatment: The multistage Westfield pilot plant. *Water Air Soil Pollut.* 233: 66. <https://doi.org/10.1007/s11270-022-05538-4>
- Opitz J, Bauer M, Alte M, Schmidtman J, Peiffer S (2022) Sedimentation kinetics of hydrous ferric oxides in ferruginous, circumneutral mine water. *Environ. Sci. Technol.* 56(10): 6360-6368. <https://doi.org/10.1021/acs.est.1c07640>
- Opitz J, Alte M, Bauer M, Peiffer S (2023) Development of a novel sizing approach for passive mine water treatment systems based on ferric iron sedimentation kinetics. *Water Res.* 233: 119770. <https://doi.org/10.1016/j.watres.2023.119770>

In preparation:

- Opitz J, Alte M, Bauer M, Peiffer S: A review of natural iron transformation and removal mechanisms in passive systems for treatment of circumneutral mine water.



List of conference papers / abstracts and presentations

- Opitz J, Alte M, Peiffer S (2018) Design and sizing of passive systems for treatment of circum-neutral ferruginous mine water. BayCEER Workshop, 11.10.2018, Bayreuth, O1.5
- Opitz J, Alte M, Bauer M, Peiffer S (2019) Testing iron removal in a trifurcated pilot plant for passive treatment of circum-neutral ferruginous mine water. In: Proc. IMWA Conference, 15.-19.07.2019, Perm, Volume 1: 256-261
- Opitz J (2020) Customised sizing of a sustainable passive mine water treatment systems: Successful upscaling of a pilot plant. International Forum Contest XVI – Topical Issues of Rational Use of Natural Resources, 17.-19.06.2020, St. Petersburg, Session 8.1

List of project reports

- Deutsche Bundesstiftung Umwelt – 1. *Zwischenbericht* (Az. 33012/01-23): Modellhafte Anwendung und Weiterentwicklung eines naturnahen, passiv-biologischen Verfahrens ohne Energie- und Chemikalieneintrag zur nachhaltigen Aufbereitung kontaminierter Bergbauabwässer. Von: BASE TECHNOLOGIES GmbH | Universität Bayreuth, Mai 2018
- Deutsche Bundesstiftung Umwelt – 2. *Zwischenbericht* (Az. 33012/01-23): Modellhafte Anwendung und Weiterentwicklung eines naturnahen, passiv-biologischen Verfahrens ohne Energie- und Chemikalieneintrag zur nachhaltigen Aufbereitung kontaminierter Bergbauabwässer. Von: BASE TECHNOLOGIES GmbH | Universität Bayreuth, Mai 2019
- Deutsche Bundesstiftung Umwelt – 3. *Zwischenbericht* (Az. 33012/01-23): Modellhafte Anwendung und Weiterentwicklung eines naturnahen, passiv-biologischen Verfahrens ohne Energie- und Chemikalieneintrag zur nachhaltigen Aufbereitung kontaminierter Bergbauabwässer. Von: BASE TECHNOLOGIES GmbH | Universität Bayreuth, April 2020
- Deutsche Bundesstiftung Umwelt – *Abschlussbericht* (Az. 33012/01-23): Modellhafte Anwendung und Weiterentwicklung eines naturnahen, passiv-biologischen Verfahrens ohne Energie- und Chemikalieneintrag zur nachhaltigen Aufbereitung kontaminierter Bergbauabwässer. Von: BASE TECHNOLOGIES GmbH | Universität Bayreuth, September 2021

Study 1 – Appl. Geochem. 122: 104731

Title	Quantifying iron removal efficiency of a passive mine water treatment system using turbidity as a proxy for (particulate) iron
Authors	Opitz J, Alte M, Bauer M, Peiffer S
Status	Published
Year	2020
Journal	Applied Geochemistry
Article	122: 104731
Pages	9
DOI	10.1016/j.apgeochem.2020.104731
SI	 No Supporting Information
Access	 http://sciencedirect.com/science/article/abs/pii/S0883292720302237 © Elsevier Ltd.



Relative contribution of the PhD student to study 1:

- Study design 60%
- Data collection and field work 60%
- Laboratory work 10%
- Data processing and analysis 80%
- Evaluation 80%
- Manuscript preparation 90%

JO, MA, MB, and SP designed the study, including setup and monitoring of the Westfield pilot plant. JO, MA, JE, and others were responsible for construction (and construction supervision) of the pilot plant. JO and JE planned and conducted both field and laboratory work, with samples and field parameters predominantly collected by JO, and chemical analyses predominantly conducted by JE. The data was processed and analysed by JO and SP, with further evaluation supported by MA and MB. JO prepared a first draft as well as figures and tables for the manuscript with input from all co-authors. All authors jointly finalised and submitted the manuscript. JO is the corresponding author.

JO: Joscha Opitz // MA: Matthias Alte // MB: Martin Bauer // JE: Jutta Eckert // SP: Stefan Peiffer



Quantifying iron removal efficiency of a passive mine water treatment system using turbidity as a proxy for (particulate) iron

Joscha Opitz^{a,b,*}, Matthias Alte^b, Martin Bauer^b, Stefan Peiffer^a

^a University of Bayreuth, Department of Hydrology, Universitätsstraße 30, 95447, Bayreuth, Germany
^b Base Technologies GmbH, Josef-Felder-Straße 53, 81241, Munich, Germany

ARTICLE INFO

Editorial handling by Prof. M. Kersten

Keywords:
Mine water
Turbidity
Iron
Mass balance
Passive treatment

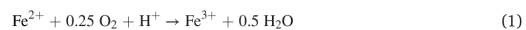
ABSTRACT

Passive treatment systems are frequently used for the removal of iron from circum-neutral, ferruginous mine discharges. Upon oxygenation, iron is quickly oxidised and precipitated, and thus predominantly present as particulate hydrous ferric oxide. The objective of this study was to quantify whether turbidity as continuously monitored via in-situ sensors could serve as a surrogate for particulate iron throughout a passive treatment system. Accordingly, a statistical relationship between turbidity and particulate iron was established for a ferruginous, circum-neutral seepage water flowing through a passive pilot plant at an abandoned mine site with $c(\text{Fe}_{\text{part}}) = 0.092 \times [\text{Turb}] + 0.031$. The multi-stage pilot plant was equipped with ten fixed turbidity sensors to obtain a high-resolution dataset for exploitation of the near-monocausal turbidity-iron-relationship. The statistical proxy-relationship obtained from extensive monitoring by way of linear regression allowed approximate conversion of continuously monitored turbidity to particulate iron concentration with reasonable degree of accuracy. The conversion was used to describe iron transport and removal at the 30-min logging interval of the turbidity sensors and to establish a corresponding high-resolution mass balance for the pilot plant. This high-resolution mass balance showed that simpler mass balances based on overall averages or frequent, yet episodic semi-weekly samplings tended to considerably overestimate iron mass flow and accumulation due to the temporal variability in hydraulic loading, especially during weekends. Therefore, continuous monitoring of turbidity as a proxy for iron can provide a more accurate estimate of iron removal and hence an improved assessment of the iron mass balance, especially if flow rate and/or inflow concentration are subject to fluctuations. Since iron is the decisive compliance parameter on site, the correlation can be used to greatly improve data resolution (in this study from semi-weekly to 30-min interval) and quality as well as cost efficiency of monitoring efforts.

1. Introduction

Turbidity and iron are crucial monitoring parameters in the field of water treatment, particularly wastewater treatment and drinking water purification. In aquatic environments, iron occurs either as ferrous (divalent) or ferric (trivalent) species. Dissolved iron concentrations are low at thermodynamic equilibrium unless the aquatic system is anaerobic, extremely acidic or basic (Stumm and Morgan, 1996). In oxygenated and neutral systems, ferrous iron is rapidly oxidised to ferric iron, which in turn precipitates as metastable hydrous ferric oxide, ultimately transforming to a variety of stable (oxyhydr)oxides (Cornell and Schwertmann, 2003; Cornell et al., 1989). Consequently, iron is predominantly present as colloidal or particulate suspended matter at

circum-neutral pH:



Turbidity of aquatic media is measured via light intensity decrease resulting from attenuation (adsorption, scattering, backscattering) by waterborne particulate matter. Thus, one can infer that the turbidity of a liquid is ultimately a bulk parameter determined by the concentration of suspended matter and their light scattering and absorbing effects. Hence, correlations or (site-specific) surrogate relationships may be established between turbidity and TSS matrix (e.g. Filip et al., 1974;

* Corresponding author. University of Bayreuth, Department of Hydrology, Universitätsstraße 30, 95447, Bayreuth, Germany.
E-mail address: joscha.opitz@uni-bayreuth.de (J. Opitz).

<https://doi.org/10.1016/j.apgeochem.2020.104731>

Received 25 April 2020; Received in revised form 7 August 2020; Accepted 10 August 2020

Available online 15 August 2020

0883-2927/© 2020 Elsevier Ltd. All rights reserved.

Harter and Mitsch, 2003; James et al., 2004; Rügner et al., 2014). If suspended matter is dominated by suspended solids, statistical relationships may be derived between turbidity and iron concentration as was demonstrated by Filip et al. (1974) in the filter effluent of a drinking water treatment plant at low iron content (<1 mg/L). It is to be expected that similar relationships may be established in ferruginous aquatic environments such as typically found in the mining or metallurgical industry. In several cases, statistical relationships of iron and associated metals with bulk parameters of dissolved or particulate species such as turbidity, TDS, TSS and specific conductivity as well as metal concentrations in sediments deposited along the flow path have been investigated to analyse or model transport and disposal mechanisms in surface water systems (e.g. Butler and Ford, 2018; Church et al., 1997; Davis et al., 1991; Hubert and Wolkersdorfer, 2015; Galván et al., 2012; Skarbøvik et al., 2012; Thomson et al., 1997). For example, Rügner et al. (2014) found statistical correlations between turbidity, TSS and particle-associated contaminants such as PAHs that helped to estimate contaminant transport on a catchment scale. Especially in waters or watersheds influenced by acid mine drainage (AMD), strong relationships and even direct correlations were observed between suspended hydrous ferric oxides and particulate matter as well as other AMD-typical metals associated with and transported by suspended matter (e.g. Karlsson et al., 1988; Kimball et al., 1995; Lee and Cheong, 2016; Sarmiento et al., 2012; Schemel et al., 2000). Lee and Cheong (2016) showed that evolution of turbidity in oxidation ponds apparently resembled the development of iron during oxidation, precipitation and sedimentation yet did not further investigate potential relationships. Recently, Cánovas et al. (2017) reported statistical relationships between not only turbidity and iron, but also turbidity and other contaminants in mining-impacted surface waters yet did not further exploit these relationships. To our knowledge, in no instance was turbidity directly utilised to estimate contaminant and especially iron loads transported by mining-impacted flowing waters or through a passive treatment system.

Aerobic passive systems for treatment of ferruginous, neutral mine water utilise and enhance natural (geo)chemical, biological and physical processes for removal of hydrolysable metals, thereby saving costs, resources and energy (Skousen et al., 2017). Removal of predominantly iron and aluminium is achieved by providing hydraulic retention time in surface-flow ponds and wetlands (at times complemented by filter units) for ferrous iron oxidation followed by sedimentation or filtration of particulate hydrous ferric oxides. In neutral mine waters, turbidity as a measure of suspended solids predominantly includes particulate metal (hydr)oxides together with natural solids such as clastic erosion material and natural organic matter. Consequently, turbidity may be a good indicator of progressing iron removal in circumneutral, thoroughly oxygenated mine waters.

The turbidity of a liquid is measured both in-situ using mobile or fixed sensors and ex-situ by measuring samples in hand-held turbidimeters ("nephelometers"). By combining turbidity sensors with a logging device, turbidity can be continuously monitored in high resolution. In contrast, iron in aqueous environments is determined ex-situ almost exclusively. Hand-collected samples are stabilised and analysed by respective field or laboratory instruments. Emerging auto-sampling/analysing equipment is costly both in acquisition and maintenance, which is why monitoring of iron and other contaminants in aqueous environments is predominantly conducted via sample collection and analysis. This manual procedure is laborious, time-consuming and costly, and respective datasets are fragmentary and low-resolution (Chapin, 2015; Frau et al., 2018; Nimick et al., 2003). Analyses of individual grab samples (even at daily routine) only represent snapshots of the actual conditions and are therefore considered insufficient for detailed documentation of general variability as well as transient environmental events or diurnal cycles (e.g. Chapin, 2015; Korostynska et al., 2013; O'Flynn et al., 2010; Revitta et al., 2004; Skarbøvik et al., 2012).

In this study, the relationship between turbidity and iron content was studied in a pilot passive mine water treatment system consisting of three consecutive stages (settling ponds, wetlands, sediment filters). The main objective was to derive a site-specific correlation between turbidity and iron to test the suitability of turbidity to establish a high-resolution iron mass balance for the passive system. Conversion of turbidity monitoring data to (particulate) iron would allow to detail transport and removal of iron within the pilot plant. For this purpose, the system was equipped with numerous fixed turbidity sensors. As the water is circum-neutral and thoroughly oxygenated, iron is almost exclusively and abundantly present as suspended hydrous ferric oxide, hence assumingly dominating turbidity. The relationship was thoroughly investigated by (1.) analysis of settled solids as representative fraction of formerly suspended particulate matter, (2.) evaluation of available monitoring data of continuously monitored turbidity and discontinuously sampled and analysed iron and (3.) an experimental dilution series using mine water and particles sampled on site to empirically reproduce the statistical field relationship between turbidity and iron under controlled conditions. The results were discussed regarding application of statistical relationships between easily measured (bulk-) parameters and laboriously monitored individual parameters with a focus on resolution and cost-effectiveness of monitoring efforts.

2. Materials and methods

2.1. Study site

The study site is located near Wackersdorf in the former lignite district of Upper Palatinate, Germany (Fig. 1). The mined open pit was subsequently used as a landfill for disposal of waste rock and overburden as well as bottom and electrostatic precipitator ash from a lignite-fired power plant. Seepage water at the lowest point of the remaining morphological depression is highly mineralised and contaminated with mining- and ash-typical substances, particularly iron, sulphate, chloride and manganese as well as alkali and alkaline earth metals (Table 1). Due to the predominantly alkalisating ashes, seepage water is circum-neutral with pH 7.1–7.5 (interquartile range) despite substantial formation of AMD in the surrounding mined land. For protection of adjacent aquifers, the seepage water is pumped out to a chemical treatment plant for iron removal before discharge to receiving surface waters (Opitz et al.,



Fig. 1. Study site.

Table 1
 Raw water chemistry: Average and standard deviation of selected parameters 2011–2020 (n = 111).

EC [mS/cm]	pH [-]	K _{s1,3} ^a [mM]	K _{b,2} ^a [mM]	Fe [mg/L]	Al [mg/L]	Mn [mg/L]	SO ₄ [mg/L]	Cl [mg/L]	Ca [mg/L]	Mg [mg/L]	K [mg/L]	Na [mg/L]
2.83 ± 0.3	7.3	2.5 ± 0.4	0.4 ± 0.2	9.3 ± 4.2	0.5 ± 0.4	1.3 ± 0.3	1784 ± 298	202 ± 79	576 ± 68	96.2 ± 18	67.0 ± 10	146 ± 35

^a Acid capacity to pH 4.3 and base capacity to pH 8.2.

2020).

The groundwater in proximity of the seepage area is highly ferruginous with iron concentrations (predominantly ferrous) exceeding 100 mg/L. Seepage water is collected in a sump and temporary impounded for discontinuous pump operation. Consequently, raw water entering the treatment plant is thoroughly oxygenated with average oxygen saturation and ORP of 88% and 104 mV, respectively, which is why iron concentrations (predominantly ferric) are reduced by an order of magnitude.

A trifurcated pilot plant for aerobic removal of iron via oxidation, precipitation and sedimentation or filtration was installed next to the conventional treatment plant as part of an ongoing research project on the suitability of passive treatment for long-term seepage water management (Opitz et al., 2019). Both turbidity and iron are intensively monitored at ten measuring points consecutively numbered MP01-MP10 for documentation of progressing iron removal. MP01 represents the system inflow from a distribution tank ("reservoir") and MP02-MP10 represent measuring points following successive parallel treatment/sampling stages in the trifurcated system (Fig. 2). MP02-MP04 stand for settling ponds for preliminary treatment, MP05-MP07 stand for constructed aerobic wetlands for fine treatment and MP08-MP10 stand for sediment filters for purification (also representing outflows). A description of pilot plant and monitoring scheme is documented in Opitz et al. (2019).

2.2. Methodology

Settled solids accumulated over approximately one year were collected in open sediment traps directly below the fixed turbidity sensors at all measuring points as a characterising sample of suspended particulate matter passing by the sensors. Sediments from parallel measuring points were blended, yielding a total of four bulk samples, namely inflow (MP01) as well as settling pond effluents (MP02-MP04), wetland effluents (MP05-MP07) and sediment filter effluents (MP08-MP10).

MP10). Solids were freeze-dried and sieved to <2 mm for removal of larger depositions unrepresentative of suspended particulate matter settled from the seepage water. Six subsamples per bulk sample were analysed for elemental composition via microwave-assisted aqua regia digestion and ICP-OES.

In the context of this study, turbidity measurements were solely conducted nephelometrically by measuring the intensity of scattered light at an angle of 90° to a light source, in this case LEDs emitting infrared light in the wavelength range of 860 nm according to ISO 7027. Measurement results are given in Formazine Nephelometric Units [FNU]. All measuring points in the pilot plant are equipped with fixed cable sensors for measuring turbidity (WTW VisoTurb®700 IQ). The sensors are connected to data loggers (WTW MIQ/TC, 2020 3G-EF) for automatic data logging every 30 min. Turbidity loggings are moving weighted median values across 1-min intervals.

Two samples, one of which filtered (0.45 µm), were collected next to the fixed sensors in sterile 15 mL PP-tubes for laboratory analysis. Filtered samples were acidified with 150 µL of 1 M HCl to immediately quench ferrous iron oxidation, whereas unfiltered samples were acidified with 150 µL of 12 M HCl to additionally re-dissolve hydrous ferric oxides. Samples were cooled to 4 °C and transported to the laboratory for spectrophotometric analysis using acetate buffer solution and 1,10-phenantroline at 512 nm. Total iron was measured by reducing ferric to ferrous iron with ascorbic acid. The spectrophotometer (Hach DR 3800 VIS) was calibrated using standard solutions prepared with high-purity Fe(II)chloride dissolved in degassed water and acidified with 1 M HNO₃. All chemicals were analytical grade.

Filtered samples were analysed for dissolved ferrous and total iron. Unfiltered samples were analysed for total iron. Particulate iron was calculated by subtracting total dissolved (filtered sample) from total iron (unfiltered sample). Thus, the conceptual approach allowed not only the determination of dissolved species, but also particulate and total content (Butler et al., 2008; Hedin, 2008). It should be noted that freshly precipitated colloidal hydrous ferric oxides as small as 1 × 10⁻⁷ m pass

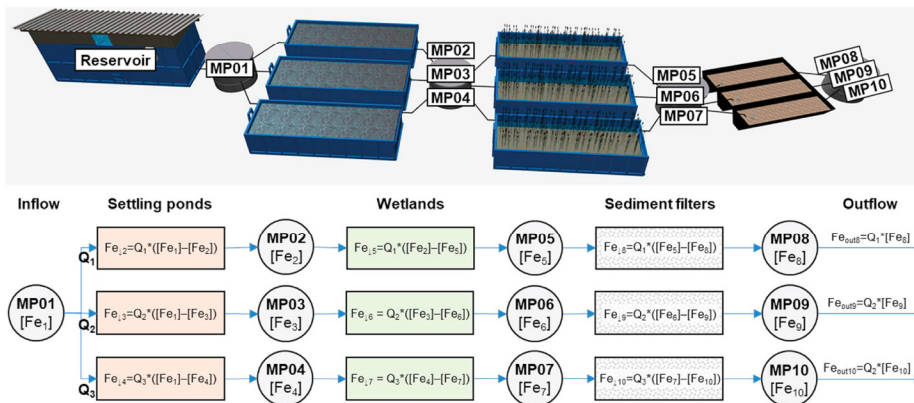


Fig. 2. Schematics of pilot plant and mass balance model with Q as flow rates, [Fe], Fe₁ and Fe_{out} as iron concentration, removed iron mass and effluent iron mass, respectively.

the 0.45 µm syringe filters and are thus analysed as part of the dissolved phase (Hoffmann et al., 1981; Kimball et al., 1992; Taillefert et al., 2000). Therefore, technical differentiation between dissolved and particulate iron as <0.45 µm and ≥0.45 µm, respectively, may cause a slight discrepancy between turbidity and iron data and the resultant correlation by omitting nanoparticulate solids from the particulate fraction (Taillefert et al., 2000). However, differentiating at 0.45 µm has become common practice despite the fact that submicron particles might pass respective filters (Filella, 2007). Since in circum-neutral, thoroughly oxygenated ferruginous waters freshly precipitated hydrous ferric oxides are metastable toward larger colloids and particles due to aggregation and crystal growth effects (Baumgartner and Faivre, 2015; Cornell et al., 1989), the resultant inaccuracy was considered small enough to be accepted for practical purposes. For the sake of completeness, dissolved iron was also considered to investigate potential effects of colloids.

For the dilution series, a bulk sample of ≈2 L was collected from the pilot plant inflow (MP01) and transported to the laboratory. A small amount of freeze-dried ocherous sludge collected from the reservoir was added to the bulk sample to bring turbidity up to approximately 1.000 FNU. The sample was left in a magnetic stirrer overnight for homogenisation at 300 rpm. Incremental subsamples were taken under constant stirring, injected into 50 mL PP-tubes and brought to volume with Millipore water to obtain a range of sample:water ratios. Diluted samples were thoroughly shaken and immediately split up three ways with two 15 mL subsamples (filtered and unfiltered) for iron analysis as described above and one subsample in a 20 mL cuvette for immediate turbidity measurement in a hand-held nephelometer (WTW pHotoFlex®Turb). Turbidity was measured thrice in quick succession and results were averaged to minimise possible variations (Gregory, 1985). The nephelometer was calibrated prior to measurements using manufacturer-adjusted formazine standards (WTW AMCO Clear®) with 0.02, 10 and 1.000 FNU.

2.3. Data collection and processing

After an adequate start-up time, research monitoring of the pilot plant started in July 2018 and continues to date, with data up to December 2019 considered in this study (452 days). Flow rates in the three system lines were adjusted by ball valves and, except for the first 9 days, continuously monitored by flowmeters with magnetic floats and reed sensor chains (Stübbe DFM200) connected to a data logger at a 30-sec interval (minimum). Water samples for iron analysis were taken approximately twice a week at all measuring points. To correlate continuous turbidity data with discontinuous iron data, each iron analysis was matched with the average of turbidity recordings in an interval of ±15 min around the respective sampling time. The resultant correlation was used to convert turbidity measurements to particulate iron concentration. For the dilution series, a total of 18 samples were examined including dilution factors 1.000, 800, 500, 400, 250, 100, 50, 25, 20, 10, 5, 4, 2.5, 2, 1.5, 1.25, 1.1 and 1.02. This theoretically leads to the following overall datasets (assuming no errors and before data cleansing):

- 216 960 turbidity measurements at a 30-min interval (21 696 per MP);
- 1200 iron analyses at a semi-weekly interval (120 per MP);
- 24 sediment analyses (6 per sampling stage);
- 18 turbidity-iron data pairs from the dilution series (18 dilution increments).

Data cleansing predominantly included removal of outliers in the order of several hundred FNU that occurred either due to maintenance measures (i.e. swirling up of flocs) or sensor errors owing to partial or full covering of sensor optics with ochre, pollen or small snails. Accordingly, most errors occurred in wetland effluents.

Finally, three mass balances were established:

- 1) **Overall mass balance** based on flow recordings and iron analyses both averaged over the entire monitoring period (1 data pair);
- 2) **Low-resolution mass balance** based on semi-weekly iron analyses and accordingly averaged flow rates (1200 data pairs);
- 3) **High-resolution mass balance** based on 30-min interval iron data derived from turbidity-iron-conversion and respectively averaged flow recordings (216 960 data pairs).

Iron mass leaving the overall system or individual components (Fe_{out}) was calculated by multiplying respective flow rates with concentrations and time interval according to equation (4). Iron mass removed in the overall system or individual components (Fe_{1}) was calculated by multiplying respective flow rates with the difference of inflow and outflow concentration and time interval according to equation (5):

$$Fe_{out_tot} = (Q_1 \times [Fe_8] + Q_2 \times [Fe_9] + Q_3 \times [Fe_{10}]) \times t \quad (4)$$

$$Fe_{1tot} = ((Q_1 + Q_2 + Q_3) \times [Fe_1] - (Q_1 \times [Fe_8] + Q_2 \times [Fe_9] + Q_3 \times [Fe_{10}])) \times t \quad (5)$$

with Fe_{1tot} as iron retained in the system during the time period t , $[Fe_{1-10}]$ as iron concentrations at MP01 to MP10 and Q_{1-3} as flow rates in lines 1 to 3 (Fig. 2). Results of the three mass balances were compared to investigate the effect of resolution on mass balances subject to fluctuating water and substance fluxes.

3. Results and evaluation

3.1. Solids

Solids from the first three sampling stages (inflow, settling pond effluents, wetland effluents) were visually similar and composed of amorphous ocherous sludge interspersed with darker blackish impurities. In contrast, solids collected after sediment filters were composed of a relatively homogeneous, fine-grained, greyish matrix. Only the wetland sample contained a noteworthy fraction >2 mm, mostly plant litter and snail shells. The amount of solids in sediment traps decreased substantially along the flow-path, with plentiful sludge at the inflow and only a tiny fraction after sediment filters. Unfortunately, quantification of accumulation rates was unfeasible with sediment traps exposed to the water current.

Elemental fractions of major cations are displayed in Table 2. As expected, iron is the major component in the first three sampling stages with similar concentrations in the range of 25–29%. Results are within the typical range of mine water treatment sludge iron content (20–53%) as compiled by Dudeney et al. (2003), although at the lower end. Further cations present at measurable concentration are Al, Ca, Mg and Mn with other metals such as Co, Cr, Cu, Pb and Zn negligible or below detection

Table 2
Average content and standard deviation of major cations in sediment samples [mg/g].

Sampling point	Al	Ca	Fe	Mg	Mn
MP01 (inflow)	43.2 ± 3.4	20.0 ± 0.3	253.6 ± 1.5	3.6 ± 0.3	3.6 ± 0.2
MP02-MP04	23.1 ± 0.5	49.9 ± 0.5	275.8 ± 3.0	3.2 ± 0.2	17.9 ± 0.5
MP05-MP07	19.4 ± 0.5	37.1 ± 0.7	285.4 ± 17.0	3.0 ± 0.2	24.7 ± 0.2
MP08-MP10	23.0 ± 0.7	17.0 ± 1.1	56.0 ± 2.4	12.5 ± 0.6	7.0 ± 0.6

limit (data not shown). Ca and Mg are likely either scavenged and co-precipitated by Fe or Mn (hydr)oxides (Ingri and Widerlund, 1994) or, in the case of Ca, precipitated as gypsum.

The totalled up sediment fraction of Fe, Al and Mn (hydr)oxides correspond well in the first three sampling stages with 62–64% assuming structural formulas $\text{Fe}(\text{OH})_3$, $\text{Al}(\text{OH})_3$ and MnO_2 . The remaining unknown fraction is composed of (allochthonous) organic and inorganic matter as indicated by visual and organoleptic inspection of the original samples as well as a small amount of silty material remaining after acid digestion. This relatively high non-iron fraction (ca. 33%) is likely attributable to wind exposition and a construction site road directly adjacent to the pilot plant. In contrast, iron concentrations are much lower in solids settled after sediment filters. Visual observation of the original sample, of which a substantial amount remained after acid digestion, and relatively increased Al and Mg indicated an inorganic, likely clastic sediment matrix resulting from abrasions and fines washed out of the granite filter gravel.

3.2. Statistical data evaluation

Linear regression analysis was used to evaluate the statistical relationship between turbidity and particulate iron for both dilution series and monitoring data with the level of significant correlation for all analyses set at $P \leq 0.05$ (95% confidence level). Coefficients of determination (R^2) were calculated to evaluate statistical significance. As was expected, neither visually evident nor statistically relevant relationships between turbidity and dissolved iron were found for dilution series and monitoring data (data not shown). Thus, no clear indications regarding the effect of dissolved or colloidal iron on turbidity were discernible. In contrast, excellent correlations were obtained between turbidity and particulate iron for dilution series and monitoring data with $R^2 = 0.986$ and 0.855, respectively (Fig. 3).

Fluctuation of the turbidity:iron ratio in the dilution series (Fig. 3A) was most likely due to inconsistent dispersion and light scattering/backscattering at (artificially induced) excessive particulate ferric (hydr)oxide concentrations (Gregory, 1985). Since turbidity in the pilot plant was typically <125 FNU (Fig. 3B) this is of no practical relevance. Scattered outliers of the monitoring dataset displayed in Fig. 3B are inevitable in near-natural open systems where sensor measurements and hand-collected samples may be disturbed by swirling up of flocs, staining of sensor optics, non-iron suspended matter, bioactivity or by the simple fact that iron and turbidity are not determined from one and the same sample with iron analysed from grab samples and turbidity continuously in-situ measured over a time interval. It should be noted that the linear regression in Fig. 3B is the overall regression for all measuring points. A distinct clustering of sampling stages in point clouds

is discernible by different colours and shapes of the symbols, nicely visualising progressing iron removal along the flow path.

Statistical parameters obtained from dilution series and monitoring data are compiled in Table 3. It should be noted that sediment filters were excluded from the statistical evaluation of the monitoring dataset because iron concentration in sediment filter effluents was invariably close to or below detection limit (only 15 out of 360 data pairs remaining). Hence, the sediment filter dataset was insufficient (in number) for statistical evaluation. This is in accordance with the small amount of solids found in sediment traps behind sediment filters and the deviating composition of the solids therein (see Table 2). The numeric effect of the remaining data pairs for sediment filter effluents on the overall correlation (and thus also on mass balances) was negligible with the effect only appearing on the fourth decimal place. For MPO1-MPO7, 731 of theoretical 840 measurements remained due to data cleansing and/or missing data, predominantly in wetland effluents (100 missing data pairs) where measurements were in most cases below detection limit, but also due to sensor errors and staining of sensor optics.

Although the freeze-dried, crystalline ferric (hydr)oxide used for the dilution series was not fully representative of suspended amorphous hydrous ferric oxides in the pilot plant, turbidity-iron-relationships obtained from monitoring data and dilution series were in good accordance with gradients almost even (rel. difference 3.3%). The y-intercept of the monitoring dataset was close to zero, whereas the negative y-intercept of the dilution series was presumably caused by the excessive floc load (y-intercept approaching zero for lower concentrations) or background turbidity caused by colloidal hydrous ferric oxides that passed filtration and/or suspended non-iron solids. Both dilution series and monitoring data showed strong linear relationships at the 95% confidence level. Uncertainty of the monitoring relationship was lower with only 2.3% of the overall turbidity:iron ratio average based on the 95% confidence interval. The larger element of uncertainty of the

Table 3
 Statistical parameters and regression equations for turbidity-iron-relationships.

Statistical parameters	Dilution series	Monitoring data
Sample size (% missing data)	18 (0%)	731 (13%)
Turbidity:iron ratio (average \pm SD)	12.4 \pm 3.0	11.1 \pm 3.5
95% confidence interval of the turbidity:iron ratio average (\pm 9%)	[11.0; 13.8] (\pm 11%)	[10.8; 11.3] (\pm 2.3%)
p-value	2.6E-16	2.6E-308
Residual standard deviation s_y	3.479	1.016
Process standard deviation s_{σ_0}	39.3 FNU	11.0 FNU
Linear function	$c(\text{Fe}_{\text{part}}) = 0.089 \times [\text{Turb}] - 1.137$	$c(\text{Fe}_{\text{part}}) = 0.092 \times [\text{Turb}] + 0.031$

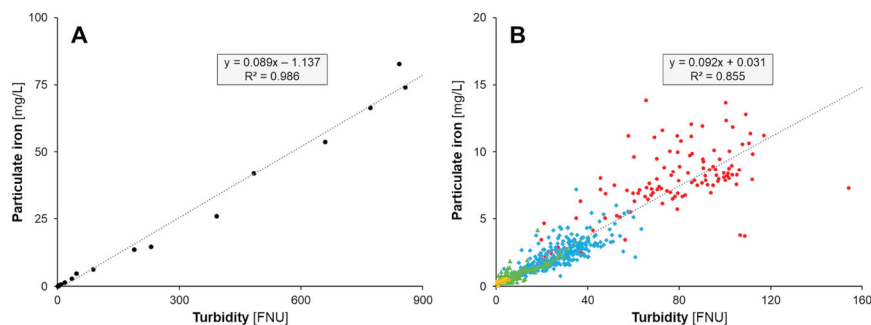


Fig. 3. Scatter plots showing correlations of particulate iron with turbidity for (A) dilution series with laboratory data as black circles and (B) monitoring data with MPO1 as red circles, MPO2-MPO4 as blue diamonds, MPO5-MPO7 as green triangles, MPO8-MPO10 as orange squares and overall linear regressions as dotted lines. (For interpretation of the references to colour in this figure legend, the reader is referred to the Web version of this article.)

dilution series was likely attributable to the small data sample where exclusion of one or more data pairs may inordinately affect the statistical relationship. Altogether, the linear function derived from the monitoring dataset was chosen for the following turbidity-iron-conversion since it was ultimately representative of the pilot plant. The statistical relationship was considered adequate and sufficiently robust for monitoring-related turbidity-iron-conversion as well as for estimation of mass flows and removal rates due to the large sample size, good coefficient of determination and reasonable element of uncertainty as displayed by statistical figures in [Table 3](#).

3.3. Mass balances

Overall flow rate in the pilot plant was about 800 L/h, evenly distributed at about 270 L/h per system line during the first 113 days and varied between 100 and 500 L/h afterwards ([Opitz et al., 2019](#)). Fluctuations in one or two system lines were inevitable subject to filling level variations in the reservoir. Missing flow rate loggings for the 9 days prior to data logger installation were surrogated with visual flowmeter readings. Data gaps in the turbidity-iron-conversion dataset due to missing turbidity data (e.g. sensor errors or data cleansing) were surrogated with medians of the respective monitoring period prior to mass balance calculation. Iron analyses below detection limit were nevertheless used for mass balances as the most conservative option to minimise distortion and to not underestimate effluent iron.

The overall mass balance based on averaged numbers of the entire monitoring period yields a total mass inflow of 67.2 kg and outflow of 1.7 kg over the 452-day period, which equals an overall mass removal and treatment efficiency of 97.5% ([Table 4](#)).

The low-resolution mass balance based on approximately semi-weekly intervals for flow rates and iron concentrations as derived from sample analyses yields a similar total mass inflow of 69.3 kg and outflow of 1.7 kg over the 452-day period, which equals an overall mass removal and treatment efficiency of 97.5% ([Table 5](#)).

The high-resolution mass balance based on 30-min intervals for flow rates and iron concentrations as derived from the turbidity-iron-conversion yields a total mass inflow of only 56.3 kg and outflow of 1.2 kg over the 452-day period, which equals an overall mass removal and treatment efficiency of 97.9% ([Table 6](#)).

In general, all three mass balances show similar, excellent iron removal efficiencies of about 98% yet differ regarding mass flows, with inflow for overall and low-resolution mass balances exceeding the high-resolution mass balance by approximately 18 and 21%, respectively, over the 452-day period. Discrepancy between mass flows could be explained by (1.) exclusion of the dissolved and colloidal iron fraction from turbidity-iron-conversion and thus the high-resolution mass balance on the one hand and (2.) substantial fluctuation of hydraulic loading due to discontinuous pump operation on the other hand. The former is considered insignificant with dissolved iron negligible in the

Table 4
Overall mass balance based on averaged flow rates and iron concentrations.

	Settling ponds (MP02-MP04)	Wetlands (MP05-MP07)	Sediment filters (MP08-MP10)
Mass inflow [kg]	67.2	19.9	6.4
Mass outflow	19.9	6.4	1.7
Fe _{out,tot} [kg]			
Mass removal Fe _i [kg] ^a	47.3 (70.3%)	13.5 (20.1%)	4.7 (7.0%)
Treatment efficiency ^b [%]	70.3	67.7	73.5
Cumulative removal ^c [%]	70.3	90.4	97.5

^a Removal fraction from system line inflow in brackets.

^b %-removal for individual stages.

^c Cumulative treatment efficiency.

Table 5
Low-resolution mass balance based on semi-weekly intervals for flow rates and iron concentrations.

	Settling ponds (MP02-MP04)	Wetlands (MP05-MP07)	Sediment filters (MP08-MP10)
Mass inflow [kg]	69.3	21.6	7.0
Mass outflow	21.6	7.0	1.7
Fe _{out,tot} [kg]			
Mass removal Fe _i [kg] ^a	47.6 (68.8%)	14.6 (21.1%)	5.3 (7.6%)
Treatment efficiency ^b [%]	68.8	67.5	75.2
Cumulative removal ^c [%]	68.8	89.9	97.5

^a Removal fraction from system line inflow in brackets.

^b %-removal for individual stages.

^c Cumulative treatment efficiency.

Table 6
High-resolution mass balance based on 30-min intervals for flow rates and turbidity-iron-conversion.

	Settling ponds (MP02-MP04)	Wetlands (MP05-MP07)	Sediment filters (MP08-MP10)
Mass inflow [kg]	56.3	21.7	5.4
Mass outflow	21.7	5.4	1.2
Fe _{out,tot} [kg]			
Mass removal Fe _i [kg] ^a	34.6 (61.4%)	16.3 (29.0%)	4.2 (7.4%)
Treatment efficiency [%] ^b	61.4	75.2	77.9
Cumulative removal [%] ^c	61.4	90.4	97.9

^a Removal fraction from system line inflow in brackets.

^b %-removal for individual stages.

^c Cumulative treatment efficiency.

inflow and close to or below detection limit throughout MP02-MP10. By contrast, considerably lower mass flows calculated for the high-resolution mass balance are attributable to decreased hydraulic loading during weekends when pump operation ceased, and the system was only fed from the (dwindling) reservoir. This progressing decrease in both flow rate and iron concentration during weekends is illustrated by periodic weekly minima in [Fig. 4](#). Respective mass flow fluctuations are not taken into consideration by both overall and low-resolution mass balances with samples for iron analysis collected during weekdays, only. Hence, overall and low-resolution mass balances naturally overestimate iron mass flows, which could have serious implications for long-term operation and maintenance of a passive system. For instance, a 20% overestimation of iron accumulation for the pilot plant would lead to shorter estimates for sludge removal intervals (i.e. four instead of five years) and correspondingly higher estimates for sludge disposal costs. Consequently, we consider using high-resolution turbidity data as a proxy for iron considerably more suitable to describe mass flows in the system.

4. Conclusion and outlook

4.1. Application, uncertainties and limitations

Both solids analysis and extensive monitoring confirm the initial hypothesis of an approximately monocausal relationship between particulate iron and suspended solids (and thus turbidity) in the pilot plant (excluding sediment filters). Most importantly, the proportion of suspended iron- and non-iron matter is relatively stable throughout the first three sampling stages. Thus, the results clearly show that turbidity can be used as a proxy for iron in a ferruginous, circum-neutral environment.

The linear correlation was successfully used to investigate iron mass

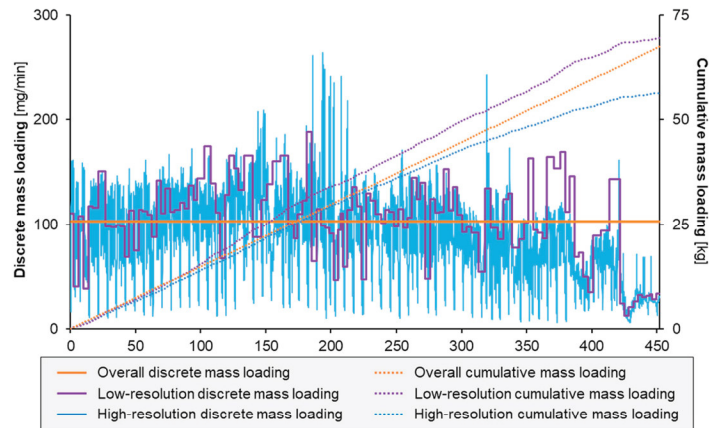


Fig. 4. Discrete hydraulic loading over mass balance intrinsic time intervals (solid lines) and cumulative mass removal (dotted lines) for overall (orange), low-resolution (purple) and high-resolution (blue) mass balances for the 452-day period. (For interpretation of the references to colour in this figure legend, the reader is referred to the Web version of this article.)

flows in the pilot plant, describing transport and removal with unprecedented degree of resolution. Evaluation of system performance was considerably improved in quality and resolution by application of the turbidity-iron-conversion. For example, the high-resolution mass balance indicates that, although iron is largely accumulated in settling ponds, both wetlands and sediment filters show relatively higher treatment efficiency despite low inflow concentrations and are thus indispensable for purification (Table 6). Altogether, the results of this study give rise to concern that mass balance models based on relatively large, but periodic datasets may feature considerable deviation due to temporal variation of flow rates and/or inflow concentrations.

Turbidity measurements depend on size and morphology of suspended particles which may vary spatially, with large flocs settling early on and small particles or colloids further transported along the flow path. In addition, it is to be expected that both autochthonous and allochthonous matter (e.g. plant litter, fine sediments, wind-borne dust, pollen or seeds) have a temporally and spatially variable effect on turbidity in the pilot plant, potentially resulting in increasing heterodispersity along the flow-path (Gregory, 1985). For instance, non-iron turbidity-sensitive suspended solids such as natural organic matter or clastic sediments may be produced in wetlands and sediment filters, respectively. Especially in wetland outflows, TSS concentration and composition is likely to vary seasonally. Moreover, it is quite possible that turbidity-sensitive, non-iron substances are either sedimented and filtered or associated (adsorbed, co-precipitated) with suspended hydrous ferric oxides and thus indiscernible from particulate iron.

Despite potentially increasing heterodispersity along the flow path, study results clearly confirm that turbidity is generally dominated by particulate iron in inflow, settling ponds and wetlands because of:

1. Coherent statistical correlation of turbidity and iron with $R^2 > 0.86$ and $p < 0.05$;
2. Solids settled thereafter are similarly composed of mainly hydrous ferric oxides;
3. The field-derived turbidity-iron-relationship is in good accordance with a laboratory-based dilution series determined from a more monodispersed suspension;
4. Other turbidity-sensitive substances (e.g. TOC, SiO_2 , PO_4 -compounds) are relatively low in concentration;
5. Both total iron and turbidity approach zero towards discharge, either indicating low “background noise” caused by non-iron suspended

solids or non-iron suspended solids are associated and settle together with hydrous ferric oxides.

Altogether, the empirical turbidity-iron-relationship is not only considered robust enough for (site-specific) data evaluation but considerably improves quality and resolution of monitoring and mass balance evaluation.

4.2. Transferability and fields of application

The results demonstrate that both overall and low-resolution mass balances based on averaged numbers overestimate mass flows in the composite treatment system due to disregarded variability in hydraulic loading. Therefore, using turbidity as a proxy for iron is a valuable tool for in-depth investigation of mass flows under conditions where hydraulic loading and/or mass flows are fluctuating or even decoupled (e.g. seasonal variation, intermittent flow, re-mobilisation effects).

Experiments by Hove et al. (2008) and Misawa et al. (1974) as well as findings by Davison (1993), Liu and Millero (1999), Moses and Herman (1989) and Peiffer et al. (1999) indicate that aqueous iron chemistry and solubility as well as formation of hydrous ferric oxides are, especially in the early stages, subject to various factors (e.g. pH, redox-state, TOC, mineralisation, oxygenation, bacterial activity). Consequently, the empirical turbidity-iron correlation at hand is only applicable to the pilot plant and the intrinsic (mine) water chemistry for the time being. Nevertheless, there is good reason to assume that similar relationships could be established for other (mine) sites where particulate iron is the predominant constituent responsible for increased turbidity. In-depth studies are necessary to elucidate the effect of mine water chemistry on particle characteristics to establish a more universal surrogate relationship. Based on a well-founded (site-specific) correlation between turbidity and (particulate) iron, monitoring of thoroughly oxygenated, circum-neutral ferruginous mine water can be greatly improved regarding cost, resolution and efficiency. This is particularly interesting for remote locations, extensive catchment scale studies and cases of application where the required resolution is unfeasible by way of manual grab sampling on site (Chapin, 2015; Nimick et al., 2003; Skarbøvik et al., 2012; Thomson et al., 1997).

Beyond that, it is easily conceivable that similar statistical relationships could be established for other turbidity-sensitive substances. As an example, suspended aluminium is frequently occurring in mine waters

J. Oplitz et al.

Applied Geochemistry 122 (2020) 104731

(e.g. Carrero et al., 2015; Peiffer et al., 1997). Moreover, suspended trivalent iron or aluminium hydroxides may be used as a proxy for associated constituents (e.g. metals, metalloids, oxyanions) in oxygenated, circum-neutral environments (Cornell and Schwertmann, 2003; Waychunas et al., 2005) where transport and distribution are thus predominantly controlled by particulate transport (Church et al., 1997; Karlsson et al., 1988; Zänker et al., 2003). For example, Cánovas et al. (2017) report non-conservative behaviour of not only iron, but also potentially scavenged (i.e. co-precipitated, adsorbed or incorporated) metal(oid)s such as As, Pb and V in a mining-influenced catchment study. It would be interesting to try and advance iron and associated contaminant transport predictions in respective mixing models by utilising turbidity-proxy-relationships to correct for mineral-phase deposition and/or re-suspension along the flow path with respective correlations between metal(oid)s and turbidity indeed reported by Cánovas et al. (2017).

Declaration of competing interest

The authors declare that they have no known competing financial interests or personal relationships that could have appeared to influence the work reported in this paper.

Acknowledgements

The study was conducted as part of a research project funded by the German Federal Environmental Foundation (project no. 33012/01-23). The study was supported by Uniper Kraftwerke GmbH (Düsseldorf) and WTW/Xylem Analytics Germany (Weilheim). The authors thank J. Eckert for meticulous assistance with field and laboratory work and Dr. S. Menzler for advice on data evaluation.

Appendix A. Supplementary data

Supplementary data to this article can be found online at <https://doi.org/10.1016/j.apgeochem.2020.104731>.

References

Baumgartner, J., Favre, D., 2015. Iron solubility, colloids and their impact on iron (oxy)hydroxide formation from solution. *Earth Sci. Rev.* 150, 520–530. <https://doi.org/10.1016/j.earscirev.2015.09.003>.

Butler, B.A., Ford, R.G., 2018. Evaluating relationships between total dissolved solids (TDS) and total suspended solids (TSS) in a mining-influenced watershed. *Mine Water Environ.* 37 (1), 18–30. <https://doi.org/10.1007/s10230-017-0484-y>.

Butler, B.A., Ranville, J.F., Ross, P.E., 2008. Direct versus indirect determination of suspended sediment associated metals in a mining-influenced watershed. *Appl. Geochem.* 23 (5), 1218–1231. <https://doi.org/10.1016/j.apgeochem.2007.11.021>.

Cánovas, C.R., Macías, F., Olias, M., Pérez López, R., Nieto, J.M., 2017. Metal-fluxes characterization at a catchment scale: study of mixing processes and end-member analysis in the Meca River watershed (SW Spain). *J. Hydrol.* 550, 590–602. <https://doi.org/10.1016/j.jhydrol.2017.05.037>.

Carrero, S., Pérez-López, R., Fernández-Martínez, A., Cruz-Hernández, P., Ayora, C., Poulain, A., 2015. The potential role of aluminium hydroxysulphates in the removal of contaminants in acid mine drainage. *Chem. Geol.* 417, 414–423. <https://doi.org/10.1016/j.chemgeo.2015.10.020>.

Chapin, T.P., 2015. High-frequency, long duration water sampling in acid mine drainage studies: a short review of current methods and recent advances in automated water samplers. *Appl. Geochem.* 59, 118–124. <https://doi.org/10.1016/j.apgeochem.2015.04.004>.

Church, S.E., Kimball, B.A., Fey, D.A., Ferderer, D.A., Yager, T.J., Vaughn, R.B., 1997. Source, Transport, and Partitioning of Metals between Water, Colloids, and Bed Sediments of the Animas River, Colorado. USGS Open File Report, pp. 97–151.

Cornell, R.M., Schwertmann, U., 2003. *The Iron Oxides*, first ed. Wiley-VCH Verlag GmbH & Co. KGaA, Weinheim. <https://doi.org/10.1002/3527602097>. 664 pp.

Cornell, R.M., Giovanoli, R., Schneider, W., 1989. Review of the hydrolysis of iron(III) and the crystallization of amorphous iron(III) hydroxide hydrate. *J. Chem. Technol. Biotechnol.* 46 (2), 115–134. <https://doi.org/10.1002/jctb.280460204>.

Davis, A., Olsen, R.L., Walker, D.R., 1991. Distribution of metals between water and entrained sediment in streams impacted by acid mine discharge, Clear Creek, Colorado, U.S.A. *Appl. Geochem.* 6 (3), 333–348. [https://doi.org/10.1016/0883-2927\(91\)90009-E](https://doi.org/10.1016/0883-2927(91)90009-E).

Davison, W., 1993. Iron and manganese in lakes. *Earth Sci. Rev.* 34 (2), 119–163. [https://doi.org/10.1016/0012-8252\(93\)90029-7](https://doi.org/10.1016/0012-8252(93)90029-7).

Dudeney, B., Demin, O., Tarasova, I., 2003. Control of ochreous deposits in mine water treatment. *Land Contam. Reclam.* 11 (2), 259–266. <https://doi.org/10.2462/09670513.823>.

Filella, M., 2007. Colloidal properties of submicron particles in natural waters. In: Wilkinson, K.J., Lead, J.R. (Eds.), *Environmental Colloids and Particles: Behaviour, Separation and Characterisation*. John Wiley & Sons (IUPAC series on analytical and physical chemistry of environmental systems), Chichester, pp. 17–93.

Filip, A., Vuskovic, B., Strundjalic, P., 1974. Correlation between turbidity and iron content of the filter effluent of well origin. *J. Am. Water Works Assoc.* 66 (3), 166–168. <https://doi.org/10.1002/j.1551-8833.1974.tb01995.x>.

Frau, I., Korostynska, O., Mason, A., Byrne, P., 2018. Comparison of electromagnetic wave sensors with optical and low-frequency spectroscopy methods for real-time monitoring of lead concentrations in mine water. *Mine Water Environ.* 37 (3), 617–624. <https://doi.org/10.1007/s10230-018-0511-7>.

Galván, L., Olias, M., Cánovas, C.R., Torres, E., Ayora, C., Nieto, J.M., Sarmiento, A.M., 2012. Refining the estimation of metal loads dissolved in acid mine drainage by continuous monitoring of specific conductivity and water level. *Appl. Geochem.* 27 (10), 1932–1943. <https://doi.org/10.1016/j.apgeochem.2012.07.011>.

Gregory, J., 1985. Turbidity fluctuations in flowing suspensions. *J. Colloid Interface Sci.* 105 (2), 357–371. [https://doi.org/10.1016/0021-9797\(85\)90309-1](https://doi.org/10.1016/0021-9797(85)90309-1).

Harter, S.K., Mitsch, W.J., 2003. Patterns of short-term sedimentation in a freshwater created marsh. *J. Environ. Qual.* 32 (1), 325–334. <https://doi.org/10.2134/jeq2003.3250>.

Hedin, R.S., 2008. Iron removal by a passive system treating alkaline coal mine drainage. *Mine Water Environ.* 27 (4), 200–209. <https://doi.org/10.1007/s10230-008-0041-9>.

Hoffmann, M.R., Yost, E.C., Eisenreich, S.J., Maier, W.J., 1981. Characterization of soluble and colloidal phase metal complexes in river water by ultrafiltration: A mass-balance approach. *Environ. Sci. Technol.* 15 (6), 655–661. <https://doi.org/10.1021/es00088a002>.

Hove, M., van Hille, R.P., Lewis, A.E., 2008. Mechanisms of formation of iron precipitates from ferrous solutions at high and low pH. *Chem. Eng. Sci.* 63 (6), 1626–1635. <https://doi.org/10.1016/j.ces.2007.11.016>.

Hubert, E., Wolkersdorfer, C., 2015. Establishing a conversion factor between electrical conductivity and total dissolved solids in South African mine waters. *Water South Africa* 41 (4), 490–500. <https://doi.org/10.4314/wsa.v41i4.08>.

Ingrt, J., Widerlund, A., 1994. Uptake of alkali and alkaline-earth elements on suspended iron and manganese in the Kalix river, northern Sweden. *Geochim. Cosmochim. Acta* 58 (24), 5433–5442. [https://doi.org/10.1016/0016-7037\(94\)90240-2](https://doi.org/10.1016/0016-7037(94)90240-2).

James, W.F., Best, E.P., Barko, J.W., 2004. Sediment resuspension and light attenuation in Peoria Lake: Can macrophytes improve water quality in this shallow system? *Hydrobiologia* 515 (1–3), 193–201. <https://doi.org/10.1023/B:HYDR.0000027328.00153.b2>.

Karlsson, S., Allard, B., Håkansson, K., 1988. Characterization of suspended solids in a stream receiving acid mine effluents, Bersbo, Sweden. *Appl. Geochem.* 3 (3), 345–356. [https://doi.org/10.1016/0883-2927\(88\)90111-4](https://doi.org/10.1016/0883-2927(88)90111-4).

Kimball, B.A., McKnight, D.M., Wetherbee, G.A., Harnish, R.A., 1992. Mechanisms of iron photoreduction in a metal-rich, acidic stream (St. Kevin Gulch, Colorado, U.S.A.). *Chem. Geol.* 96 (1–2), 227–239. [https://doi.org/10.1016/0009-2541\(92\)90130-W](https://doi.org/10.1016/0009-2541(92)90130-W).

Kimball, B.A., Callender, E., Axtmann, E.V., 1995. Effects of colloids on metal transport in a river receiving acid mine drainage, upper Arkansas River, Colorado, U.S.A. *Appl. Geochem.* 10 (3), 285–306. [https://doi.org/10.1016/0883-2927\(95\)00011-8](https://doi.org/10.1016/0883-2927(95)00011-8).

Korostynska, O., Mason, A., Al-Shamma'a, A.L., 2013. Monitoring pollutants in wastewater: Traditional lab based versus modern real-time approaches. In: Mukhopadhyay, S.C., Mason, A. (Eds.), *Smart Sensors for Real-Time Water Quality Monitoring*, vol. 4. Springer (Smart Sensors, Measurement and Instrumentation, 4), New York, pp. 1–24.

Lee, D.K., Cheong, Y.W., 2016. The relationship between flow paths and water quality in mine water oxidation ponds in South Korea. *Mine Water Environ.* 35 (4), 469–479. <https://doi.org/10.1007/s10230-016-0383-7>.

Liu, X., Millero, F.J., 1999. The solubility of iron hydroxide in sodium chloride solutions. *Geochim. Cosmochim. Acta* 63 (19–20), 3487–3497. [https://doi.org/10.1016/S0016-7037\(99\)00270-7](https://doi.org/10.1016/S0016-7037(99)00270-7).

Misawa, T., Hashimoto, K., Shimodaira, S., 1974. The mechanism of formation of iron oxide and oxyhydroxides in aqueous solutions at room temperature. *Corrosion Sci.* 14 (2), 131–149. [https://doi.org/10.1016/S0010-938X\(74\)80051-X](https://doi.org/10.1016/S0010-938X(74)80051-X).

Moses, C.O., Herman, J.S., 1989. Homogeneous oxidation kinetics of aqueous ferrous iron at circumneutral pH. *J. Solut. Chem.* 18 (8), 705–725. <https://doi.org/10.1007/BF00651804>.

Ninick, D.A., Gannons, C.H., Cleasby, T.E., Madison, J.P., Skaar, D., Brick, C.M., 2003. Diel cycles in dissolved metal concentrations in streams: Occurrence and possible causes. *Water Resour. Res.* 39 (9), 1742–1759. <https://doi.org/10.1029/2002WR001571>.

O'Flynn, B., Regan, F., Lawlor, A., Wallace, J., Torres, J., O'Mathuna, C., 2010. Experiences and recommendations in deploying a real-time, water quality monitoring system. *Meas. Sci. Technol.* 21 (12), 124004. <https://doi.org/10.1088/0957-0233/21/12/124004>.

Oplitz, J., Alte, M., Bauer, M., Peiffer, S., 2019. Testing iron removal in a trifurcated pilot plant for passive treatment of circum-neutral ferruginous mine water. In: Khayrulina, E., Wolkersdorfer, C., Polyakova, S., Bogush, A. (Eds.), *Proceedings IMWA 2019 Conference*. Mine Water: Technological and Ecological Challenges, pp. 256–262. Perm.

Oplitz, J., Alte, M., Bauer, M., Schäfer, W., Söll, T., 2020. Estimation of self-neutralisation rates in a lignite pit lake. *Mine Water Environ.* 39 (3), 556–571. <https://doi.org/10.1007/s10230-020-00692-9>.

J. Oplitz et al.

Applied Geochemistry 122 (2020) 104731

- Peiffer, S., Beierkuhnlein, C., Sandhage-Hofmann, A., Kaupenjohann, M., Bär, S., 1997. Impact of high aluminium loading on a small catchment area (Thuringia slate mining area) – Geochemical transformations and hydrological transport. *Water, Air, Soil Pollut.* 94 (3/4), 401–416. <https://doi.org/10.1023/A:1026415905628>.
- Peiffer, S., Walton-Day, K., Macalady, D.L., 1999. The interaction of natural organic matter with iron in a wetland (Tennessee Park, Colorado) receiving acid mine drainage. *Aquat. Geochem.* 5 (2), 207–223. <https://doi.org/10.1023/A:1009617925959>.
- Revitta, D.M., Shutes, R.B.E., Jones, R.H., Forshaw, M., Winter, B., 2004. The performances of vegetative treatment systems for highway runoff during dry and wet conditions. *Sci. Total Environ.* 334–335, 261–270. <https://doi.org/10.1016/j.scitotenv.2004.04.046>.
- Rügner, H., Schwientek, M., Egner, M., Grathwohl, P., 2014. Monitoring of event-based mobilization of hydrophobic pollutants in rivers: Calibration of turbidity as a proxy for particle facilitated transport in field and laboratory. *Sci. Total Environ.* 490, 191–198. <https://doi.org/10.1016/j.scitotenv.2014.04.110>.
- Sarmiento, A.M., Caraballo, M.A., Sanchez-Rodas, D., Nieto, J.M., Parviainen, A., 2012. Dissolved and particulate metals and arsenic species mobility along a stream affected by Acid Mine Drainage in the Iberian Pyrite Belt (SW Spain). *Appl. Geochem.* 27 (10), 1944–1952. <https://doi.org/10.1016/j.apgeochem.2012.07.012>.
- Schenel, L.E., Kimball, B.A., Bencala, K.E., 2000. Colloid formation and metal transport through two mixing zones affected by acid mine drainage near Silverton, Colorado. *Appl. Geochem.* 15 (7), 1003–1018. [https://doi.org/10.1016/S0883-2927\(99\)00104-3](https://doi.org/10.1016/S0883-2927(99)00104-3).
- Skarbovik, E., Stålnacke, P., Bogen, J., Bonsnes, T.E., 2012. Impact of sampling frequency on mean concentrations and estimated loads of suspended sediment in a Norwegian river: Implications for water management. *Sci. Total Environ.* 433, 462–471. <https://doi.org/10.1016/j.scitotenv.2012.06.072>.
- Skousen, J., Zipper, C.E., Rose, A., Zienkiewicz, P.F., Nairn, R., McDonald, L.M., Kleinmann, R.L.P., 2017. Review of passive systems for acid mine drainage treatment. *Mine Water Environ.* 36 (1), 133–153. <https://doi.org/10.1007/s10230-016-0417-1>.
- Stumm, W., Morgan, J.J., 1996. *Aquatic Chemistry. Chemical Equilibria and Rates in Natural Waters*, third ed. John Wiley & Sons Inc., New York. 1024 pp.
- Taillefert, M., Lienemann, C.P., Gaillard, J.F., Perret, D., 2000. Speciation, reactivity, and cycling of Fe and Pb in a meromictic lake. *Geochim. Cosmochim. Acta* 64 (2), 169–183. [https://doi.org/10.1016/S0016-7037\(99\)00285-9](https://doi.org/10.1016/S0016-7037(99)00285-9).
- Thomson, N.R., McBean, E.A., Snodgrass, W., Monstrenko, I.B., 1997. Highway stormwater runoff quality: Development of surrogate parameter relationships. *Water, Air, Soil Pollut.* 94 (3), 307–347. <https://doi.org/10.1007/BF02406066>.
- Waychunas, G.A., Kim, C.S., Banfield, J.F., 2005. Nanoparticulate iron oxide minerals in soils and sediments: Unique properties and contaminant scavenging mechanisms. *J. Nanoparticle Res.* 7 (4–5), 409–433. <https://doi.org/10.1007/s11051-005-6931-x>.
- Zänker, H., Richter, W., Hüttig, G., 2003. Scavenging and immobilization of trace contaminants by colloids in the waters of abandoned ore mines. *Colloid. Surface. Physicochem. Eng. Aspect.* 217 (1–3), 21–31. [https://doi.org/10.1016/S0927-7752\(02\)00555-1](https://doi.org/10.1016/S0927-7752(02)00555-1).

Study 2 – Mine Water Environ. 40: 587

Title The role of macrophytes in constructed surface-flow wetlands for mine water treatment: A review

Authors Opitz J, Alte M, Bauer M, Peiffer S

Status Published


Year 2021

Journal Mine Water and the Environment

Article 40(3): 587-605

Pages 19

DOI 10.1007/s10230-021-00779-x

SI  No Supporting Information

Access  <https://link.springer.com/article/10.1007/s10230-021-00779-x>
© The authors (Open Access)



Relative contribution of the PhD student to study 2:

- Study design 80%
- Literature compilation 90%
- Literature review 90%
- Data integration and analysis 70%
- Manuscript preparation 80%

JO and SP designed the study. JO compiled and evaluated the relevant literature and conducted the review with support by all co-authors. All authors contributed to integration and analysis of relevant data for the review. JO prepared a first draft as well as figures and tables for the manuscript with input from all co-authors. All authors jointly finalised and submitted the manuscript. JO is the corresponding author.

JO: Joscha Opitz // MA: Matthias Alte // MB: Martin Bauer // SP: Stefan Peiffer



The Role of Macrophytes in Constructed Surface-flow Wetlands for Mine Water Treatment: A Review

Joscha Opitz^{1,2} · Matthias Alte² · Martin Bauer² · Stefan Peiffer¹

Received: 16 August 2020 / Accepted: 1 April 2021 / Published online: 20 April 2021
© The Author(s) 2021

Abstract

Constructed wetlands are a standard sustainable technology in waste and mine water treatment. Whereas macrophytes actively contribute to decomposition and/or removal of wastewater's organic pollutants, removal of hydrolysable metals from mine water is not attributable to direct metabolic, but rather various indirect macrophyte-related mechanisms. These mechanisms result in higher treatment efficiency of (vegetated) wetlands relative to (unvegetated) settling ponds. Contribution of macrophytes to treatment predominantly includes: enhanced biogeochemical oxidation and precipitation of hydrolysable metals due to catalytic reactions and bacterial activity, particularly on immersed macrophyte surfaces; physical filtration of suspended hydrous ferric oxides by dense wetland vegetation down to colloids that are unlikely to gravitationally settle efficiently; scavenging and heteroaggregation of dissolved and colloidal iron, respectively, by plant-derived natural organic matter; and improved hydrodynamics and hydraulic efficiency, considerably augmenting retention and exposure time. The review shows that constructed surface-flow wetlands have considerable advantages that are often underestimated. In addition to treatment enhancement, there are socio-environmental benefits such as aesthetic appearance, biotope/habitat value, and landscape diversity that need to be considered. However, there is currently no quantitative, transferrable approach to adequately describe the effect and magnitude of macrophyte-related benefits on mine water amelioration, let alone clearly assign optimal operational deployment of either settling ponds or wetlands. A better (quantitative) understanding of underlying processes and kinetics is needed to optimise assembly and sizing of settling ponds and wetlands in composite passive mine water treatment systems.

Keywords Passive treatment · Filtration · Biogeochemistry · Settling pond · Hydrodynamics

Introduction

Constructing wetlands for treatment of municipal, domestic, agricultural, and industrial wastewater dates back to the early 1950s (Seidel 1966; Vymazal 2014). In the late 1970s and early 1980s, observation of positive effects of natural wetlands on mine drainage chemistry in the Appalachian coal-fields led to adaptation of wetlands for treatment of acidic and/or metalliferous mine water (Huntsman et al. 1978; Wieder 1989). Nowadays, constructed wetlands are used to passively remove a variety of mine water contaminants,

predominantly hydrolysable metals (Al, Fe, Mn), but also other metals typically associated with mining activities (Ag, Cd, Co, Cr, Cu, Hg, Mo, Ni, Pb, U, V, Zn), metalloids (e.g., As, Sb, Se), and other pollutants (e.g., cyanide, ammonia) (e.g., Noller et al. 1994; Pedescoll et al. 2015; Sobolewski 1999; Walton-Day 1997). Since then, application of mine water treatment wetlands has been spreading worldwide, with a focus on legacy mine sites.

Both aerobic (free water surface-flow) and anaerobic (vertical/subsurface-flow) wetlands as well as composite systems are used for passive mine water treatment according to mine discharge chemistry. Anaerobic wetlands are primarily used to treat acidic mine drainage (AMD) by way of alkalinity generation and metal sulphide precipitation, whereas aerobic wetlands are used to treat neutral, metalliferous mine drainage by way of oxidation and precipitation of hydrolysable metals (Skousen et al. 2017). This study is focussed on

✉ Joscha Opitz
joscha.opitz@uni-bayreuth.de

¹ Department of Hydrology, University of Bayreuth, Universitätsstraße 30, 95447 Bayreuth, Germany

² Base Technologies GmbH, Josef-Felder-Straße 53, 81241 Munich, Germany

aerobic surface-flow wetlands (hereinafter “wetlands”), with macrophytes prevalent in the free water column.

It is generally hypothesised that macrophytes have a considerable effect on treatment performance and are the keystone of surface-flow wetlands, which are in turn the key “polishing” component to achieve a specific compliance target for most passive treatment systems (Batty 2003; Batty and Younger 2002). The importance of macrophytes is undebated for wastewater treatment wetlands, where plants actively participate in central elemental cycles (C, N, P) and release allelochemicals or antibacterial substances (Bavor et al. 2001; Kadlec and Wallace 2009; Vymazal 2014). Ample literature based on quantitative studies exists on the design and sizing of wetlands for wastewater treatment (e.g., Kadlec and Wallace 2009; Kadlec et al. 2000; Pedescoll et al. 2015).

In contrast, there has been a long-standing discussion whether mine water treatment wetlands outperform unvegetated settling ponds, since macrophytes do not take a metabolically active role in metal removal. With numerous studies indicating better treatment performance and hydraulic efficiency for wetlands compared to settling ponds, recently including direct juxtaposition of large data sets (e.g., Opitz et al. 2019; Pedescoll et al. 2015; Sapsford 2013; Sapsford and Watson 2011), there is general agreement that wetlands are superior in terms of treatment efficiency, particularly for low iron concentrations (Batty et al. 2008). It was consequently concluded that, beyond the aesthetic value, macrophytes play an important role even without substantial direct uptake of hydrolysable metals or metabolic effects on metal removal mechanisms (Batty 2003; Brix 1994; Sheoran and Sheoran 2006). For instance, some aspects, such as improved hydrodynamics and floc filtration by macrophytes are frequently quoted (Skousen et al. 2017), and Batty and Younger (2002) even showed that metal uptake may be a factor at residual iron concentrations. However, to this day, the processes and effects bringing about superior metal removal efficiency in wetlands are described rather vaguely, particularly from a quantitative perspective (Johnson and Hallberg 2002). In addition, there is still an ongoing discussion whether better treatment performance justifies increased operation and maintenance requirements, shorter refurbishment cycles, and complicated disposal of both metalliferous and organic-rich sediments.

A holistic view of core advantages and disadvantages as well as underlying processes and effects of wetlands is required to facilitate well-founded decisions regarding the deployment of vegetated or unvegetated ponds, both as stand-alone units and in composite passive systems (Sapsford 2013). In this context, it stands to reason that macrophytes are the decisive difference between wetlands and settling ponds. The purpose of this study is to give a literature-based overview of the current state of knowledge

regarding the contribution of macrophytes to mine water amelioration in surface-flow wetlands. The goal is to identify and describe the determining macrophyte-related processes and effects contributing to mine water contaminant removal as a (qualitative) basis for future in-depth investigation and quantification of these effects. A better understanding of macrophyte-related effects would go a long way towards circumscribing or parameterising the difference between settling ponds and wetlands and to ultimately improving the design and sizing of composite passive systems. Exemplary hydrochemical and environmental juxtaposition of settling ponds and wetlands in this study is provided from international literature and a closely monitored passive pilot plant featuring equally sized, consecutive settling ponds and wetlands, as described in Opitz et al. (2019, 2020).

Ecological Background

Treatment wetlands are designed to artificially emulate natural wetlands, creating a near-natural and densely vegetated aquatic environment. Wetlands are exceptional in that various transitional and sometimes opposed environmental conditions (e.g., stagnant to flowing, clear to turbid, oligotrophic to eutrophic) and gradients (e.g., temperature, pH, oxygenation, light exposure, redox potential) are found in a spatially confined area and may display considerable temporal (e.g., diurnal, seasonal, or hydrological cycles) variation (Bezbaruah and Zhang 2004; Feierabend 1989; García et al. 2003; Kadlec and Wallace 2009). Wetlands are exceedingly dynamic systems that generally display substantial biomass production and mineralisation, thus supporting intensive substance and nutrient cycles (Mitsch et al. 2012). Consequently, wetlands are a hotspot of (micro)biological activity and productivity, usually supporting a particularly vibrant and diverse ecosystem. It is therefore hardly surprising that wetland biogeochemistry also affects metal (redox) cycles and transformations with demonstrably positive effects on water quality (Fennessy and Mitsch 1989; Sobolewski 1999; Wildemann et al. 1993).

According to Kadlec et al. (2000), macrophytes are “*the dominant structural component of most wetland treatment systems.*” Early field observations and trials of shallow *Sphagnum* bogs showed promising metal removal capacities, especially for mildly acidic and neutral mine water (Kleinmann et al. 1983; Wieder et al. 1982). However, overall and especially long-term performance of hybrid *Sphagnum* bogs was rather variable due to progressive armouring of the plants, especially when faced with acidic and/or highly ferruginous loadings (Brenner et al. 1993; Henrot and Wieder 1990). To further augment metal removal and alkalisation, early mine water treatment wetlands were soon being constructed as hybrid marsh-like wetlands with low water

depth (5–25 cm) and high substrate depth (\approx 50 cm) to facilitate both open water and pore space flow with limestone-amended organic or peat substrates for metal adsorption and alkalinity generation (Girts et al. 1987; Wieder 1989). Eventually, this led to the more targeted forking into anaerobic and aerobic wetlands seen today (Hedin et al. 1994; McIntire and Edenborn 1990). Nowadays, aerobic wetlands are constructed as shallow basins with a loose rooting substrate predominantly planted with emergent, tall-growing herbaceous macrophytes, although submerged or floating plants may occur alongside. Recommendations for water depths range from 15–25 cm (Younger et al. 2002) to 10–50 cm (Hedin et al. 1994). Generally, a water depth of 50 cm was reported as the maximum tolerable by emergent, tall-growing macrophytes, e.g. *Typha* and *Phragmites* genera, to reliably develop dense vegetation coverage (Brodie 1991; Wildemann et al. 1993). However, most wetlands are designed with water depths of 10–40 cm to promote vegetation diversity and to accommodate other hydrophilous plants from genera such as *Juncus*, *Scirpus/Schoenoplectus*, *Carex*, *Acorus*, *Eleocharis*, and *Sphagnum*. Planting of constructed wetlands is guided by environmental conditions and local species, with, for instance, *Phalaris* or *Cyperus* preferred in warm, subtropical or tropical climates. Plant community in constructed wetlands may display considerable floral diversity, although over time, dominance of fast-growing reeds and cattails is to be expected in temperate climates due to their environmental resilience, competitive vegetative growth, and reproduction (Brodie 1991; Maine et al. 2009; Stark et al. 1994). Population density varies depending on water level, water quality, plant community, and climate, yet may quickly reach up to several dozen cattails (Sencindiver and Bhumbra 1988; Stark et al. 1994) or several hundred reed shoots per m^2 (Tanner 1996).

Due to the dynamic environmental conditions of wetlands, respective macrophytes are adapted to or tolerate chemical and biophysical stress. Hence, most wetland plants are robust towards the detrimental or even potentially toxic conditions that are characteristic for both acidic and metalliferous mine drainage, including but not limited to low pH, high pollutant levels (metals, metalloids, sulphate, ammonia), high levels of dissolved and/or suspended solids, increased salinity and turbidity (the latter also reducing light transition), and low dissolved oxygen and nutrient levels (e.g., Batty and Younger 2003; Karathanasis and Johnson 2003; Manios et al. 2003; Nixdorf et al. 2001; Tanner 1996; Taylor and Crowder 1983; Wu et al. 2015) as well as ochre plaque on plants, roots, and rooting soil (e.g., Chabbi 1999; Fernandes and Henriques 1990; Snowden and Wheeler 1995). Respective tolerance or phytotoxicity thresholds as well as uptake capacity and bioaccumulation were observed to be high in wetland macrophytes, both towards surrounding water and rooting substrate or soil solution (e.g., Batty

and Younger 2003; Maine et al. 2006; Matthews et al. 2004; Outridge and Noller 1991; Ye et al. 1997b). Although impairment of both physiological development and nutrient metabolism were observed for macrophytes in mining influenced waters by Batty and Younger (2003, 2004) and Wenerick et al. (1989), most treatment wetlands achieve full vegetation cover within a few years, even under at times life-hostile conditions (Mayes et al. 2009; Stark et al. 1994).

Contributing Processes and Aspects

The following review of the various effects of macrophytes on mine water treatment in wetlands is sorted by the nature of the process or effect as much as possible. Where overlap is intrinsic, assignment was done to the best of our judgement. Most effects are related to iron removal as the principal treatment goal in surface-flow mine water treatment wetlands.

Filtration Effects

Submerged parts of aquatic macrophytes such as shoots, leaves, rhizomes, and roots as well as fresh litter and decaying detritus provide substantial surface area for particle filtration through interception and trapping of suspended solids. Various field and laboratory studies have shown significantly increased particulate matter retention in vegetated compared to unvegetated flowing waters (e.g. Cotton et al. 2006; Elliot 2000; Horvath 2004; Pluntke and Kozerski 2003; Saiers et al. 2003; Verschoren et al. 2017). Most studies were able to pinpoint macrophytes as the ultimate cause. For example, Verschoren et al. (2017) compared a lowland river reach in fully vegetated (77–90% cover), partly mown (48–56% cover) and unvegetated (0% cover) state and found an increase in mean particle travel distance (e.g., 14.0 vs. 15.4 vs. 25.4 m for wood chips) as well as a decrease in particle retention (e.g., 97.2 vs. 96.1 vs. 86.0% for wood chips) and hydraulic efficiency (0.83 ± 0.03 vs. 0.76 ± 0.03 vs. 0.67 ± 0.03 for NaCl tracer tests) with progressing vegetation removal. Analogously, Pluntke and Kozerski (2003) observed approximate doubling of particle retention in vegetated compared to unvegetated experimental littoral conditions using particles and spores in the size range of 3–120 μm . What is more, Saiers et al. (2003) found increasing removal of colloidal TiO_2 (average diameter 0.3 μm) in a surface-water flume facility vegetated with *Eleocharis* spp. and estimated that “a single stem was capable of scavenging 29% of the particles that approached its projected cross-sectional area from the upstream direction”. Consequently, macrophyte-related

filtration of particulate matter is not limited to macro-flocs in the upper micrometre range that are predestined to gravitationally settle quickly according to the ratio of flow and settling velocity (Sheoran and Sheoran 2006), but also affects dispersed nanoparticles and colloids that are not susceptible to effective gravitational sedimentation and would thus pass through settling ponds unimpeded. Fennessey and Mitsch (1989) observed a significant increase in particulate iron removal rates from mine water, from 20–30% before up to 50–60% after full development and maturation of cattail populations. Interestingly, the authors also positively correlated iron removal and *Typha* biomass production in the three consecutive wetland cells, although the relationship may be affected by differences in influent water chemistry.

Generally, particle interception increases with increasing vegetation cover. Therefore, existing approaches to quantification of improved particle retention by dense aquatic vegetation are often based on or include respective physical, plant-related parameters (e.g., immersed surface area, stalk diameter, plant density, biomass) and ecological factors (e.g., plant species, vegetation development; e.g., Nepf 1999; Saiers et al. 2003; Schmid et al. 2005; Verschoren et al. 2017). Since filtration of suspended particles by macrophytes was also observed to be influenced by hydrodynamics (e.g., flow velocity, velocity distribution, shear stress) and particle characteristics (e.g., concentration, size, morphology, or charge), further approaches to quantification of particle retention by wetland macrophytes are based on modelling of particle-macrophyte interaction at laminar flow related to, for example, plant-related alteration in velocity distribution, turbulence, shear velocity, and drag. Most models and relationships are, however, based on specific assumptions or site-specific, empirical wetland and particle characteristics, respectively. Since wetlands are very diverse and dynamic systems and the examined particles are a variety of organic and inorganic materials that are easy to handle and reasonably representative of natural waterborne particles (e.g., polymers, spores, chips, clay, corundum, quartz), findings from existing studies are hardly transferrable to mining environments. In this context, periphyton coating of macrophytes may considerably alter colloid filtration, depending on the particle surface charge, as speculated by Saiers et al. (2003). Unfortunately, the authors of this study know of no (quantitative and transferrable) results regarding increased removal of hydrous ferric oxides by macrophytes in mine water treatment wetlands to date.

Physico-chemical Effects

Plant surfaces in general, and ochre-covered tissues in particular, provide extensive catalytic surfaces for adsorption,

heterogeneous oxidation, and precipitation of dissolved (supersaturated) metals (Batty et al. 2008). Reactive surfaces greatly increase reaction kinetics and thus accelerate removal of divalent iron and manganese from mine waters (Dempsey et al. 2001). Heterogeneous ferrous iron oxidation is assumed to be either closely linked to or in competition with biological oxidation (van der Beek et al. 2012), although the borderline or interrelation between surface-catalysed (chemical) and bacterially-catalysed (biological) ferrous iron oxidation as well as between inorganic plaque and biofilms in circumneutral aquatic environments is still unclear and the subject of current research. Similar uncertainties are found in the field of drinking water purification (Mouchet 1992; van Beek et al. 2012). Irrespective of this discussion, oxidation of divalent iron and manganese ions is clearly expected to increase in the presence of reactive surfaces and/or respective iron-oxidising bacteria (Batty et al. 2008; Luan et al. 2012) and it is well-known that other metals associated with mine waters are susceptible to sorption on submerged macrophyte surfaces, as reported by Lesage et al. (2007). Ochreous surfaces and biofilms are most important at low or residual iron concentrations where hydrous ferric oxides (and the catalytic effect they can provide) are negligible.

Biochemical Effects

In the context of this study, biological and biochemical effects describe a passive or indirect contribution by wetland macrophytes to metal transformation or removal that does not (directly) involve the plant's intrinsic metabolism.

First and foremost, the near-natural aquatic and benthic environment created by hydrophytes with at times steep gradients in dissolved oxygen, redox potential, and pH favours development of microorganisms benefiting from environmental heterogeneity. Roots and submerged plant tissue as well as root exudations provide a suitable, nurturing environment and growth surface for development of extensive biofilms and periphyton, and generally stimulate bacterial activity and diversity (Dunbabin and Bowmer 1992; Pietrangelo et al. 2018; Weiss et al. 2003). Field observations of mining-influenced waters indicate that macrophytes stimulate biogeochemical activity in the water column, rhizosphere, and sediment, including but not limited to biological metal oxidation and subsequent precipitation of respective (hydr)oxides (especially the iron redox-cycle) as well as trace metal assimilation and sequestration (e.g., Chabbi 1999; Doyle and Otte 1997; Emerson et al. 1999; Hansel et al. 2001; Neubauer et al. 2002). Moreover, bacteria can also increase particle flocculation due to particle bridging by way of secreted extracellular polymeric fibres (Banfield et al. 2000; Droppo and Ongley 1994). Ferrous iron oxidation and concomitant precipitation and removal of hydrous

ferric oxides in passive system was evaluated by way of a performance index (ϵ), comparing observed with anticipated ideal iron removal via respective first-order kinetics by Sapsford and Watson (2011). With $\epsilon = 1$ indicating ideal performance, the results showed that iron removal in wetlands lived up to expectations (median $\epsilon \approx 0.89$, $n = 12$), whereas settling ponds broadly underperformed (median $\epsilon \approx 0.59$, $n = 10$), indicating “that lagoons are less efficient for iron removal than wetlands” (Sapsford and Watson 2011). This is in accordance with the findings of Kadlec (2003), who reported larger removal rate constants for typical wastewater contaminants (TSS, BOD, $\text{NH}_4\text{-N}$, P_{tot} , fecal coliforms) without exception in unvegetated ponds, attributable to various biogeochemical processes in addition to filtration.

On top of that, field studies indicate a similar, potentially even stronger effect for manganese oxidation. Chemical Mn(II)-oxidation is kinetically limited at $\text{pH} < 8$ and in the presence of ferrous iron, yet may increase in wetlands compared to settling ponds after lowering iron concentrations, as observed by Stark et al. (1995) and Wildemann et al. (1993). The effect is illustrated for the exemplifying pilot system in Fig. 1, with wetlands showing similar (Fe) or better (Mn) removal efficiency than settling ponds despite lower inflow concentrations. Stimulation of metal oxidation processes in wetlands may enhance overall metal removal kinetics, yet the effect of macrophytes on both/either heterogeneous (physico-chemical) and/or bacterial (biological) oxidation is yet to be elucidated.

Current and future research on biological ferrous iron oxidation by neutrophilic bacteria may show if and how chemical and biological oxidation are coupled in circumneutral environments (Emerson and de Vet 2015; Ilbert and Bonnefoy 2013; Kappler et al. 2015), although ferruginous mine waters may pose an additional challenge. At the current state of science, it must be assumed that ferrous iron oxidation in circumneutral mine waters is predominantly driven by chemical oxidation mechanisms (Kirby et al. 1999). Notwithstanding this, bacteria not only contribute to short-term formation of transient amorphous or hydrous metal oxide phases, but also to subsequent long-term transformation to more stable, increasingly crystalline minerals (Tuhela et al. 1992). Beyond that, it is conceivable that biological oxidation of divalent iron and manganese may be increasingly important at more acidic pH and/or low oxygen concentrations (Kirby et al. 1999; Sobolev and Roden 2001), for residual concentration levels in the compliance range (Batty and Younger 2002; Batty et al. 2008) and in the presence of adequate biofilm growth surfaces (Mouchet 1992; van Beek et al. 2012; Weber et al. 2006).

Furthermore, the generation of dissolved, colloidal, and particulate natural organic matter (NOM) in wetland environments is important for metal cycles and removal due to their affinity for metals and complex organic molecules. The

abundance of organic substances in wetlands contributes to further decreases in residual ferrous and ferric iron concentrations in different ways:

First, heteroaggregation of suspended NOM and hydrous ferric oxides was identified as a major iron removal mechanism in estuarine and wetland environments (Mayer 1982; Tipping and Cooke 1982; Tipping and Ohnstad 1984). Put simply, at circumneutral pH, humic substances are negatively charged due to ionisation of carboxyl groups, whereas hydrous ferric oxides are positively charged due to hydrolytic reactions. Consequently, charge neutralisation is achieved by adsorptive aggregation of hydrous ferric oxides and humic substances, resulting in increased aggregate size, stability, and altered zeta potential (Liang et al. 1993). Organic colloids or particles may therefore act as “natural coagulants” for dissolved and suspended iron and enhance formation of larger aggregates that gravitationally settle more easily (Pizarro et al. 1995; Sholkovitz 1978). Iron removal in connection with NOM is particularly important for low or residual iron concentrations, which is not to be underestimated in the context of strict compliance limits (Opitz et al. 2019).

Second, decomposition of plant tissue and detritus releases organic (poly)ligands such as humic and fulvic acids. These anionic groups contribute to scavenging of dissolved iron through organic complexation, sorption, and chelation (Peiffer et al. 1999; Tipping and Hurley 1992). Studies show that organic matter decomposition over time exposes additional ligands and functional groups, resulting in (relative) accumulation and stable immobilisation of iron and other metals within and near the organic-interspersed wetland sediment (Larsen and Schierup 1981; Sobolewski 1999). The potential for remobilisation towards the water phase is considered small since metals are usually bound in stable metal-chelate complexes (Galletti et al. 2010; Sobolewski 1999).

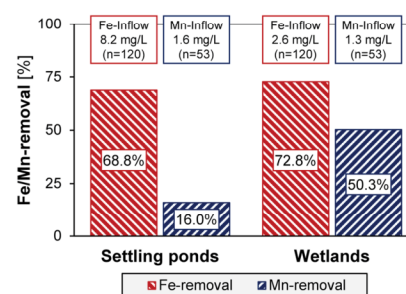


Fig. 1 Relative ferric iron and manganese removal (inflow=100%) in consecutive settling ponds and wetlands from the pilot system described in Opitz et al. (2019)

Third, organic matter generated by plant growth and decay is used as an energy source by various microorganisms that contribute to metal transformation and fixation in the aqueous and particularly the benthic zone (Hansel et al. 2001). As a consequence, iron and other metals from soil-solution are precipitated as sulphide minerals in deeper reaches of the sediment and substrate. This metal removal mechanism based on dissimilatory sulphate reduction is, however, characteristic of anaerobic wetlands and covers only a small share of the overall iron load in aerobic wetlands. Nevertheless, the process may be important for polishing and even more so for the removal of trace metals such as Cu, Pb and Zn (Sobolewski 1999).

Phytologic Effects

Besides the indirect effects described above, macrophytes also actively contribute to mine water treatment and quality by way of several intrinsic phytologic processes and characteristics. Plants are used in environmental remediation for accumulation of contaminants and metals through direct uptake and incorporation into plant tissues (phytoextraction) (Ernst 1996; Khalid et al. 2017). With regard to mine waters, it was firmly established that bioaccumulation of major contaminants such as Fe, Al, and Mn in wetlands is negligible at high loadings, for example accounting for less than 1% of overall iron removal (Fernandes and Henriques 1990; Mitsch and Wise 1998; Sencindiver and Bhumbla 1988). The same is true for other metals associated with mining activities present at noteworthy loadings such as Cd, Cr, Cu, Ni, Pb, and Zn (Liu et al. 2007; Mays and Edwards 2001; Nyquist and Greger 2009) as well as U (Overall and Parry 2004). For example, Ye et al. (2001b) found low accumulation of Fe (0.91%), Co (0.19%), and Ni (0.38%) in *Typha latifolia*, despite relatively low loadings and good overall removal throughout the wetland system, indicating that metals were removed by other means than bioaccumulation. It is, however, important to note that numbers on metal uptake in wetlands are generally difficult to compare and sometimes conflicting due to the different (e.g., lab vs. field, metal loading, pH, redox potential, contact time) testing conditions (Marchand et al. 2010).

Nevertheless, many field and mesocosm studies of mine and waste water treatment wetlands indicate that active bioaccumulation by hydrophytes might be relevant for metals at trace concentration levels (e.g., Dunbabin and Bowmer 1992; Ellis et al. 1994; Maine et al. 2006; Outridge and Noller 1991; Schierup and Larsen 1981; Scholes et al. 1998; Ye et al. 1997b). By way of example, Maine et al. (2006) found root tissue metal concentrations of *T. domingensis* to multiply by factors of about 7 (Cr) and 8 (Ni) at low mean water concentrations (22 and 17 µg/L, respectively) within a year of wetland operation, and even

a doubling of Zn, despite water concentrations below detection limit (<0.05 µg/L). Perhaps most interestingly, Batty and Younger (2002) reported a maximal iron uptake by *P. australis* seedlings in laboratory exposure experiments of ≈ 100% at an iron supply of 1 mg/L, dropping at both higher and lower iron concentrations, with < 50% at 0.5 and 2 mg/L, and < 25% at < 0.1 and ≥ 5 mg/L. Metal uptake—including iron—by macrophytes in terms of mass content was shown to increase at greater concentrations (Batty and Younger 2003)—and decrease with increasing water column or flow velocity, presumably due to declining contact time between contaminated water and plant (roots) (Kumari and Tripathi 2015; Schierup and Larsen 1981; Stark et al. 1996). For instance, iron contents in shoots, rhizomes, and roots of up to almost 1, 10, and 100 g/kg dry weight, respectively, were observed at solution concentrations of 50 mg/L in the *P. australis* seedling exposure experiments by Batty and Younger (2003) mentioned above. It was also shown that wetland macrophytes accumulate different metals in different plant components, with the highest concentrations usually found in roots and rhizomes, especially compared to above-ground tissues (e.g., Ellis et al. 1994; Kumari and Tripathi 2015; Liu et al. 2007; Stark et al. 1988; Tanner 1996; Taylor and Crowder 1981; Ye et al. 2001a, b, c). For instance, Ellis et al. (1994) found Cd, Cu, Pb, and Zn in *T. latifolia* from low exposure field sites was approximately two thirds in root and rhizome tissues and only one third in leaf tissues. In comparison, up to two orders of magnitude higher concentrations of Cd, Cu, Fe, Ni, Pb, and Zn were found in roots and rhizomes compared to shoots of *T. latifolia* and *P. australis* in high exposure laboratory experiments (Batty and Younger 2003; Ye et al. 1997a, b). Furthermore, O'Sullivan et al. (2004) and Schierup and Larsen (1981) showed that metal (bio)availability for macrophytes is governed by geochemical and environmental factors, such as pH, redox potential, speciation, carbon content, and temperature. Conversely, sediment pH and redox potential are in turn influenced by wetland plants, as reported for *Typha* populations by Sencindiver and Bhumbla (1988). Altogether, bioaccumulation is expected to prevail in shallow, bog-like wetlands and waterlogged anaerobic soils or sediments with low flow velocities allowing for adequate contact time between contaminated water and plant (roots) where metal uptake and fixation is correlated with soil-sediment concentration (Taylor and Crowder 1981). Nevertheless, most of the metals that are not precipitated in the water column are expected to be retained within the soil-sediment matrix, chiefly by sorption on plant detritus and sulphide precipitation in a reducing environment (e.g., Galletti et al. 2010; Karathanasis and Johnson 2003; Maine et al. 2006; Mays and Edwards 2001; O'Sullivan et al. 2004; Ye et al. 2001c).

A more complex biogeochemical interaction is found in the rhizosphere where radial oxygen release from plant roots creates an aerobic-anaerobic interface of substantial areal extent (Armstrong et al. 1992; Dunbabin and Bowmer 1992). Iron and manganese plaque formation was observed for various plants and (metalliferous) environments directly on the root surface and throughout the sediment (Snowden and Wheeler 1995). It is still unclear whether this is simply a consequence of radial oxygen loss from roots or in fact a protective plant mechanism controlling metal phytotoxicity and uptake rates. In any case, it is clear that metal depositions act as a sink for not only iron, manganese, and aluminium (Batty and Younger 2003), but also several other trace contaminants associated with mining activities (As, Cd, Cu, Pb, Ni, and Zn) as well as phosphate (e.g., Batty et al. 2000, 2002; Hansel et al. 2001; St-Cyr and Campbell 1996; Ye et al. 1997a, 2001a).

Environmental Effects

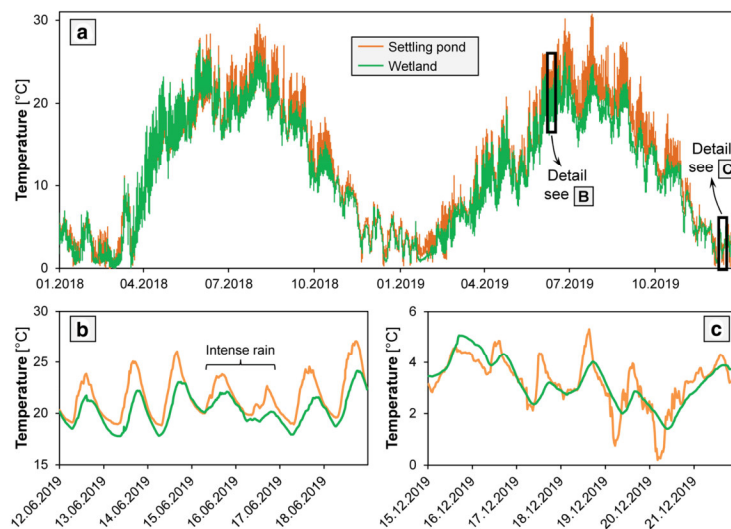
Dense macrophyte stands have considerable beneficial effects on constructed wetland functionality. Wetland macrophytes develop extensive rhizome and root systems throughout and above the substrate that physically stabilise the sediment, preventing resuspension of the accumulating ochre (James et al. 2004; Kadlec et al. 2000; Nyquist and Greger 2009). In addition, extensive and dense hydrophyte populations improve the microclimate through evapotranspiration and shading in summer as well as insulation and windbreak by senescent, erect macrophytes in winter (Brix

1994; García et al. 2003; Wittgren and Maehlum 1997). Water temperature in wetlands displays a more sluggish reaction and lower amplitude relative to settling ponds (Gearheart 1992). This effect is illustrated in Fig. 2 for the exemplifying pilot system, becoming slightly more pronounced in the second vegetation period due to increased maturity. In addition, fewer and less extreme water temperatures, particularly warm temperatures, were observed in the wetland compared to the settling pond, with maximum temperatures of 30.7 and 27.2 °C measured in settling pond and wetland, respectively. More stable temperature conditions in wetlands prevent thermal currents or buoyancy effects and thus improve gravitational settling of particulate hydrous ferric oxides, although it may also lead to semi-permanent thermal stratifications that reduce the effective volume. Additionally, windbreaking by emergent stems and leaves contributes to the hydraulic efficiency of wetlands, especially compared to bare settling ponds, by reducing wave formation, water turbulence, dispersion, and most importantly, by preventing wind-driven currents transporting contaminated water from inflow to outflow with minimal retention time (Goodarzi et al. 2018; Thackston et al. 1987). Windbreaking also contributes to corrosion control, preventing resuspension of settled flocs (Batty 2003; Braskerud 2001; Brix 1994).

Hydraulic Effects

Both settling ponds and wetlands basically provide retention time for natural biogeochemical reactions and

Fig. 2 Water temperature data from settling pond (orange lines) and wetland (green lines) of the pilot system described in Opitz et al. (2019) with **a** development over 2 years, **b** week detail from summer 2019 and **c** week detail from winter 2019 (all at 30-min measurement interval)



physical processes to proceed to completion (Jing et al. 2002). Besides accelerating or providing a better environment for respective reactions and processes as described above, macrophytes improve overall hydraulic efficiency and may ultimately increase the actual hydraulic retention time compared to bare settling ponds of equal size (Jadhav and Buchberger 1995; Persson et al. 1999). For example, Verschoren et al. (2017) conducted an experimental field comparison of a lowland river reach with fully developed, partially removed, and fully removed aquatic vegetation and reported that “*vegetation free treatments [...] had the lowest hydraulic resistance, the highest flow velocity, the highest longitudinal dispersion coefficient, the largest transient storage zone, and the lowest retention of particulate matter.*” Improved hydraulics in wetlands compared to unvegetated ponds are attributable to several effects that are directly related to macrophyte vegetation as natural hydraulic obstacles (e.g., Braskerud 2001; Buchberger and Shaw 1995; Horvath 2004; Jadhav and Buchberger 1995; Kadlec 1994; Laurent et al. 2015; Nepf 1999; Persson et al. 1999; Su et al. 2009), including but not limited to:

- Increased mixing, flow distribution and flow regulation encouraging more homogeneous hydrodynamics (approaching “plug flow”);
- Reduced flow velocities and more regular velocity profiles in the vertical direction;
- Less dead or stagnant zones, stratification, dispersion, and preferential or open-channel flow (“short-circuiting”);
- Reduced wind-related effects (see above).

For details on quantitative aspects such as hydraulic efficiency in general and effects of wetland vegetation in particular, the reader is kindly referred to respective specialised literature (e.g., Kadlec 1994; Persson et al. 1999; Thackston et al. 1987). Altogether, hydraulic retention time and advective transport increase with greater vegetation density (Braskerud 2001; Jadhav and Buchberger 1995). It is important to note that the effect of vegetation on hydraulic efficiency strongly depends on flow regime, vegetation type and density, as well as pond shape, length:width ratio, and layout (Guo et al. 2017; Persson et al. 1999; Persson and Wittgren 2003; Su et al. 2009). Badly maintained wetlands with spatially irregular vegetation distribution or silting up can have opposite effects, such as flow channelling or plugging (Brix 1994; Jadhav and Buchberger 1995; Klerk et al. 2016; Persson et al. 1999; Wahl et al. 2012). Field tracer tests of various settling ponds and wetlands in UK passive mine water treatment systems showed better hydraulic efficiency for wetlands, whereas the effective volume of settling ponds was often considerably reduced due to dispersed flow,

poor mixing, and short-circuiting (Kruse et al. 2009; Kusun et al. 2010; Sapsford 2013).

Ancillary and Secondary Benefits

Besides contributing to water quality improvement and system operation, the supplemental benefits of wetland vegetation should not be underestimated (Batty and Younger 2002). First and foremost, the near-natural appearance of lush, green wetlands increases the aesthetic appearance of the treatment system, especially compared to bare settling ponds or conventional reactor-based (chemical) treatment plants (Batty 2003). The value of wetland ecosystems beyond the intrinsic treatment purpose nowadays represented and evaluated by various ecosystem services is, without going into further detail, often widely underestimated (e.g., Liquele et al. 2016; Masi et al. 2018; McInnes 2013; Mitsch et al. 2014). In addition, constructed wetlands provide wildlife shelter and habitat with diverse biotopes and ecological or structural niches for various (even protected) aquatic and semi-aquatic species (Knight 1997; Knight et al. 2001; Lacki et al. 1992). Although constructed wetlands may develop a spatially inclusive and comprehensive, yet structurally diverse mosaic of predominantly reed beds or sedge reeds, most mine water treatment wetlands display less overall floral (and faunal) diversity compared to natural wetlands due to the monocultural reed or cattail structure (Knight 1997). This is mostly due to the technical design and management of treatment wetlands, where the primary consideration is preservation of hydraulic and treatment performance (Thullen et al. 2005). Nevertheless, constructed wetlands contribute to the restoration, development, and conservation of functioning ecological interrelations, biodiversity, wildlife corridors, and biotope networks in post-mining landscapes (Batty 2005; Feierabend 1989; Klerk et al. 2016; Yang et al. 2006). Biological water quality, which is increasingly introduced as a monitoring and valuation parameter (e.g., EU Water Framework Directive biological quality elements, U.S. EPA Biological Water Quality Criteria Program), is considerably improved through development of the increasingly diverse aquatic micro- and macro fauna within passive systems, and thus before discharge to freshwater environments. Secondary benefits such as these may become increasingly important to the acceptance level of passive mine water treatment plants amongst stakeholders, particularly residents, and environmental authorities.

Macrophyte metabolism (especially uptake and assimilation) as well as stimulation of biological activity and self-sustaining nutrient or substance cycles in wetlands lead to biotransformation of organic compounds potentially present in mine waters, such as carbon- or nitrogen-based residues from explosives or cyanidation (Koren et al. 2000; Zaitsev

et al. 2008) as well as carbon fixation (Mitsch et al. 2012). Elevated ammonia in coal mining discharges originating from degradation of organic residues in coal or lignite deposits is reduced through plant uptake and assimilation as well as autoxidative transformation towards nitrate in oxygenated wetland environments (Vymazal 2013). It is, however, important to note that the aquatic nitrogen cycle is predominantly limited to nitrification in the prevailing oxygenated environment in mine water treatment wetlands (Demim and Dudeney 2003). In any case, wetland macrophytes show high organic pollutant assimilation and removal capacities that may additionally improve mine water quality (Tanner 1996). Synergetic cotreatment of mine- and wastewater in constructed wetlands is also increasingly tested worldwide (Makhathini et al. 2020).

In summary, noteworthy (ecological) effects, amenity value, ecosystem services, and secondary benefits of wetland macrophytes, although not directly contributing to metal removal, are of considerable and increasing importance to stakeholder management, approval procedures, and environmental impact assessments. Respective environmental and ecological aspects as well as landscape diversity should not be underestimated, particularly in post-mining landscapes. Environmental benefits and ecological value are expected to increase with long-term operation and concomitant wetland maturation (Kadlec et al. 2000; Stark et al. 1988). Therefore, ecological development of constructed wetlands should be given due consideration during the technical planning stage and approval procedure.

Drawbacks and Limitations

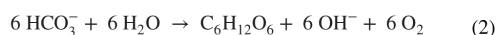
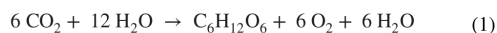
Biochemical Problems

From a biogeochemical perspective, continuous decomposition of plant litter in wetlands increases dissolved and particulate organic carbon in the water (Noller et al. 2003). Ensuing metabolic, photolytic, or autoxidative decomposition result in oxygen consumption throughout the water column. In extreme cases, this may lead to oxygen depletion, not only along the flow path, but also towards the sediment surface, and even reducing conditions within the substrate or directly above the sediment–water interface. Especially at low flow velocities or (temporally) stagnant conditions, intensive NOM generation and concomitant decomposition can substantially decrease both dissolved oxygen and redox potential (Kirby et al. 1999; Pedescoll et al. 2015). This is not to be underestimated, particularly during the growing season, as illustrated in Fig. 4 for the exemplifying pilot system where, in contrast to the settling pond, oxygen saturation in the wetland dropped below 50% in summer when NOM generation was highest and oxygen solubility lowest.

This may lead to retarded ferrous iron oxidation in the water and even ferric iron reduction in the sediment, the latter temporarily remobilising iron. This spatially and temporally increase in iron redox cycle complexity may potentially affect overall treatment performance (Johnson and Hallberg 2002), although no corresponding observations of significantly compromised treatment performance are reported.

Seasonal Variability

It is important to note that most macrophyte-related effects are subject to considerable variability, mostly due to seasonal, hydraulic, and stochastic fluctuations in wetland environments (Johnson and Hallberg 2002; Kadlec et al. 2000). First and foremost, plants directly participate in material cycles in their immediate environment through photorespiration, i.e., photosynthesis during the day and cellular respiration during the night, with the overall O₂–CO₂ budget benefitting oxygen production. Unlike terrestrial plants, hydrophytes not only affect gas equilibria in the atmosphere but also in the surrounding aqueous environment. Mine discharges are often suboxic and oversaturated with CO₂, the latter lowering the pH of the water. This directly and substantially affects metal oxidation reaction kinetics, with oxidation rates declining with a decrease in dissolved oxygen and/or pH (Geroni et al. 2012). During the day, wetland macrophytes vertically transport oxygen through the aerenchyma to the roots and thus into the water column and sediment (Armstrong et al. 1992; Brix et al. 1992). Concomitantly, dissolved CO₂ or bicarbonate diffuse into the plant, promoting photosynthesis:



This uptake of dissolved inorganic carbon accelerates CO₂-stripping in respectively oversaturated mine waters and thus increases or stabilises the pH, which in turn is one of the determining factors in most biogeochemical redox cycles. In the circumneutral range, an increase by up to one pH-unit thorough CO₂-stripping was reported by Geroni et al. (2012) and Opitz et al. (2019), which may increase iron oxidation 100-fold (Dempsey et al. 2001). However, while the pH increase would have a positive impact on ferrous iron oxidation, wetlands may display considerable pH fluctuation in either direction due to uptake of dissolved inorganic carbon by algae and macrophytes as well as the release of organic acids, as illustrated for the exemplifying pilot system in Fig. 3. Overall, biological processes in the wetland resulted in a lower median pH (about 0.5 units) compared to the preceding settling pond that only featured

Fig. 3 pH data from settling pond (orange lines) and wetland (green lines) of the pilot system described in Opitz et al. (2019) with **a** development over 1 year, **b** week detail from April 2019 and **c** distribution curve of the year-round pH-dataset (all at 30-min measurement interval)

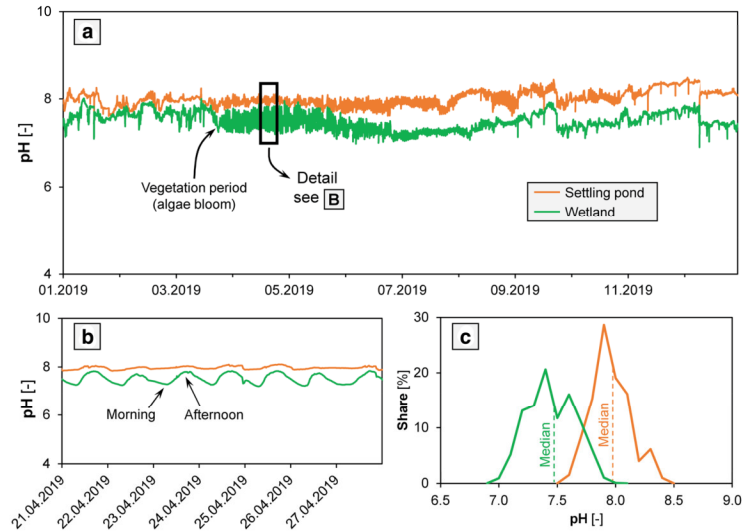
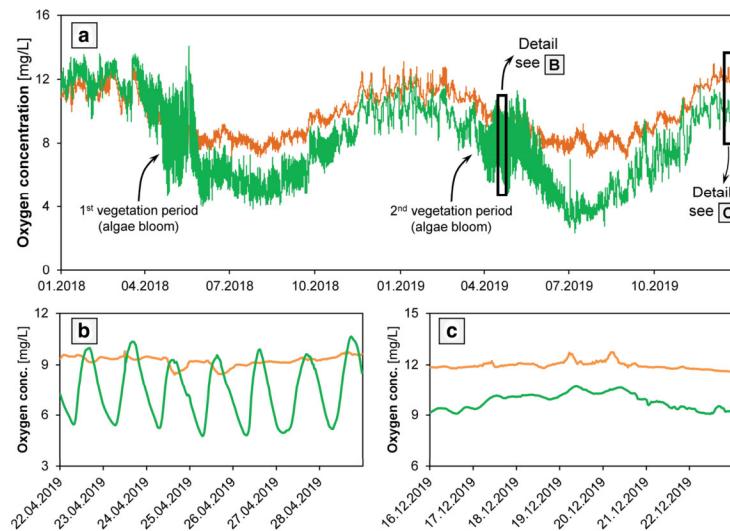


Fig. 4 Dissolved oxygen data from settling pond (orange lines) and wetland (green lines) of the pilot system described in Opitz et al. (2019) with **a** development over 2 years, **b** week detail from April 2019 and **c** distribution curve of the year-round oxygen concentration dataset (all at 30-min measurement interval)



natural CO₂-degassing, especially during spring and summer (Fig. 3c).

Common wetland macrophytes can transfer to and radiatively release up to several hundred mg/m²/h of oxygen from the rhizomes (Brix and Schierup 1990; Watson et al. 1989). Reversal of the process during the night results in diurnal

oxygen cycles with maxima early in the afternoon and minima during the night, further amplified by microbial oxygen consumption upon NOM decomposition and temperature-dependence of oxygen solubility (Dempsey et al. 2001). Since only the latter is relevant in settling ponds, the dissolved oxygen amplitude is, again, considerably larger in

wetlands compared to settling ponds as illustrated for the exemplifying pilot system in Fig. 4a. Diurnal fluctuation of dissolved oxygen in wetlands is exceptionally pronounced during algae blooms with amplitudes easily between 50 and 110% saturation (Fig. 4b) and still noticeable after full emergence of herbaceous macrophytes, yet negligible in winter (Fig. 4c). In contrast, settling ponds are expected to display relatively stable and high oxygen saturation throughout the year unless oxygen is consumed by ferrous iron oxidation. Altogether, increased oxygen solubility with decreasing temperature results in lower oxygen concentrations in summer and in the night and higher oxygen concentrations in winter at daytime for both settling ponds and wetlands, yet this is considerably pronounced in wetlands during the vegetation period (Gu et al. 2006). With homogeneous ferrous iron oxidation showing first-order dependency on oxygen concentration and inversely second-order dependency on proton activity, a shift in dissolved oxygen and/or pH inevitably affects oxidation rates and thus treatment efficiency (Dempsey et al. 2001; Hustwit et al. 1992).

Total suspended solids (TSS) content in wetland outflows can also display considerable seasonal patterns, with increased effluent TSS during the growing season due to generation of particulate NOM by vegetation growth and decay (Kadlec et al. 2000). Regarding mine water treatment wetlands, it is important to note that increased effluent TSS in summer predominantly concerns wetland-derived particulate matter (i.e., the “natural background”; Gearheart 1992), whereas effluent suspended hydrous ferric oxides are expected to decrease with vegetation development (filtration) and NOM generation during the growing season (scavenging) and increase with vegetation dieback in winter (Opitz et al. 2020). Moreover, Braskerud (2001) found that the effect of wetland vegetation on hydraulic efficiency was linked to seasonal vegetation development, increasing during the summer and decreasing during winter, with hydraulic efficiencies of 0.86 and 0.78, respectively.

Altogether, ecological and thus macrophyte-related fluctuations in hydrochemical parameters such as pI, dissolved oxygen, and TSS, as well as temperature (see Fig. 2) have both positive and negative effects on metal removal mechanisms and kinetics. Therefore, wetland performance evaluation is usually recommended on an averaged time span basis (several seasons or years) rather than on individual measured values to accommodate natural fluctuations in open systems (Kadlec et al. 2000). In contrast to surface-flow wastewater treatment wetlands, mine water treatment wetlands usually display less performance fluctuation due to ecological or seasonal variability, with physico-chemical iron and TSS removal only moderately affected by environmental variations (Gu et al. 2006; Hedin 2008). Rather, treatment efficiency is more often affected by stochastic fluctuations as well as distinct variations in consequence of inconsistent

hydraulic loading or retention time (Opitz et al. 2020; Stark et al. 1994). The effect of environmental and especially gas transfer effects on passive system performance may be reduced by ensuring thorough aeration at the inlet of (and potentially between) ponds (Cravotta 2007, 2015; Geroni et al. 2012).

Technical Difficulties

With treatment efficiency governed by wetland macrophytes, there are nevertheless drawbacks of near-natural wetlands compared to settling ponds. Although wetlands are considered a low-cost and low-maintenance technology, regular service is required to maintain ecological as well as biogeochemical and hydraulic integrity (Hedin 2020). First and foremost, wetlands require maintenance to prevent deterioration of hydraulic performance as the carefully engineered conditions that facilitate initial macrophyte establishment degrade over time. The most frequent problems include plugging, silting up, and hydrosere due to accumulating plant litter, detritus, and ochre. Receding plant cover may lead to laterally fringing vegetation with increased flow velocity through the unvegetated middle (“short-circuiting”; Jenkins and Greenway 2005; Persson et al. 1999). Detrimental conditions or pest infestation may lead to deterioration of vegetation structure and habitat value or altogether perishing of (monocultural) vegetation, warranting accompanying landscape preservation measures (Brodie 1991; Snoddy et al. 1989; Thullen et al. 2005).

It was also noted at several sites that newly constructed wetlands require up to three vegetation cycles for full maturation, which was mostly attributed to progressive development and coverage of plant communities (Fennessy and Mitsch 1989; Stark et al. 1988; Wildemann et al. 1993), but likely also applies to bacterial communities (Samsó and García 2013). If regulatory standards must be met from day one, it may prove necessary to either oversize the system, as recommended by Wildemann et al. (1993) or to (transitionally) install an additional sediment filter for effluent polishing, as successfully demonstrated by Opitz et al. (2019, 2020).

Waste Disposal

In surface-flow wetlands, a substrate depth of about 0.3 m is usually sufficient for macrophyte roots to find stable grounding, although the root zone may naturally extend much deeper, and to support hydrophytic plant life (Kadlec and Wallace 2009; Laine and Jarvis 2003). Accretion of metal (hydr)oxides and plant litter on top of the rooting soil results in an accruing sediment. Most organic residues (e.g., cellulose, hemicellulose) are readily biodegradable and thus decomposed and overturned rapidly, especially during

elevated summer temperatures (Álvarez and Bécares 2006; Chimney and Pietro 2006). However, Álvarez and Bécares (2006) estimated that only approximately two thirds of *T. latifolia* detritus decomposes within the first year, with persistent structural polymers such as lignin remaining. Consequently, sediment accumulation in wetlands is faster and characterised by a more heterogeneous composition than settling ponds. In the long run, this may ultimately result in sediment build-up and hydrosere, necessitating excavation and refurbishment of the constructed wetland.

Generally, settling ponds are designed to retain the bulk of ochre solids and thus require more frequent sludge removal than wetlands (Nuttal 2003). The accumulating sediment in settling ponds predominantly consists of hydrous ferric oxides, with some allochthonous (e.g., biotic or wind-borne) material (Fig. 5a). The ochreous sludge is easily removed and dewatered (Dempsey and Jeon 2001), and either disposed of or used for various purposes, subject to composition (e.g., Hedin 2003; Sapsford et al. 2015). Polishing wetlands exhibit longer life spans, despite the additional accumulation of organic matter. Wetland sediments consist of the original soil substrate, accumulated hydrous ferric oxides, and a substantial amount of organic matter comprising litter, roots, and detritus in various stages of decomposition (Fig. 5b) (Kadlec et al. 2000). The heterogeneous material is usually unfit for valorisation, and the organic content complicates or altogether prevents landfill disposal. There is a longstanding discussion regarding appropriate utilisation as opposed to disposal of ochreous and organic-rich substrates excavated from mine water treatment wetlands that is ultimately governed by the applicable legal framework. Even if contamination of the mine water and thus the sediment is basically limited to Fe, Al, and Mn, the material may still be technically classified as waste material and thus require complex screening and permission procedures as well as pre-treatment (i.e., oxidation and stabilisation) for reuse in

the environment as, for instance, soil amendment or top-soil. Furthermore, wetlands may require a little more routine effort for maintenance of optimal hydraulic, ecological, and technical conditions (e.g., prevention of clogging or silting up, pest prevention) and refurbishment, the latter requiring the removal of rhizomes prior to sludge removal for reuse after replenishing of the substrate layer.

Discussion

Designing and planning of passive systems, particularly at legacy or socialised mine sites, is often inevitably guided by economic considerations and land area availability. Obviously, iron removal in unvegetated settling ponds is mostly limited to chemical oxidation of dissolved ferrous iron and physical sedimentation of settleable hydrous ferric oxides, whereas colloidal hydrous ferric oxides often break through settling ponds due to their low settling velocities. In contrast, this review clearly shows that vegetated surface-flow wetlands are in many ways more effective for iron removal due to a variety of auxiliary processes and effects. Most importantly, macrophyte-related filtration, in combination with physico-chemical, biogeochemical, and hydraulic effects, are indispensable for not only removal of settleable hydrous ferric oxides, but also polishing of residual dissolved ferrous iron and ferric colloids where mere gravitational sedimentation would require several days. The effective removal of residual iron is of major importance to reliably meet (strict) regulatory standards.

However, it is important to note that the macrophyte-related advantage in treatment performance goes hand in hand with additional effort and expenditure in operation, maintenance, cleanout, and restoration (Kadlec et al. 2000). Accordingly, overloading of wetlands will rapidly smother and clog macrophyte stands, resulting in declining treatment efficiency and shorter restoration cycles. This trade-off led to the current state of the art, where settling ponds and wetlands are serially connected in composite passive systems for pre-treatment of the bulk iron loading and polishing of residual iron, respectively, as outlined in Table 1 (Hedin et al. 1994). This way, both overall system performance and efficiency are increased, whilst protecting wetlands from overloading.

Unfortunately, quantitative target criteria recommendations, especially for pre-treatment, are limited to rather rough approximations, for instance aiming at 50–70% iron removal in upstream settling ponds (Dey et al. 2003; Parker 2003). A 50% reduction of a highly ferruginous inflow may, however, still result in wetland overloading, especially if the wetland receives high concentrations of ferrous iron. Similar problems may be observed for the long-established area-adjusted iron removal concept for neutral or alkaline mine water outlined by Hedin et al.

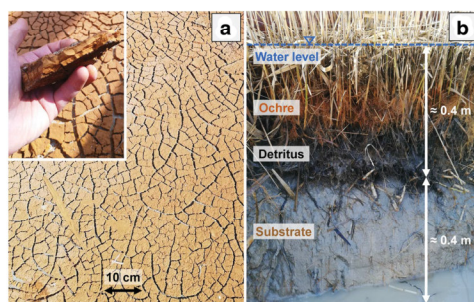


Fig. 5 Photos of **a** sun-dried ochre in a settling pond and **b** profile of a drained surface-flow reed wetland from the pilot system described in Opitz et al. (2019)

Table 1 Juxtaposition of core advantages and disadvantages of settling ponds and wetlands for iron removal

Iron removal process	Settling ponds	Wetlands
Ferrous iron oxidation	+ Good oxygen transfer + Ample residence time + Plentiful dispersed catalytic surfaces + Warm summer temperatures + Mixing and turbulence (wind, buoyancy, etc.) + Effective CO ₂ degassing – Poor hydraulic efficiency – Cold winter temperatures	+ Catalytic plant surfaces + Growth surfaces for bacteria + Hydraulic efficiency + Vertical oxygen transport by plants – Decompositional oxygen depletion – pH amplitude – Little mixing – Diurnal and seasonal variability
Removal of hydrous ferric oxides	+ Gravitational settling + Intensive (homo)aggregation + Large sludge storage capacity + Ample residence time – Mixing and turbulence – Potential re-suspension – Poor hydraulic efficiency	+ Gravitational settling + Filtration by dense vegetation + Heteroaggregation + Scavenging by organic matter + Quiescent body of water + Hydraulic efficiency – Small sludge storage capacity
Primary field of application	Broad ferrous iron oxidation and aggregation-based sedimentation of the bulk loading	Effective removal of both dissolved and suspended residual iron

(1994). Both percentage- and area-adjusted removal concepts are, according to the principles of mass action, concentration-independent (i.e., linear) approaches and thus tend to under- and overestimate iron removal at high and low iron loadings, respectively (Hedin et al. 1994; Hedin 2008). Thus, current engineering guidelines fail to provide an adequate quantitative basis for customised design and sizing of settling ponds for pre-treatment and wetlands for polishing (Sapsford and Watson 2011). To optimally exploit the respective advantages of both treatment units and thus minimise the areal footprint and overhead of composite passive systems, it will be necessary to develop a better quantitative understanding of the concentration-dependent relationships between pond size (or hydraulic retention time) and iron removal kinetics.

- Physical filtration of colloidal hydrous ferric oxides that are unlikely to gravitationally settle within a given retention time by dense wetland vegetation;
- Scavenging and heteroaggregation of dissolved and colloidal iron, respectively, by plant-derived NOM;
- Improved hydrodynamics and hydraulic efficiency of vegetated treatment ponds, considerably augmenting retention and exposure time.

Summary

Positive effects of macrophytes on passive mine water treatment are mostly attributable to a variety of (interrelated) processes and factors conglomerated in the wetland-specific aquatic and benthic environment (Fig. 6). The main conclusion of this review is that the contribution of macrophytes to water quality in general and iron/metal removal from mine drainage in particular becomes especially important for low or residual iron concentrations due to a number of mechanisms and effects that are intrinsic to wetland environments and do not occur in bare settling ponds:

- Enhanced biogeochemical oxidation and precipitation of hydrolysable metals due to catalytic reactions and bacterial activity on immersed macrophyte surfaces;

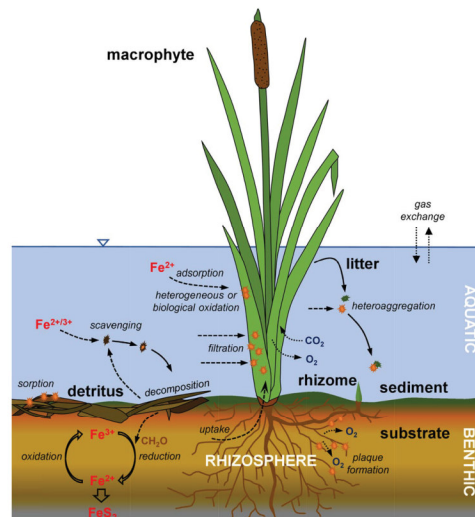


Fig. 6 Schematised effects of macrophytes on iron (metal) removal in surface-flow wetlands

While this review provides an extensive qualitative overview of macrophyte-related effects on passive mine water treatment, we emphasise that quantification of, for a start, the individual effects described above, but principally the overall contribution of macrophytes specifically to metal/iron removal is limited to complex, predominantly site-specific, and thus untransferable model approaches. One of the main reasons is the unknown number and magnitude as well as the variability of vegetation-related influencing factors (Brisson and Chazarenc 2009; Kuehn and Moore 1995). Comparative studies of settling ponds and especially wetlands showed that performance may be similar under comparable conditions yet may vary considerably due to primary influencing factors, such as contaminant loading or retention time, and potential secondary (i.e., ecological) factors such as plant species, density, and development as well as seasonal patterns, and water and substrate depth. Although the literature provides various approaches to estimate macrophyte effects on the removal of particulate matter (especially clastic sediments and other natural particles) in wetlands and small lotic systems, little of this data is easily transferable to other cases, much less usable or applicable for actually designing or sizing constructed mine water treatment wetlands. Nevertheless, as both Pluntke and Kozerski (2003) and Saiers et al. (2003) found the suspended concentration of micro-metre particles and submicron colloids, respectively, to be the most likely determining factor for macrophyte-related particle retention under similar hydrodynamic conditions, we speculate that a way forward may be the systematic empirical or model-based determination of simplified iron removal relationships or rates. At the very least, a roughly estimated “filtration-factor” for wetlands compared with or relative to settling ponds would help to more specifically deploy either component in composite passive systems.

Well-designed and -maintained, fully mature constructed wetlands continually and reliably achieve iron removal rates > 90%, little short of conventional, chemical treatment plants. Nevertheless, this study shows that the choice between and optimal sizing of settling ponds and wetlands in a composite passive system must consider the intrinsic advantages and limitations of the two components. Optimal system design requires an elaborate concept that duly considers economic, ecologic, and legal aspects. A much better knowledge of iron/metal removal kinetics in surface-flow mine water treatment systems would facilitate optimised apportionment and consequential specific sizing of the two treatment stages, for instance settling ponds and wetlands deliberately designed to first lower iron concentration to $\approx 5\text{--}10$ mg/L and then below the site-specific legal limit (polishing).

Acknowledgements The study was conducted as part of a research project funded by the German Federal Environmental Foundation (project 33012/01-23).

Funding Open Access funding enabled and organized by Projekt DEAL.

Open Access This article is licensed under a Creative Commons Attribution 4.0 International License, which permits use, sharing, adaptation, distribution and reproduction in any medium or format, as long as you give appropriate credit to the original author(s) and the source, provide a link to the Creative Commons licence, and indicate if changes were made. The images or other third party material in this article are included in the article's Creative Commons licence, unless indicated otherwise in a credit line to the material. If material is not included in the article's Creative Commons licence and your intended use is not permitted by statutory regulation or exceeds the permitted use, you will need to obtain permission directly from the copyright holder. To view a copy of this licence, visit <http://creativecommons.org/licenses/by/4.0/>.

References

- Álvarez JA, Bécarea E (2006) Seasonal decomposition of *Typha latifolia* in a free-water surface constructed wetland. *Ecol Eng* 28(2):99–105. <https://doi.org/10.1016/j.ecoleng.2006.05.001>
- Armstrong J, Armstrong W, Beckett PM (1992) *Phragmites australis*: Venturi- and humidity-induced pressure flows enhance rhizome aeration and rhizosphere oxidation. *New Phytol* 120(2):197–207. <https://doi.org/10.1111/j.1469-8137.1992.tb05655.x>
- Banfield JF, Welch SA, Zhang H, Ebert TT, Penn RL (2000) Aggregation-based crystal growth and microstructure development in natural iron oxyhydroxide biomineralization products. *Science* 289(5480):751–754. <https://doi.org/10.1126/science.289.5480.751>
- Batty LC (2003) Wetland plants—more than just a pretty face? *Land Contam Reclamat* 11(2):173–180. <https://doi.org/10.2462/09670513.812>
- Batty LC (2005) Wetland systems associated with mine sites as a source of biodiversity. In: Loredó J, Pendás F (eds), *Proc, 9th IMWA Congress, Oviedo*, pp 525–531
- Batty LC, Younger PL (2002) Critical role of macrophytes in achieving low iron concentrations in mine water treatment wetlands. *Environ Sci Technol* 36(18):3997–4002. <https://doi.org/10.1021/es020033+>
- Batty LC, Younger PL (2003) Effects of external iron concentration upon seedling growth and uptake of Fe and phosphate by the common reed, *Phragmites australis* (Cav.) Trin ex. Steudel. *Ann Bot* 92(6):801–806. <https://doi.org/10.1093/aob/mcg205>
- Batty LC, Younger PL (2004) Growth of *Phragmites australis* (Cav.) Trin ex. Steudel in mine water treatment wetlands: effects of metal and nutrient uptake. *Environ Pollut* 132(1):85–93. <https://doi.org/10.1016/j.envpol.2004.03.022>
- Batty LC, Baker AJ, Wheeler BD, Curtis CD (2000) The Effect of pH and plaque on the uptake of Cu and Mn in *Phragmites australis* (Cav.) Trin ex. Steudel. *Ann Bot* 86(3):647–653. <https://doi.org/10.1006/anbo.2000.1191>
- Batty LC, Hooley D, Younger PL (2008) Iron and manganese removal in wetland treatment systems: rates, processes and implications for management. *Sci Total Environ* 394(1):1–8. <https://doi.org/10.1016/j.scitotenv.2008.01.002>
- Bavor HJ, Davies CM, Sakadevan K (2001) Stormwater treatment: do constructed wetlands yield improved pollutant management

- performance over a detention pond system? *Water Sci Technol* 44(11–12):565–570. <https://doi.org/10.2166/wst.2001.0881>
- Bezbaruah AN, Zhang TC (2004) pH, Redox, and oxygen microprofiles in rhizosphere of bulrush (*Scirpus validus*) in a constructed wetland treating municipal wastewater. *Biotechnol Bioeng* 88(1):60–70. <https://doi.org/10.1002/bit.20208>
- Braskerud BC (2001) The influence of vegetation on sedimentation and resuspension of soil particles in small constructed wetlands. *J Environ Qual* 30(4):1447–1457. <https://doi.org/10.2134/jeq2001.3041447x>
- Brenner EK, Brenner FJ, Brovard S, Schwartz TE (1993) Analysis of wetland treatment systems for acid mine drainage. *J Penn Acad Sci* 67(2):85–93
- Brisson J, Chazarenc F (2009) Maximizing pollutant removal in constructed wetlands: Should we pay more attention to macrophyte species selection? *Sci Total Environ* 407(13):3923–3930. <https://doi.org/10.1016/j.scitotenv.2008.05.047>
- Brix H (1994) Functions of macrophytes in constructed wetlands. *Water Sci Technol* 29(4):71–78. <https://doi.org/10.2166/wst.1994.0160>
- Brix H, Schierup HH (1990) Soil oxygenation in constructed reed beds: the role of macrophyte and soil-atmosphere interface oxygen transport. *Proc, International Conf on the Use of Constructed Wetlands in Water Pollution Control*, Cambridge, pp 53–66
- Brix H, Sorrell BK, Orr PT (1992) Internal pressurization and convective gas flow in some emergent freshwater macrophytes. *Limnol Oceanogr* 37(7):1420–1433. <https://doi.org/10.4319/lo.1992.37.7.1420>
- Brodie GA (1991) Achieving compliance with staged, aerobic, constructed wetlands to acid drainage. *Proc, 1991 National ASMR Meeting, Durango*, pp 151–174. <https://doi.org/10.21000/ASMR91010151>
- Buchberger SG, Shaw GB (1995) An approach toward rational design of constructed wetlands for wastewater treatment. *Ecol Eng* 4(4):249–275. [https://doi.org/10.1016/0925-8574\(94\)00053-8](https://doi.org/10.1016/0925-8574(94)00053-8)
- Chabbi A (1999) *Juncus bulbosus* as a pioneer species in acidic lignite mining lakes: interactions, mechanism and survival strategies. *New Phytol* 144(1):133–142. <https://doi.org/10.1046/j.1469-8137.1999.00503.x>
- Chimney MJ, Pietro KC (2006) Decomposition of macrophyte litter in a subtropical constructed wetland in south Florida (USA). *Ecol Eng* 27(4):301–321. <https://doi.org/10.1016/j.ecoleng.2006.05.016>
- Cotton JA, Wharton G, Bass JA, Heppell CM, Wotton RS (2006) The effects of seasonal changes to in-stream vegetation cover on patterns of flow and accumulation of sediment. *Geomorphology* 77(3–4):320–334. <https://doi.org/10.1016/j.geomorph.2006.01.010>
- Cravotta CA (2007) Passive aerobic treatment of net-alkaline, iron-laden drainage from a flooded underground anthracite mine, Pennsylvania, USA. *Mine Water Environ* 26(3):128–149. <https://doi.org/10.1007/s10230-007-0002-8>
- Cravotta CA (2015) Monitoring, field experiments, and geochemical modeling of Fe(II) oxidation kinetics in a stream dominated by net-alkaline coal-mine drainage, Pennsylvania, USA. *Appl Geochem* 62:96–107. <https://doi.org/10.1016/j.apgeochem.2015.02.009>
- de Klerk AR, Oberholster PJ, van Wyk JH, Truter JC, Schaefer LM, Botha AM (2016) The effect of rehabilitation measures on ecological infrastructure in response to acid mine drainage from coal mining. *Ecol Eng* 95(1):463–474. <https://doi.org/10.1016/j.ecoleng.2016.06.070>
- Demim OA, Dudeney AWL (2003) Nitrification in constructed wetlands treating ochreous mine water. *Mine Water Environ* 22(1):15–21. <https://doi.org/10.1007/s102300300003>
- Dempsey BA, Jeon BH (2001) Characteristics of sludge produced from passive treatment of mine drainage. *Geochem Explor Env Anal* 1(1):89–94. <https://doi.org/10.1144/geochem.1.1.89>
- Dempsey BA, Roscoe HC, Ames R, Hedin RS, Jeon BH (2001) Ferrous oxidation chemistry in passive abiotic systems for the treatment of mine drainage. *Geochem Explor Env Anal* 1(1):81–88. <https://doi.org/10.1144/geochem.1.1.81>
- Dey M, Sadler PJK, Williams KP (2003) A novel approach to mine water treatment. *Land Contam Reclam* 11(2):253–258. <https://doi.org/10.2462/09670513.822>
- Doyle MO, Otte ML (1997) Organism-induced accumulation of iron, zinc and arsenic in wetland soils. *Environ Poll* 96(1):1–11. [https://doi.org/10.1016/S0269-7491\(97\)00014-6](https://doi.org/10.1016/S0269-7491(97)00014-6)
- Droppo IG, Ongley ED (1994) Flocculation of suspended sediment in rivers of southeastern Canada. *Water Res* 28(8):1799–1809. [https://doi.org/10.1016/0043-1354\(94\)90253-4](https://doi.org/10.1016/0043-1354(94)90253-4)
- Dunbabin JS, Bowmer KH (1992) Potential use of constructed wetlands for treatment of industrial wastewaters containing metals. *Sci Total Environ* 111(2–3):151–168. [https://doi.org/10.1016/0048-9697\(92\)90353-T](https://doi.org/10.1016/0048-9697(92)90353-T)
- Elliot AH (2000) Settling of fine sediment in a channel with emergent vegetation. *J Hydraul Eng* 126(8):570–577. [https://doi.org/10.1061/\(ASCE\)0733-9429\(2000\)126:8\(570\)](https://doi.org/10.1061/(ASCE)0733-9429(2000)126:8(570))
- Ellis JB, Shutes RB, Revitt DM, Zhang TT (1994) Use of macrophytes for pollution treatment in urban wetlands. *Resour Conserv Recy* 11(1–4):1–12. [https://doi.org/10.1016/0921-3449\(94\)90074-4](https://doi.org/10.1016/0921-3449(94)90074-4)
- Emerson D, de Vet W (2015) The role of FeOB in engineered water ecosystems: a review. *J Am Water Works Ass* 107(1):47–57. <https://doi.org/10.5942/jawwa.2015.107.0004>
- Emerson D, Weiss JV, Magonigal JP (1999) Iron-oxidizing bacteria are associated with ferric hydroxide precipitates (Fe-plaque) on the roots of wetland plants. *Appl Environ Microb* 65(6):2758–2761. <https://doi.org/10.1128/AEM.65.6.2758-2761.1999>
- Ernst (1996) Bioavailability of heavy metals and decontamination of soils by plants. *Appl Geochem* 11(1–2):163–167. [https://doi.org/10.1016/0883-2927\(95\)00040-2](https://doi.org/10.1016/0883-2927(95)00040-2)
- Feierabend JS (1989) Wetlands: the lifeblood of wildlife. In: Hammer DA (ed), *Proc, 1st International Conf on Constructed Wetlands for Wastewater Treatment*, pp 107–118
- Fennessey MS, Mitsch WJ (1989) Treating coal mine drainage with an artificial wetland. *Res J Water Pollut C* 61(11/12):1691–1701
- Fernandes JC, Henriques FS (1990) Metal levels in soils and cattail (*Typha latifolia* L.) plants in a pyrites mine area at Lousal, Portugal. *Int J Environ Stud* 36(3):205–210. <https://doi.org/10.1080/00207239008710597>
- Galletti A, Verlicchi P, Ranieri E (2010) Removal and accumulation of Cu, Ni and Zn in horizontal subsurface flow constructed wetlands: Contribution of vegetation and filling medium. *Sci Total Environ* 408(21):5097–5105. <https://doi.org/10.1016/j.scitotenv.2010.07.045>
- García J, Ojeda E, Sales E, Chico F, Píriz T, Aguirre P, Mujeriego R (2003) Spatial variations of temperature, redox potential, and contaminants in horizontal flow reed beds. *Ecol Eng* 21(2–3):129–142. <https://doi.org/10.1016/j.ecoleng.2003.10.001>
- Gearheart RA (1992) Use of constructed wetlands to treat domestic wastewater, city of Arcata. *California Water Sci Technol* 26(7–8):1625–1637. <https://doi.org/10.2166/wst.1992.0606>
- Geroni JN, Cravotta CA III, Sapsford DJ (2012) Evolution of the chemistry of Fe bearing waters during CO₂ degassing. *Appl Geochem* 27(12):2335–2347. <https://doi.org/10.1016/j.apgeochem.2012.07.017>
- Girts MA, Kleinmann RL, Erickson PM (1987) Performance data on *Typha* and *Sphagnum* wetlands constructed to treat coal mine drainage. *Proc, 8th Annual West Virginia Surface Mine Drainage Task Force Symp*

- Goodarzi D, Lari KS, Alighardashi A (2018) A Large Eddy Simulation study to assess low-speed wind and baffle orientation effects in a water treatment sedimentation basin. *Water Sci Technol* 2:412–421. <https://doi.org/10.2166/wst.2018.171>
- Gu B, Chimney MH, Newman J, Nungesser MK (2006) Limnological characteristics of a subtropical constructed wetland in south Florida (USA). *Ecol Eng* 27(4):345–360. <https://doi.org/10.1016/j.ecoleng.2006.05.013>
- Guo C, Cui Y, Dong B, Liu F (2017) Tracer study of the hydraulic performance of constructed wetlands planted with three different aquatic plant species. *Ecol Eng* 102(1):433–442. <https://doi.org/10.1016/j.ecoleng.2017.02.040>
- Hansel CM, Fendorf S, Suttons S, Newville M (2001) Characterization of Fe plaque and associated metals on the roots of mine-waste impacted aquatic plants. *Environ Sci Technol* 35(19):3863–3868. <https://doi.org/10.1021/es0105459>
- Hedin RS (2003) Recovery of marketable iron oxide from mine drainage in the USA. *Land Contam Reclam* 11(2):93–97. <https://doi.org/10.2462/09670513.802>
- Hedin RS (2008) Iron removal by a passive system treating alkaline coal mine drainage. *Mine Water Environ* 27(4):200–209. <https://doi.org/10.1007/s10230-008-0041-9>
- Hedin RS (2020) Long-term performance and costs for the Anna S mine passive treatment systems. *Mine Water Environ* 39(2):345–355. <https://doi.org/10.1007/s10230-020-00676-9>
- Hedin RS, Narin RW, Kleinmann RLP (1994) Passive treatment of coal mine drainage. US Bureau of Mines, Information Circular 9389
- Henrot J, Wieder RK (1990) Processes of iron and manganese retention in laboratory peat microcosms subjected to acid mine drainage. *J Environ Qual* 19(2):312–320. <https://doi.org/10.2134/jeq1990.00472425001900020018x>
- Horvath TG (2004) Retention of particulate matter by macrophytes in a first-order stream. *Aquat Bot* 78(1):27–36. <https://doi.org/10.1016/j.aquabot.2003.09.003>
- Huntsman RF, Solch JG, Porter MD (1978) Utilization of *Sphagnum* species dominated bog for coal acid mine drainage abatement. In: Proc, 91st Annual GSA Meeting, Toronto 10(7), 426 pp
- Hustwit CC, Ackman TE, Erickson PE (1992) The role of oxygen transfer in acid mine drainage (AMD) treatment. *Water Environ Res* 64(6):817–823. <https://doi.org/10.2175/WER.64.6.10>
- Ilbert M, Bonnefoy V (2013) Insight into the evolution of the iron oxidation pathways. *Biochim Biophys Acta* 1827(2):161–175. <https://doi.org/10.1016/j.bbabi.2012.10.001>
- Jadhav RS, Buchberger SG (1995) Effects of vegetation on flow through free water surface wetlands. *Ecol Eng* 5(4):481–496. [https://doi.org/10.1016/0925-8574\(95\)00039-9](https://doi.org/10.1016/0925-8574(95)00039-9)
- James WF, Barko JW, Butler MG (2004) Shear stress and sediment resuspension in relation to submersed macrophyte biomass. *Hydrobiologia* 515(1–3):181–191. <https://doi.org/10.1023/B:HYDR.0000027329.67391.c6>
- Jenkins GA, Greenway M (2005) The hydraulic efficiency of fringing versus banded vegetation in constructed wetlands. *Ecol Eng* 25(1):61–72. <https://doi.org/10.1016/j.ecoleng.2005.03.001>
- Jing SR, Lin YF, Wang TW, Lee DY (2002) Microcosm wetlands for wastewater treatment with different hydraulic loading rates and macrophytes. *J Environ Qual* 31(2):690–696. <https://doi.org/10.2134/jeq2002.0690>
- Johnson DB, Hallberg KB (2002) Pitfalls of passive mine water treatment. *Rev Environ Sci Bio* 1(4):335–343. <https://doi.org/10.1023/A:1023219300286>
- Kadlec RH (1994) Detention and mixing in free water wetlands. *Ecol Eng* 3(4):345–380. [https://doi.org/10.1016/0925-8574\(94\)00007-7](https://doi.org/10.1016/0925-8574(94)00007-7)
- Kadlec RH (2003) Pond and wetland treatment. *Water Sci Technol* 48(5):1–8. <https://doi.org/10.2166/wst.2003.0266>
- Kadlec RH, Wallace SD (2009) *Treatment wetlands* (2nd Edition). CRC Press, 1046 pp
- Kadlec RH, Knight RL, Vymazal J, Brix H, Cooper P, Haberl R (2000) *Constructed wetlands for pollution control: Processes, performance, design and operation*. IWA Publishing, Scientific and Technical Report No. 8, 156 pp
- Kappler A, Emerson D, Gralnick J, Roden E, Muehe EM (2015) *Geomicrobiology of iron*. Chapter 17 In: Ehrlich's *Geomicrobiology* (6th Edition), Taylor & Francis Ltd., 635 pp. <https://doi.org/10.1201/b19121-18>
- Karathanasis AD, Johnson CM (2003) Metal removal potential by three aquatic plants in an acid mine drainage wetland. *Mine Water Environ* 22(1):22–30. <https://doi.org/10.1007/s102300300004>
- Khalid S, Shahid M, Niazi KK, Murtaza B, Bibi I, Dumat C (2017) A comparison of technologies for remediation of heavy metal contaminated soils. *J Geochem Explor* 182(B):247–268. <https://doi.org/10.1016/j.gexplo.2016.11.021>
- Kirby CS, Thomas HM, Southam G, Donald R (1999) Relative contributions of abiotic and biological factors in Fe(II) oxidation in mine drainage. *Appl Geochem* 14(4):511–530. [https://doi.org/10.1016/S0883-2927\(98\)00071-7](https://doi.org/10.1016/S0883-2927(98)00071-7)
- Kleinmann RL, Tiernan TO, Solch JG, Harris RL (1983) A low-cost, low-maintenance treatment system for acid mine drainage using *Sphagnum* moss and limestone. In: Graves DH (ed), Proc, 1983 Symp on Surface Mining, Hydrology, Sedimentology, and Reclamation, Lexington, pp 241–245
- Knight RL (1997) Wildlife habitat and public use benefits of treatment wetlands. *Water Sci Technol* 35(5):35–43. [https://doi.org/10.1016/S0273-1223\(97\)00050-4](https://doi.org/10.1016/S0273-1223(97)00050-4)
- Knight RL, Clarke RA Jr, Bastian RK (2001) Surface flow (sf) treatment wetlands as a habitat for wildlife and humans. *Water Sci Technol* 44(11–12):27–38. <https://doi.org/10.2166/wst.2001.0806>
- Koren DW, Gould WD, Bédard P (2000) Biological removal of ammonia and nitrate from simulated mine and mill effluents. *Hydrometallurgy* 56(2):127–144. [https://doi.org/10.1016/S0304-386X\(99\)00088-2](https://doi.org/10.1016/S0304-386X(99)00088-2)
- Kruse NA, Gozzard E, Jarvis AP (2009) Determination of hydraulic residence times in several UK mine water treatment systems and their relationship to iron removal. *Mine Water Environ* 28(2):115–123. <https://doi.org/10.1007/s10230-009-0068-6>
- Kuehn E, Moore JA (1995) Variability of treatment performance in constructed wetlands. *Water Sci Technol* 32(3):241–250. [https://doi.org/10.1016/0273-1223\(95\)00625-7](https://doi.org/10.1016/0273-1223(95)00625-7)
- Kumari M, Tripathi BD (2015) Efficiency of *Phragmites australis* and *Typha latifolia* for heavy metal removal from wastewater. *Ecotox Environ Safe* 112(1):80–86. <https://doi.org/10.1016/j.ecoenv.2014.10.034>
- Kusin FM, Jarvis AP, Gandy CJ (2010) Hydraulic residence time and iron removal in a wetland receiving ferruginous mine water over a 4 year period from commissioning. *Water Sci Technol* 62(8):937–946. <https://doi.org/10.2166/wst.2010.495>
- Lacki MJ, Hummer JW, Webster HJ (1992) Mine-drainage treatment wetland as habitat for herpetofaunal wildlife. *Environ Manage* 16(4):513–520. <https://doi.org/10.1007/BF02394127>
- Laine DM, Jarvis AP (2003) Engineering design aspects of passive in situ remediation of mining effluents. *Land Contam Reclam* 11(2):113–125. <https://doi.org/10.2462/09670513.805>
- Larsen VJ, Schierup HH (1981) Macophyte cycling of zinc, copper, lead and cadmium in the littoral zone of a polluted and a non-polluted lake. II. Seasonal changes in heavy metal content of above-ground biomass and decomposing leaves of *Phragmites australis* (Cav.) Trin. *Aquat Bot* 11(1):211–230. [https://doi.org/10.1016/0304-3770\(81\)90062-0](https://doi.org/10.1016/0304-3770(81)90062-0)
- Laurent J, Bois P, Nuel M, Wanko A (2015) Systemic models of full-scale surface flow treatment wetlands: determination by

- Goodarzi D, Lari KS, Alighardashi A (2018) A Large Eddy Simulation study to assess low-speed wind and baffle orientation effects in a water treatment sedimentation basin. *Water Sci Technol* 2:412–421. <https://doi.org/10.2166/wst.2018.171>
- Gu B, Chimney MH, Newman J, Nungesser MK (2006) Limnological characteristics of a subtropical constructed wetland in south Florida (USA). *Ecol Eng* 27(4):345–360. <https://doi.org/10.1016/j.ecoleng.2006.05.013>
- Guo C, Cui Y, Dong B, Liu F (2017) Tracer study of the hydraulic performance of constructed wetlands planted with three different aquatic plant species. *Ecol Eng* 102(1):433–442. <https://doi.org/10.1016/j.ecoleng.2017.02.040>
- Hansel CM, Fendorf S, Suttons S, Newville M (2001) Characterization of Fe plaque and associated metals on the roots of mine-waste impacted aquatic plants. *Environ Sci Technol* 35(19):3863–3868. <https://doi.org/10.1021/es0105459>
- Hedin RS (2003) Recovery of marketable iron oxide from mine drainage in the USA. *Land Contam Reclam* 11(2):93–97. <https://doi.org/10.2462/09670513.802>
- Hedin RS (2008) Iron removal by a passive system treating alkaline coal mine drainage. *Mine Water Environ* 27(4):200–209. <https://doi.org/10.1007/s10230-008-0041-9>
- Hedin RS (2020) Long-term performance and costs for the Anna S mine passive treatment systems. *Mine Water Environ* 39(2):345–355. <https://doi.org/10.1007/s10230-020-00676-9>
- Hedin RS, Narin RW, Kleinmann RLP (1994) Passive treatment of coal mine drainage. US Bureau of Mines, Information Circular 9389
- Henrot J, Wieder RK (1990) Processes of iron and manganese retention in laboratory peat microcosms subjected to acid mine drainage. *J Environ Qual* 19(2):312–320. <https://doi.org/10.2134/jeq1990.00472425001900020018x>
- Horvath TG (2004) Retention of particulate matter by macrophytes in a first-order stream. *Aquat Bot* 78(1):27–36. <https://doi.org/10.1016/j.aquabot.2003.09.003>
- Huntsman RF, Solch JG, Porter MD (1978) Utilization of *Sphagnum* species dominated bog for coal acid mine drainage abatement. In: Proc, 91st Annual GSA Meeting, Toronto 10(7), 426 pp
- Hustwit CC, Ackman TE, Erickson PE (1992) The role of oxygen transfer in acid mine drainage (AMD) treatment. *Water Environ Res* 64(6):817–823. <https://doi.org/10.2175/WER.64.6.10>
- Ilbert M, Bonnefoy V (2013) Insight into the evolution of the iron oxidation pathways. *Biochim Biophys Acta* 1827(2):161–175. <https://doi.org/10.1016/j.bbap.2012.10.001>
- Jadhav RS, Buchberger SG (1995) Effects of vegetation on flow through free water surface wetlands. *Ecol Eng* 5(4):481–496. [https://doi.org/10.1016/0925-8574\(95\)00039-9](https://doi.org/10.1016/0925-8574(95)00039-9)
- James WF, Barko JW, Butler MG (2004) Shear stress and sediment resuspension in relation to submersed macrophyte biomass. *Hydrobiologia* 515(1–3):181–191. <https://doi.org/10.1023/B:HYDR.0000027329.67391.c6>
- Jenkins GA, Greenway M (2005) The hydraulic efficiency of fringing versus banded vegetation in constructed wetlands. *Ecol Eng* 25(1):61–72. <https://doi.org/10.1016/j.ecoleng.2005.03.001>
- Jing SR, Lin YF, Wang TW, Lee DY (2002) Microcosm wetlands for wastewater treatment with different hydraulic loading rates and macrophytes. *J Environ Qual* 31(2):690–696. <https://doi.org/10.2134/jeq2002.0690>
- Johnson DB, Hallberg KB (2002) Pitfalls of passive mine water treatment. *Rev Environ Sci Bio* 1(4):335–343. <https://doi.org/10.1023/A:1023219300286>
- Kadlec RH (1994) Detention and mixing in free water wetlands. *Ecol Eng* 3(4):345–380. [https://doi.org/10.1016/0925-8574\(94\)00007-7](https://doi.org/10.1016/0925-8574(94)00007-7)
- Kadlec RH (2003) Pond and wetland treatment. *Water Sci Technol* 48(5):1–8. <https://doi.org/10.2166/wst.2003.0266>
- Kadlec RH, Wallace SD (2009) *Treatment wetlands* (2nd Edition). CRC Press, 1046 pp
- Kadlec RH, Knight RL, Vymazal J, Brix H, Cooper P, Haberl R (2000) *Constructed wetlands for pollution control: Processes, performance, design and operation*. IWA Publishing, Scientific and Technical Report No. 8, 156 pp
- Kappler A, Emerson D, Gralnick J, Roden E, Muehe EM (2015) *Geomicrobiology of iron*. Chapter 17 In: Ehrlich's *Geomicrobiology* (6th Edition), Taylor & Francis Ltd., 635 pp. <https://doi.org/10.1201/b19121-18>
- Karathanasis AD, Johnson CM (2003) Metal removal potential by three aquatic plants in an acid mine drainage wetland. *Mine Water Environ* 22(1):22–30. <https://doi.org/10.1007/s102300300004>
- Khalid S, Shahid M, Niazi KK, Murtaza B, Bibi I, Dumat C (2017) A comparison of technologies for remediation of heavy metal contaminated soils. *J Geochem Explor* 182(B):247–268. <https://doi.org/10.1016/j.gexplo.2016.11.021>
- Kirby CS, Thomas HM, Southam G, Donald R (1999) Relative contributions of abiotic and biological factors in Fe(II) oxidation in mine drainage. *Appl Geochem* 14(4):511–530. [https://doi.org/10.1016/S0883-2927\(98\)00071-7](https://doi.org/10.1016/S0883-2927(98)00071-7)
- Kleinmann RL, Tiernan TO, Solch JG, Harris RL (1983) A low-cost, low-maintenance treatment system for acid mine drainage using *Sphagnum* moss and limestone. In: Graves DH (ed), Proc, 1983 Symp on Surface Mining, Hydrology, Sedimentology, and Reclamation, Lexington, pp 241–245
- Knight RL (1997) Wildlife habitat and public use benefits of treatment wetlands. *Water Sci Technol* 35(5):35–43. [https://doi.org/10.1016/S0273-1223\(97\)00050-4](https://doi.org/10.1016/S0273-1223(97)00050-4)
- Knight RL, Clarke RA Jr, Bastian RK (2001) Surface flow (sf) treatment wetlands as a habitat for wildlife and humans. *Water Sci Technol* 44(11–12):27–38. <https://doi.org/10.2166/wst.2001.0806>
- Koren DW, Gould WD, Bédard P (2000) Biological removal of ammonia and nitrate from simulated mine and mill effluents. *Hydrometallurgy* 56(2):127–144. [https://doi.org/10.1016/S0304-386X\(99\)00088-2](https://doi.org/10.1016/S0304-386X(99)00088-2)
- Kruse NA, Gozzard E, Jarvis AP (2009) Determination of hydraulic residence times in several UK mine water treatment systems and their relationship to iron removal. *Mine Water Environ* 28(2):115–123. <https://doi.org/10.1007/s10230-009-0068-6>
- Kuehn E, Moore JA (1995) Variability of treatment performance in constructed wetlands. *Water Sci Technol* 32(3):241–250. [https://doi.org/10.1016/0273-1223\(95\)00625-7](https://doi.org/10.1016/0273-1223(95)00625-7)
- Kumari M, Tripathi BD (2015) Efficiency of *Phragmites australis* and *Typha latifolia* for heavy metal removal from wastewater. *Ecotox Environ Safe* 112(1):80–86. <https://doi.org/10.1016/j.ecoenv.2014.10.034>
- Kusin FM, Jarvis AP, Gandy CJ (2010) Hydraulic residence time and iron removal in a wetland receiving ferruginous mine water over a 4 year period from commissioning. *Water Sci Technol* 62(8):937–946. <https://doi.org/10.2166/wst.2010.495>
- Lacki MJ, Hummer JW, Webster HJ (1992) Mine-drainage treatment wetland as habitat for herpetofaunal wildlife. *Environ Manage* 16(4):513–520. <https://doi.org/10.1007/BF02394127>
- Laine DM, Jarvis AP (2003) Engineering design aspects of passive in situ remediation of mining effluents. *Land Contam Reclam* 11(2):113–125. <https://doi.org/10.2462/09670513.805>
- Larsen VJ, Schierup HH (1981) Macophyte cycling of zinc, copper, lead and cadmium in the littoral zone of a polluted and a non-polluted lake. II. Seasonal changes in heavy metal content of above-ground biomass and decomposing leaves of *Phragmites australis* (Cav.) Trin. *Aquat Bot* 11(1):211–230. [https://doi.org/10.1016/0304-3770\(81\)90062-0](https://doi.org/10.1016/0304-3770(81)90062-0)
- Laurent J, Bois P, Nuel M, Wanko A (2015) Systemic models of full-scale surface flow treatment wetlands: determination by

- Outridge PM, Noller BN (1991) Accumulation of toxic trace elements by freshwater vascular plants. *Rev Environ Contam T* 121:1–63. https://doi.org/10.1007/978-1-4612-3196-7_1
- Overall RA, Parry DL (2004) The uptake of uranium by *Eleocharis dulcis* (Chinese water chestnut) in the Ranger Uranium Mine constructed wetland filter. *Environ Pollut* 132(2):307–320. <https://doi.org/10.1016/j.envpol.2004.04.005>
- Parker K (2003) Mine water management on a national scale—experiences from the Coal Authority. *Land Contam Reclam* 11(2):181–190. <https://doi.org/10.2462/09670513.813>
- Pedescoll A, Sidrach Cardona R, Hijosa Valsero M, Bécáres E (2015) Design parameters affecting metals removal in horizontal constructed wetlands for domestic wastewater treatment. *Ecol Eng* 80(1):92–99. <https://doi.org/10.1016/j.ecoleng.2014.10.035>
- Peiffer S, Walton-Day K, Macalady DL (1999) The interaction of natural organic matter with iron in a wetland (Tennessee Park, Colorado) receiving acid mine drainage. *Aquat Geochem* 5(2):207–233. <https://doi.org/10.1023/A:1009617925959>
- Persson J, Wittgren HB (2003) How hydrological and hydraulic conditions affect performance of ponds. *Ecol Eng* 21(4–5):259–269. <https://doi.org/10.1016/j.ecoleng.2003.12.004>
- Persson J, Somes NL, Wong TH (1999) Hydraulics efficiency of constructed wetlands and ponds. *Water Sci Technol* 40(3):291–300. [https://doi.org/10.1016/S0273-1223\(99\)00448-5](https://doi.org/10.1016/S0273-1223(99)00448-5)
- Pietrangelo L, Buccì A, Maiuro L, Bulgarelli D, Naclerio G (2018) Unraveling the composition of the root-associated bacterial microbiota of *Phragmites australis* and *Typha latifolia*. *Front Microbiol* 9:1650. <https://doi.org/10.3389/fmicb.2018.01650>
- Pizarro J, Belzile N, Filella M, Leppard GG, Negre JC, Perret D, Buffle J (1995) Coagulation/sedimentation of submicron iron particles in a eutrophic lake. *Water Res* 29(2):617–632. [https://doi.org/10.1016/0043-1354\(94\)00167-6](https://doi.org/10.1016/0043-1354(94)00167-6)
- Pluntke T, Kozerski HP (2003) Particle trapping on leaves and on the bottom in simulated submerged plant stands. *Hydrobiologia* 506(1–3):575–581. <https://doi.org/10.1023/B:HYDR.0000008569.29286.ec>
- Saiers JE, Harvey JW, Mylon SE (2003) Surface-water transport of suspended matter through wetland vegetation of the Florida everglades. *Geophys Res Lett.* <https://doi.org/10.1029/2003GL018132>
- Samsó R, García J (2013) Bacteria distribution and dynamics in constructed wetlands based on modelling results. *Sci Total Environ* 461–462:430–440. <https://doi.org/10.1016/j.scitotenv.2013.04.073>
- Sapsford DJ (2013) New perspectives on the passive treatment of ferruginous circumneutral mine waters in the UK. *Environ Sci Pollut R* 20:7827–7836. <https://doi.org/10.1007/s11356-013-1737-3>
- Sapsford DJ, Watson I (2011) A process-orientated design and performance assessment methodology for passive mine water treatment systems. *Ecol Eng* 37(6):970–975. <https://doi.org/10.1016/j.ecoleng.2010.12.010>
- Sapsford DJ, Santonastaso M, Thorn P, Kershaw S (2015) Conversion of coal mine drainage ochre to water treatment reagent: production, characterisation and application for P and Zn removal. *J Environ Manage* 160(1):7–15. <https://doi.org/10.1016/j.jenvman.2015.06.004>
- Schierup HH, Larsen VJ (1981) Macrophyte cycling of zinc, copper, lead and cadmium in the littoral zone of a polluted and a non-polluted lake. I. Availability, uptake and translocation of heavy metals in *Phragmites australis* (Cav.) Trin. *Aquat Bot* 11(1):197–210. [https://doi.org/10.1016/0304-3770\(81\)90061-9](https://doi.org/10.1016/0304-3770(81)90061-9)
- Schmid BH, Stephan U, Hengl MA (2005) Sediment deposition in constructed wetland ponds with emergent vegetation: laboratory study and mathematical model. *Water Sci Technol* 51(9):307–314. <https://doi.org/10.2166/wst.2005.0342>
- Scholes L, Shutes RB, Revitt DM, Forshaw M, Purchase D (1998) The treatment of metals in urban runoff by constructed wetlands. *Sci Total Environ* 214(1–3):211–219. [https://doi.org/10.1016/S0048-9697\(98\)00072-2](https://doi.org/10.1016/S0048-9697(98)00072-2)
- Seidel K (1966) Reinigung von Gewässern durch höhere Pflanzen [Water treatment by higher plants]. *Naturwissenschaften* 53(12):289–297. <https://doi.org/10.1007/BF00712211>
- Sencindiver JC, Bhumbra DK (1988) Effects of cattails (*Typha*) on metal removal from mine drainage. In: Proc, 1988 Mine Drainage and Surface Mine Reclamation Conf, US Bureau of Mines Information Circular 9184, Volume 1: Mine Water and Mine Waste. 359–366. <https://doi.org/10.21000/JASMR88010359>
- Sheoran AS, Sheoran V (2006) Heavy metal removal mechanism of acid mine drainage in wetlands: a critical review. *Miner Eng* 19(2):105–116. <https://doi.org/10.1016/j.mineng.2005.08.006>
- Sholkovitz ER (1978) The flocculation of dissolved Fe, Mn, Al, Cu, Ni, Co and Cd during estuarine mixing. *Earth Planet Sc Lett* 41(1):77–86. [https://doi.org/10.1016/0012-821X\(78\)90043-2](https://doi.org/10.1016/0012-821X(78)90043-2)
- Skousen J, Zipper CE, Rose A, Ziemkiewicz PF, Narin R, McDonald LM, Kleinmann RL (2017) Review of passive systems for acid mine drainage treatment. *Mine Water Environ* 36(1):133–153. <https://doi.org/10.1007/s10230-016-0417-1>
- Snoddy EL, Brodie GA, Hammer DA, Tomljanovich DA (1989) Control of the armyworm, *Simyra henrici*, on cattail plantings in acid mine drainage treatment wetlands at Widows Creek steam-electric plant. In: Hammer DA (ed) Constructed wetlands for wastewater treatment: Municipal, industrial, and agricultural, 808–811
- Snowden RE, Wheeler BD (1995) Chemical changes in selected wetland plant species with increasing Fe supply, with specific reference to root precipitates and Fe tolerance. *New Phytol* 131(4):503–520. <https://doi.org/10.1111/j.1469-8137.1995.tb03087.x>
- Sobolev D, Roden EE (2001) Suboxic deposition of ferric iron by bacteria in opposing gradients of Fe(II) and oxygen at circum-neutral pH. *Appl Environ Microb* 67(3):1328–1334. <https://doi.org/10.1128/AEM.67.3.1328-1334.2001>
- Sobolewski A (1999) A review of processes responsible for metal removal in wetlands treating contaminated mine drainage. *Int J Phytoremediat* 1(1):19–51. <https://doi.org/10.1080/15226519908500003>
- Stark LR, Kolbash RL, Webster HJ, Stevens SE, Dionis KA, Murphy ER (1988) The Simco#4 wetland: Biological patterns and performance. In: Mine Drainage and Surface Mine Reclamation, Vol. I: Mine Water and Mine Waste, US Bureau of Mines IC9183, 332–344. <https://doi.org/10.21000/JASMR88010332>
- Stark LR, Williams FR, Stevens Jr. SE, Eddy DP (1994) Iron retention and vegetative cover at the Simco constructed wetland: An appraisal through year eight of operation. In: Proc, International Land Reclamation and Mine Drainage Conf and 3rd International Conf on the Abatement of Acidic Drainage, Pittsburgh
- Stark LR, Williams FM, Wenerick WR, Wuest PJ, Urban C (1996) The effects of substrate type, surface water depth, and flow rate on manganese retention in mesocosm wetlands. *J Environ Qual* 25(1):97–106. <https://doi.org/10.2134/jeq1996.00472425002500010013x>
- St-Cyr L, Campbell PG (1996) Metals (Fe, Mn, Zn) in the root plaque of submerged aquatic plants collected in situ: relations with metal concentrations in the adjacent sediments and in the root tissue. *Biogeochemistry* 33(1):45–76. <https://doi.org/10.1007/BF00000969>
- Stumm W, Morgan JJ (1996) Aquatic chemistry—chemical equilibria and rates in natural waters (3rd Ed.) John Wiley & Sons, 1019 pp
- Su TM, Yang SC, Shih SS, Lee HY (2009) Optimal design for hydraulic efficiency performance of free-water-surface constructed

- wetlands. *Ecol Eng* 35(8):1200–1207. <https://doi.org/10.1016/j.ecoleng.2009.03.024>
- Tanner CC (1996) Plants for constructed wetland treatment systems—a comparison of the growth and nutrient uptake of eight emergent species. *Ecol Eng* 7(1):59–83. [https://doi.org/10.1016/0925-8574\(95\)00066-6](https://doi.org/10.1016/0925-8574(95)00066-6)
- Taylor GJ, Crowder AA (1981) Uptake and accumulation of heavy metals by *Typha latifolia* in wetlands of the Sudbury, Ontario region. *Can J Botany* 61(1):63–73. <https://doi.org/10.1139/b83-005>
- Taylor GJ, Crowder AA (1983) Uptake and accumulation of copper, nickel, and iron by *Typha latifolia* grown in solution culture. *Can J Botany* 61(7):1825–1830. <https://doi.org/10.1139/b83-193>
- Thackston EL, Shields FD, Schroeder PR (1987) Residence time distributions of shallow basins. *J Environ Eng* 113(6):1319–1332. [https://doi.org/10.1061/\(ASCE\)0733-9372\(1987\)113:6\(1319\)](https://doi.org/10.1061/(ASCE)0733-9372(1987)113:6(1319))
- Thullen JS, Sartoris JJ, Nelson SM (2005) Managing vegetation in surface-flow wastewater-treatment wetlands for optimal treatment performance. *Ecol Eng* 25(5):583–593. <https://doi.org/10.1016/j.ecoleng.2005.07.013>
- Tipping E, Cooke D (1982) The effects of adsorbed humic substances on the surface charge of goethite (α -FeOOH) in freshwaters. *Geochim Cosmochim Acta* 46(1):75–80. [https://doi.org/10.1016/0016-7037\(82\)90292-7](https://doi.org/10.1016/0016-7037(82)90292-7)
- Tipping E, Hurley MA (1992) A unifying model of cation binding by humic substances. *Geochim Cosmochim Acta* 56(10):3627–3641. [https://doi.org/10.1016/0016-7037\(92\)90158-F](https://doi.org/10.1016/0016-7037(92)90158-F)
- Tipping E, Ohnstad M (1984) Colloid stability of iron oxide particles from a freshwater lake. *Nature* 308(5956):266–268. <https://doi.org/10.1038/308266a0>
- Tuhela L, Carlson L, Tuovinen OH (1992) Ferrihydrite in water wells and bacterial enrichment cultures. *Water Res* 26(9):1159–1162. [https://doi.org/10.1016/0043-1354\(92\)90175-4](https://doi.org/10.1016/0043-1354(92)90175-4)
- van der Beek CG, Hiemstra T, Hofs B, Nederlof MM, van Paassen JA, Reijnen GK (2012) Homogeneous, heterogeneous and biological oxidation of iron(II) in rapid sand filtration. *J Water Supply Res T* 61(1):1–13. <https://doi.org/10.2166/aqua.2012.033>
- Verschoren V, Schoelynck J, Cox T, Schoutens K, Temmerman S, Meire P (2017) Opposing effects of aquatic vegetation on hydraulic functioning and transport of dissolved and organic particulate matter in a lowland river: a field experiment. *Ecol Eng* 105(1):221–230. <https://doi.org/10.1016/j.ecoleng.2017.04.064>
- Vymazal J (2013) The use of hybrid constructed wetlands for wastewater treatment with special attention to nitrogen removal: a review of a recent development. *Water Res* 47(14):4795–4811. <https://doi.org/10.1016/j.watres.2013.05.029>
- Vymazal J (2014) Constructed wetlands for treatment of industrial wastewaters: a review. *Ecol Eng* 73(1):724–751. <https://doi.org/10.1016/j.ecoleng.2014.09.034>
- Wahl MD, Brown LC, Soboyejo AO, Dong B (2012) Quantifying the hydraulic performance of treatment wetlands using reliability functions. *Ecol Eng* 47(1):120–125. <https://doi.org/10.1016/j.ecoleng.2012.06.009>
- Walton-Day K (1997) Geochemistry of the processes that attenuate acid mine drainage in wetlands. *Rev Econ Geol* 6A:215–228. <https://doi.org/10.5382/Rev.06.10>
- Watson J, Sherwood SC, Kadlec RH, Knight R, Whitehouse R (1989) Performance expectations and loading rates for constructed wetlands. In: *Constructed Wetlands for Wastewater Treatment: Municipal, Industrial, and Agricultural*, Lewis Publishers, pp 319–352
- Weber KA, Achenbach LA, Coates JD (2006) Microorganisms pumping iron: anaerobic microbial iron oxidation and reduction. *Nat Rev Microbiol* 4(10):752–764. <https://doi.org/10.1038/nrmicro1490>
- Weiss JV, Emerson D, Backer SM, Megonigal JP (2003) Enumeration of Fe(II)-oxidizing and Fe(III)-reducing bacteria in the root zone of wetland plants: implications for a rhizosphere iron cycle. *Biogeochemistry* 64(1):77–96. <https://doi.org/10.1023/A:1024953027726>
- Wenerick WR, Stevens SE, Webster HJ, Stark LR, DeVeau E (1989) Tolerance of three wetlands plant species to acid mine drainage: a greenhouse study. In: Hammer DA (ed.) *Constructed Wetlands for Wastewater Treatment: Municipal, Industrial, and Agricultural*, 801–807
- Wieder RK (1989) A survey of constructed wetlands for acid coal mine drainage treatment in the eastern United States. *Wetlands* 9(2):299–315. <https://doi.org/10.1007/BF03160750>
- Wieder RK, Lang GE, Whitehouse AE (1982) Modification of acid mine drainage in a freshwater wetland. In: Behling RE (ed.), *Proc. Symp on Wetlands of the Unglaciated Appalachian Region*, pp 43–53
- Wildemann T, Brodie G, Gusek J (1993) *Wetland Design for Mining Operations*. BiTech Publishers Ltd
- Wittgren HB, Maehlum T (1997) Wastewater treatment wetlands in cold climates. *Water Sci Technol* 35(5):45–53. [https://doi.org/10.1016/S0273-1223\(97\)00051-6](https://doi.org/10.1016/S0273-1223(97)00051-6)
- Wu H, Zhank J, Ngo HH, Guo W, Hu Z, Liang S, Fan J, Liu H (2015) A review on the sustainability of constructed wetlands for wastewater treatment: Design and operation. *Bioresour Technol* 175(1):594–601. <https://doi.org/10.1016/j.biortech.2014.10.068>
- Yang B, Lan CY, Yang CS, Liao WB, Chang H, Shu WS (2006) Long-term efficiency and stability of wetlands for treating wastewater of a lead/zinc mine and the concurrent ecosystem development. *Environ Pollut* 143(3):499–512. <https://doi.org/10.1016/j.envpol.2005.11.045>
- Ye ZH, Baker JM, Wong MH, Willis AJ (1997a) Copper and nickel uptake, accumulation and tolerance in *Typha latifolia* with and without iron plaque on the root surface. *New Phytol* 136(3):481–488. <https://doi.org/10.1046/j.1469-8137.1997.00758.x>
- Ye ZH, Baker JM, Wong MH, Willis AJ (1997b) Zinc, lead and cadmium tolerance, uptake and accumulation by *Typha latifolia*. *New Phytol* 136(3):469–480. <https://doi.org/10.1046/j.1469-8137.1997.00759.x>
- Ye ZH, Cheung KC, Wong MH (2001a) Copper uptake in *Typha latifolia* as affected by iron and manganese plaque on the root surface. *Can J Botany* 79(3):314–320. <https://doi.org/10.1139/b01-012>
- Ye ZH, Whiting SN, Lin ZQ, Lytle CM, Qian JH, Terry N (2001b) Removal and distribution of iron, manganese, cobalt, and nickel within a Pennsylvania constructed wetland treating coal combustion by-product leachate. *J Environ Qual* 30(4):1464–1473. <https://doi.org/10.2134/jeq2001.3041464x>
- Ye ZH, Whiting SN, Qian JH, Lytle CM, Lin ZQ, Terry N (2001c) Trace element removal from coal ash leachate by a 10-year-old constructed wetland. *J Environ Qual* 30(5):1710–1719. <https://doi.org/10.2134/jeq2001.3051710x>
- Younger PL, Banwart SA, Hedin RS (2002) *Mine water—hydrology, pollution, remediation*. Springer Science, <https://doi.org/10.1007/978-94-010-0610-1>
- Zaitsev G, Mettänen T, Langwaldt J (2008) Removal of ammonium and nitrate from cold inorganic mine water by fixed-bed biofilm reactors. *Miner Eng* 21(1):10–15. <https://doi.org/10.1016/j.mineng.2007.08.014>

Study 3 – Water Air Soil Pollut. 233: 66

Title Optimising operational reliability and performance in aerobic passive mine water treatment: The multistage Westfield pilot plant

Authors Opitz J, Bauer M, Eckert J, Peiffer S, Alte M

Status Published

Year 2022

Journal Water, Air, and Soil Pollution

Article 233: 66

Pages 16

DOI 10.1007/s11270-022-05538-4



SI  https://static-content.springer.com/esm/art%3A10.1007%2F11270-022-05538-4/MediaObjects/11270_2022_5538_MOESM1_ESM.pdf

Access  <https://link.springer.com/article/10.1007/s11270-022-05538-4>
© The authors (Open Access)

Relative contribution of the PhD student to study 3:

- Study design 40%
- Data collection and field work 70%
- Data processing and analysis 80%
- Evaluation 70%
- Manuscript preparation 80%

JO, MB, JE, SP, and MA designed the study. JO, MA, and JE acquired equipment and chemicals. JO and JE planned and conducted both field and laboratory work, with samples and field parameters predominantly collected by JO, and chemical analyses conducted by JE. JO, MB, and MA obtained comparison datasets from the full-scale conventional treatment plant on site. The data was evaluated and analysed by JO, with further evaluation supported by MB, SP, and MA. JO prepared a first draft as well as figures and tables for the manuscript. All authors jointly finalised and submitted the manuscript. JO is the corresponding author.

JO: Joscha Opitz // MA: Matthias Alte // MB: Martin Bauer // JE: Jutta Eckert // SP: Stefan Peiffer



Optimising Operational Reliability and Performance in Aerobic Passive Mine Water Treatment: the Multistage Westfield Pilot Plant

Joscha Opitz[✉] · Martin Bauer · Jutta Eckert · Stefan Peiffer · Matthias Alte

Received: 25 October 2021 / Accepted: 3 February 2022
© The Author(s) 2022

Abstract A three-stage pilot system was implemented for passive treatment of circumneutral, ferruginous seepage water at a former opencast lignite mine in southeast Germany. The pilot system consisted of consecutive, increasingly efficient treatment stages with settling ponds for pre-treatment, surface-flow wetlands for polishing and sediment filters for purification. The overall objective of the multistage approach was to demonstrate applicability and operational reliability for successive removal of iron as the primary contaminant broadly following Pareto's principle in due consideration of the strict site-specific effluent limit of 1 mg/L. Average inflow total iron concentration was $8.4(\pm 2.4)$ mg/L, and effluent concentration averaged $0.21(\pm 0.07)$ mg/L. The bulk iron load ($\approx 69\%$) was retained in settling ponds, thus effectively protecting wetlands and sediment filter from overloading. In turn,

wetlands and sediment filters displayed similar discrete treatment efficiency ($\approx 73\%$ each) relative to settling ponds and thus proved indispensable to reliably meet regulatory requirements. Moreover, the wetlands were found to additionally stimulate and enhance biogeochemical processes that facilitated effective removal of secondary contaminants such as Mn and NH_4 . The sediment filters were found to reliably polish particulate and redox-sensitive compounds (Fe, As, Mn, NH_4 , TSS) whilst concomitantly mitigating natural spatiotemporal fluctuations that inevitably arise in open systems. Both treatment performance and operational reliability of the multistage pilot system were comparable to the conventional treatment plant currently operated on site. Altogether the study fully confirmed suitability of the multistage passive setup as a long-term alternative for seepage water treatment on site and provided new insights into the performance and interrelation of consecutive treatment stages. Most importantly, it was demonstrated that strategically combining increasingly efficient components may be used for optimisation of treatment performance and operational reliability whilst providing an opportunity to minimise land consumption and overall costs.

Supplementary Information The online version contains supplementary material available at <https://doi.org/10.1007/s11270-022-05538-4>.

J. Opitz (✉) · J. Eckert · S. Peiffer
BayCEER, Department of Hydrology, University of Bayreuth, Universitätsstraße 30, 95447 Bayreuth, Germany
e-mail: joscha.opitz@uni-bayreuth.de

J. Opitz · M. Bauer · M. Alte
BASE TECHNOLOGIES GmbH, Josef-Felder-Straße 53, 81241 Munich, Germany

Keywords Constructed wetland · Settling pond · Iron removal · Manganese removal · Nitrification

Published online: 12 February 2022

Springer

1 Introduction

Passive treatment is a rapidly spreading, eco-technological approach for the removal of various organic and inorganic contaminants from wastewaters through exploitation and amplification of natural biogeochemical and physical processes (Kadlec & Wallace, 2009; Vymazal, 2014). In the mining industry, passive technologies are increasingly used for economic and resource-conserving treatment of acidic and/or metaliferous mine water (e.g. Hedin et al., 1994; Skousen et al., 2017; Younger, 2000a). This study is focussed on aerobic surface-flow systems that are commonly used for passive removal of hydrolysable metals (Fe, Al, Mn) from circumneutral, primarily ferruginous mine water (Sapsford, 2013; Wildemann et al., 1993). Aerobic systems predominantly include classic water treatment components such as aeration cascades, settling ponds, surface-flow wetlands and oxic sediment filters or leach beds where contaminant removal and water quality improvement are governed by naturally occurring physical and biogeochemical processes (Skousen et al., 2017).

Trivalent Fe and Al readily precipitate at circumneutral pH, forming particulate (oxy)hydroxides (Stumm & Morgan, 1996) that are subsequently removed through gravitational sedimentation and/or filtration in settling ponds and wetlands, respectively (Hedin, 2008). In contrast, Mn(II) oxidation and Mn(III/IV) precipitation in aerobic passive systems are relatively low unless ameliorated in a favourable environment that promotes distribution of Mn-oxidising bacteria and concomitant formation of (auto)catalytic surfaces (e.g. Luan et al., 2012; Neculita & Rosa, 2019; Tan et al., 2010; Tebo et al., 2004). Therefore, Mn removal from mine water is commonly promoted in limestone drains/beds (e.g. Christenson et al., 2019; Silva et al., 2010) or low-flow wetlands, the latter potentially amended with organic or limestone-based substrates (e.g. Batty et al., 2008; Hallberg & Johnson, 2005; Stark et al., 1996). Removal of additional mining-associated metal(loid)s (e.g. As, Cd, Cu, Ni, Pb, Zn) is frequently observed in aerobic passive systems, although it is important to note that this is predominantly attributable to either adsorption and complexation in wetland substrates (Opitz et al., 2021; Sobolewski, 1999) or to the omnipresence of Fe/Al/Mn (oxyhydr)oxides through scavenging, adsorption or co-precipitation (Burrows et al., 2017;

Schaider et al., 2014; Zänker et al., 2003). Beyond that, aerobic passive systems may contribute to biotransformation and decomposition of organic and particularly nitrogen compounds that originate from the use of explosives and extraction chemicals (Johnson, 2015) or as coalification by-products (Chlot et al., 2011). Most notably, elevated NH_4 levels in mine waters may be mitigated in aerobic passive systems through nitrification and assimilation by hydrophytes in surface-flow wetlands (Demin et al., 2002; Eteib et al., 2021; Vymazal, 2013). Surface-flow ponds and oxic filter beds further improve basic water quality criteria such as oxygen concentration, redox-potential, total suspended solids (TSS) and turbidity (García et al., 2003; Kadlec & Wallace, 2009).

Compared to conventional treatment plants, passive systems are open to environmental influences such as wind, precipitation, evapotranspiration, temperature variation and biological activity that unavoidably result in higher performance fluctuation (Kadlec et al., 2000; Mitsch et al., 2012). Such effects depend, however, on the nature and magnitude of the underlying treatment mechanisms and may thus vary between different mine sites and contaminants with, for instance, biogeochemical processes more susceptible to seasonal variation compared to physicochemical processes (Gu et al., 2006; Opitz et al., 2021). At worst, seasonal variation of water chemistry, temperature or biomass may even result in re-mobilisation of contaminants from wetlands as reported by Goulet and Pick (2001). Therefore, the planning and permission of passive mine water treatment systems requires a thorough decision process in due consideration of the expectable treatment efficiency, operational reliability and environmental impact as well as investment and operating costs, land consumption and at times secondary factors such as waste disposal, site-specific regulatory requirements and ecosystem services (Eppink et al., 2020; Ziemkiewicz et al., 2003). The weighing between passive and conventional treatment may be further complicated by high or fluctuating pollutant loading, spatial restrictions on site, secondary contaminants or site-specific legal and other (environmental) requirements (Trumm, 2010). Whereas hundreds of passive systems were implemented particularly in the Anglo-American area despite initial scepticism as noted by Kleinmann et al. (2021), application of passive technologies for mine water treatment in Germany is still in its infancy,

which is why both operators and regulators also face a lack of successful domestic showcases as well as a standardised technical and legal basis of valuation.

This study reports on a three-stage pilot plant that was implemented for passive treatment of circum-neutral, mining-influenced seepage water at a former lignite open pit in southeast Germany. As opposed to the numerous previous (pilot) studies on passive treatment, the novel pilot system in this study was designed with three consecutive, increasingly efficient treatment stages to increase overall treatment performance and operational reliability. The main objectives of the pilot plant were to (1) demonstrate operational reliability for passive treatment in due consideration of the strict, site-specific discharge limit, (2) assess the multistage setup according to efficacy and limitations of the consecutive treatment stages and (3) generate a database for well-founded upscaling of the pilot plant to full scale. Preliminary results were reported for Fe as the primary contaminant at the study site, showing effective Fe removal in the pilot system (Opitz et al., 2019). This study investigates the interrelationship and individual contribution of the three consecutive treatment stages for removal of relevant contaminants over the entire 452-day study period. To further assess the suitability of passive treatment for the study site, the treatment performance of the pilot system is ancillary compared

to the long-term performance of the conventional treatment plant currently operated on site. The overall objective of this study is to evaluate the conceptual multistage approach for optimising operational reliability and performance of passive mine water treatment systems.

2 Study Site

The study site is located near Wackersdorf in the former lignite district of Upper Palatinate in south-east Germany (Fig. 1a). Industrial-scale mining in the Wackersdorf area ceased in 1982, and the post-mining landscape is currently in an advanced stage of rehabilitation. Progressing oxidation of sulphide minerals in the backfilled pits results in extensive formation of acid mine drainage (AMD) in the post-mining landscape (Evangelou & Zhang, 1995).

The Westfield is an opencast segment in the southern Upper Palatine district (Fig. 1b). Two major lignite seams were mined in the Westfield between 1941 and 1982, and parts of the pit were concurrently backfilled with waste rock and ashes from the nearby lignite-fired power plant. In 1984, the northern ≈ 51.5 ha of the Westfield pit were approved as a landfill for combustion residues under waste law (Fig. 1c). An estimated 3.1×10^6 m³ bottom and electrostatic

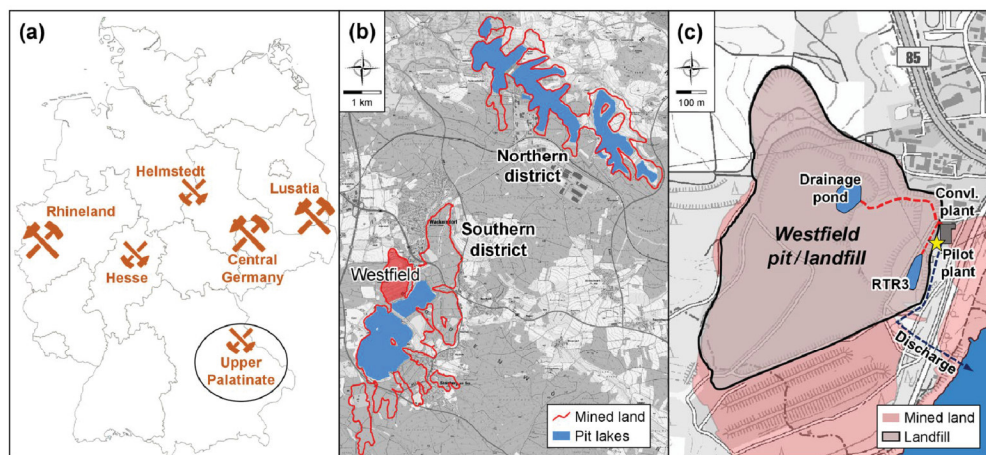


Fig. 1 Geographic location: (a) Germany's lignite mining regions, (b) the historic Upper Palatine lignite district and (c) the Westfield project site (modified maps © BayernAtlas 2021)

Table 1 Raw water chemistry of the conventional Westfield treatment plant 2011–2021 ($n = 128$)

Parameter		Lower to upper quartiles
EC	[mS/cm]	2.7–3.0
pH	[-]	7.2–7.5
Fe ¹	[mg/L]	5.0–12.0
Al	[mg/L]	0.1–0.3
Mn	[mg/L]	1.2–1.4
Cl ²	[mg/L]	140–245
SO ₄	[mg/L]	1639–1960
Mg	[mg/L]	88–113
Ca	[mg/L]	554–603
Na	[mg/L]	127–157
K	[mg/L]	62–72

¹ Fe decreased after commissioning of the RTR3 in 2019 owing to intrinsic sedimentation

² Cl steadily dropped from 250–350 in 2011 to 100–150 mg/L since 2018

precipitator ash ($\approx 4 \times 10^6$ t) were deposited in the Westfield landfill until decommissioning in 2003, still leaving a morphological depression behind. Artificial dewatering of the Westfield pit/landfill was maintained for geohydraulic reasons because it was found that groundwater runoff would have affected surrounding aquifer systems and thus threatened regional drinking water resources in the long term. Therefore, seepage water is continually pumped out from a “drainage pond” at the lowest point of the former pit/landfill for protection of adjacent aquifers, thus creating a groundwater drawdown cone that collects ground- and seepage water from the surrounding mined land.

In 1995, a conventional treatment plant was implemented east of the Westfield site for treatment of the ferruginous seepage water. The plant is discontinuously fed from the drainage pond via an intermediate reservoir, the “RTR3”, that was commissioned in 2019 (Fig. 1c). Removal of dissolved and particulate Fe is achieved in a classical physicochemical reactor system through addition of lime slurry for alkalisation followed by addition of flocculants, recycled sludge and flocculant aids. The treated water is discharged to a nearby pit lake. As treatment and discharge of seepage water from the decommissioned landfill were permitted under (waste)water law rather than mining law, a strict site-specific discharge limit for total Fe of 1 mg/L was imposed to protect the receiving water.

Groundwater in the mined land surrounding the Westfield is heavily affected by AMD, yet the seepage water leaking in the drainage pond is circumneutral

due to the predominantly alkalisating character of deposited ashes. The seepage water is mineralised and contaminated with both mining- and ash-typical substances such as Fe, Mn, SO₄, Cl and alkali(ne) earth metals (Table 1). Concentrations of metal(loid)s other than Fe or Mn are low despite considerable mobility in the surrounding mined land, which is attributable to the high sorption capacity of the electrostatic precipitator ashes (Mishra & Tripathi, 2008) and to the circumneutral character of the seepage water where solubility of most metals is low (Stumm & Morgan, 1996). Seepage water pumped to the conventional treatment plant is thoroughly oxygenated due to the temporary impoundment in drainage pond and RTR3, which is why Fe levels in the raw water are relatively low (Opitz et al., 2020). Temporal fluctuations in seepage water chemistry are attributable to the varying mixing ratio of seepage water, rainwater and surface runoff in drainage pond and RTR3 in consequence of the discontinuous pump operation. Overall, the (geo)technical, hydrogeological and regulatory setup of the Westfield legacy may be unique, especially regarding the artificial water management system.

3 Materials and Methods

3.1 Setup of the Westfield Pilot Plant

The Westfield pilot plant was implemented in 2017 next to the conventional treatment plant (Fig. 1c). The

conceptual approach for passive treatment of the mining-influenced seepage water in due consideration of the strict discharge permit criteria was a three-stage system (Fig. 2) for progressing Fe removal broadly following Pareto’s principle:

1. Pre-treatment in settling ponds
2. Polishing in surface-flow wetlands
3. Purification in sediment filters

The innovative pilot plant was implemented with three parallel lines. As opposed to most multi-line (pilot) systems that were installed to test different materials or setups (e.g. Cravotta & Trahan, 1999; García et al., 2004; Nyquist & Greger, 2009; Whitehead & Prior, 2005), the trifurcated Westfield pilot plant was designed with three identical, parallel lines to generate hydraulic and hydrochemical comparison datasets for investigation of treatment performance, kinetic relationships and critical influencing factors as a basis for upscaling (Opitz et al., 2019).

A large roll-off container (7.0×2.35×2.25 m) precedes the pilot plant as a distribution “reservoir” that is (discontinuously) filled from the feeding pipe of the conventional plant. Lower roll-off containers (7.0×2.35×1.25 m) were utilised as settling ponds and wetlands, with all steel containers embedded into the ground for isolation. The wetland containers received a sandy ≈0.3-m substrate layer and were planted with common reed. Lastly,

three parallel trenches with approximately semi-ellipsoidal cross section (ca. 4.0×0.5×0.25 m) were sealed with a plastic liner and filled with granite gravel (8–16 mm) as sediment filters (Fig. 2a). A total of ten monitoring points (MP01–MP10) for installation of fixed sensors and sampling taps were incorporated into the pipework system in four protected concrete manholes in between treatment stages. The outflow of one component corresponds to the inflow of the subsequent one, with MP01 representing the overall system inflow from the reservoir to the three parallel settling ponds, MP02–MP04 representing settling pond outflows and wetland inflows, MP05–MP07 representing wetland outflows and sediment filter inflows and MP08–MP10 representing sediment filter outflows and thus system effluent (Fig. 2b).

3.2 Pilot Plant Operation and Hydraulics

The first months of operation in 2017/2018 were used for vegetational development in wetlands and as a test phase. Following this, the main 452-day study period (July 2018 to December 2019) was commenced where hydraulic loading of the three system lines was varied in four 113-day monitoring periods with a short maintenance break in the summer of 2019. Flow rates in the three system lines were set between 100 and 500 L/h each to investigate treatment performance as a function of hydraulic loading.

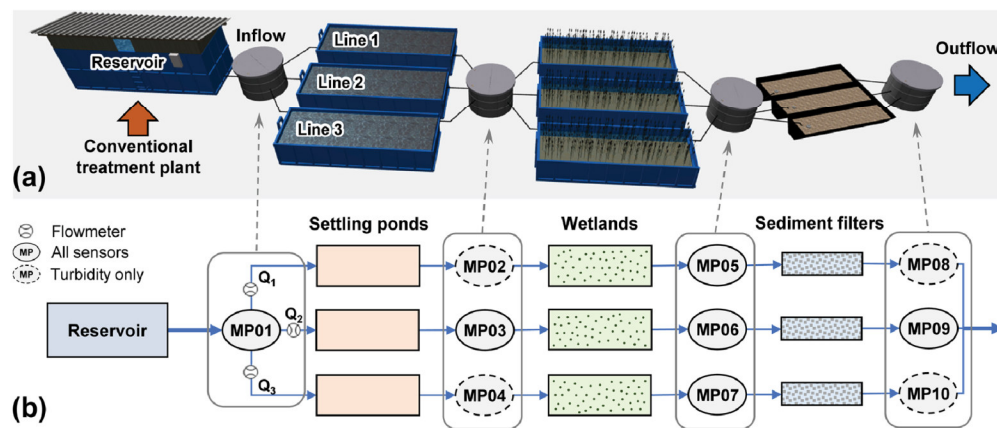


Fig. 2 Pilot plant setup: (a) 3D-illustration (without terrain) and (b) schematic

The overall flow rate in the pilot plant was governed by the filling level of the gravitationally drained reservoir, which was in turn discontinuously filled during operation of the conventional plant on site. At normal operation, the reservoir allowed operation of the pilot system at ≈ 800 L/h (lower to upper quartiles 746–851 L/h). During weekends, progressing emptying of the reservoir resulted in considerable flow fluctuations in at least one of the three system lines with temporary drops in the overall flow rate as low as 400 L/h.

According to the hydraulic monitoring of the drainage pond, the overall water yield after sealing and rehabilitation of the Westfield landfill is estimated in the order of 175,000–200,000 m³/a. Accordingly, the Westfield pilot plant continuously treated up to 4% of the overall (seepage) water yield, underlining the scale of the Westfield legacy.

3.3 Hydrochemical Monitoring

A multiparameter monitoring system (WTW IQ Sensor Net) was installed at the Westfield pilot plant for continuous logging of basic hydrochemical parameters at a 30-min interval. All monitoring points were equipped with turbidity sensors. Additionally, the central line and wetland outflows (MP01, MP03, MP05–MP07, MP09) were equipped with temperature, electrical conductivity, pH and dissolved oxygen sensors (Fig. 2b). The fixed sensors were doublechecked weekly and further complemented by redox potential measurements with hand-held metres (WTW Multi 3530).

Water samples for multiparameter analysis were collected weekly at all monitoring points. One sample was immediately filtered (0.45 μ m) and stabilised with 150 μ L of 3.6% HCl for cation analysis via ICP-OES (Al, Ba, Ca, Cr, Cu, K, Mg, Na, Ni, Pb, V, Zn) and trace analysis via graphite tube AAS for Mn (weekly) and As (monthly). A second sample was collected and immediately frozen for (an)ion analysis via ion chromatography (Br, Cl, F, NO₂, NO₃, PO₄, SO₄) and photometry (NH₄, PO₄, SO₄). A third sample was collected for total organic and inorganic carbon (TOC, TIC) measurements. Samples for analysis of Fe as the primary contaminant were collected twice weekly at all monitoring points and subjected to spectrophotometric analysis of

dissolved ferrous and ferric as well as particulate and total Fe as described by Matthies et al. (2012) and Opitz et al. (2020). Acidity was calculated from analytical results and corrected for CO₂ using PHREEQC broadly following Kirby and Cravotta (2005). After the initial test period, the analytical scope was considerably reduced as several parameters (especially metals) were consistently close to or below detection limit as already established by the long-term seepage water monitoring. Furthermore, TSS monitoring was substituted by daily averaged, in situ turbidity monitoring as an indirect, yet higher resolution measurand of suspended solids (Pfannkuche & Schmidt, 2003) because TSS in sediment filter outflows was invariably below detection limit. All chemicals used for stabilisation, analytics and standards were analytical grade.

For comparison of the consecutive treatment stages of the trifurcated pilot system, substance concentrations along the three system lines (C_1 to C_3) are weight proportional to the respective flow rate (Q_1 to Q_3) to calculate a median concentration (C_m):

$$C_m = \frac{\sum_{i=1}^3 (Q_i \times C_i)}{\sum_{i=1}^3 Q_i} \quad (1)$$

Rough mass balance estimates are based on the respective sampling intervals noted above. Mass loading (m_i) is calculated from concentrations and flow rates of the three system lines multiplied with the respective time interval around the sampling event (t_i) over the entire study period (t).

$$m_i = \sum_0^t t_s \times \sum_{i=1}^3 (C_i \times Q_i) \quad (2)$$

The average (daily) loading (L) is calculated by dividing the mass loading (m_i) by the length of the respective study period (t_i):

$$L = \frac{m_i}{t_i} \quad (3)$$

Hydrochemical monitoring data from the conventional treatment plant operated at the Westfield site was provided by courtesy of the plant operator. The database comprised monthly chemical analyses of raw and treated water (inflow/outflow) since the last major restoration of the conventional treatment plant in 2010.

4 Results and Discussion

4.1 Hydrochemistry

In a first step, the extensive dataset collected from the Westfield pilot plant over the 452-day study period was used to categorise basic parameters and chemical species by their overall change from inflow to outflow. Four distinct categories were identified by evaluating flow-weighted medians irrespective of minor spatiotemporal variations: Firstly, easily soluble compounds (Br, Ca, Cl, F, K, Mg, Na, SO₄) and electrical conductivity displayed a conservative behaviour with overall changes <5%. Besides quality control, this also shows that external effects such as dilution by rainwater or evapoconcentration are negligible for the aggregated datasets. Secondly, several compounds (Fe, As, Mn, NH₄, TSS/turbidity) displayed a substantial decrease in concentration ≥25%, whereas thirdly, a major increase was only observed for NO₃ and redox potential. Fourthly, minor removal or increase in the order of 5–25% was observed for TOC and TIC as well as acidity, oxygen saturation and pH. As noted above, most metals (Al, Cr, Cu, Ni, Pb, V, Zn) are negligible in the seepage water.

In a second step, the development of relevant parameters and especially contaminants was further analysed. Beyond the mere change in overall concentration, the comprehensive individual monitoring of consecutive treatment stages allowed identification of specific patterns and trends as well as clear assignment of overall (i.e. for the entire system) and discrete (i.e. for individual stages) treatment efficiency for relevant contaminants (Fe, As, Mn, NH₄, NO₃, turbidity).

First and foremost, similar removal patterns for Fe, turbidity and As on the one hand and Mn, NH₄ and NO₃ (inverse) on the other hand are clearly discernible in Fig. 3 as indicated by concave and convex arrows, respectively, and as further detailed below. The development of basic hydrochemical parameters from the first and fourth category is displayed in Fig. S1 with selected trends particularly in wetlands briefly outlined in the following, predominantly based on lower and upper quartiles to take account of natural and stochastic fluctuations in the open system. For instance, dissolved oxygen was close to saturation in the open system with a notable drop from settling ponds (94–101%) to wetlands (67–82%) and little further change in sediment filters. Correspondingly, the redox potential slightly decreased from 102–174 in

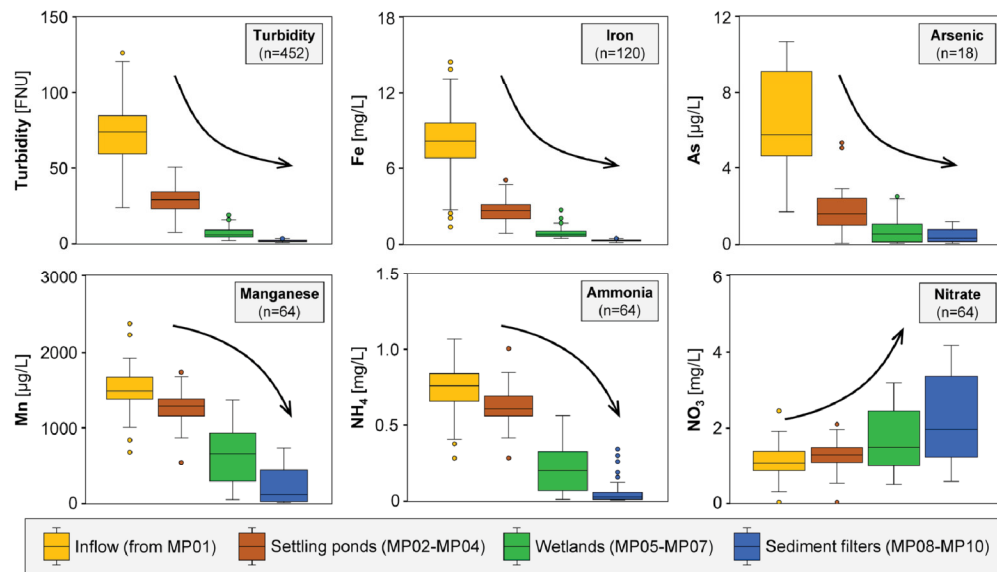


Fig. 3 Development of relevant contaminants in the Westfield pilot plant through the study period as median concentrations (C_m) with number of samples per boxplot in brackets and arrows indicating removal progression

settling ponds to 88–140 mV in wetlands—yet consistently increased to 179–222 mV in sediment filters. TOC increased in settling ponds and especially wetlands by 10–15%, each. This increase, albeit at a relatively low TOC level of 0.6–1.1 mg/L, is in accordance with visual observation of organic residues and biofilms attached to pipework and sensors at wetland outflows (MP05–MP07). However, TOC decreased again in sediment filters, resulting in a moderate overall TOC increase (median 15%) throughout the pilot plant. Overall, the monitoring indicated the onset of microbial and/or oxidation processes in wetlands that continued in sediment filters, with the latter effectively removing redox-sensitive and wetland-derived organic compounds, presumably through filtration, attachment and mineralisation in the filter matrix (García et al., 2003).

Additionally, several temporal environmental and ecological patterns were identified through the high-resolution in situ monitoring of basic hydrochemical parameters. For instance, spring blooms of floating and epiphytic algae in wetlands caused a diurnal cycle in oxygen concentration with a sharp increase during the day (up to 14 mg/L) that was reversed after sunset (as low as 4 mg/L). Concomitantly, the photorespiratory cycle of algae and macrophytes caused a diurnal pH amplitude in wetlands (up to one pH unit). Both amplitudes were, again, mitigated in sediment filters

and rapidly declined after emergence of dense, tall-growing reed stands and concomitant senescence of algae, dwindling away over the course of the summer. Beyond that, seepage water pH was relatively stable throughout the pilot system at 7.4–7.6 with an interim peak at 7.8–8.0 in settling ponds. This pH increase is attributable to CO₂ degassing as confirmed by a slight decrease (≈7%) in TIC and stable CO₂-corrected acidity (Fig. S1).

4.2 Contaminant Removal

4.2.1 Iron, Arsenic and TSS/Turbidity

Generally, Fe, As and TSS were predominantly retained in settling ponds (63–77%) with little further accumulation in wetlands (20–31%) and sediment filters (4–6%). However, the discrete treatment efficiency of the three consecutive treatment stages for Fe, As and TSS was very similar or even increased in wetlands and/or sediment filters even though the latter stages received substantially lower loadings. By way of example, discrete median removal in settling ponds, wetlands and sediment filters was 69, 73 and 72% for Fe and 62, 82 and 78% for turbidity, respectively (Table 2). Overall, Fe levels decreased from an average of 8.4(±2.4) in the inflow to 0.21(±0.07) mg/L in sediment filter outflows during the study

Table 2 Transport and removal of relevant contaminants in the Westfield pilot plant through the study period: Concentration development¹ and contaminant removal²

Parameter		Inflow (MP01)	Settling pond outflows (MP02–MP04)	Wetland outflows (MP05–MP07)	Sediment filter outflows (MP08–MP10)
Turbidity	Conc. [FNU]	73 (55–85)	27 (21–33)	4.9 (3.8–8.1)	1.1 (0.72–1.5)
	Removal	0% (0%)	62% (62%)	93% (82%)	99% (78%)
Fe	Conc. [mg/L]	8.1 (6.9–9.6)	2.5 (1.8–3.0)	0.69 (0.55–0.93)	0.19 (0.17–0.25)
	Removal	0% (0%)	69% (69%)	92% (73%)	98% (72%)
As	Conc. [µg/L]	5.8 (4.7–8.9)	1.6 (0.99–2.3)	0.48 (0.10–0.91)	0.27 (0.10–0.64)
	Removal	0% (0%)	73% (73%)	92% (69%)	95% (44%)
Mn	Conc. [mg/L]	1.5 (1.4–1.7)	1.3 (1.2–1.4)	0.66 (0.29–0.92)	0.11 (0.02–0.43)
	Removal	0% (0%)	13% (13%)	56% (49%)	92% (83%)
NH ₄	Conc. [mg/L]	0.76 (0.66–0.84)	0.61 (0.57–0.69)	0.20 (0.07–0.32)	0.02 (0.01–0.05)
	Removal	0% (0%)	20% (20%)	74% (68%)	97% (90%)
NO ₃	Conc. [mg/L]	1.1 (0.84–1.4)	1.3 (1.1–1.5)	1.5 (1.0–2.4)	2.0 (1.2–3.4)
	Removal	0% (0%)	–21% (–21%)	–40% (–16%)	–85% (–32%)

¹Median concentrations with the spread characterised by lower and upper quartiles in brackets.

²Overall cumulative removal through the system and (as *italics in brackets*) discrete removal for individual components.

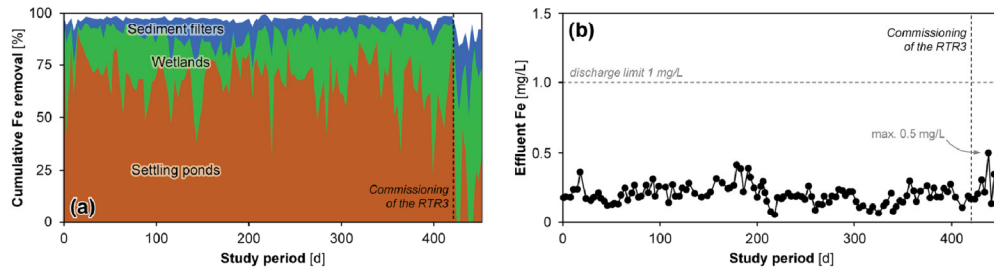


Fig. 4 Iron monitoring through the study period with (a) cumulative removal and (b) effluent concentration

period. The maximum effluent Fe concentration was 0.50 mg/L for flow-weighted ($n=120$) or 0.67 mg/L for individual ($n=360$) measurements, respectively, and thus well below the site-specific discharge limit of 1 mg/L (Fig. 4b). In mining environments, it is commonly observed that TSS and turbidity are predominantly attributable to dispersed hydrous ferric oxides that also cause the characteristic ochreous discoloration of ferruginous, circumneutral mine waters. This was previously established for the Westfield pilot plant where turbidity and (particulate) Fe are closely correlated (Opitz et al., 2020). Accordingly, Fe and turbidity show similar removal patterns along the consecutive treatment stages, with turbidity decreasing from an average of $69(\pm 22)$ FNU in the inflow to $1.2(\pm 0.6)$ FNU in the outflow (Fig. S2).

The trace levels of As detected in the inflow were consistently decreased close to or below detection limit in sediment filter outflows (Table 2). There is good reason to assume that As was largely associated (and thus removed) with the hydrous ferric oxide phases as commonly reported for As in ferruginous mining environments (Park et al., 2016). This is substantiated by the fact that the median Fe:As molar ratios were almost even at approx. 2000:1 throughout inflow, settling ponds and wetlands, eventually decreasing to about 1000:1 in sediment filters where Fe and especially As were marginally low.

Altogether, the removal of particulate (ferric) solids and associated compounds such as As throughout the multistage system was predominantly governed by physical processes such as sedimentation and filtration. This is substantiated by the fact that no major seasonal or other spatiotemporal trends were discernible over the study period for Fe, turbidity or

As. Overall, the objective of progressing treatment broadly following Pareto's principle was achieved for Fe as the primary contaminant, confirming the application potential of passive treatment at the Westfield site and providing proof of operational reliability in due consideration of the strict regulatory requirements (Fig. 4b).

4.2.2 Manganese, Ammonia and Nitrate

As the seepage water pH showed a peak in settling ponds at up to pH 8, it may have been expected that Mn(II) oxidation rates were highest in settling ponds. However, only minor Mn removal in the order of 13% was observed in settling ponds (Table 2). In contrast, Fig. 5a shows that Mn removal was stimulated in wetlands and further soared in sediment filters with discrete median removal of 49 and 83%, respectively, effectively reducing Mn levels from an average of $1.5(\pm 0.3)$ mg/L in the inflow to <0.5 mg/L in the outflow. There is good reason to assume that Mn(II) oxidation and subsequent precipitation in the Westfield pilot plant was catalysed by respective microbial communities closely linked with reactive surfaces in wetlands and especially in the sediment filter matrix (Luan et al., 2012; Neculita & Rosa, 2019). This is substantiated by black Mn(III/IV)-(oxyhydr)oxide coatings of plant litter in wetlands, the pipework succeeding wetland outflows and especially the granite gravel in sediment filters (Fig. S3). Also, the lowest Mn removal in the Westfield pilot system was observed in winter (January 2018 and January 2019). Nevertheless, even at low temperatures, Mn removal exceeded 50% from inflow to outflow, and no remobilisation or net export of Mn as reported by Goulet and Pick (2001) was observed.

Analogously, only minor NH_4 removal in the order of 20% was observed in settling ponds (Fig. 5b). Nitrification showed a similar trend as Mn(II) oxidation, soaring in wetlands and further increasing in sediment filters with median discrete NH_4 removal rates of 68 and 90%, respectively (Table 2). A simple correlation analysis highlights that removal of both Mn and NH_4 is correlated with temperature in settling ponds as would be expected for predominantly physicochemical oxidation. Only moderate correlations are found in wetlands where a potential temperature effect is likely masked by phytologic, microbial and

surface-catalytic effects. Overall, wetlands accounted for 56% of NH_4 removal, thus highlighting the importance of the densely vegetated, near-natural environment for nitrification (Cui et al., 2020). Nitrification caused a concomitant increase in NO_3 (median 85%), nearly doubling median NO_3 levels from an average of $1.1(\pm 0.4)$ in the inflow to $2.2(\pm 1.0)$ mg/L in the outflow. However, it is interesting to note that NH_4 basically decreased year-round, whereas NO_3 increase was apparently higher in autumn and winter (approx. September to April) as illustrated in Fig. 5b,c. There is reason to assume that NO_3 generation did not decrease in spring and summer, but rather that a nitrogen fraction was fixed in plants, litter and sediment as a result of primary production (algae, macrophytes) and/or lost to the atmosphere as N_2 as a result of denitrification in sediment and substrate (Griffiths et al., 2021). The nitrogen mass balance and deficit are further explored below.

4.3 Mass Balances

For Fe, the average time interval of the mass balance was 3.7 days. Mass loading is estimated at 69 kg over the study period with an average loading of 153 g/d. About 48 kg were retained in settling ponds, 15 kg in wetlands and 5.3 kg in sediment filter, and only 1.8 kg (<3%) were discharged which is in accordance with previous estimates (Opitz et al., 2020). Thus, most (69%) Fe was retained in settling ponds as hydrous ochre, thereby protecting subsequent treatment stages as well as allowing for efficient desludging and potential valorisation of the relatively pure ochre (Hedin, 2003).

For As, the average time interval of the mass balance was 25 days and should thus be treated with caution. The mass loading is estimated at 55 g over the study period with an average loading of 121 mg/d. About 38 g were retained in settling ponds, 9.9 g in wetlands and 3.2 g in sediment filters, and only 3.2 g (<6%) were discharged. For Mn, the average time interval of the mass balance was 7.1 days. The mass loading is estimated at 13 kg over the study period with an average loading of 29 g/d. Only about 2.1 kg were retained in settling ponds, whereas 5.4 and 3.6 kg were retained in wetlands and sediment filters, respectively. About 1.8 kg (<14%) were discharged, most of it in winter. The divergence between the median removal efficiency in Table 3 and the

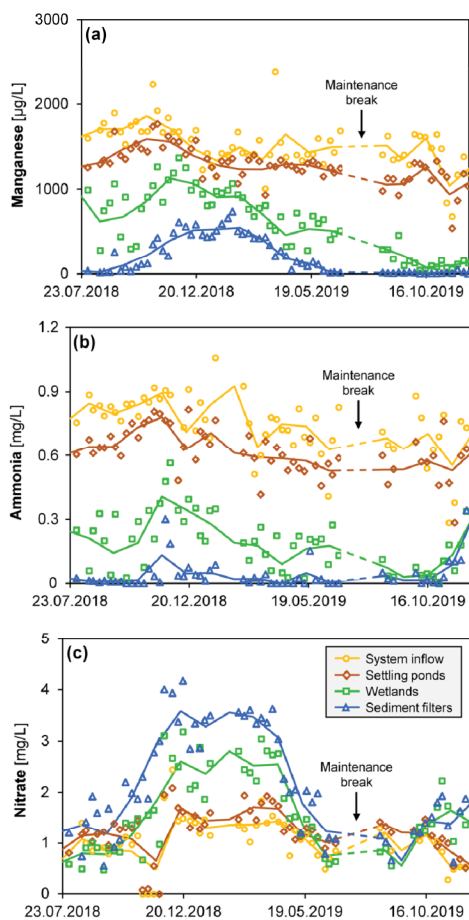


Fig. 5 Monitoring of (a) Mn, (b) NH_4 and (c) NO_3 in the Westfield pilot plant through the study period with solid lines indicating monthly averages (legend applies to all diagrams)

Table 3 Mass balance of the Westfield pilot plant for relevant contaminants through the study period: Mass loading (m_i) with average daily loading (L) in brackets

Loading	Fe	As	Mn	NH ₄ -N	NO ₃ -N
Settling pond loading (MP01)	69 kg (153 g/d)	55 g (121 mg/d)	13 kg (29 g/d)	349 mol (0.77 mol/d)	145 mol (0.32 mol/d)
Wetland loading (MP02–MP04)	22 kg (48 g/d)	16 g (36 mg/d)	11 kg (24 g/d)	294 mol (0.65 mol/d)	171 mol (0.38 mol/d)
Sediment filter loading (MP05–MP07)	7.0 kg (16 g/d)	6.4 g (14 mg/d)	5.4 kg (12 g/d)	96 mol (0.21 mol/d)	224 mol (0.50 mol/d)
Discharge (MP08–MP10)	1.8 kg (3.9 g/d)	3.2 kg (7.1 mg/d)	1.8 kg (4.0 g/d)	21 mol (0.05 mol/d)	296 mol (0.66 mol/d)

mass balance estimates is attributable to the seasonal variation of Mn(II) oxidation rates in sediment filters (Table S2) with overall Mn removal ranging from > 90% in summer to 60–70% in winter.

A simple nitrogen mass balance was established based on NH₄-N and NO₃-N as notable nitrogen species in the seepage water with NO₂ largely below detection limit (Fig. 6). The overall nitrogen loading is estimated at 495 mol over the study period at an average loading of 1.1 mol/d, with an estimated overall NH₄-N removal of ≈328 mol and NO₃-N generation of ≈151 mol over the study period. Most notably, the wetlands showed a substantial nitrogen deficit in the order of 144 mol that correlates with the seasonal variation in NO₃ outlined above. Investigation of monospecific reed stands by Schieferstein (1999) showed that nitrogen assimilation by common reed is highest in early spring, whereas nitrogen re-cycling from plant litter and detritus may be expected as of late summer. This is in accordance with year-round nitrate mobility in wetlands of the Westfield pilot system (Fig. 5c), which leads us to believe that a sizeable nitrogen fraction is assimilated by plants during spring and summer, yet partly re-mobilised upon decomposition and mineralisation of plant litter during autumn and winter. This is substantiated by the correlation analysis, showing that the seasonal effect induces a

positive correlation in wetlands as opposed to negative correlations in settling ponds and sediment filters (Table S2). Overall, the Westfield pilot system showed a net-negative nitrogen budget of ≈178 mol (≈36%) over the study period, with allocation of the deficit to (temporary) fixation (plants, sediment, litter) and N₂ degassing unknown. Median NH₄-N removal rates in wetlands may be broadly estimated at up to 8.8 mmol/m²/d, which is in accordance with literature reports in the order of 1–20 mmol/m²/d (Dzakpasu et al., 2014; Mitsch & Gosselink, 2000).

4.4 Comparison of Conventional Plant and Passive Pilot System

The aggregated median concentration development of relevant parameters in the Westfield passive pilot system and the full-scale conventional treatment plant operated on site are illustrated in Fig. 7. It should be noted that juxtaposition of relative treatment efficiencies for two water treatment plants is only valid if the underlying absolute inflow levels are broadly similar. Although the pilot system was directly fed from the conventional plant, a comparability test was made for the aggregated long-term datasets as the respective monitoring periods are non-identical. The comparison in Table S1 shows that inflow concentrations consistently overlap

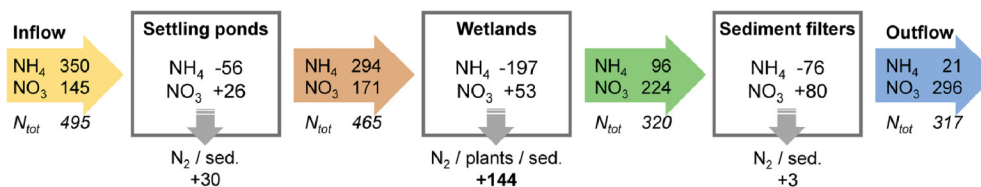


Fig. 6 Overall nitrogen mass balance for the Westfield pilot plant over the study period in [mol]

with relative differences of long-term medians well below 20%. The sole exception is Cl due to the long-time falling trend noted in Table 1. Hence, seepage water chemistry remained relatively stable over the years, and we consider the two aggregated databases as broadly comparable as long as differences indicated by Table S1 are taken into account.

First and foremost, Fig. 7 shows that the two treatment plants are comparable in terms of Fe removal as the primary contaminant, both reliably meeting the regulatory requirements. The same holds true for TSS/turbidity and As. However, both Mn and NH₄ mostly pass the conventional treatment plant with overall median removal in the order of 5–10%, rarely exceeding 20%. This goes to show that the biogeochemical processes stimulated in the near-natural wetland environment together with the high-surface sediment filters provide a technological benefit regarding overall water quality amelioration.

The addition of lime slurry and ferric chloride solution in the conventional treatment plant as alkalis and flocculating agents, respectively, measurably increase the intrinsically conservative ions Ca and Cl (data not shown). The median percentage increase is relatively minor (Ca ≈3%; Cl ≈9%), yet because of the high initial loadings noted in Table 1, the additional yearly discharge of Ca and Cl from the conventional treatment plant to the receiving surface

water is estimated at 2.6–3.0 and 3.0–3.4 t/a, respectively. Although the conventional treatment plant at the Westfield site is relatively old and might thus fall short of the expected efficiency of modern physicochemical treatment plants, the underlying resource consumption of conventional mine water treatment is broadly transferrable and an environmental concern in the long run. In this context, passive treatment provides a more sustainable alternative for long-term water treatment, particularly at abandoned mining legacies.

5 Evaluation of the Multistage Setup

It is generally well-established that adequately designed and sized passive mine water treatment systems facilitate effective removal of Fe as the primary, ubiquitous contaminant in ferruginous, circumneutral mine waters and reliably meet regulatory discharge standards (e.g. Hedin, 2020; Sapsford & Watson, 2011; Younger, 2000b). The multistage approach tested for the Westfield pilot system further advanced Fe removal efficiency, consistently achieving effluent concentrations well below the strict site-specific limit of 1 mg/L despite the heterogeneity in hydraulic loading and year-round environmental conditions as well as the predisposition of pilot-scale systems to performance fluctuations or operational failures. The

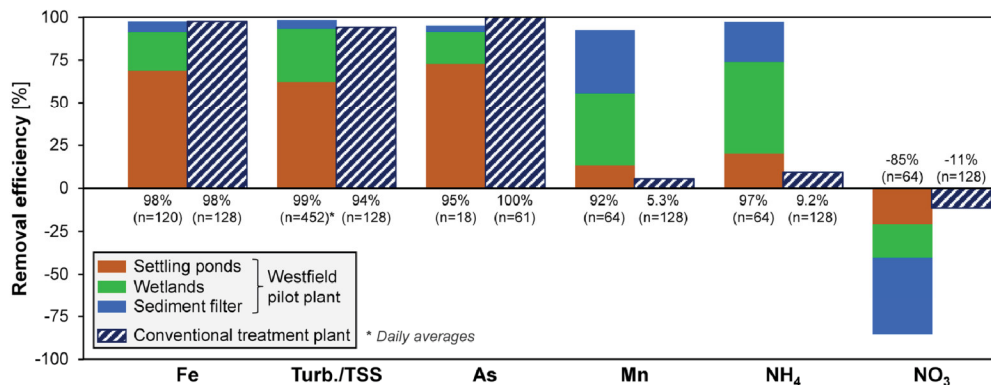


Fig. 7 Removal efficiency of relevant contaminants based on median inflow-outflow concentrations for the Westfield pilot plant (2018–2019) and the full-scale conventional treatment

plant (2011–2021) with overall removal and number of samples indicated below columns

removal of Fe as the primary contaminant as well as TSS/turbidity and As (broadly) followed the designated removal pattern according to Pareto's principle, with similar discrete removal efficiencies in the three consecutive stages of 60–80% (Table 2). By retaining the bulk Fe loading, the settling ponds effectively protected the more efficient, but also more delicate wetlands and sediment filters from overloading (i.e. clogging or colmation). Wetlands and sediment filters in turn ensured polishing at similar or even slightly higher discrete treatment efficiency despite substantially lower loading. Thus, the strategical combination of classical passive treatment stages is an effective means to facilitate reliable and effective treatment whilst potentially minimising maintenance and land requirements.

Generally, water quality improvement in settling ponds is predominantly limited to physicochemical processes such as gas exchange, autoxidation and sedimentation. Hence, the removal or decomposition of secondary contaminants such as Mn and NH_4 was primarily stimulated in the vibrant and dynamic, near-natural environment of the densely vegetated wetlands and continued in sediment filters. Thus, the surface-flow wetlands are the centrepiece for not only polishing of residual Fe, but also beneficial biogeochemical substance and redox cycles (Opitz et al., 2021). These observations are in accordance with previous studies on composite passive mine water treatment systems where wetlands were found to outperform settling ponds, not only for Fe but also Mn removal (e.g. Batty et al., 2008; Sapsford, 2013). Finally, the sediment filters were found to be a suitable means for overall polishing of particulate and redox-sensitive compounds (Fe, As, Mn, NH_4 , TSS) whilst concomitantly mitigating spatiotemporal fluctuations that inevitably arise in near-natural open systems, including but not limited to turbidity, oxygen level, redox potential and TOC (Fig. 4 and Fig. S1).

Comprehensive, year-round datasets such as collected for the Westfield pilot plant provide a robust basis for assessment of treatment performance. Nevertheless, in-depth evaluation of the underlying temporal profiles is indispensable to identify spatiotemporal variations and interrelations in individual treatment stages. This was highlighted for the biogeochemical removal of Mn and NH_4 which both (1) displayed an establishment phase with higher removal rates in the second and third compared to the first

year of operation (data not shown) and (2) were subject to seasonal variation. The comprehensive monitoring together with visual observations indicate that development of plant cover, adapted microbial populations, biofilms, sediments and reactive surface coatings were the driving factors for Mn(II) oxidation and nitrification in surface-flow wetlands as previously suggested by Demin et al. (2002). The spatiotemporal fluctuations should, however, be kept in mind when interpreting treatment efficiency and mass balance estimates based on periodic samplings (Opitz et al., 2020). Altogether, it is to be expected that contaminant removal improves with maturation of the system until, eventually, sediment accumulation compromises the hydraulic efficiency. As biogeochemical trends and cycles in eco-technological systems are rather sluggish, necessary maintenance measures may be adequately predicted.

6 Conclusions

The study confirmed suitability and operational reliability of the multistage passive system for treatment of ferruginous, mining-influenced seepage water at the project site. The Westfield pilot system achieved excellent removal rates for Fe as the primary contaminant in the order of 98% with effluent concentrations averaging $0.21(\pm 0.07)$ mg/L, thus reliably meeting the strict site-specific effluent limit of 1 mg/L.

In-depth evaluation of the consecutive treatment stages showed that, whilst the bulk Fe load was retained in bare settling ponds, wetlands and sediment filters displayed similar discrete treatment efficiency and thus proved indispensable for polishing. The surface-flow wetlands were found to be the centrepiece of the multistage system, not only for Fe removal but also by stimulating and enhancing biogeochemical processes that contribute to the removal of secondary contaminants such as Mn and NH_4 . The sediment filters were found to be an eminently suitable means for overall polishing and to mitigate spatiotemporal variations of various hydrochemical parameters in the open system, including but not limited to TSS/turbidity, oxygen level, redox potential, Fe, As, Mn, NH_4 and TOC.

Fe removal efficiency of the multistage pilot system was comparable to the full-scale conventional treatment plant currently operated on site and even

surpassed the latter in terms of Mn/NH₄ removal, thus demonstrating that passive treatment is a suitable and more sustainable alternative for long-term seepage water treatment at the project site.

Altogether, the pilot study showed that strategically combing increasingly efficient passive treatment stages broadly following the Pareto principle may allow for optimisation of treatment performance and operational reliability whilst providing an opportunity to minimise land consumption, maintenance requirements and overall costs. In addition, the multistage setup ensures that performance fluctuations in one stage are reliably mitigated in the consecutive treatment stage(s), thus minimising the overall risk of exceeding regulatory requirements.

Acknowledgements The study was conducted as part of a research project funded by the German Federal Environmental Foundation (project no. 33012/01-23). The authors thank Uniper Kraftwerke GmbH (Düsseldorf) for the support and for providing extensive datasets, as well as the laboratory staff of the University of Bayreuth, Department of Hydrology, for the meticulous assistance with sample analysis.

Funding Open Access funding enabled and organized by Projekt DEAL. The study was conducted as part of a research project funded by the German Federal Environmental Foundation (project no. 33012/01-23). The study was supported by Uniper Kraftwerke GmbH (Düsseldorf).

Data Availability The datasets used in this study are available from the corresponding author on reasonable request except for data that is subject to third party restrictions.

Declarations

Conflict of Interest The authors declare no competing interests.

Open Access This article is licensed under a Creative Commons Attribution 4.0 International License, which permits use, sharing, adaptation, distribution and reproduction in any medium or format, as long as you give appropriate credit to the original author(s) and the source, provide a link to the Creative Commons licence, and indicate if changes were made. The images or other third party material in this article are included in the article's Creative Commons licence, unless indicated otherwise in a credit line to the material. If material is not included in the article's Creative Commons licence and your intended use is not permitted by statutory regulation or exceeds the permitted use, you will need to obtain permission directly from the copyright holder. To view a copy of this licence, visit <http://creativecommons.org/licenses/by/4.0/>.

References

- Batty, L., Hooley, D., & Younger, P. (2008). Iron and manganese removal in wetland treatment systems: Rates, processes and implications for management. *Science of the Total Environment*, 394(1), 1–8. <https://doi.org/10.1016/j.scitotenv.2008.01.002>
- Burrows, J., Cravotta, C., & Peters, S. (2017). Enhanced Al and Zn removal from coal-mine drainage during rapid oxidation and precipitation of Fe oxides at near-neutral pH. *Applied Geochemistry*, 78(1), 194–201. <https://doi.org/10.1016/j.apgeochem.2016.12.019>
- Chlot, S., Widerlund, A., Siergieiev, D., Ecke, F., Husson, E., & Öhlander, B. (2011). Modelling nitrogen transformations in waters receiving mine effluents. *Science of the Total Environment*, 409, 4585–4595. <https://doi.org/10.1016/j.scitotenv.2011.07.024>
- Christenson, H., Pope, J., Trumm, D., Newman, N., Blanco, I., Kerr, G., Young, M., & Uster, B. (2019). Manganese and trace element removal from New Zealand coal mine drainage using limestone leaching beds. *New Zealand Journal of Geology and Geophysics*, 62(2), 217–228. <https://doi.org/10.1080/002883306.2018.1540995>
- Cravotta, C., & Trahan, M. K. (1999). Limestone drains to increase pH and remove dissolved metals from acidic mine drainage. *Applied Geochemistry*, 14(5), 581–606. [https://doi.org/10.1016/S0883-2927\(98\)00066-3](https://doi.org/10.1016/S0883-2927(98)00066-3)
- Cui, N., Thang, X., Zhou, L., Chen, G., & Zou, G. (2020). Roles of vegetation in nutrient removal and structuring microbial communities in different types of agricultural drainage ditches for treating farmland runoff. *Ecological Engineering*, 155, 105941. <https://doi.org/10.1016/j.ecoleng.2020.105941>
- Demin, O., Dudeney, A., & Tarasova, I. (2002). Remediation of ammonia-rich minewater in constructed wetlands. *Environmental Technology*, 23(5), 497–514. <https://doi.org/10.1080/09593332308618388>
- Dzakupas, M., Scholz, M., McCarthy, V., & Jordan, S. (2014). Nitrogen transformations and mass balance in an integrated constructed wetland treating domestic wastewater. *Water Science & Technology*, 70(9), 1496–1502. <https://doi.org/10.2166/wst.2014.402>
- Eppink, F., Trumm, D., Weber, P., Olds, W., Pope, J., & Cavanagh, J. (2020). Economic performance of active and passive AMD treatment systems under uncertainty: Case studies from the Brunner coal measures in New Zealand. *Mine Water and the Environment*, 39(4), 785–796. <https://doi.org/10.1007/s10230-020-00710-w>
- Etteib, S., Zolfaghari, M., Magdoui, S., Kaur Brar, K., & Kaur Brar, S. (2021). Performance of constructed wetland for selenium, nutrient and heavy metals removal from mine effluents. *Chemosphere*, 281, 130921. <https://doi.org/10.1016/j.chemosphere.2021.130921>
- Evangelou, V., & Zhang, Y. (1995). A review: Pyrite oxidation mechanisms and acid mine drainage prevention. *Critical Reviews in Environmental Science and Technology*, 25(2), 141–199. <https://doi.org/10.1080/10643389509388477>
- García, J., Ojeda, E., Sales, E., Chico, F., Píriz, T., Aguirre, P., & Mujeriego, R. (2003). Spatial variations of temperature,

- redox potential, and contaminants in horizontal flow reed beds. *Ecological Engineering*, 21(2), 129–142. <https://doi.org/10.1016/j.ecoleng.2003.10.001>
- García, J., Chiva, J., Aguirre, P., Álvarez, E., Sierra, J., & Mujeriego, R. (2004). Hydraulic behaviour of horizontal subsurface flow constructed wetlands with different aspect ratio and granular medium size. *Ecological Engineering*, 23(3), 177–187. <https://doi.org/10.1016/j.ecoleng.2004.09.002>
- Goulet, R., & Pick, F. R. (2001). Changes in dissolved and total Fe and Mn in a young constructed wetland: Implications for retention performance. *Ecological Engineering*, 17(4), 373–384. [https://doi.org/10.1016/S0925-8574\(00\)00161-0](https://doi.org/10.1016/S0925-8574(00)00161-0)
- Griffiths, L., Haupt, T., Zhang, L., & Mitsch, W. (2021). Role of emergent and submerged vegetation and algal communities on nutrient retention and management in a subtropical urban stormwater treatment wetland. *Wetlands Ecology and Management*, 29(5), 245–264. <https://doi.org/10.1007/s11273-020-09781-6>
- Gu, B., Chimney, M., Newman, J., & Nungesser, M. (2006). Limnological characteristics of a subtropical constructed wetland in south Florida (USA). *Ecological Engineering*, 27(4), 345–360. <https://doi.org/10.1016/j.ecoleng.2006.05.013>
- Hallberg, K., & Johnson, D. (2005). Biological manganese removal from acid mine drainage in constructed wetlands and prototype bioreactors. *Science of the Total Environment*, 338(1–2), 115–124. <https://doi.org/10.1016/j.scitotenv.2004.09.011>
- Hedin, R. (2003). Recovery of marketable iron oxide from mine drainage in the USA. *Land Contamination and Reclamation*, 11(2), 93–97. <https://doi.org/10.2462/09670513.802>
- Hedin, R. (2008). Iron removal by a passive system treating alkaline coal mine drainage. *Mine Water and the Environment*, 27(4), 200–209. <https://doi.org/10.1007/s10230-008-0041-9>
- Hedin, R. (2020). Long-term performance and costs for the Anna S mine passive treatment systems. *Mine Water and the Environment*, 39(2), 345–355. <https://doi.org/10.1007/s10230-020-00676-9>
- Hedin R, Nairn R, Kleinmann R, (1994) Passive treatment of coal mine drainage. Information Circular 9389, US Bureau of Mines.
- Johnson, C. (2015). The fate of cyanide in leach wastes at gold mines: An environmental perspective. *Applied Geochemistry*, 57, 194–205. <https://doi.org/10.1016/j.apgeochem.2014.05.023>
- Kadlec R, Wallace S, (2009) Treatment wetlands (2nd ed.). CRC Press.
- Kadlec R, Knight R, Vymazal J, Brix H, Cooper P, Haberl R, (2000). Constructed wetlands for pollution control: Processes, performance, design and operation. IWA Publishing.
- Kirby, C., & Cravotta, C. (2005). Net alkalinity and net acidity 1: Theoretical considerations. *Applied Geochemistry*, 20(10), 1920–1940. <https://doi.org/10.1016/j.apgeochem.2005.07.002>
- Kleinmann, R., Skousen, J., Wildemann, T., Hedin, R., Nairn, R., & Gusek, J. (2021). The early development of passive treatment systems for mining-influenced water: A North American perspective. *Mine Water and the Environment*, 40(4), 818–830. <https://doi.org/10.1007/s10230-021-00817-8>
- Luan, F., Santelli, C., Hansel, C., & Burgos, W. (2012). Defining manganese(II) removal processes in passive coal mine drainage treatment systems through laboratory incubation experiments. *Applied Geochemistry*, 27(8), 1567–1578. <https://doi.org/10.1016/j.apgeochem.2012.03.010>
- Matthies, R., Aplin, A., Horrocks, B., & Mudashiru, L. (2012). Occurrence and behaviour of dissolved, nano-particulate and microparticulate iron in waste waters and treatment systems: New insights from electrochemical analysis. *Journal of Environmental Monitoring*, 14(4), 1173–1180. <https://doi.org/10.1039/C2EM10846A>
- Mishra, A., & Tripathi, B. (2008). Utilization of fly ash in adsorption of heavy metals from wastewater. *Environmental Toxicology and Chemistry*, 90(6), 1091–1097. <https://doi.org/10.1080/02772240801936786>
- Mitsch, W., Zhang, L., Stefanik, K., Nahlik, A., Anderson, C., Bernal, B., Hernandez, M., & Song, K. (2012). Creating wetlands: Primary succession, water quality changes, and self-design over 15 years. *BioScience*, 62(3), 237–250. <https://doi.org/10.1525/bio.2012.62.3.5>
- Mitsch W, Gosselink J, (2000) Wetlands (5th ed.). John Wiley & Sons.
- Neculita, C., & Rosa, E. (2019). A review of the implications and challenges of manganese removal from mine drainage. *Chemosphere*, 214, 491–510. <https://doi.org/10.1016/j.chemosphere.2018.09.106>
- Nyquist, J., & Greger, M. (2009). A field study of constructed wetlands for preventing and treating acid mine drainage. *Ecological Engineering*, 35(5), 630–642. <https://doi.org/10.1016/j.ecoleng.2008.10.018>
- Opitz, J., Alte, M., Bauer, M., & Peiffer, S. (2020). Quantifying iron removal efficiency of a passive mine water treatment system using turbidity as a proxy for (particulate) iron. *Applied Geochemistry*, 120, 104731. <https://doi.org/10.1016/j.apgeochem.2020.104731>
- Opitz, J., Alte, M., Bauer, M., & Peiffer, S. (2021). The role of macrophytes in constructed surface-flow wetlands for mine water treatment: A review. *Mine Water and the Environment*, 40(3), 587–605. <https://doi.org/10.1007/s10230-021-00779-x>
- Opitz J, Alte M, Bauer M, Peiffer S (2019) Testing iron removal in a trifurcated pilot plant for passive treatment of circumneutral ferruginous mine water. In: Proc. IMWA 2019 Conf., Perm (Russia), 256–262.
- Park, J., Han, Y., & Ahn, J. (2016). Comparison of arsenic co-precipitation and adsorption by iron minerals and the mechanism of arsenic natural attenuation in a mine stream. *Water Research*, 106(1), 295–303. <https://doi.org/10.1016/j.watres.2016.10.006>
- Pfannkuche, J., & Schmidt, A. (2003). Determination of suspended particulate matter concentration from turbidity measurements: Particle size effects and calibration procedures. *Hydrological Processes*, 17(10), 1951–1963. <https://doi.org/10.1002/hyp.1220>
- Sapsford, D. J. (2013). New perspectives on the passive treatment of ferruginous circumneutral mine waters in the UK. *Environmental Science and Pollution Research*, 20(11), 7827–7836. <https://doi.org/10.1007/s11356-013-1737-3>

- Sapsford, D., & Watson, I. (2011). A process-orientated design and performance assessment methodology for passive mine water treatment systems. *Ecological Engineering*, 37(6), 970–975. <https://doi.org/10.1016/j.ecoleng.2010.12.010>
- Schaidler, L., Senn, D., Estes, E., Brabander, D., & Shine, J. (2014). Sources and fates of heavy metals in a mining-impacted stream: Temporal variability and the role of iron oxides. *Science of the Total Environment*, 490, 456–466. <https://doi.org/10.1016/j.scitotenv.2014.04.126>
- Schieferstein, B. (1999). Ecological and molecular biological investigations on reed (*Phragmites australis* (Cav.) Trin. ex Steudel) in lakes of northern Germany - An overview. *Limnologica*, 29(1), 28–35. [https://doi.org/10.1016/s0075-9511\(99\)80036-x](https://doi.org/10.1016/s0075-9511(99)80036-x)
- Silva, A., Cruz, F., Lima, R., Teixeira, M., & Leão, V. (2010). Manganese and limestone interactions during mine water treatment. *Journal of Hazardous Materials*, 181(1–3), 514–520. <https://doi.org/10.1016/j.jhazmat.2010.05.044>
- Skousen, J., Zipper, C., Rose, A., Ziemkiewicz, P., Nairn, R., McDonald, L., & Kleinmann, R. (2017). Review of passive systems for acid mine drainage treatment. *Mine Water and the Environment*, 36(1), 133–153. <https://doi.org/10.1007/s10230-016-0417-1>
- Sobolewski, A. (1999). A review of processes responsible for metal removal in wetlands treating contaminated mine drainage. *International Journal of Phytoremediation*, 1(1), 19–51. <https://doi.org/10.1080/15226519908500003>
- Stark, L., Williams, F., Wenerick, W., Wuest, P., & Urban, C. (1996). The effects of substrate type, surface water depth, and flow rate on manganese retention in mesocosm wetlands. *Journal of Environmental Quality*, 25(1), 97–106. <https://doi.org/10.2134/jeq1996.00472425002500010013x>
- Stumm W; Morgan J (1996) Aquatic chemistry: Chemical equilibria and rates in natural waters (3rd ed.). John Wiley & Sons.
- Tan, H., Zhang, G., Heaney, P. J., Webb, S., & Burgos, W. (2010). Characterization of manganese oxide precipitates from Appalachian coal mine drainage treatment systems. *Applied Geochemistry*, 25(3), 389–399. <https://doi.org/10.1016/j.apgeochem.2009.12.006>
- Tebo, B., Bargar, J., Clement, B., Dick, G., Murray, K., Parker, D., Verity, R., & Webb, S. (2004). Biogenic manganese oxides: Properties and mechanisms of formation. *Annual Review of Earth and Planetary Sciences*, 32, 287–328. <https://doi.org/10.1146/annurev.earth.32.101802.120213>
- Trumm, D. (2010). Selection of active and passive treatment systems for AMD – Flow charts for New Zealand conditions. *New Zealand Journal of Geology and Geophysics*, 53(2–3), 195–210. <https://doi.org/10.1080/00288306.2010.500715>
- Vymazal, J. (2013). The use of hybrid constructed wetlands for wastewater treatment with special attention to nitrogen removal: A review of a recent development. *Water Research*, 47(14), 4795–4811. <https://doi.org/10.1016/j.watres.2013.05.029>
- Vymazal, J. (2014). Constructed wetlands for treatment of industrial wastewaters: A review. *Ecological Engineering*, 73, 724–751. <https://doi.org/10.1016/j.ecoleng.2014.09.034>
- Whitehead, P., & Prior, H. (2005). Bioremediation of acid mine drainage: An introduction to the Wheal Jane wetlands project. *Science of the Total Environment*, 338(1–2), 15–21. <https://doi.org/10.1016/j.scitotenv.2004.09.016>
- Wildemann T, Brodie G, Gusek, J., (1993). Wetland design for mining operations. BiTech Publishers.
- Younger, P. (2000a). The adoption and adaptation of passive treatment technologies for mine waters in the United Kingdom. *Mine Water and the Environment*, 19(2), 84–97. <https://doi.org/10.1007/BF02687257>
- Younger, P. (2000b). Holistic remedial strategies for short- and long-term water pollution from abandoned mines. *Mining Technology*, 109(3), 210–2018. <https://doi.org/10.1179/mnt.2000.109.3.210>
- Zänker, H., Richter, W., & Hüttig, G. (2003). Scavenging and immobilization of trace contaminants by colloids in the waters of abandoned ore mines. *Colloids and Surfaces A*, 217(1), 21–31. [https://doi.org/10.1016/S0927-7757\(02\)00555-1](https://doi.org/10.1016/S0927-7757(02)00555-1)
- Ziemkiewicz, P., Skousen, J., & Simmons, J. (2003). Long-term performance of passive acid mine drainage treatment systems. *Mine Water and the Environment*, 22(3), 11a8–129. <https://doi.org/10.1007/s10230-003-0012-0>

Publisher's Note Springer Nature remains neutral with regard to jurisdictional claims in published maps and institutional affiliations.

SUPPLEMENTARY INFORMATION

**Optimising Operational Reliability and Performance in
Aerobic Passive Mine Water Treatment: The Multistage
Westfield Pilot Plant**

Joscha Opitz^{1,2,*}, Martin Bauer², Jutta Eckert¹, Stefan Peiffer¹, Matthias Alte²

¹ Department of Hydrology, University of Bayreuth, Bayreuth Center for Ecology and Environmental Research (BayCEER), Universitätsstraße 30, D-95447 Bayreuth, Germany

² BASE Technologies GmbH, D-81241 Munich, Germany

* Corresponding author: joscha.opitz@uni-bayreuth.de

Water, Air, & Soil Pollution (2022)

DOI: 10.1007/s11270-022-05538-4

Received: 25 October 2021 / Accepted: 3 February 2022

Number of Pages: 3

Supporting Figures: 3

Supporting Tables: 2

SUPPLEMENTARY FIGURES

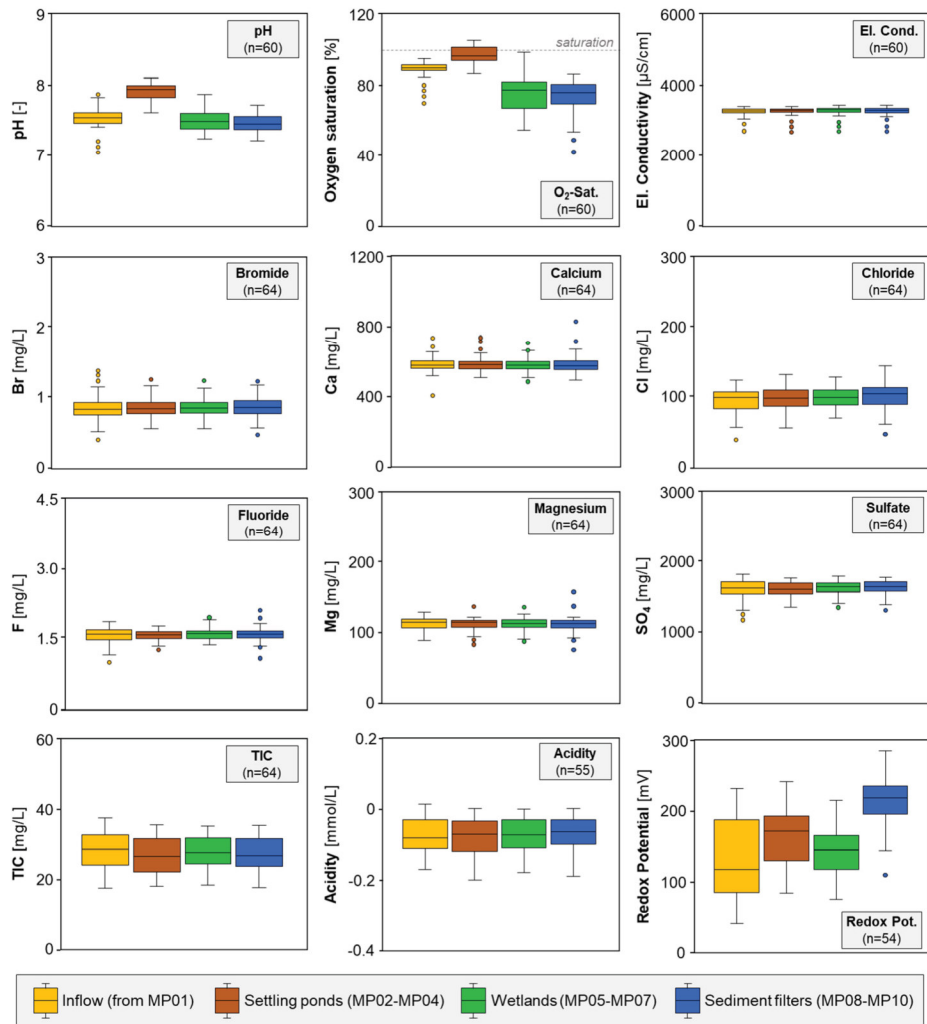


Figure S1 Development of chemical parameters in the Westfield pilot plant through the study period as median concentrations (C_m) with number of samples per boxplot in brackets

SI-1

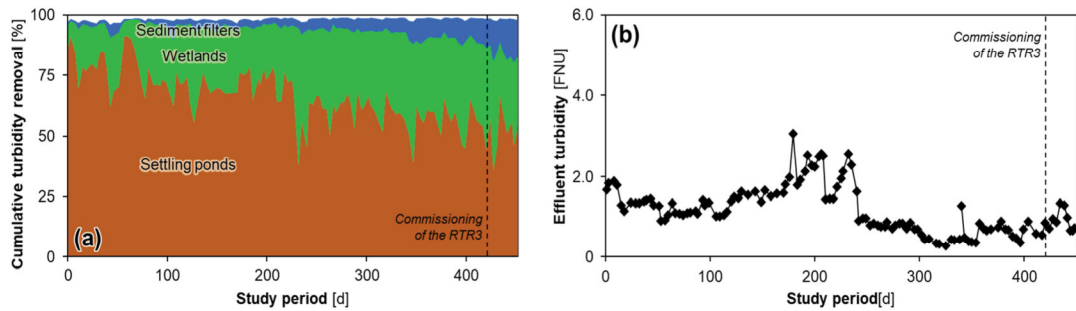


Figure S2 Turbidity monitoring through the study period with (a) cumulative removal and (b) effluent turbidity



Figure S3. Photo of fresh, unused granite filter gravel (on the right) and used filter gravel from the pilot plant after approx. two years of operation (on the left) with black coating of Mn-(oxyhydr)oxides

SUPPLEMENTARY TABLES

Table S1 Juxtaposition of inflow concentrations for conventional treatment plant (n=128) and Westfield pilot plant (n=64) as lower and upper quartiles with deviating number of samples in brackets

Parameter	Conventional treatment plant (2011-2021)	Westfield pilot plant (MP01) (2018-2019)
pH [-]	7.2 – 7.5	7.4 – 7.6 (n=60)
As [$\mu\text{g/L}$]	0 – 10 (n=61)	4.7 – 8.9 (n=18)
B [$\mu\text{g/L}$]	860 – 1022 (n=88)	n/a
Br [mg/L]	n/a	0.7 – 0.9
Ca [mg/L]	554 – 603	556 – 600
Cl [mg/L]	140 – 245 (n=101)	82 – 105
F [mg/L]	1.4 – 1.8 (n=61)	1.5 – 1.7
Fe [mg/L]	5.0 – 12.0	6.9 – 9.6 (n=120)
K [mg/L]	62 – 72	n/a
Mg [mg/L]	88 – 113	106 – 119
Mn [mg/L]	1.2 – 1.4	1.4 – 1.7
Na [mg/L]	127 – 157	n/a
NH ₄ [mg/L]	1.0 – 1.4	0.7 – 0.9
NO ₃ [mg/L]	0.9 – 3.7	0.8 – 1.4
SO ₄ [mg/L]	1639 – 1960	1540 – 1702
TOC [mg/L]	1.0 – 1.9	0.6 – 1.1
TIC [mg/L]	26 – 33	24 – 33

Table S2 Pearson correlation coefficients between treatment efficiency (Mn, NH₄, NO₃) and in-situ monitored water temperature, both aggregated to monthly averages (n=17)

Treatment stage	Mn removal	NH ₄ removal	NO ₃ removal
Settling ponds	0.76*	0.75*	-0.22
Wetlands	0.13	0.45	0.83*
Sediment filters	0.73*	0.38	-0.40

* p < 0.05

Study 4 – Environ. Sci. Technol. 56: 6360

Title Sedimentation kinetics of hydrous ferric oxides in ferruginous, circumneutral mine water

Authors Opitz J, Bauer M, Alte M, Schmidtman J, Peiffer S

Status Published

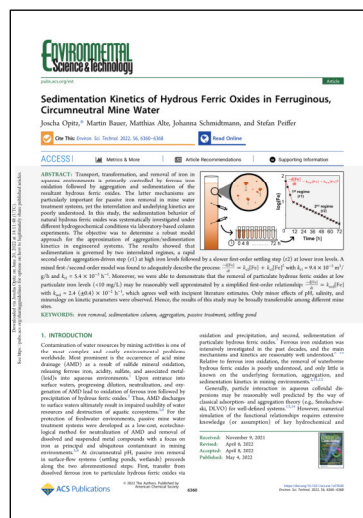
Year 2022

Journal Environmental Science & Technology


Article 56(10): 6360-6368

Pages 9

DOI 10.1021/acs.est.1c07640



SI <https://pubs.acs.org/doi/10.1021/acs.est.1c07640?goto=supporting-info>

Access  <https://pubs.acs.org/doi/10.1021/acs.est.1c07640>
 © American Chemical Society

Relative contribution of the PhD student to study 4:

- Study design 70%
- Data collection and lab work 70%
- Data processing and analysis 90%
- Evaluation 80%
- Manuscript preparation 80%

JO, JE, MA, and SP designed the study. JO, JE, and SP obtained access to suitable laboratory facilities and designed the experimental setup. JO and JE obtained and assembled the novel equipment. JO, JS, and JE planned and conducted the laboratory work, with the sedimentation experiments conducted by JO and JE, sample analyses conducted by JE, and specific additional measurements conducted by JS. The data was evaluated and analysed by JO, JS, and SP. JO and SP evaluated the results, with input from MA and MB. JO prepared a first draft as well as figures and tables for the manuscript. All authors jointly finalised and submitted the manuscript. JO is the corresponding author.

JO: Joscha Opitz // MA: Matthias Alte // MB: Martin Bauer // JE: Jutta Eckert // JS: Johanna Schmidtman // SP: Stefan Peiffer

Reprinted (adapted) with permission from Opitz et al. (2022), ES&T 56(19): 6360-6368.
<https://doi.org/10.1021/acs.est.1c07640>. Copyright 2022, American Chemical Society (ACS).

Sedimentation Kinetics of Hydrous Ferric Oxides in Ferruginous, Circumneutral Mine Water

Joscha Opitz,* Martin Bauer, Matthias Alte, Johanna Schmidtman, and Stefan Peiffer

Cite This: *Environ. Sci. Technol.* 2022, 56, 6360–6368

Read Online

ACCESS |

Metrics & More

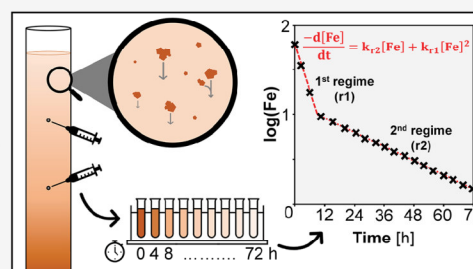
Article Recommendations

Supporting Information

Downloaded via Joscha Opitz on June 20, 2022 at 14:11:48 (UTC).
 See <https://pubs.acs.org/sharingguidelines> for options on how to legitimately share published articles.

ABSTRACT: Transport, transformation, and removal of iron in aqueous environments is primarily controlled by ferrous iron oxidation followed by aggregation and sedimentation of the resultant hydrous ferric oxides. The latter mechanisms are particularly important for passive iron removal in mine water treatment systems, yet the interrelation and underlying kinetics are poorly understood. In this study, the sedimentation behavior of natural hydrous ferric oxides was systematically investigated under different hydrogeochemical conditions via laboratory-based column experiments. The objective was to determine a robust model approach for the approximation of aggregation/sedimentation kinetics in engineered systems. The results showed that sedimentation is governed by two interrelated regimes, a rapid second-order aggregation-driven step (r1) at high iron levels followed by a slower first-order settling step (r2) at lower iron levels. A mixed first-/second-order model was found to adequately describe the process: $\frac{-d[\text{Fe}]}{dt} = k_{r2}[\text{Fe}] + k_{r1}[\text{Fe}]^2$ with $k_{r1} = 9.4 \times 10^{-3} \text{ m}^3/\text{g/h}$ and $k_{r2} = 5.4 \times 10^{-3} \text{ h}^{-1}$. Moreover, we were able to demonstrate that the removal of particulate hydrous ferric oxides at low particulate iron levels (<10 mg/L) may be reasonably well approximated by a simplified first-order relationship: $\frac{-d[\text{Fe}]}{dt} = k_{\text{sed}}[\text{Fe}]$ with $k_{\text{sed}} = 2.4 (\pm 0.4) \times 10^{-2} \text{ h}^{-1}$, which agrees well with incipient literature estimates. Only minor effects of pH, salinity, and mineralogy on kinetic parameters were observed. Hence, the results of this study may be broadly transferrable among different mine sites.

KEYWORDS: iron removal, sedimentation column, aggregation, passive treatment, settling pond



1. INTRODUCTION

Contamination of water resources by mining activities is one of the most complex and costly environmental problems worldwide. Most prominent is the occurrence of acid mine drainage (AMD) as a result of sulfide mineral oxidation, releasing ferrous iron, acidity, sulfate, and associated metal-(loid)s into aqueous environments.¹ Upon entrance into surface waters, progressing dilution, neutralization, and oxygenation of AMD lead to oxidation of ferrous iron followed by precipitation of hydrous ferric oxides.² Thus, AMD discharges to surface waters ultimately result in impaired usability of water resources and destruction of aquatic ecosystems.^{3,4} For the protection of freshwater environments, passive mine water treatment systems were developed as a low-cost, ecotechnological method for neutralization of AMD and removal of dissolved and suspended metal compounds with a focus on iron as principal and ubiquitous contaminant in mining environments.^{5,6} At circumneutral pH, passive iron removal in surface-flow systems (settling ponds, wetlands) proceeds along the two aforementioned steps: First, transfer from dissolved ferrous iron to particulate hydrous ferric oxides via

oxidation and precipitation, and second, sedimentation of particulate hydrous ferric oxides.⁷ Ferrous iron oxidation was intensively investigated in the past decades, and the main mechanisms and kinetics are reasonably well understood.^{8–10} Relative to ferrous iron oxidation, the removal of waterborne hydrous ferric oxides is poorly understood, and only little is known on the underlying formation, aggregation, and sedimentation kinetics in mining environments.^{2,7,11,12}

Generally, particle interaction in aqueous colloidal dispersions may be reasonably well predicted by the way of classical adsorption- and aggregation theory (e.g., Smoluchowski, DLVO) for well-defined systems.^{13,14} However, numerical simulation of the functional relationships requires extensive knowledge (or assumption) of key hydrochemical and

Received: November 9, 2021

Revised: April 6, 2022

Accepted: April 8, 2022

Published: May 4, 2022



hydrodynamic parameters governing the different aggregation and sedimentation regimes,^{15–17} which is a complex task in real mining environments and, most importantly, of little practical use in environmental engineering.¹⁸ Therefore, simplified rate laws or kinetic relationships were developed to estimate the removal of waterborne hydrous ferric oxides as engineering rather than scientific model approaches. For instance, a first-order relationship was proposed to approximate sedimentation of ferric solids:^{7,19}

$$-\frac{d[\text{Fe}]}{dt} = k_{\text{sed}}[\text{Fe}] \quad (1)$$

Similar yet widespread ranges for the constant k_{sed} were estimated from both column experiments and field data from 1.3×10^{-2} to $2.1 \times 10^{-1} \text{ h}^{-1}$ by Pizarro et al.¹⁹ and 9.6×10^{-3} to $3.2 \times 10^{-1} \text{ h}^{-1}$ by Sapsford.¹² Sutton et al.²⁰ conducted a single experiment with preoxygenated mine water from a New Zealand mine site containing $\approx 6.7 \text{ mg/L}$ of freshly precipitated ferric solids, with the exponential decay graph yielding $k_{\text{sed}} \approx 2.3 \times 10^{-2} \text{ h}^{-1}$ to reach a stable, residual level $< 1 \text{ mg/L}$ after $\approx 135 \text{ h}$. However, the studies differed in terms of the setup and methodology, and no further systematic investigations have been conducted to explore the applicability and limitations of simple first-order kinetics for the sedimentation of hydrous ferric oxides in mining environments.

Alternatively, higher-order relationships were proposed based on the assumption that the removal of waterborne ferric solids is governed by aggregation rather than sedimentation.²¹ For instance, a second-order relationship was suggested as a fair approximation for binary collisions of particles in dilute dispersions:^{22,23}

$$-\frac{d[\text{Fe}]}{dt} = k_{\text{sed}}[\text{Fe}]^2 \quad (2)$$

For ferric solids, ranges for k_{sed} were reported in the order of 2.3×10^{-3} to $9.3 \times 10^{-2} \text{ m}^3/\text{g/h}$ in agitated batch experiments studying estuarine environments.^{24,25} Again, the rates should be treated with caution because aggregation of ferric solids in natural waters is often associated with natural organic matter. Additionally, it was observed that the salinity gradient from freshwater to seawater significantly affected aggregation rates through double-layer compression and charge neutralization.^{22,26} Farley and Morel²⁷ found k_{sed} in the order of $7.3 \times 10^{-3} \text{ m}^3/\text{g/h}$ for goethite particles in seawater but concluded that a mixed rate law was necessary to account for the interrelated aggregation and settling regimes.

Hydrous ferric oxides in circumneutral (mine) water were generally found to display a natural tendency toward aggregation,^{28,29} presumably due to surface charge neutralization and double-layer compression in ubiquitously mineralized mining environments.³⁰ Hence, aggregation of freshly precipitated, colloidal hydrous ferric oxides results in proceeding growth toward a critical aggregate size that facilitates effective sedimentation.³¹ The critical window governing transition from dispersed colloids to effectively settleable particles is to be expected in the upper nanometer and lower micrometer range.^{26,32} This estimate is substantiated by the examination of artificial hydrous ferric oxides from controlled precipitation experiments^{30,33,34} and ochreous sediments from various mine sites, where ferric aggregates predominantly occurred between 0.2 and 10 μm .^{8,35–38} This is in accordance with a recent study by Chikanda et al.,¹¹ reporting effective gravitational separation of hydrous ferric

oxides in a drain and pond system once the ferric aggregates considerably exceeded 0.3 μm . Moreover, the size range is in accordance with early sizing approaches for settling ponds in the mining industry, which recommended an overflow rate of $1 \times 10^{-3} \text{ m/s}$ based on the estimated settling time of shale-sized particles with a diameter of $\approx 4 \mu\text{m}$.³⁹ However, despite the broad knowledge on the occurrence and mineralogy of hydrous ferric oxides in mining environments, the interrelation and kinetics of aggregation and sedimentation remain poorly understood. The integer-order models outlined above appear to be inadequate to model the removal of particulate hydrous ferric oxides over wider concentration ranges. According to Grant et al.,¹⁶ particle coagulation and sedimentation may be reasonably well predicted by simplified rate expressions in due consideration of the respective characteristic regimes. However, no respective practical mixed or noninteger order model approach for aggregation and sedimentation of hydrous ferric oxides was proposed thus far.

In this study, we systematically investigated the sedimentation behavior of hydrous ferric oxides under different hydrogeochemical conditions via laboratory-based column experiments. In the first step, we investigated the sedimentation of naturally precipitated hydrous ferric oxides (sampled at an abandoned mine site) at incrementally increasing concentrations to determine and parameterize the underlying kinetics across a wide concentration range. In the second step, we investigated several potentially critical influencing factors such as hydrochemistry of the ambient solution and mineralogy of the ferric solids on aggregation and sedimentation. The overall objective of this study was to determine a simple and robust (engineering) approach for practical approximation of aggregation-driven sedimentation of hydrous ferric oxides. A better understanding of iron transport, transformation, and removal may ultimately lead to more reliable sizing of passive systems.

2. MATERIALS AND METHODS

2.1. Materials. Naturally precipitated hydrous ferric oxides (“natural ochre”) were collected from the closed reservoir tank of a passive pilot plant that was implemented for the treatment of circumneutral ($\text{pH} \approx 7.4$), ferruginous seepage water at a former opencast lignite mine.^{40,41} The natural ochre was collected with PP-buckets and sieved using stainless-steel wire mesh sieves with 1.0 and 0.1 mm mesh size to remove foreign matter (e.g., insects) and larger agglomerates. The sieved ochre was immediately transported to the laboratory and stored in an aqueous state at 4 °C.

Additional samples were collected from the same mine site at lower pH owing to higher ferrous iron concentrations with one slightly acidic ($\text{pH} 5\text{--}7$) and one acidic ($\text{pH} 2\text{--}5$) ochre sample. The samples were subjected to the same processing and storage as outlined above. Furthermore, synthetic ferrihydrite and lepidocrocite were produced in the laboratory following Schwertmann and Cornell.⁴² Briefly summarized, 6-line ferrihydrite was synthesized by bringing a 0.1 M $\text{Fe}(\text{NO}_3)_3$ solution to pH 8 through dropwise addition of 1 M NaOH followed by aging, dialyzing, and freeze-drying of the dispersion. Lepidocrocite was synthesized by mixing 0.2 M FeCl_2 and urotropine solutions to precipitate $\text{Fe}(\text{OH})_2$, which was oxidized by adding 1 M NaNO_2 solution followed by decanting, washing, and freeze-drying of the solids.

Iron content of the ferric solids was analyzed from triplicate freeze-dried and washed subsamples via aqua regia digestion

and inductively coupled plasma optical emission spectroscopy (ICP-OES). Mineralogy of the ferric solids was examined by X-ray diffraction in a diffractometer (AXS D4 Endeavor, Bruker) equipped with a Co X-ray source and a LynxEye detector. Dried samples were mounted on X-ray diffraction (XRD) sample holders during analysis with diffractograms collected from 10° – 80° 2θ with a 0.06° 2θ step size and 2 s acquisition time.

The zeta potential and the z-average hydrodynamic diameter of the natural ochre were obtained via electrophoresis using a zetasizer (Nano ZS, Malvern). Triplicate measurements were conducted on approx. 1 mL subsamples at 25 °C using folded capillary zeta cells (DTS1070, Malvern). The isoelectric points (IEPs) of the natural ochre and synthetic ferrihydrite were exemplarily determined by measuring the electrophoretic mobility of subsamples with pH adjusted between 4 and 8.²⁵

2.2. Experimental Setup and Procedure. The setup of the sedimentation columns was broadly adopted from Sapsford¹² with key modifications. Plexiglass columns with an internal diameter of 19.4 cm were cut to a height of 200 cm and capped at the top while the bottom was left open. The cap was fitted with a brazen hose barb. Two sampling ports were set at heights of 60 and 120 cm and fitted with airtight septa (Mininert Precision Sampling Valves, Resteck). The columns were strapped to a framework, allowing only vertical movement. Round 90 L PE-tubs were set below the columns as reservoirs. A vacuum pump was connected to the column top via a three-way valve, as illustrated in Figure 1a.

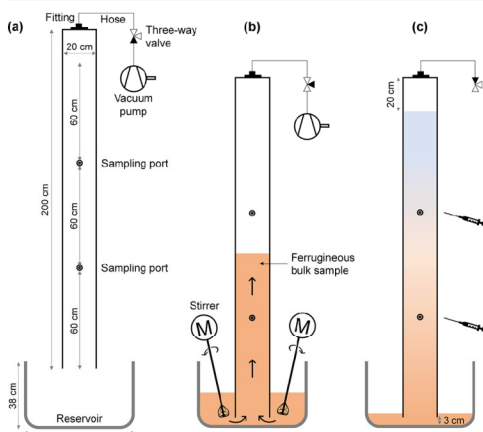


Figure 1. Experimental setup during (a) preparation, (b) mixing and filling, and (c) sampling.

Up to six columns were run in parallel. To mix the ferruginous bulk samples, stock solutions were freshly prepared the day before experiments by adding field-collected ferric solids to tap water to obtain iron concentrations in the order of 20–50 g/L. Stock solutions were homogenized over night with a magnetic stirrer at 320 rpm to break up loose aggregates and thoroughly disperse the ferric solids. To start the experiments, the reservoirs below the columns were filled with ≈ 80 L of tap water and allowed to adjust to the laboratory temperature (20 ± 2 °C). Incremental amounts of the stock solution were

added, and the resultant ferruginous bulk samples thoroughly homogenized with motor-operated basket stirrers. At constant stirring, the columns were lowered into the reservoirs, and the ferruginous bulk sample immediately pumped to a height of 180 cm within 30–45 s (Figure 1b). Vacuum filling allowed for easy mixing and vertically uniform dispersion throughout the column. After closing the three-way valve, the pump could be disconnected for filling of the next column.

Initial samples were taken 30 s after filling and sampling continued at a 4 h interval for 60–80 h (Figure 1c). Samples were collected using syringes (5 mL Inject, B.Braun) fitted with stainless-steel hypodermic needles (Sterican 0.8 \times 120 mm, B.Braun). To that end, the safety interlock of a sampling port was opened, the hypodermic needle pierced through the septum, and fully inserted to collect a 5 mL sample from the exact column center. The sampling procedure ensured minimal hydraulic, static, or temperature-related boundary effects, which are expected to increase toward the column walls. Samples were acidified to pH < 2 using 12 M HCl and left for >24 h to dissolve particulate hydrous ferric oxides. Ferric iron was reduced to ferrous iron by ascorbic acid and the iron concentration determined spectrophotometrically at 512 nm using acetate buffer solution and 1,10-phenanthroline. The spectrophotometer (DR 3800 VIS, Hach) was calibrated using standard solutions prepared with high-purity FeCl₂ dissolved in degassed water and acidified with 1 M HNO₃. All chemicals used during this study were of analytical grade.

2.3. Experimental Series and Data Evaluation. First of all, an extensive *basic series* was conducted with incrementally increasing iron concentrations to investigate the overall kinetics across a wide concentration range spanning almost two orders of magnitude (3–240 mg/L). Following this, additional experimental series was conducted to investigate the variation of hydrochemistry and mineralogy on the aggregation and sedimentation behavior of hydrous ferric oxides with an overview provided in Table 1.

Two extensive series were conducted to investigate the effect of pH and salinity as primary factors on the aggregation behavior of dispersed hydrous ferric oxides.^{43,44} For the *pH series*, the pH of the ferruginous bulk solution was varied across the neutral range in increments of 0.5 pH units (5.5, 6.0, 6.5, 7.0, 7.5, and 8.0) by buffering the bulk sample with 2 mM 3-(*N*-morpholino)propanesulfonic acid and carefully adjusting pH to within ± 0.1 through dropwise addition of either 10 M NaOH or 12 M HCl. For the *salinity series*, electrical conductivity (EC) of the ferruginous bulk solution was adjusted through the addition of NaCl salt to approx. 5, 10, 50, 100, 150, and 250 mS/cm. Both series were conducted at low (10–15 mg/L) and high (60–80 mg/L) initial iron levels as the particle interaction is expected to increase with increasing concentration.

The *solids' series* was run to investigate differences in mineralogy and composition, including but not limited to mass density, impurities, texture, and surface charge.⁴⁶ To that end, experiments were conducted with synthetic ferrihydrite and lepidocrocite as well as the field-collected slightly acidic (pH 5–7) and acidic (pH 2–5) ochre.

Lastly, a *real mine water series* was run to verify transferability of tap water experiments to field conditions following Wan et al.⁴⁵ To that end, ≈ 400 L of “real” mine water with negligible iron concentration were collected from a large, quiescent reservoir at the project mine site and transported to the laboratory. Results of the *real mine water series* confirmed that

Table 1. Overview of Experimental Series

experimental series	datasets	solids	iron concentration	bulk sample chemistry
basic series	36	natural ochre	3–240 mg/L	tap water
pH series	24	natural ochre	10–80 mg/L	tap water, pH adjusted to 5.5–8.0
salinity series	22	natural ochre	10–80 mg/L	tap water, EC adjusted to 5–240 mS/cm
solids' series	8	synthetic ferrihydrite	15–35 mg/L	tap water
	4	synthetic lepidocrocite	50 mg/L	tap water
	8	slightly acidic ochre (pH 5–7)	15–40 mg/L	tap water
	6	acidic ochre (pH 2–5)	10–30 mg/L	tap water
real mine water series ^{a†}	10	natural ochre	10–175 mg/L	real mine water

^{a†}Results reported in the Supporting Information.

Table 2. Chemical, Physical, and Mineralogical Properties of the Solids

sample	pH	iron content (as FeOOH)	hydrodynamic diameter ^{a†}	isoelectric pH (IEP)	mineralogy of ferric solids
natural ochre	7.39	50–70%	2679 (±185) nm	≈5.7	ferrihydrite, little goethite
slightly acidic ochre (pH 5–7)	5–7	81–87%	n/a	n/a	nanocrystalline goethite
acidic ochre (pH 2–5)	2–5	80%	n/a	n/a	nanocrystalline goethite
synthetic ferrihydrite	n/a	>90%	1000–4000 nm	≈7.0	6-line ferrihydrite
synthetic lepidocrocite	n/a	>90%	n/a	n/a	lepidocrocite

^{a†}Hydrodynamic diameter determined in the pH-range 6–8

tap water is a suitable substitute for real mine water and the former was therefore used throughout this study.

Data validation included identification of potential outliers by rank-order-based outlier detection. Only outliers that were obviously due to experimental or analytical errors were manually removed. For the sake of transparency, all datapoints are included as empty symbols in appropriate Supporting Information figures.

3. RESULTS AND DISCUSSION

3.1. Material Characterization. The natural ochre predominantly consists of a mixture of amorphous and poorly crystalline ferric phases, likely ferrihydrite, as indicated by weak diffraction patterns. XRD scans also show a minor goethite fraction and impurities such as quartz, gypsum, and Mn oxides (Figure S1). The slightly acidic and acidic ochre samples both predominantly consist of goethite of high disorder and/or small particle size, as indicated by broad peaks with negligible other fractions, although amorphous ferric solids such as ferrihydrite or schwertmannite cannot be ruled out.

The IEP of natural ochre and synthetic ferrihydrite are found just below pH 6 and at pH ≈ 7, respectively. The low electrophoretic mobility observed for both ferric solids between pH 6 and 8 indicates that the particles display little surface charge at circumneutral pH and thus naturally tend toward aggregation. These observations are consistent with literature reports where the IEP of synthetic ferric (oxyhydr)-oxides is commonly reported in the neutral or alkaline range,⁴⁷ whereas the IEP of naturally precipitated hydrous ferric oxides from mining environments was reported in the slightly acidic range.^{28,29,48} The median hydrodynamic particle diameters of natural ochre and synthetic ferrihydrite at pH 6–8 are found at 2–3 and 1–4 μm, respectively, perfectly falling into the particle size range outlined in the introduction.^{8,35–38} Characteristics of the different ferric solids used in this study are compiled in Table 2.

3.2. Kinetics of Sedimentation. Visual monitoring of the experiments revealed that columns with high initial concentrations and opaque water body cleared noticeably faster compared to columns with low initial concentrations. In

addition, all columns featured a slight turbidity at the end of the experimental runs. These observations already indicate that sedimentation-based removal of hydrous ferric oxides is effective in the beginning yet inherently limited at residual concentrations, with some dispersed ferric colloids remaining in suspension and unlikely to settle within reasonable time—if at all. Accordingly, temporal concentration profiles confirm that all experiments display initially steep slopes yet converge after ≈20 h, asymptotically leveling off at residual iron levels in the order of 0.7–2.0 mg/L after 60–80 h (Figure 2).

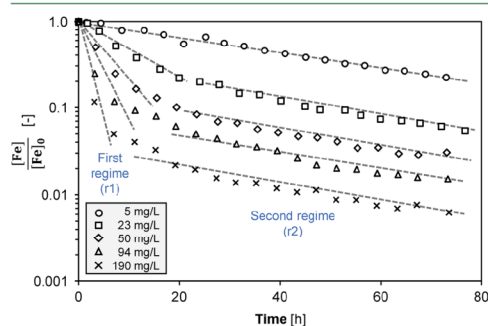


Figure 2. Normalized, semilogarithmic concentration profiles vs time for five exemplary experiments at different initial concentrations (range 5–190 mg/L) with dashed lines indicating slopes (the principle is consistent for all experiments).

Sedimentation rates were found to be independent of depth (data not shown), as previously reported by Sapsford¹² and Sutton et al.²⁰ Therefore, results from the two sampling ports were evaluated as individual datasets such that each column generated two datasets per experiment. The concentration profiles reveal a removal pattern that can be separated into a rapid initial step (r1 in Figure 2) and a slower, second step (r2 in Figure 2). The linear slopes of the two regimes indicate removal that appears to depend on the initial iron

concentration in the first regime and to be independent of concentration in the second regime. The slopes of the second regime approach a constant value in the order of $\approx 2 \times 10^{-2} \text{ h}^{-1}$ below a certain threshold concentration.

Reaction orders of the two mechanisms were determined differentially by plotting the initial sedimentation rate ($\Delta[\text{Fe}]/\Delta t$) of all 36 datasets of the *basic series* against the respective initial concentration $[\text{Fe}]_0$, as illustrated in Figure 3. The two

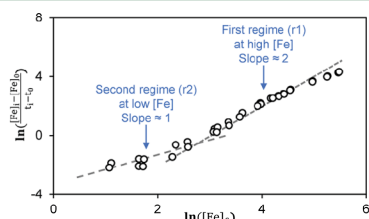


Figure 3. Double-logarithmic plot of initial sedimentation rates as $\Delta[\text{Fe}]/\Delta t$ vs the initial concentration of the corresponding interval ($t_i \approx 4 \text{ h}$) for all 36 datasets of the *basic series* at different initial iron concentrations $[\text{Fe}]_0$ (3–240 mg/L) with dashed lines indicating slopes.

regimes are again discernible in the double-logarithmic plot. The respective slopes show that the removal of hydrous ferric oxides is governed by second- and first-order kinetics at high and low concentrations, respectively. Hence, our results indicate that the two removal regimes (r1, r2) can be collectively described by a mixed first- and second-order removal model:

$$-\frac{d[\text{Fe}]}{dt} = k_{r2}[\text{Fe}] + k_{r1}[\text{Fe}]^2 \quad (3)$$

The rate constants k_{r1} and k_{r2} for the overall removal model cannot be graphically determined from Figure 3 as the two parallel regimes are interrelated.⁴⁹ Nevertheless, it is worth noting that both Figures 2 and 3 show that the reaction order progresses from 2 to 1 below a concentration range of 10 mg/L. This observation implies that at concentrations below such threshold, the removal of iron may be approximated by a simple first-order expression.

Derivation of the rate coefficients k_{r1} and k_{r2} following Espenson⁴⁹ and Chao and Espenson⁵⁰ is detailed in the Supporting Information. The coefficients were determined with $k_{r1} = 9.4 \times 10^{-3} \text{ m}^3/\text{g}/\text{h}$ and $k_{r2} = 5.4 \times 10^{-3} \text{ h}^{-1}$, with the first-order term only appreciably contributing to the mixed model at low particulate iron levels (<10 mg/L) and the second-order term being rate-determining at higher iron levels, as illustrated in Figure S4. Respective plots of the 36 datasets of the *basic series* are provided in Figure S5 using the integrated form of the mixed expression in eq 3:

$$[\text{Fe}]_t = \frac{k_{r2}[\text{Fe}]_0}{(k_{r2} + k_{r1}[\text{Fe}]_0) \times e^{k_{r2} \times t} - k_{r1}[\text{Fe}]_0} \quad (4)$$

It is important to note that experimentally determining k_{r2} as outlined in the Supporting Information should be regarded with caution as the residual iron concentration of the respective experiment was above the critical concentration (k_{r2}/k_{r1}) of 0.57 mg/L. Notwithstanding this, the mixed model and coefficients allowed good reproduction of the experiments.

Accordingly, statistical analysis of the overall regression in Figure S3a yields a confidence interval of $\pm 1.7\%$ and a process standard deviation of 1.1 mg/L, which is an excellent outcome considering the simple experimental approach and the wide concentration range used in this study.

The observation of increased iron removal at high concentration levels indicates aggregation-driven sedimentation, which corresponds well with the tendency of naturally precipitated hydrous ferric oxides toward (homo)aggregation, as highlighted by zeta potential measurements of the natural ochre (Table 2). The change in the reaction order becoming noticeable below 10 mg/L indicates that the reaction order decreases to exponential decay owing to the declining collision frequency, with progressively less settleable particles generated through aggregation than lost from the system through gravitational settling.⁵¹ Aggregation-driven sedimentation at high iron levels facilitates effective removal of the bulk solids in the order of minutes or hours. As opposed to this, sedimentation at low iron levels is limited by slowed aggregation and thus allows dispersed hydrous ferric oxides to traverse over long distances. Altogether, the *basic series* for the first time provided a foundation to quantitatively describe aggregation-driven sedimentation of particulate hydrous ferric oxides in circumneutral mine water.

3.3. Potential Influencing Factors. The additional series listed in Table 1 are evaluated regarding sedimentation and aggregation behavior by computing k_{r1} , following the procedure outlined in the Supporting Information with k_{r2} fixed to $5.4 \times 10^{-3} \text{ h}^{-1}$ for comparison with the *basic series* (Table 3). Furthermore, the additional series are also evaluated via approach (B) for graphical illustration and comparison with the *basic series* in Figure S6.

Table 3. Results of the Additional Experimental Series for k_{r1} with k_{r2} Fixed to $5.4 \times 10^{-3} \text{ h}^{-1}$

experimental series ^a	k_{r1} ($\times 10^{-3}$) in [$\text{m}^3/\text{g}/\text{h}$]
basic series ($n = 35$)	9.7 (± 2.2)
pH series ($n = 24$)	10.8 (± 1.8)
salinity series, EC < 100 mS/cm ($n = 14$)	8.3 (± 1.7)
salinity series, EC > 100 mS/cm ($n = 8$)	6.2 (± 2.7)
synthetic ferrihydrite ($n = 8$)	8.6 (± 2.3)
synthetic lepidocrocite ($n = 4$)	8.8 (± 1.5)
slightly acidic natural ochre, pH 5–7 ($n = 8$)	9.5 (± 2.1)
acidic natural ochre, pH 2–5 ($n = 6$)	14.5 (± 1.2)

^aUnderlying number of datasets in brackets, with results given as average (\pm SD).

Despite considerable changes in hydrochemical and mineralogical conditions, the evaluation of the additional series is in good agreement with the *basic series* (Figure S6), substantiating the mixed first-/second-order pattern. Rate constants k_{r1} for the additional experimental series are mostly comparable to the *basic series* (Table 3) with an overall mean value of $9.9 (\pm 2.4) \times 10^{-3} \text{ m}^3/\text{g}/\text{h}$. Only the *salinity series* shows a distinct decrease of k_{r1} at excessive NaCl levels (EC > 100 mS/cm), whereas the more moderate salinity experiments (EC < 100 mS/cm) correspond reasonably well with the *basic series*. Salinity increments in this study were deliberately chosen to not only cover but also considerably exceed values encountered even in mining environments. Therefore, the decrease in gravitational settling at extreme salinity levels is most likely attributable to the change in solution density

(increase up to $\approx 1.3 \text{ g/cm}^3$) and viscosity, as previously reported for natural sediments by Wan et al.⁴⁵

For the *solids' series*, both synthetic ferrihydrite and lepidocrocite as well as the slightly acidic ochre (pH 5–7) align reasonably well with results obtained from the natural ochre in the *basic*, *pH*, and *salinity series*. In contrast, the acidic ochre (pH 2–5) consistently shows a higher k_{t1} compared to all other constellations, as illustrated in Figure S6d. As this is evidently attributable to the second sedimentation regime (Table 3), there is a reason to assume that this observation is due to surface characteristics rather than mass density or morphology.

Altogether, variation of pH and salinity caused no substantial change in the aggregation or sedimentation behavior of waterborne hydrous ferric oxides at levels typically observed in circumneutral, ferruginous mine waters. This indicates that the passive removal of hydrous ferric oxides at circumneutral pH is primarily governed by the particle interaction and size as a function of concentration, whereas variations in hydrochemistry or mineralogy such as those tested in this study seem to be of secondary importance. Hence, the results of this study may be broadly transferrable among different mine sites. The slight differences displayed in Table 3 and Figure S6 may be indicative of experimental variance rather than mineralogical or hydrochemical variation.

4. IMPLICATIONS

4.1. Practical Applications. Graphical illustration of the overall aggregation and sedimentation kinetics in Figures 3 and S4 shows that a mixed model is required to adequately model sedimentation-based iron removal over wider concentration ranges. Nevertheless, Figure 3 also indicates that the removal of hydrous ferric oxides at low concentration levels may be reasonably well approximated by a simple, stand-alone first-order expression as per eq 1. For practical application of a simplified first-order model approach, it is important to note that the respective coefficient k_{sed} must be chosen such that it adequately approximates the mixed model in the relevant (i.e., application-related) concentration range. Above and below this range, the simplified first-order approach will inevitably tend to progressively underestimate and overestimate iron removal, respectively. In passive mine water treatment systems, the concentration of particulate hydrous ferric oxides is usually low because ferric solids are only gradually generated upon ferrous iron oxidation³⁷ and concomitantly removed through sedimentation.¹¹ What is more, low iron levels are ultimately most relevant for sizing purposes to ensure reliable compliance with typical discharge limits in the order of 1–3 mg/L total iron.

For the 36 datasets of the *basic series*, the most robust coefficient for the simple first-order approach was determined with $k_{sed} = 2.4 (\pm 0.4) \times 10^{-2} \text{ h}^{-1}$, which corresponds well with the slope of the second regime (r2) marked in Figure 2 and incipient estimates from the literature.^{12,19,20} The results from the *basic series* are also well reproducible for the additional experimental series (Table S1). In Figure 4, five exemplary experiments are provided as logarithmic profiles for measurements <10 mg/L in juxtaposition with the simplified first-order model approach. The slight curvature of the logarithmic profiles approaches a relatively constant slope that is well described by the first-order model, but it is also noticeable that the profiles curve upward toward residual iron levels <1 mg/L where the simplified model will thus progressively overestimate

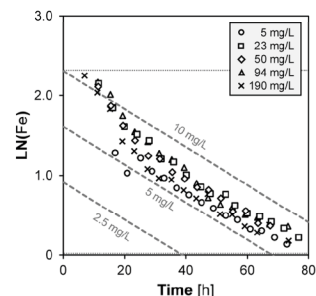


Figure 4. Excerpt of concentration development for the same five exemplary experiments displayed in Figure 2 below 10 mg/L as logarithmic iron profiles vs time with the simplified first-order model slope ($k_{sed} = 2.4 \times 10^{-2} \text{ h}^{-1}$) exemplarily indicated as dashed gray lines as of 2.5, 5, and 10 mg/L (the principle is consistent for all experiments).

the removal of hydrous ferric oxides. This is in accordance with the initial observation of a residual amount of finely dispersed hydrous ferric oxides remaining in all sedimentation experiments.

Overall, this study provides a consistent, quantitative approach and (laboratory-based) parametrization for the two-step aggregation/sedimentation-based removal of hydrous ferric oxides in circumneutral mine water. Moreover, the results also confirm the hypothesis of Sapsford and Watson⁷ that sedimentation may be approximated by a first-order expression at moderate iron levels. The explicitly conservative value for k_{sed} suggested above ensures that iron removal is underestimated rather than overestimated in the relevant concentration range (1–10 mg/L) as is common practice in engineering sciences.

4.2. Perspectives. The study highlighted that passive removal of hydrous ferric oxides in ferruginous, circumneutral mine waters is primarily governed by (homo)aggregation of ferric solids toward a settleable size that facilitates subsequent gravitational settling. As illustrated in Figure S4, the removal rate decreases rapidly toward residual iron levels <1 mg/L, effectively limiting the degree of purity that may (realistically) be achieved in full-scale settling ponds. Consequently, more efficient passive components such as wetlands or sediment filters are necessary for polishing of finely dispersed hydrous ferric oxides from settling pond effluents.^{41,52}

The sedimentation kinetics determined in this study could considerably improve our quantitative understanding of iron transport and removal in mining environments. For instance, the relationships may be integrated into transport models or used for the calculation of temporal iron removal profiles in passive treatment systems to determine the optimal application range of settling ponds and wetlands for pretreatment and polishing, respectively. The k_{sed} of $2.4 \times 10^{-2} \text{ h}^{-1}$ recommended above corresponds to a time requirement in the order of 28 h to remove 50% of initial ferric solids. Such “half live” is in good agreement with the retention time recommended for sizing of settling ponds in passive mine water treatment systems in the order of 12–48 h.^{6,53,54} Moreover, in systems containing ferrous iron, the first-order sedimentation approach may be readily combined with the corresponding rate law for ferrous iron oxidation, allowing for

the approximation of overall iron removal as suggested by Sapsford and Watson.⁷ Such application-oriented, physico-chemical model approaches inevitably entail a certain degree of simplification—especially in mining environments, where iron transformation and removal are considerably affected by various environmental factors and spatiotemporal fluctuations (pH, redox potential, temperature, hydrodynamics, and so forth).⁵⁵ However, this is of minor importance for practical applications in environmental engineering, where the overall objective is to (conservatively) estimate the underlying process dynamics on a relatively large scale. In this context, it is important to note that further transfer to freshwater environments is unclear at this stage as the transport of colloidal ferric (oxyhydr)oxides in surface waters is known to be considerably affected by dilution⁵⁶ and interaction with natural organic matter.^{43,57}

Sedimentation experiments in this study were conducted in quiescent columns, where particle migration was limited to vertical, gravitational settling and largely unaffected by hydrodynamic effects. Thus, the controlled batch experiments can be regarded as an idealized approximation of the sluggish flow conditions in settling ponds. However, surface-flow ponds are inevitably subject to complex hydrodynamic and environmental effects that affect the migration of waterborne particles: on the one hand, sedimentation may be reduced by currents and turbulences⁵⁸ or altogether disrupted by thermal or wind-induced mixing and buoyancy.^{59,60} On the other hand, particle interaction may be increased by shear forces or scavenging^{27,34} and further accelerated through heterogeneous ferrous iron oxidation on particle surfaces.^{20,29} Therefore, parameterization of sedimentation kinetics as obtained from this study requires verification by in-depth field studies. In the first step, our future work will focus on the evaluation of the hydrochemical and hydraulic monitoring of the passive pilot plant from whence the ochre was sampled for direct comparison of laboratory and field data.

■ ASSOCIATED CONTENT

SI Supporting Information

The Supporting Information is available free of charge at <https://pubs.acs.org/doi/10.1021/acs.est.1c07640>.

Seven supporting figures showing additional results, namely, X-ray diffractograms of ferric solids, individual plots of the *basic series* for the derivation of rate constants, results of the additional experimental series, and a table with the results of the additional experimental series for the first-order approach. In addition, the methodology to derive the rate coefficients k_{r1} and k_{r2} is briefly outlined (PDF)

The datasets used in this study are published on Zenodo at <https://doi.org/10.5281/zenodo.6482292>.

■ AUTHOR INFORMATION

Corresponding Author

Joscha Opitz – Department of Hydrology, University of Bayreuth, BayCEER, Bayreuth D-95447, Germany; BASE Technologies GmbH, Munich D-81241, Germany; orcid.org/0000-0002-0414-9211; Email: Joscha.opitz@uni-bayreuth.de

Authors

Martin Bauer – BASE Technologies GmbH, Munich D-81241, Germany

Matthias Alte – BASE Technologies GmbH, Munich D-81241, Germany

Johanna Schmidtman – Department of Hydrology, University of Bayreuth, BayCEER, Bayreuth D-95447, Germany; orcid.org/0000-0003-2589-9043

Stefan Peiffer – Department of Hydrology, University of Bayreuth, BayCEER, Bayreuth D-95447, Germany; orcid.org/0000-0002-8326-0240

Complete contact information is available at: <https://pubs.acs.org/10.1021/acs.est.1c07640>

Funding

The study was funded by the Deutsche Bundesstiftung Umwelt (DBU, German Federal Environmental Foundation) – project no. 33012/01-23, and by the Deutsche Forschungsgemeinschaft (DFG, German Research Foundation) – SFB 1357 - 391977956.

Notes

The authors declare no competing financial interest.

■ ACKNOWLEDGMENTS

The study was conducted as part of a research project funded by the German Federal Environmental Foundation (project no. 33012/01-23) and by the Deutsche Forschungsgemeinschaft (DFG, German Research Foundation) – Project Number 391977956 – SFB 1357. We are grateful to Prof. Papastavrou for providing access to the laboratories of Physical Chemistry II at the University of Bayreuth for measurements of electrophoretic mobility.

■ REFERENCES

- (1) Nordstrom, D. Mine waters: Acidic to circumneutral. *Elements* **2011**, *7*, 393–398.
- (2) Yazbek, L.; Cole, K.; Shedleski, A.; Singer, D.; Herndon, E. Hydrogeochemical processes limiting aqueous and colloidal Fe export in a headwater stream impaired by acid mine drainage. *ACS ES&T Water* **2021**, *1*, 68–78.
- (3) Byrne, P.; Wood, P.; Reid, I. The impairment of river systems by metal mine contamination: A review including remediation options. *Crit. Rev. Environ. Sci. Technol.* **2012**, *42*, 2017–2077.
- (4) Cadmus, P.; Clements, W.; Williamson, J.; Ranville, J.; Meyer, J.; Gutiérrez Ginés, M. The use of field and mesocosm experiments to quantify effects of physical and chemical stressors in mining-contaminated streams. *Environ. Sci. Technol.* **2016**, *50*, 7825–7833.
- (5) Skousen, J.; Zipper, C.; Rose, A.; Ziemkiewicz, P.; Nairn, R.; McDonald, L.; Kleinmann, R. Review of passive systems for acid mine drainage treatment. *Mine Water Environ.* **2017**, *36*, 133–153.
- (6) Younger, P.; Banwart, S.; Hedin, R. *Mine Water – Hydrology, Pollution, Remediation*; Springer Science: Dordrecht, Netherlands, 2002.
- (7) Sapsford, D.; Watson, I. A process-orientated design and performance assessment methodology for passive mine water treatment systems. *Ecol. Eng.* **2011**, *37*, 970–975.
- (8) Dietz, J.; Dempsey, B. Heterogeneous oxidation of Fe(II) in AMD. *Appl. Geochem.* **2017**, *81*, 90–97.
- (9) Millero, F. The effect of ionic interactions on the oxidation of metals in natural waters. *Geochim. Cosmochim. Acta* **1985**, *49*, 547–553.
- (10) Singer, P.; Stumm, W. Acidic mine drainage. The rate-determining step. *Science* **1970**, *167*, 1121–1123.
- (11) Chikanda, F.; Otake, T.; Koide, A.; Ito, A.; Sato, T. The formation of Fe colloids and layered double hydroxides as

- sequestration agents in the natural remediation of mine drainage. *Sci. Tot. Environ.* **2021**, *774*, No. 145183.
- (12) Sapsford, D. New perspectives on the passive treatment of ferruginous circumneutral mine waters in the UK. *Environ. Sci. Pollut. Res.* **2013**, *20*, 7827–7836.
- (13) Berka, M.; Rice, J. Relation between aggregation kinetics and the structure of kaolinite aggregates. *Langmuir* **2005**, *21*, 1223–1229.
- (14) Buffle, J.; Wilkinson, K.; Stoll, S.; Filella, M.; Zhang, J. A generalized description of aquatic colloidal interactions: The three-colloidal component approach. *Environ. Sci. Technol.* **1998**, *32*, 2887–2899.
- (15) González, A.; Odriozola, G.; Leone, R. Colloidal aggregation with sedimentation: Concentration effects. *Eur. Phys. J. E: Soft Matter Biol. Phys.* **2004**, *13*, 165–178.
- (16) Grant, S.; Kim, J.; Poor, C. Kinetic theories for the coagulation and sedimentation of particles. *J. Colloid Interface Sci.* **2001**, *238*, 238–250.
- (17) Phenrat, T.; Saleh, N.; Sirk, K.; Tilton, R.; Lowry, G. Aggregation and sedimentation of aqueous nanoscale zerovalent iron dispersions. *Environ. Sci. Technol.* **2007**, *41*, 284–290.
- (18) Rand, L.; Ranville, J. Characteristics and stability of incidental iron oxide nanoparticles during remediation of a mining-impacted stream. *Environ. Sci. Technol.* **2019**, *53*, 11214–11222.
- (19) Pizarro, J.; Belzile, N.; Filella, M.; Leppard, G.; Negre, J.; Perret, D.; Buffle, J. Coagulation/sedimentation of submicron iron particles in a eutrophic lake. *Water Res.* **1995**, *29*, 617–632.
- (20) Sutton, A.; Sapsford, D.; Moorhouse, A. *Mine water treatability studies for passive treatment of coal mine drainage*. In: Proc. 10th ICARD & IMWA Annual Conference, 2015.
- (21) Hunt, J.; Pandya, J. Sewage sludge coagulation and settling in seawater. *Environ. Sci. Technol.* **1984**, *18*, 119–121.
- (22) Gunnars, A.; Blomqvist, S.; Johansson, P.; Andersson, C. Formation of Fe(III) oxyhydroxide colloids in freshwater and brackish seawater, with incorporation of phosphate and calcium. *Geochim. Cosmochim. Acta* **2002**, *66*, 745–758.
- (23) Hiemenz, P.; Rajagopalan, R. *Principles of Colloid and Surface Chemistry*, 3rd ed.; Taylor & Francis: New York, USA, 1997.
- (24) Fox, L.; Wofsy, S. Kinetics of removal of iron colloids from estuaries. *Geochim. Cosmochim. Acta* **1983**, *47*, 211–216.
- (25) Mayer, L. Aggregation of colloidal iron during estuarine mixing: Kinetics, mechanism, and seasonality. *Geochim. Cosmochim. Acta* **1982**, *46*, 2527–2535.
- (26) Hunter, K.; Leonard, M.; Carpenter, P.; Smitz, J. Aggregation of iron colloids in estuaries: A heterogeneous kinetics study using continuous mixing of river and sea waters. *Colloids Surf, A* **1997**, *120*, 111–121.
- (27) Farley, K.; Morel, F. Role of coagulation in the kinetics of sedimentation. *Environ. Sci. Technol.* **1986**, *20*, 187–195.
- (28) Barnes, A.; Sapsford, D.; Dey, M.; Williams, K. Heterogeneous Fe(II) oxidation and zeta potential. *J. Geochem. Explor.* **2009**, *100*, 192–198.
- (29) Dempsey, B.; Jeon, B. Characteristics of sludge produced from passive treatment of mine drainage. *Geochem.: Explor., Environ., Anal.* **2001**, *1*, 89–94.
- (30) Xiao, F.; Yi, P.; Pan, X.; Zhang, B.; Lee, C. Comparative study of the effects of experimental variables on growth rates of aluminum and iron hydroxide flocs during coagulation and their structural characteristics. *Desalination* **2010**, *250*, 902–907.
- (31) Banfield, J.; Welch, S.; Zhang, H.; Ebert, T.; Penn, R. Aggregation-based crystal growth and microstructure development in natural iron oxyhydroxide biomineralization products. *Science* **2000**, *289*, 751–754.
- (32) Gibbs, R.; Matthews, M.; Link, D. The relationship between sphere size and settling velocity. *J. Sediment. Petrol.* **1971**, *41*, 7–18.
- (33) Hove, M.; van Hille, R.; Lewis, A. Mechanisms of formation of iron precipitates from ferrous solutions at high and low pH. *Chem. Eng. Sci.* **2008**, *63*, 1626–1635.
- (34) Lo, B.; Waite, T. Structure of hydrous ferric oxide aggregates. *J. Colloid Interface Sci.* **2000**, *222*, 83–89.
- (35) Fenton, O.; Healy, M.; Rodgers, M.; O'Huallachain, D. Site-specific P absorbency of ochre from acid mine drainage near an abandoned Cu-S mine in the Avoca-Avonmore catchment, Ireland. *Clay Miner.* **2009**, *44*, 113–123.
- (36) Marcello, R.; Galato, S.; Peterson, M.; Riella, H.; Bernardin, A. Inorganic pigments made from the recycling of coal mine drainage treatment sludge. *J. Environ. Manage.* **2008**, *88*, 1280–1284.
- (37) Matthies, R.; Aplin, A.; Horrocks, B.; Mudashiru, L. Occurrence and behaviour of dissolved, nano-particulate and micro-particulate iron in waste waters and treatment systems: New insights from electrochemical analysis. *J. Environ. Monit.* **2012**, *14*, 1174–1181.
- (38) Wang, N.; Deng, N.; Qiu, Y.; Su, Z.; Hunag, C.; Hu, K.; Wang, J.; Ma, L.; Xiao, E.; Xiao, T. Efficient removal of antimony with natural secondary iron minerals: Effect of structural properties and sorption mechanism. *Environ. Chem.* **2020**, *17*, 332–344.
- (39) National Coal Board. *Technical management of water in the coal mining industry*; Westminster Press: London, UK, 1982.
- (40) Opitz, J.; Alte, M.; Bauer, M.; Peiffer, S. Quantifying iron removal efficiency of a passive mine water treatment system using turbidity as a proxy for (particulate) iron. *Appl. Geochem.* **2020**, *122*, No. 104731.
- (41) Opitz, J.; Bauer, M.; Eckert, J.; Peiffer, S.; Alte, M. Optimising operational reliability and performance in aerobic passive mine water treatment: The multistage Westfield pilot plant. *Water, Air, Soil Pollut.* **2022**, *233*, 66.
- (42) Schwertmann, U.; Cornell, R. *Iron Oxides in the Laboratory: Preparation and Characterization*, 2nd ed.; Wiley-VCH: Weinheim, Germany, 1991.
- (43) Mylon, S.; Chen, K.; Elimelech, M. Influence of natural organic matter and ionic composition on the kinetics and structure of hematite colloid aggregation: Implications to iron depletion in estuaries. *Langmuir* **2004**, *20*, 9000–9006.
- (44) Vikesland, P.; Rebodos, R.; Bottero, J.; Rose, J.; Mason, A. Aggregation and sedimentation of magnetite nanoparticle clusters. *Environ. Sci.: Nano* **2016**, *3*, 567–577.
- (45) Wan, Y.; Wu, H.; Roelvink, D.; Gu, F. Experimental study on fall velocity of fine sediment in the Yangtze Estuary, China. *Ocean Eng.* **2015**, *103*, 180–187.
- (46) Baumgartner, J.; Faivre, D. Iron solubility, colloids and their impact on iron (oxyhydr)oxide formation from solution. *Earth-Sci. Rev.* **2015**, *150*, 520–530.
- (47) Kosmulski, M. Isoelectric points and points of zero charge of metal (hydr)oxides: 50 years after Parks' review. *Adv. Colloid Interface Sci.* **2016**, *238*, 1–61.
- (48) Schwertmann, U.; Fechtner, H. The point of zero charge of natural and synthetic ferrihydrites and its relation to adsorbed silicate. *Clay Miner.* **1982**, *17*, 471–476.
- (49) Espenson, J. *Chemical Kinetics and Reaction Mechanisms; McGraw-Hill Series in Advanced Chemistry*; New York, USA, 1981.
- (50) Chao, T.; Espenson, J. Mechanism of hydrogen evolution from hydriocobaloxime. *J. Am. Chem. Soc.* **1978**, *100*, 129–133.
- (51) Filella, M.; Buffle, J. Factors controlling the stability of submicron colloids in natural waters. *Colloids Surf, A* **1993**, *73*, 255–273.
- (52) Opitz, J.; Alte, M.; Bauer, M.; Peiffer, S. The role of macrophytes in constructed surface-flow wetlands for mine water treatment: A review. *Mine Water Environ.* **2021**, *40*, 587–605.
- (53) Parker, K. Mine water management on a national scale – Experiences from the Coal Authority. *Land Contam. Reclam.* **2003**, *11*, 181–190.
- (54) PIRAMID Consortium. *Engineering guidelines for the passive remediation of acidic and/or metalliferous mine drainage and similar wastewaters*; Project No. EVK1-CT-1999-000021: Newcastle upon Tyne, UK, 2003.
- (55) Cravotta, C. Interactive PHREEQ-N-AMDTreat water-quality modeling tools to evaluate performance and design of treatment systems for acid mine drainage. *Appl. Geochem.* **2021**, *126*, No. 104845.

(56) Mills, T.; Anderson, S.; Bern, C.; Aguirre, A.; Derry, L. Colloid mobilization and seasonal variability in a semiarid headwater stream. *J. Environ. Qual.* **2017**, *46*, 88–95.

(57) Liao, P.; Li, W.; Jian, Y.; Wu, J.; Yuan, S.; Fortner, J.; Giammar, D. Formation, aggregation, and deposition dynamics of NOM-iron colloids at anoxic-oxic interfaces. *Environ. Sci. Technol.* **2017**, *51*, 12235–12245.

(58) Goula, A.; Kostoglou, M.; Karapantsios, T.; Zouboulis, A. The effect of influent temperature variations in a sedimentation tank for potable water treatment – A computational fluid dynamics study. *Water Res.* **2008**, *42*, 3405–3414.

(59) Goodarzi, D.; Sookhak-Lari, K.; Mossaiby, F. Thermal effects on the hydraulic performance of sedimentation ponds. *J. Water Process Eng.* **2020**, *33*, No. 101100.

(60) Thackston, E.; Shields, F.; Schroeder, P. Residence time distributions of shallow basins. *J. Environ. Eng.* **1987**, *113*, 1319–1332.

Recommended by ACS

Iron(II)-Catalyzed Iron Atom Exchange and Mineralogical Changes in Iron-rich Organic Freshwater Floccs: An Iron Isotope Tracer Study

Laurel K. ThomasArrigo, Ruben Kretzschmar, *et al.*

JUNE 07, 2017

ENVIRONMENTAL SCIENCE & TECHNOLOGY

READ 

Stabilization of Ferrihydrite and Lepidocrocite by Silicate during Fe(II)-Catalyzed Mineral Transformation: Impact on Particle Morphology and ...

Katrin Schulz, Ruben Kretzschmar, *et al.*

APRIL 18, 2022

ENVIRONMENTAL SCIENCE & TECHNOLOGY

READ 

Salinity Effects on Iron Speciation in Boreal River Waters

Simon D. Herzog, Emma S. Kritzberg, *et al.*

AUGUST 24, 2017

ENVIRONMENTAL SCIENCE & TECHNOLOGY

READ 

Biological Reduction of Ferrihydrite with Silica Addition: Rates and Controlling Mechanisms

Yufeng Gong, Xuefei Zhou, *et al.*

SEPTEMBER 20, 2021

ACS EARTH AND SPACE CHEMISTRY

READ 

Get More Suggestions >

SUPPORTING INFORMATION

**Sedimentation Kinetics of Hydrous Ferric Oxides in
Ferruginous, Circumneutral Mine Water**

Joscha Opitz^{1,2,*}, Martin Bauer², Matthias Alte², Johanna Schmidtman¹, Stefan Peiffer¹

¹ Department of Hydrology, University of Bayreuth, BayCEER, Universitätsstraße 30,
D-95447 Bayreuth, Germany

² BASE Technologies GmbH, D-81241 Munich, Germany

* Corresponding author: joscha.opitz@uni-bayreuth.de

Published: Environmental Science & Technology

DOI: <https://doi.org/10.1021/acs.est.1c07640>

Received: November 9, 2021

Revised: April 6, 2022

Accepted: April 8, 2022

Number of Pages: 8

Supporting Figures: 7

Supporting Tables: 1

SUPPORTING FIGURES

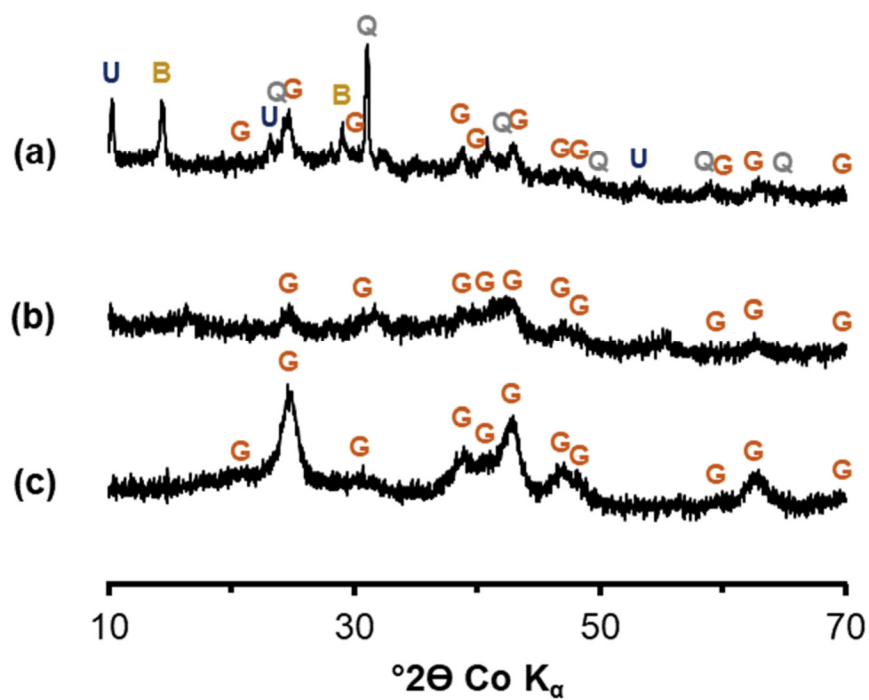


Figure S1. X-ray diffractograms of ferric solids: (a) natural ochre, (b) slightly acidic ochre precipitated at pH 5-7, and (c) acidic ochre precipitated at pH 2-5; G = goethite, Q = quartz, B = birnessite, U = unknown.

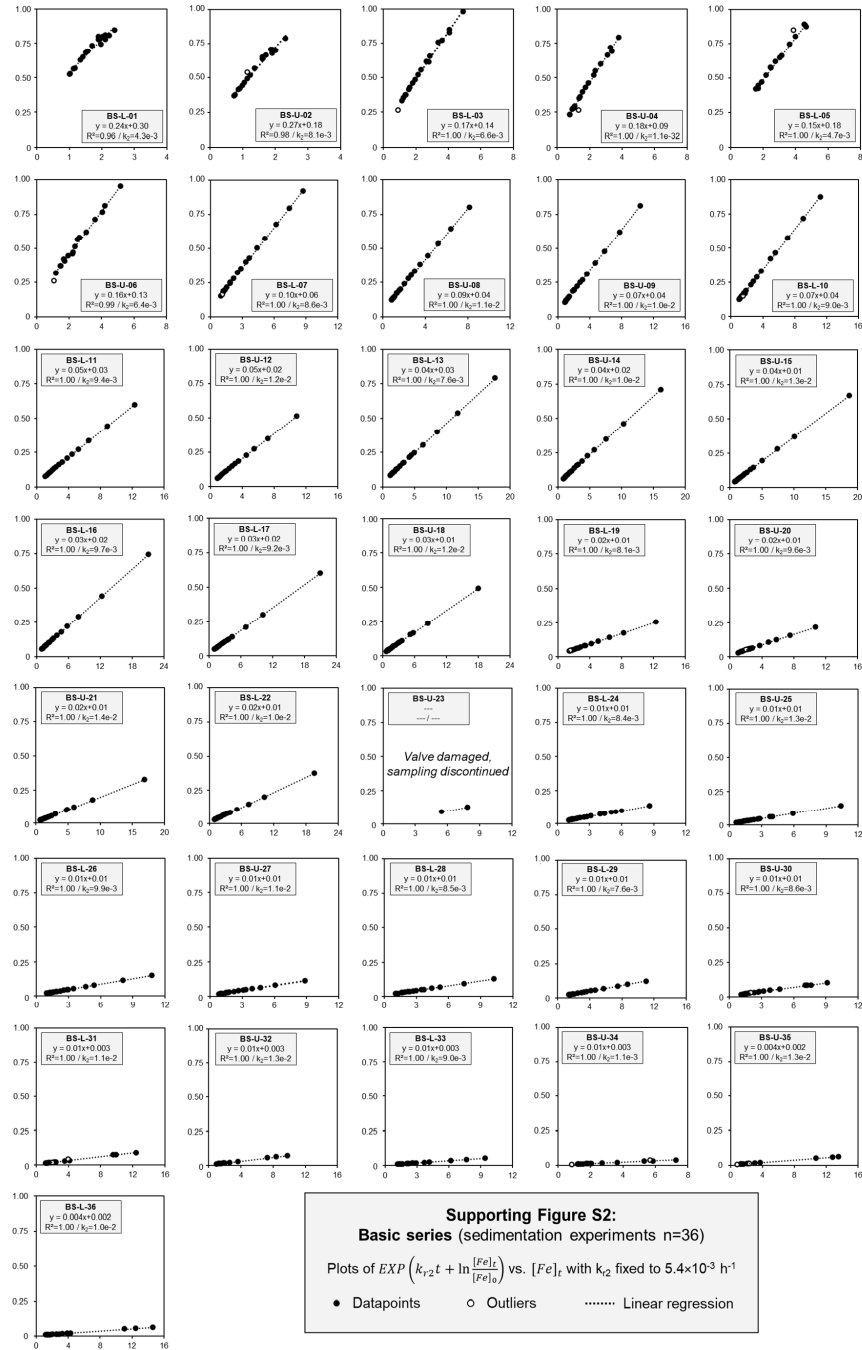


Figure S2. Plots of $EXP\left(k_{r2}t + \ln\frac{[Fe]_t}{[Fe]_0}\right)$ vs. $[Fe]_t$ with k_{r2} fixed to $5.4 \times 10^{-3} \text{ h}^{-1}$ for the 36 experiments of the basic series.

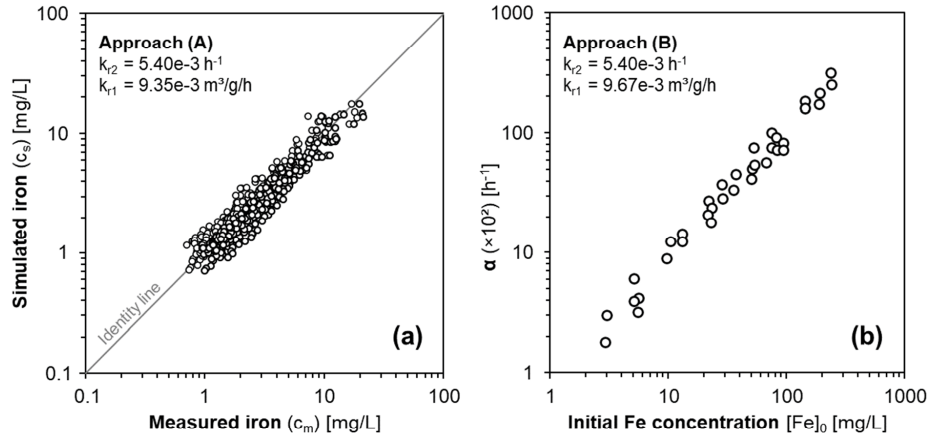


Figure S3. Determination of k_{r1} with a fixed $k_{r2} = 5.5 \times 10^{-3} \text{ h}^{-1}$ via approach (A): Logarithmic plot of the computational least-squares relative error regression of simulated (c_s) vs. measured (c_m) concentrations, and approach (B): Logarithmic plot of $\alpha = k_{r2} + k_{r1}[Fe]_0$ vs. the initial iron concentrations $[Fe]_0$.

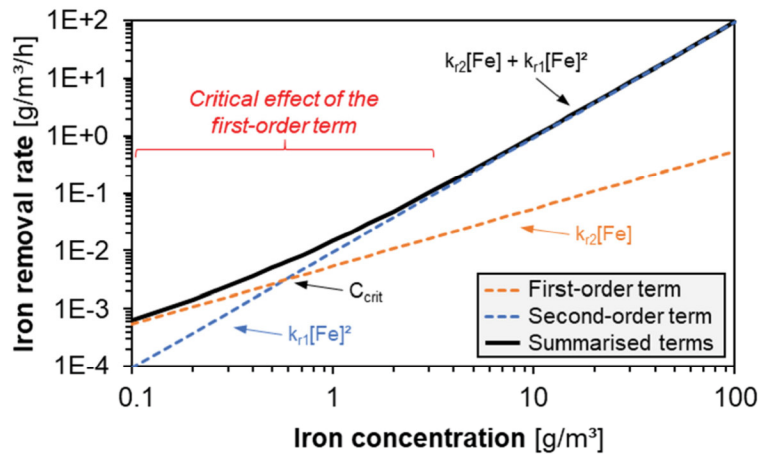


Figure S4. Contribution of the two terms of the mixed first-/second-order rate law to the sedimentation-based removal of hydrous ferric oxides with $k_{r1} = 9.4 \times 10^{-3} \text{ m}^3/\text{g/h}$ and $k_{r2} = 5.4 \times 10^{-3} \text{ h}^{-1}$ as dashed orange and blue lines, respectively, and their sum as unbroken black line.

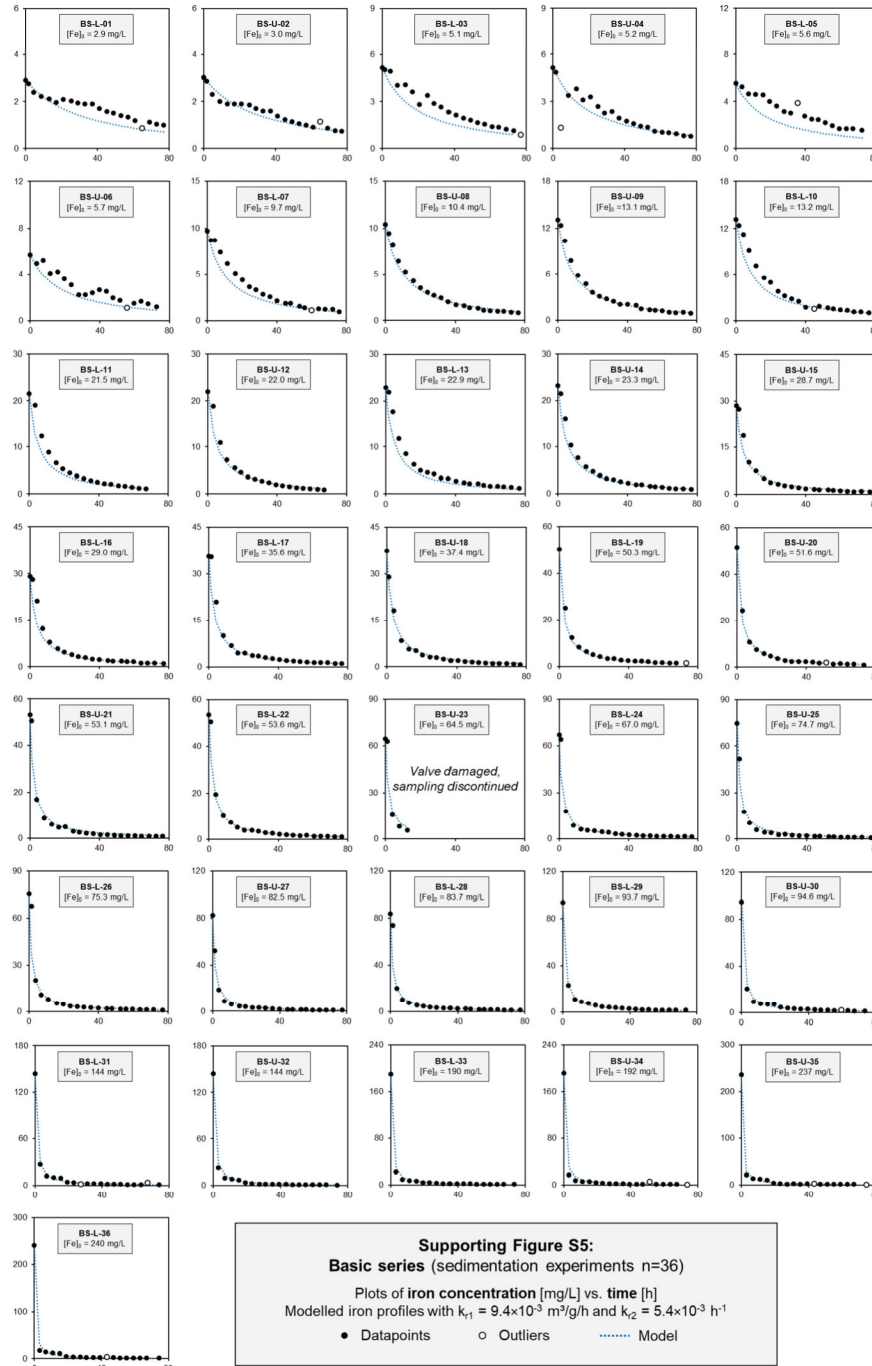


Figure S5. Plots of the 36 sedimentation experiments of the basic series based on the mixed first-/second order model.

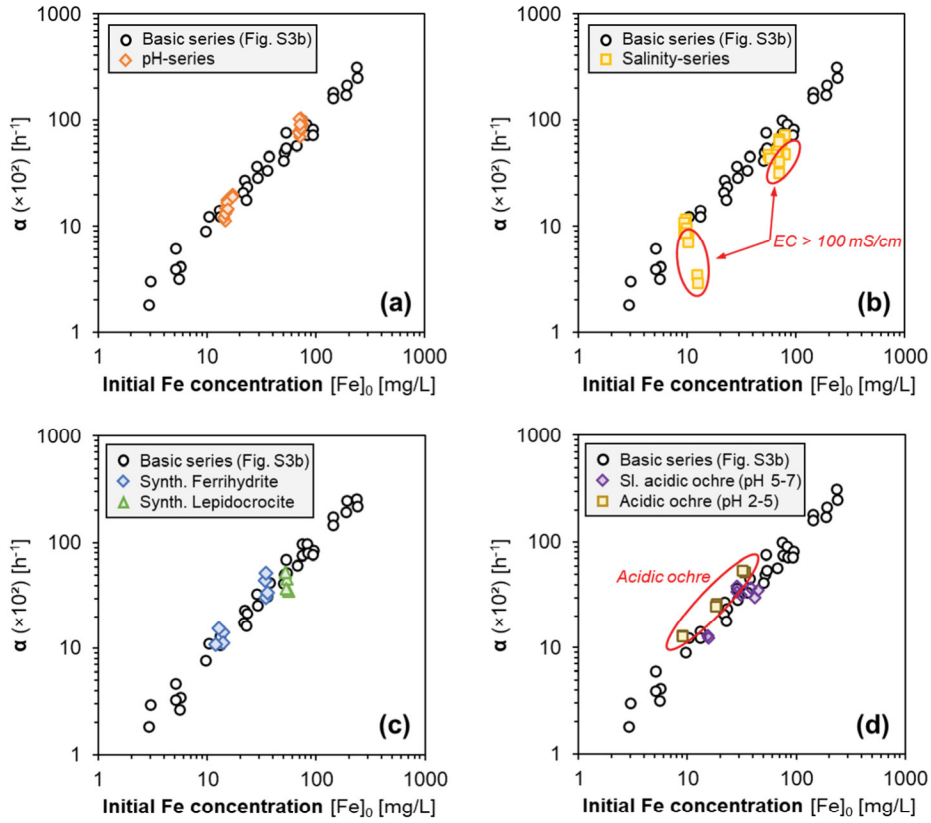


Figure S6. Logarithmic plots of $\alpha = k_{r2} + k_{r1}[Fe]_0$ with k_{r2} fixed to $5.4 \times 10^{-3} \text{ h}^{-1}$ vs. the initial iron concentration $[Fe]_0$ for the additional experimental series inserted into Figure S3b with (a) pH-series, (b) salinity series, (c) synthetic ferric solids and (d) natural, slightly acidic and acidic ochre.

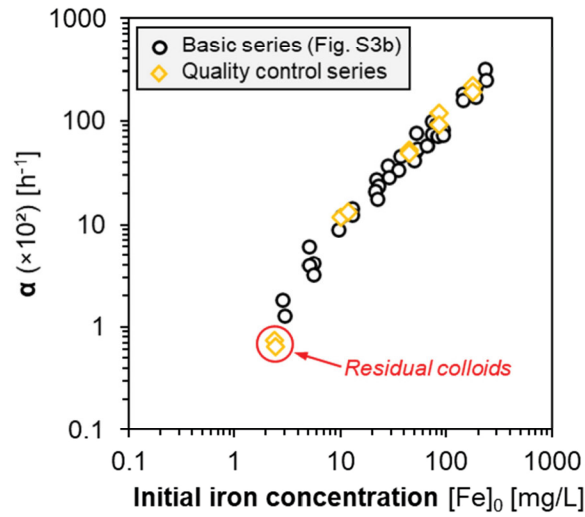


Figure S7. Logarithmic plot of $\alpha = k_{r2} + k_{r1}[Fe]_0$ with k_{r2} fixed to $5.4 \times 10^{-3} \text{ h}^{-1}$ vs. the initial concentration of ferric solids $[Fe]_0$ for the *real mine water series* inserted into Figure S3b with specific marking of the residual colloids experiments that was used to experimentally determine k_{r2} .

SUPPORTING TABLE(S)

Table S1. Results of the additional experimental series for the first-order coefficient k_{sed} below a threshold concentration of 4.25 mg/L as average (\pm SD).

experimental series ^a	k_{sed} ($\times 10^{-2}$) in [h^{-1}]
basic series (n=36)	2.4(\pm 0.4)
pH series (n=24)	2.6(\pm 0.1)
salinity series, EC < 100 mS/cm (n=14)	2.3(\pm 0.5)
salinity series, EC > 100 mS/cm (n=4)	1.8(\pm 0.2)
synthetic ferrihydrite (n=8)	2.2(\pm 0.4)
synthetic lepidocrocite (n=4)	2.4(\pm 0.1)
slightly acidic natural ochre, pH 5-7 (n=8)	2.5(\pm 0.4)
acidic natural ochre, pH 2-5 (n=6)	2.3(\pm 0.1)
real mine water series ^b (n=8)	2.5(\pm 0.1)

^a Underlying number of datasets in brackets.

^b Real mine water series without residual-colloids-experiments (see Fig. S7).

SUPPORTING TABLE(S)

Table S1. Results of the additional experimental series for the first-order coefficient k_{sed} below a threshold concentration of 4.25 mg/L as average (\pm SD).

experimental series ^a	k_{sed} ($\times 10^{-2}$) in [h^{-1}]
basic series (n=36)	2.4(\pm 0.4)
pH series (n=24)	2.6(\pm 0.1)
salinity series, EC < 100 mS/cm (n=14)	2.3(\pm 0.5)
salinity series, EC > 100 mS/cm (n=4)	1.8(\pm 0.2)
synthetic ferrihydrite (n=8)	2.2(\pm 0.4)
synthetic lepidocrocite (n=4)	2.4(\pm 0.1)
slightly acidic natural ochre, pH 5-7 (n=8)	2.5(\pm 0.4)
acidic natural ochre, pH 2-5 (n=6)	2.3(\pm 0.1)
real mine water series ^b (n=8)	2.5(\pm 0.1)

^a Underlying number of datasets in brackets.

^b Real mine water series without residual-colloids-experiments (see Fig. S7).

Study 5 – Water Res. 233: 119770

Title Development of a novel sizing approach for passive mine water treatment systems based on ferric iron sedimentation kinetics

Authors Opitz J, Alte M, Bauer M, Peiffer S

Status Published

Year 2023

Journal Water Research

Article 233: 119770

Pages 10

DOI 10.1016/j.watres.2023.119770

SI  <https://linkinghub.elsevier.com/retrieve/pii/S0043135423002051>

Access  <https://linkinghub.elsevier.com/retrieve/pii/S0043135423002051>
© Elsevier Ltd.



Relative contribution of the PhD student to study 5:

- Study design 60%
- Data collection and field work 60%
- Data processing and analysis 80%
- Evaluation 70%
- Manuscript preparation 80%

JO, MA, MB, and SP were responsible for funding acquisition as well as project administration and controlling. JO, MA, MB, and SP designed the study. JO and JE planned and conducted both field and laboratory work, with samples and field parameters predominantly collected by JO, and chemical analyses predominantly conducted by JE. The data was processed and analysed by JO and SP. All authors evaluated the results. JO prepared a first draft as well as figures and tables for the manuscript with input from all co-authors. All authors jointly finalised and submitted the manuscript. JO is the corresponding author.

JO: Joscha Opitz // MA: Matthias Alte // MB: Martin Bauer // JE: Jutta Eckert // SP: Stefan Peiffer



Development of a novel sizing approach for passive mine water treatment systems based on ferric iron sedimentation kinetics

Joscha Opitz^{a,b,*}, Martin Bauer^b, Matthias Alte^b, Stefan Peiffer^a

^a Department of Hydrology, University of Bayreuth, BayCEER, Universitätsstraße 30, Bayreuth D-95447, Germany
^b Base technologies GmbH, Josef-Felder-Straße 53, Munich D-81241, Germany

ARTICLE INFO

Keywords:

Iron removal
Mine drainage
Settling ponds
Constructed wetlands
Area-adjusted removal rate
Residence time

ABSTRACT

The removal of dissolved and particulate iron (Fe) from contaminated mine drainage is an omnipresent challenge in, and legacy of, the mining industry worldwide. The sizing of settling ponds and surface-flow wetlands for passive Fe removal from circumneutral, ferruginous mine water is based either on a linear (concentration-independent) area-adjusted removal rate or flat assignment of an experience-based retention time, neither of which reflects the underlying Fe removal kinetics. In this study, we evaluated the Fe removal performance of a pilot-scale passive system operating in three identical, parallel lines for treatment of mining-influenced, ferruginous seepage water to determine and parameterise a robust, application-orientated model approach for sizing of settling ponds and surface-flow wetlands, each. By systematically varying flow rates (and thus residence time), we were able to demonstrate that the sedimentation-driven removal of particulate hydrous ferric oxides in settling ponds may be approximated by a simplified first-order approach at low to moderate Fe levels. The first-order coefficient was found in the order of $2.1(\pm 0.7) \times 10^{-2} \text{ h}^{-1}$, which corresponds well with previous laboratory studies. The sedimentation kinetics may be combined with the preceding Fe(II) oxidation kinetics to estimate the required residence time for pre-treatment of ferruginous mine water in settling ponds. In contrast, Fe removal in surface-flow wetlands is more complex due to the phytologic component, which is why we advanced the established area-adjusted Fe removal approach by parameterising the underlying concentration-dependency for polishing of pre-treated mine water. The quantitative results of this study provide a novel, conservative approach for customised sizing of settling ponds and wetlands in integrated passive mine water treatment systems.

Glossary

A	Surface area of the pond or wetland [m^2]
V	Volume of the water body [m^3]
z	Water depth [m]
Q	Volumetric flow rate [m^3/h]
t	Residence time [h]
$t_n / t_m / t_p$	Nominal / mean / peak HRT [h]
σ^2	Variance [h^2]
λ	Hydraulic efficiency [-]
$C, [\text{O}_2], \{\text{H}^+\}$	Tracer / O_2 concentration, H^+ activity [mg/L, mol/L]
$E(t), F(t)$	Normalised and cumulative RTD functions [-]
$[\text{Fe}]_m / [\text{Fe}]_{mr}$	Inflow / outflow Fe concentration [mg/L]
$[\text{Fe}(\text{II})]$	Dissolved ferrous Fe concentration [mg/L]
$[\text{Fe}(\text{OH})_3]$	Suspended hydrous ferric oxide concentration [mg/L]

$[\text{Fe}(\text{tot})]$	Total Fe concentration [mg/L]
R_A	Area-adjusted Fe removal rate [$\text{g}/\text{m}^2/\text{d}$]
k_{sed}	First-order sedimentation constant [h^{-1}]
k_{ox}, k'_{ox}	(Pseudo) First-order oxidation constant [$\text{mol}/\text{L}/\text{s}, \text{h}^{-1}$]
m, n	Model fitting parameters [m/d, -]

1. Introduction

Industrial-scale coal, lignite, and metal mining are commonly associated with the generation of contaminated mine drainage that requires treatment to protect receiving freshwater environments. Mine water treatment is increasingly facilitated in eco-technological “passive” systems that harness and enhance natural biogeochemical and physical processes for removal of various contaminants (Skousen et al., 2017). Passive systems are often regarded as a more sustainable and

* Corresponding author.
E-mail address: joscha.opitz@uni-bayreuth.de (J. Opitz).

<https://doi.org/10.1016/j.watres.2023.119770>

Received 20 October 2022; Received in revised form 13 February 2023; Accepted 18 February 2023

Available online 21 February 2023

0043-1354/© 2023 Elsevier Ltd. All rights reserved.

cost-effective approach for mine water treatment, especially for circumneutral, ferruginous mine waters that predominantly require the removal of iron (Fe) as ubiquitous contaminant in mining environments (Hedin, 2008). Passive Fe removal is commonly achieved in surface flow systems through oxidation of dissolved Fe(II) and subsequent sedimentation or filtration of the resultant particulate hydrous ferric oxides (hereinafter Fe(OH)₃) (Hedin et al., 1994; Skousen et al., 2017).

Aerobic passive systems for iron removal commonly consist of consecutive aeration cascades for oxygenation, settling ponds for pre-treatment, and surface-flow wetlands for polishing (Hedin et al., 1994). Basically, settling ponds provide retention time for oxidation of Fe(II) and sedimentation of the bulk Fe(OH)₃ load, whereas subsequent wetlands facilitate sedimentation or filtration of the remaining colloidal Fe(OH)₃ in the dense vegetation to reliably meet specific discharge limits (Opitz et al., 2021). The assembly of consecutive treatment stages in integrated systems for treatment of circumneutral, ferruginous mine water is rather vaguely defined in the literature, broadly aiming at 50 to 80% Fe removal in settling ponds (depending on Fe loading) to protect the subsequent wetlands from overloading (Kruse et al., 2009; Parker, 2003). This latent ambiguity is attributable to the underlying sizing practice for both settling ponds and wetlands that is largely based on concentration-independent rules of thumb, which are ill-defined for more customised designing and sizing of integrated passive systems (Banks, 2003; Sapsford, 2013).

Only few approaches for sizing of settling ponds are to be found in the literature as compiled in Tab. S1a, none of which became standard practice to date (Kruse et al., 2009). Early recommendations were derived from the wastewater sector, for instance assigning an overflow rate of 1×10^{-5} m/s to broadly allow for settling of clay-sized particles (National Coal Board, 1982). However, mine discharges often require additional (retention) time to allow for Fe(II) oxidation, and it was also found that the aggregation and sedimentation behaviour of freshly precipitated Fe(OH)₃ distinctly differs from soil or sewage particles (Hove et al., 2008; Sapsford, 2013). Commonest in the literature is the experience-based assignment of either a flat hydraulic retention time (HRT) in the order of 8 to 48 h or a hydraulic loading rate in the order of 100 m²/L/s to broadly allow for both Fe(II) oxidation and settling of larger particles (Tab. S1b). Overall, Banks (2003) noted that performance evaluation of settling ponds is rather scarce relative to wetlands, which is why wetland sizing is at times transferred to settling ponds.

Various sizing approaches for surface-flow wetlands were developed for treatment of acidic and neutral mine water, most of which are based on empirical, area-adjusted Fe removal rates as compiled in Tab. S1b. Eventually, a recommendation for areal sizing of wetlands was issued by the former US Bureau of Mines (Hedin et al., 1994) that was henceforth adopted in various guidelines (e.g., PIRAMID Consortium, 2003; Skousen et al., 1998; Watzlaf et al., 2004). The wetland area (A) is calculated from Fe loading and an empirical, area-adjusted sizing constant (R_A):

$$A = \frac{Q \times ([Fe]_{in} - [Fe]_{out})}{R_A} \quad (1)$$

with Q as volumetric flow rate, and [Fe]_{in} and [Fe]_{out} as inflow and (target) effluent Fe concentration, respectively. This approach suggests that Fe removal rates in wetlands are constant over time and independent of concentration, which corresponds to a zero-order removal process.

The areal sizing coefficient R_A was estimated from operational full-scale wetlands, ranging from 10 g/m²/d for formal approval procedures to 20 g/m²/d for basic water quality improvement at legacy mine sites. However, it should be noted that the established sizing criteria were derived from passive systems treating highly ferruginous mine discharges, which is why Hedin et al. (1994) noted that the areal approach is subject to a "loading limitation". Accordingly, a wide range from < 1 up to and above 50 g/m²/d were reported for full-scale settling ponds and wetlands as compiled in Tab. S2. Most observations are

markedly below 10 g/m²/d, and it was shown that areal Fe removal is predominantly governed by Fe loading and pH (Mayes et al., 2009; Younger, 2000). Although the areal approach is commonly considered (and has proven to be) relatively robust for "classic" ferruginous coal mine discharges, there is general agreement that the multicausal relationship between overall Fe removal on the one hand and the size of settling ponds or wetlands on the other hand is inadequately described by a linear relationship (e.g., Flanagan et al., 1994; Johnson and Hallberg, 2002; Kruse et al., 2009; Mayes et al., 2009; Sapsford, 2013; Stark and Williams, 1995).

From a process-based perspective, passive Fe removal in settling ponds proceeds along two major, presumably rate determining steps; namely (1.) oxidation of dissolved Fe(II) followed by (2.) sedimentation of the resultant Fe(OH)₃. The oxidative transition from ferrous to ferric Fe has been investigated intensively and respective kinetics are well-described in the literature (e.g., Millero et al., 1987; Stumm and Morgan, 1996). The basic (homogeneous) Fe(II)-oxidation process may be approximated by the following kinetic equation where the oxidation constant (k_{ox}) is substituted by a pseudo first-order constant (k'_{ox}) at stable pH and oxygen levels that is second order with respect to {H⁺} and {OH⁻} and first order with respect to [O₂]:

$$\frac{-d[Fe(II)]}{dt} = k_{ox} \frac{[Fe(II)] \times [O_2]}{[H^+]^2} = k'_{ox} [Fe(II)] \quad (2)$$

This relationship was broadly confirmed for mining environments by extensive field studies (Dempsey et al., 2001; Kirby et al., 1999), although it is important to note that the process is considerably accelerated in ferruginous mine waters by heterogeneous Fe(II)-oxidation owing to the autocatalytic effect of omnipresent, freshly precipitated Fe(OH)₃ as demonstrated by Dietz and Dempsey (2017).

A quantitative assessment of Fe(OH)₃ sedimentation in mining environments was made by Sapsford and Watson (2011) and Sapsford (2013), reporting that "settling of these precipitates can be described by a first-order process with rates varying for different mine waters":

$$\frac{-d[Fe(OH)_3]}{dt} = k_{sed} [Fe(OH)_3] \quad (3)$$

The first-order sedimentation coefficient k_{sed} was initially estimated in the order of 9.4 × 10⁻³ to 3.2 × 10⁻¹ h⁻¹ based on column experiments by Sapsford (2013). Whereas laboratory experiments containing both ferrous and ferric Fe displayed rather complex or inconclusive patterns, a targeted experiment with oxygenated mine water containing only Fe(OH)₃ displayed an exponential decay curve with k_{sed} ≈ 2.3 × 10⁻² h⁻¹ (Sutton et al., 2015). Sapsford and Watson (2011) noted that application of Fe removal kinetics may be a way forward to describe the performance of passive mine water treatment systems more accurately, encouraging abandonment of the established areal approach for more application-orientated model approaches governed by HRT when designing integrated passive treatment schemes. Such empirical, simplified (first-order) models are frequently utilised in ecological engineering sciences, above all for passive wastewater treatment systems, to estimate the exponential removal or decay of dissolved and suspended compounds through natural biogeochemical and physical processes (Kadlec and Wallace, 2009).

In a recent sedimentation study (Opitz et al., 2022a), we were able to demonstrate that Fe(OH)₃ sedimentation across a wide concentration range (3 – 240 mg/L) may be described by a mixed first- and second-order model. The sedimentation process is governed by two interrelated regimes with a rapid aggregation-driven step (of second order) at high iron levels followed by a slower settling step (of first order) at lower iron levels. The respective coefficients were determined with k_{r1} = 9.4 × 10⁻³ m³/g/h and k_{r2} = 5.4 × 10⁻³ h⁻¹:

$$\frac{-d[Fe(OH)_3]}{dt} = k_{r2} [Fe(OH)_3] + k_{r1} [Fe(OH)_3]^2 \quad (4)$$

Moreover, we were able to demonstrate that $\text{Fe}(\text{OH})_3$ removal at moderate Fe levels ($< 10 \text{ mg/L}$) may be reasonably well approximated by the simplifying first-order relationship in Eq. (3) as proposed by Sapsford (2013). The respective sedimentation coefficient k_{sed} was determined with $2.4(\pm 0.4) \times 10^{-2} \text{ h}^{-1}$ in column experiments (Opitz et al., 2022a), which is consistent with the initial estimates reported by Sapsford (2013) and Sutton et al. (2015).

In summary, the current state of knowledge implies that it is necessary to advance the established sizing practices for both settling ponds and wetlands to account for Fe removal dynamics, especially in the face of progressively strict environmental regulation. In this study, we evaluated the $\text{Fe}(\text{OH})_3$ removal performance of a trifurcated pilot system for passive treatment of a mining-influenced, ferruginous seepage water. Variation of flow rates in the identical triplicate system lines allowed for evaluation of $\text{Fe}(\text{OH})_3$ removal as a function of mass flow. Further on, $\text{Fe}(\text{OH})_3$ removal in the pilot-scale settling ponds and wetlands was evaluated regarding different model approaches as outlined above. The overall objective was to determine and parameterise robust, application-orientated Fe removal models that could also be used for sizing of settling ponds and wetlands. The dual approach combining fundamental laboratory studies with pilot-scale field trials offers considerable prospects to advance our knowledge on Fe removal mechanisms and kinetics in passive mine water treatment systems.

2. Materials and methods

2.1. Study site and pilot plant

The Westfield study site is a former open pit in the historic lignite district of Upper Palatinate (southeast Germany). The pit was only partly backfilled with waste rock and power plant ashes, leaving a morphological depression behind. Seepage water collecting in a “drainage pond” at the lowest point of the former pit is ferruginous and highly mineralised owing to pyrite oxidation and lixiviation of soluble compounds from the backfill, yet circumneutral due to the alkalis-

character of the dumped electrostatic precipitator ashes (Tab. S3). The seepage water is continuously pumped out from the drainage pond for protection of adjacent aquifers to a conventional (physico-chemical) treatment plant for Fe removal (Opitz et al., 2022b).

The Westfield pilot plant was implemented in 2017 next to the operational, conventional treatment plant to test an integrated three-stage passive scheme with settling ponds for pre-treatment, surface-flow wetlands for polishing and sediment filters for purification as long-term alternative for treatment of the mining-influenced seepage water (Fig. 1). The three consecutive treatment stages were built as identical, parallel triplicates such that hydraulic variation in the three system lines generated a comprehensive database. The primary objective of the pilot plant was to lower total Fe below the strict site-specific discharge limit of 1 mg/L . The basic setup and performance of the multistage pilot plant for removal of relevant contaminants (e.g., Fe, Mn, As, NH_4 , turbidity) are detailed in Opitz et al. (2022b). In this study, we focus on $\text{Fe}(\text{OH})_3$ removal in settling ponds and wetlands.

Standard roll-off containers ($7.0 \times 2.35 \times 1.25 \text{ m}$) were utilised as both settling ponds and wetlands with water depth adjusted to approx. 1.0 and 0.45 m, respectively. The wetlands were planted with common reed at 20 plants/m^2 in a sandy 0.3 m substrate. The steel containers were embedded into the ground for isolation and connected by a polyethylene pipework system. Ten monitoring points (MP01-MP10) for sensor installation and sample collection were installed in protected concrete manholes before and after the containers with settling ponds fed from MP01, settling pond outflows corresponding to wetland inflows (MP02-MP04), and wetland outflows corresponding to sediment filter inflows (MP05-MP07) as schematically illustrated in Fig. 1. The ferruginous seepage water is thoroughly oxygenated within the seepage water distribution system, which is why the pilot plant’s inflow Fe concentration was relatively low with ferrous and total Fe in the order of < 1 and $\approx 8 \text{ mg/L}$, respectively. Thus, the Westfield pilot plant provided a comparatively rare opportunity to quantify $\text{Fe}(\text{OH})_3$ removal kinetics independent of $\text{Fe}(\text{II})$ oxidation.

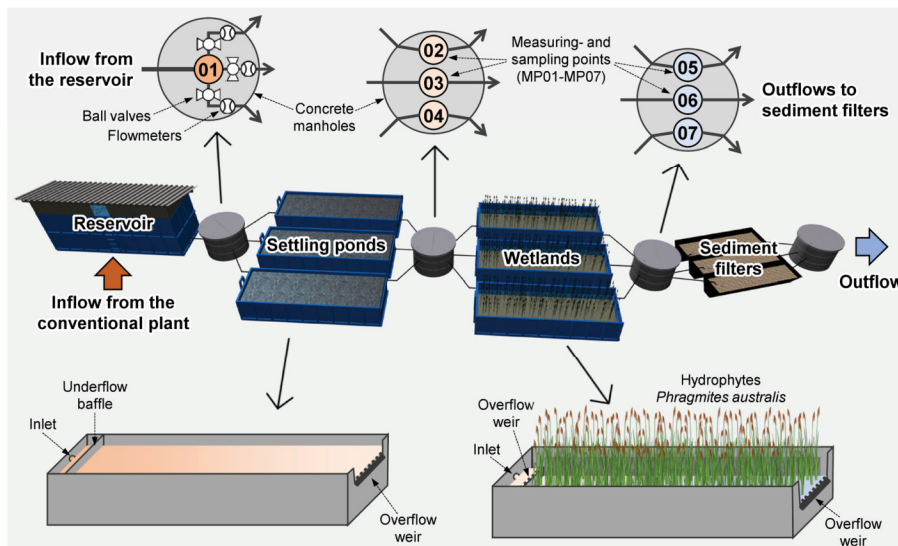


Fig. 1. Layout of the trifurcated Westfield pilot plant with details of sampling manholes (top) as well as settling ponds and wetlands (bottom).

2.2. Hydraulic characterisation

Flow rates in the three parallel system lines of the pilot plant were adjusted by ball valves and recorded by flowmeters (Stübbe DFM200) at a 30 s interval in the three feeding lines branching off MPO1 (Fig. 1). In addition, impulse-response tracer tests were conducted for hydraulic characterisation of the container-based system. Several tracer tests were conducted in both settling ponds and wetlands at incremental (steady) flow rates by pulse injection of Rhodamin WT (Acros Organics) into the inlets. Outflow fluorescence was recorded by a Cyclops 7 fluorometer (Turner Designs) at a 30 s interval. Tracer tests were conducted in winter when plant density and thermal mixing are relatively low to obtain a conservative estimate of the actual residence time distribution (RTD) (Braskerud, 2001). Fluorescence measurements were corrected for temperature following Smart and Laidlaw (1977) and converted to tracer concentration following Bodin et al. (2012) to determine concentration-normalised and cumulative RTD functions $E(t)$ and $F(t)$:

$$E(t) \approx \frac{Q \times C(t)}{\sum_{i=1}^n Q \times C_i(t) \Delta t} \quad (5)$$

$$F(t) \approx \sum_{i=1}^n E(t) \Delta t \quad (6)$$

Flow rate (Q) and effluent tracer concentration (C) were averaged to a 10 min interval (Δt) for ease of handling and to smooth tracer response curves. Cumulative effluent tracer mass (m_{out}), mean HRT (t_m) and variance (σ^2) were calculated as the zeroth, first and second moments of the RTD to determine tracer recovery, centroid and spread of the tracer response curves, respectively:

$$m_{out} \approx \sum_{i=1}^n Q \times C_i(t) \Delta t \quad (7)$$

$$t_m \approx \sum_{i=1}^n t E(t) \Delta t \quad (8)$$

$$\sigma^2 \approx \sum_{i=1}^n (t_m - t)^2 E(t) \Delta t \quad (9)$$

The hydraulic efficiency (λ) of settling ponds and wetlands was calculated as the ratio of nominal HRT (t_n) and tracer peak time (t_p) following Persson et al. (1999), with the intrinsic nominal HRT calculated from the container geometry with water depth (z) and volume (V):

$$t_n = \frac{A \times z}{Q} = \frac{V}{Q} \quad (10)$$

$$\lambda = \frac{t_p}{t_n} \quad (11)$$

2.3. Hydrochemical monitoring

Water samples for Fe analysis were collected twice weekly at all measuring points over approx. one year (07/2018 to 06/2019). Two samples were collected, one filtered at 0.45 μm and acidified with 150 μL of 1 M HCl to immediately quench Fe(II)-oxidation, the other unfiltered and acidified with 150 μL of 12 M HCl to additionally re-dissolve dispersed Fe(OH)₃. Samples were cooled to 4 °C before transport to the laboratory for spectrophotometric analysis at 512 nm (Hach DR 3800 VIS) using acetate buffer solution and 1,10-phenantroline. Filtered samples were analysed for dissolved Fe(II) and unfiltered samples for total Fe using ascorbic acid for Fe(III) reduction. This procedure allowed determination of not only dissolved species, but also particulate and total Fe (Oplitz et al., 2020). All chemicals used for stabilisation, calibration or standards were analytical grade.

2.4. Data analysis

Fe removal in the pilot plant was evaluated based on inflow/outflow Fe concentration, system geometry, flow rate, and HRT as illustrated in Fig. 2. To generate a comprehensive dataset, flow rates in the three parallel system lines were alternated between 100 and 500 L/h to vary hydraulic loading. Flow rates were aggregated as medians around the Fe samplings to smooth hydraulic fluctuations. Thus, the final semi-weekly dataset based on Fe analyses and respectively aggregated flow rates includes 270 measurements (90 per system line) for settling ponds and wetlands, each.

In a first step, Fe(OH)₃ removal rates in both settling ponds and wetlands were evaluated as the change in concentration from inflow to outflow over (retention) time assuming approximately stationary conditions in the containers. As Fe(II) was negligible throughout the pilot system, total Fe concentration [Fe] was used for evaluation of Fe(OH)₃ removal:

$$\frac{\Delta[Fe]}{\Delta t} = \frac{[Fe]_{out} - [Fe]_{in}}{t_n} \quad (12)$$

As the surface area of the pilot-scale settling ponds and wetlands remained constant throughout the study, Eq. (12) basically evaluates Fe mass flow through the system as governed by flow rate. From this it follows that Fe removal rates as $\Delta[Fe]/\Delta t$ are (directly) proportional to the area-adjusted Fe removal rate R_A from Eq. (1):

$$\frac{\Delta[Fe]}{\Delta t} = \frac{[Fe]_{out} - [Fe]_{in}}{t_n} = \frac{([Fe]_{in} - [Fe]_{out}) \times Q}{A \times z} = R_A \times z^{-1} \quad (13)$$

The water depth (z) of settling ponds and especially wetlands is usually infinitesimal relative to length and width, although it should be noted that water depth effects in shallow wetlands are complex and not yet fully understood (Guo and Cui, 2021; Shih and Wang, 2020).

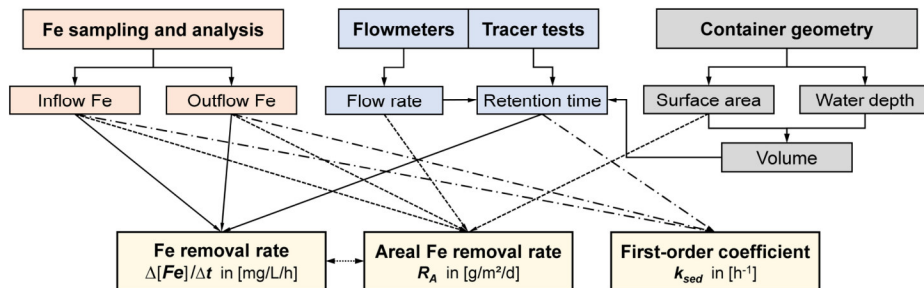


Fig. 2. Schematic illustration of the monitoring and data evaluation approach.

In a second step, the extensive datasets were used to assess Fe removal kinetics in the Westfield pilot system. Based on the preceding column experiments, it is reasonable to assume that $\text{Fe}(\text{OH})_3$ removal in bare settling ponds is ultimately governed by sedimentation and may thus be approximated by the relationships provided by Oplitz et al. (2022a). As the inflow Fe level of the Westfield pilot plant was consistently below 15 mg/L, the simplified first-order approach (rather than the mixed first-/second-order model) was used with the coefficient k_{sed} obtained through integration and rearrangement of Eq. (3):

$$k_{\text{sed}} = -\ln \left[\frac{[Fe]_{\text{out}}}{[Fe]_{\text{in}}} \right] \times t_n^{-1} \quad (14)$$

The investigation of contaminant removal kinetics in passive treatment systems is generally complicated by the fact that usually just two datapoints (namely inflow and outflow) are measured that can only be related to system geometry and/or HRT as illustrated in Fig. 2. Also, the Westfield pilot plant was inevitably subject to various technical, environmental, and hydrodynamic effects, including but not limited to:

- Small constructional differences between the three parallel system lines;
- Increasing reed density in wetlands during the second vegetation period;
- Intermittent flow rates and Fe spikes in the reservoir feed caused by filling flushes;
- Wind-driven currents, rainfall, or buoyancy in the open system.

Such intrinsic and external spatiotemporal effects are commonly the primary limitation of pilot-scale field trials, all the more because most efficiency and performance criteria are developed for full-scale systems with small dispersion indices (Chang et al., 2016; Philips et al., 2005). Therefore, three strategies were adopted in this study to minimise potential errors: Firstly, a comprehensive dataset was gathered from a trifurcated system to smooth inevitable fluctuations. Secondly, collection of data extended over one year to ensure that different environmental conditions are represented in the dataset, thus avoiding seasonal, phytologic, or meteorologic biases. Thirdly, tracer tests were conducted to assess potential hydraulic or hydrodynamic shortcomings of the pilot-scale system.

3. Results and discussion

3.1. Hydraulics

Generally, both settling ponds and wetlands show unimodal, positively skewed breakthrough curves with elongated tails. The tracer tests were terminated after ≈ 192 h to minimise imminent re-cycling of tracer dye to the pilot plant via the Westfields' seepage water distribution system. The lengthy exponential tail of the curves was extrapolated beyond truncation if needed, not only for the sake of completeness but also to ensure a conservative estimate of the median HRT (Headley and Kadlec, 2007). Extrapolation accounted for a small dye fraction only, e.g. an average of 3.4% of total tracer mass for wetlands.

In-depth evaluation revealed significant differences between settling ponds and wetlands. Settling pond RTD curves are characterised by an early tracer peak after only 3 to 11 h that is broadly independent of flow rate, followed by a pronounced tail (Fig. 3a). The shape indicates that part of the dye was transported through advective zones and exited the container early, whereas the remaining dye scattered throughout the container before slowly bleeding out of mixed or stagnant zones. These findings are in accordance with visual observations of the spreading dye.

Wetland RTD curves show a more consistent, "classic" shape (Fig. 3b). Stretching of the curves with decreasing flow rate indicates increased mixing, which is substantiated by a (negative) correlation between flow rate and variance ($R^2=0.80$). Apparently, preferential flow paths that are relevant at higher flow rates are stalled at lower flow rates (Table 1). The tracer peak is observed close to the nominal HRT with t_n/t_p ratios of $0.68(\pm 0.08)$. Visual observations showed effective flow distribution by the dense reed stands with dead zones confined to

Table 1
Tracer test results from the Westfield pilot plant.

Hydraulic characterisation	Unit	Settling pond	Wetland
Tracer injection	n/a	MP01	MP02
Fluorescence monitoring	n/a	MP03	MP05
Number of tracer tests	[-]	5	8
Dye recovery*	[%]	n/a	89(±8)
Flow rates (see Fig. 3)	[L/h]	162 – 519	172 – 500
t_n	[h]	31.7 – 102	14.9 – 43.2
t_p	[h]	3.0 – 11.0	7.5 – 30.8
t_m	[h]	27.5 – 119	13.0 – 68.0
σ	[h]	38.4 – 145	13.2 – 48.0
λ^*	[-]	0.13(±0.06)	0.60(±0.06)

* Average (±SD).

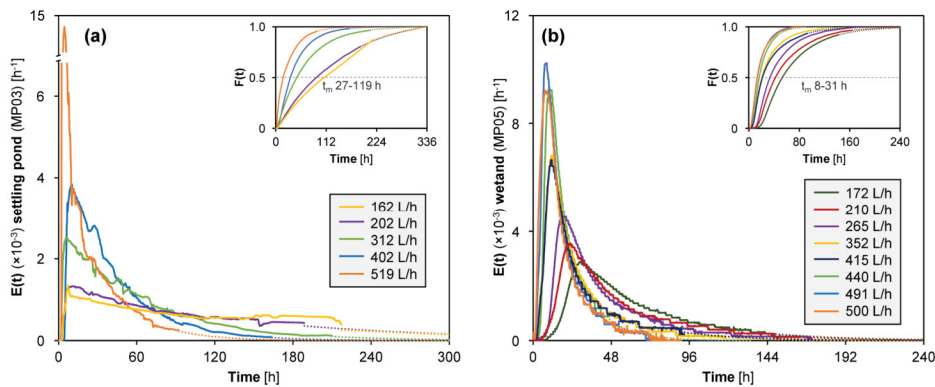


Fig. 3. Normalised RTD curves $E(t)$ at different flow rates with cumulative RTD curves $F(t)$ as small details for (a) settling ponds and (b) wetlands. Extrapolation indicated as dotted lines.

edge areas. Although Rhodamin WT may be lost in wetlands due to sorption or photolysis (Lin et al., 2003), average tracer recovery was around 90%.

Results compiled in Table 1 should be regarded with caution as to potential re-cycling of tracer dye and tailing effects, which was particularly problematic for prolonged tracer retention in settling ponds (Stephenson and Sheridan, 2021). Nevertheless, the tracer tests provide valuable insights into the hydraulics and hydrodynamics of the pilot plant. According to the classification by Persson et al. (1999), hydraulic efficiency was poor in settling ponds and satisfactory in wetlands. Poor settling pond hydraulics are likely attributable to the unfavourable geometry (i.e. low surface-to-depth ratio) that is prone to preferential flow and dead zones (Shih and Wang, 2020). Better wetland hydraulics are likely attributable to the higher surface-to-depth ratio (Shih et al., 2013) and flow distribution by the dense vegetation (Verschoren et al., 2017). Altogether, the hydraulic and hydrodynamic limitations of the Westfield pilot plant prevent a robust linking of temporal Fe removal and RTD (Guo and Cui, 2021; Sheridan et al., 2014; von Sperling, 2002). Consequently, the nominal HRT was used as a simplistic, yet conservative estimate of actual residence time for evaluation of (inversely exponential) $\text{Fe}(\text{OH})_3$ removal because the pre-nominal water portion discharged from the containers is subject to the highest removal rates, whereas the post-nominal water portion is subject to receding removal rates (Sapsford, 2013; Wahl et al., 2010).

3.2. Iron removal

Inflow Fe levels ranged from 2.7 to 14.5 mg/L (average 8.3 ± 2.2 mg/L) in settling ponds and 0.64 to 7.3 mg/L (average 2.4 ± 1.0 mg/L) in subsequent wetlands. Combined with the respective flow rates, Fe loading of settling ponds and wetlands as first to third quartiles ranged from 41.4 to 67.9 and 9.3 to 21.2 g/h, respectively, over the course of the study period. The Westfield pilot plant was successful in reducing effluent Fe levels below the site-specific discharge limit of 1 mg/L (Fig. S1). The excellent treatment performance and operational reliability are attributable to the multistage setup where residual effluent concentrations are reliably polished in the successive stage(s), thus optimising overall treatment performance and mitigating natural performance fluctuations in the open system (Opitz et al., 2022b).

As noted in the introduction, the major Fe removal mechanisms are expected to be nonlinearly correlated with inflow concentration. To examine the relevance of the initial Fe level on removal, the Fe removal rates in settling ponds and wetlands are plotted against the respective initial Fe concentration for all 270 samplings. Both datasets in Fig. 4

show a significant concentration-dependency, with Fe removal rates increasing with increasing initial concentration.

For settling ponds, the concentration-dependency in Fig. 4 may be reasonably well described by a linear regression, although the adumbrated increase of the slope at higher Fe levels could be indicative of a transition from settling- to aggregation-driven Fe removal as suggested by the mixed model in Eq. (4). Unfortunately, the range of inflow Fe concentrations (max. 14.5 mg/L) is insufficient for respective in-depth evaluation. Interestingly, the x-intercept of the regression at ≈ 1.5 mg/L indicates that sedimentation-based Fe removal in settling ponds is inherently limited at residual Fe levels, which corresponds with similar observations in the preceding sedimentation experiments where a residual colloidal fraction remained suspended for long time spans (Opitz et al., 2022a).

For wetlands, the concentration-dependency in Fig. 4 is best described by a superlinear regression, implying that Fe removal in densely vegetated wetlands follows a more complex overall mechanism compared to bare settling ponds. The multicausal polishing process may include, but not be limited to sedimentation, filtration, adsorption and heteroaggregation (Verschoren et al., 2017). Hence, there is good reason to assume that Fe removal in wetlands is inadequately described by the same sedimentation model approach as in bare settling ponds. It is, however, interesting to note that the regression asymptotically approaches the origin, illustrating that wetlands (in contrast to settling ponds) are effective in retaining even finely dispersed, residual colloids in the dense hydrophyte stands. Altogether, the direct juxtaposition of both treatment stages highlights the superior treatment efficiency of densely vegetated wetlands relative to (unvegetated) settling ponds, especially for polishing at low Fe levels.

A tentative indication of the order of Fe removal can be obtained by the double-logarithmic plot of Fe removal rates vs. initial Fe concentration in Fig. 5. For settling ponds, the plot provides limited information due to the relatively stable inflow Fe level from the reservoir with 50% of datapoints clustered between 7.2 and 9.6 mg/L. Nevertheless, the slope in the order of 1.3 indicates that Fe removal may be reasonably well approximated by the simplified first-order model at low to moderate Fe levels such as observed in the Westfield pilot plant. Moreover, it is conceivable that the slope of 1.3 may in fact split in slopes of 1 (sedimentation-driven) and 2 (aggregation-driven) at lower and higher Fe levels, respectively, as observed in the preceding column experiments; yet again, Fig. 5 gives no indication of the development of Fe removal kinetics at higher initial Fe levels and thus no empirical confirmation of the aggregation-driven increase of Fe removal dynamics. Evaluation of the settling ponds' dataset for first-order removal

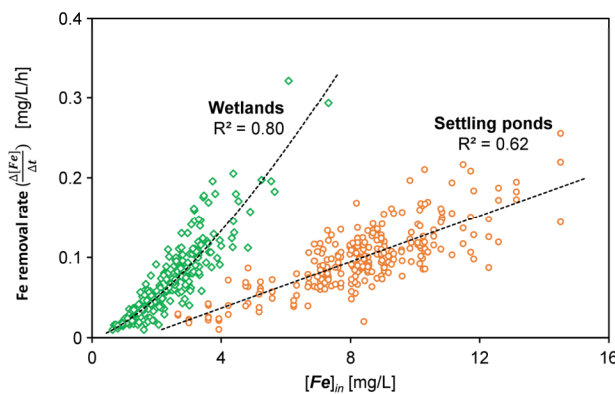


Fig. 4. Correlation of Fe removal rates as $\Delta[\text{Fe}]/\Delta t$ and inflow Fe concentration in settling ponds (orange circles) and wetlands (green diamonds) with overall regressions as dashed lines.

J. Opitz et al.

Water Research 233 (2023) 119770

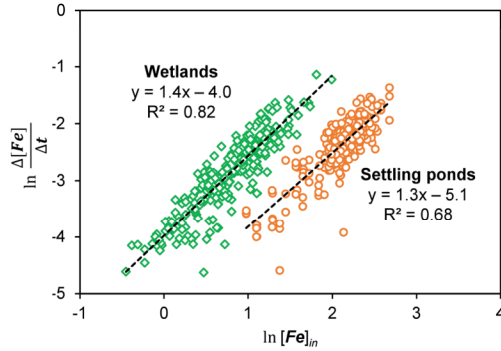


Fig. 5. Double-logarithmic plot of Fe removal rates vs. initial Fe concentration in settling ponds (orange circles) and wetlands (green diamonds) with dashed lines indicating slopes.

via Eq. (14) yields an overall coefficient k_{sed} of $2.1(\pm 0.7) \times 10^{-2} \text{ h}^{-1}$ (Fig. S1a), which corresponds well with initial laboratory findings noted in the introduction. The spread in k_{sed} is attributable to a slight concentration-dependency, which is in accordance with the preceding column experiments that showed a similar effect due to receding homoaggregation of dispersed Fe at lower Fe levels (Opitz et al., 2022a).

In wetlands, the complexity of Fe removal is substantiated by both the double-logarithmic plot in Fig. 5 which clearly shows a broken-order relationship over the dataset, and by the scattering observed in Fig. S1b for the coefficient k_{sed} as evaluated on a trial basis via Eq. (14). As Fe removal in wetlands should also be expected to vary depending on ecological factors (macrophyte species, plant density, water depth, etc.), we propose to advance the established areal sizing approach by incorporating the concentration-dependency empirically determined in this study rather than trying to establish an overall kinetic equation for the multicausal process. To parameterise the extended areal Fe removal model, the removal rates in Fig. 4 were converted to areal Fe removal rates following Eq. (13). The concentration-dependency of R_A for the pilot-scale wetlands was fitted as $R_A = m \times [Fe]_{in}^n$ with $m = 0.2$ and $n = 1.4$ as illustrated by the superlinear regression in Fig. S2b.

3.3. Comparison with literature data

In order to compare the Westfield pilot plant data with literature data, the area-adjusted Fe removal rates from Tab. S2 are compared to the converted areal Fe removal rates from this study from Fig. S2. All passive systems compiled in Tab. S2 were implemented at (abandoned) coal mines in the Anglo-American area for treatment of ferruginous, weakly acidic to weakly alkaline mine water (pH-range 4.7 to 8.1). It should be noted that the literature reports are often individual measurements rather than robust, aggregated long-term monitoring data and should thus be treated with caution.

For settling ponds, the literature data corresponds reasonably well with the relationship derived in this study, especially at low and moderate inflow Fe levels. This is somewhat surprising considering the wide range of pond configurations, ferrous-ferric ratios, and pH of the literature data. Notably, settling ponds with higher inflow Fe levels display higher areal Fe removal rates relative to the (extrapolated) relationship, presumably owing to homoaggregation effects as demonstrated in the preceding column experiments (Opitz et al., 2022a). The three outliers marked in Fig. 6a correspond to exceptionally deep settling ponds ($z \geq 2.5 \text{ m}$), indicating a maximised residence time per unit area. Such mass flux effects are altogether disregarded by an area-based approach. Further evaluation of $Fe(OH)_3$ removal kinetics from the data in Tab. S2a is precluded by missing data on HRT and/or pond geometry as well as the usually large $Fe(II)$ fraction in the inflow.

For wetlands, an inconclusive pattern is observed in Fig. 6b with literature reports scattered both below and above the relationship from this study, largely well below the established sizing criteria. The main difficulty in comparing and evaluating wetland performance is the heterogeneity in not only mine water chemistry (pH, Fe loading, ferrous-ferric-ratio, etc.), but also wetland configuration (shape, water depth, substrate amendment, macrophyte species, plant density, hydraulic efficiency, etc.) as noted in respective surveys (e.g., Cravotta and Brady, 2015; Stark and Williams, 1995; Tarutis et al., 1999; Wieder, 1989). The concentration-dependant relationship developed in this study applies to polishing of residual, colloidal Fe from pre-treated ferruginous mine water in relatively deep, reed-planted wetlands and is, to the best of our knowledge, the first such relationship developed for mine water treatment wetlands.

3.4. Simulation of iron removal in full-scale settling ponds

Coupling of contaminant removal and (retention) time is increasingly used to model Fe transport, transformation, and removal in mining-impacted waters (e.g., Baken et al., 2015; Cravotta, 2021;

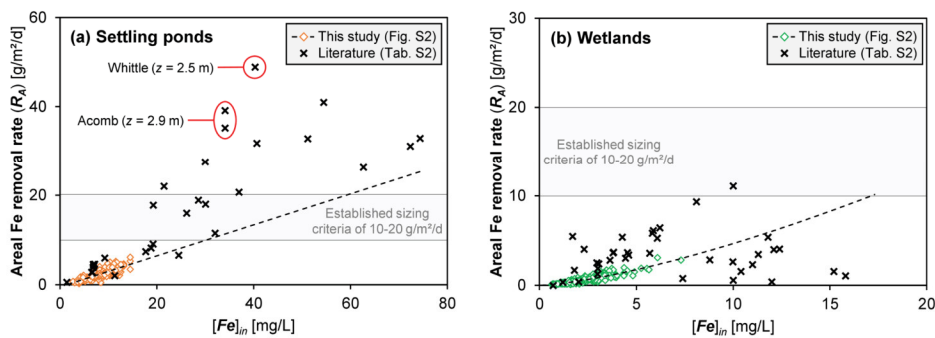


Fig. 6. Correlation of area-adjusted Fe removal (R_A) and inflow Fe concentration in (a) settling ponds and (b) wetlands, with results of this study as coloured diamonds and dashed (extrapolated) regression lines, and literature data from Tab. S2 as black crosses.

J. Oplitz et al.

Water Research 233 (2023) 119770

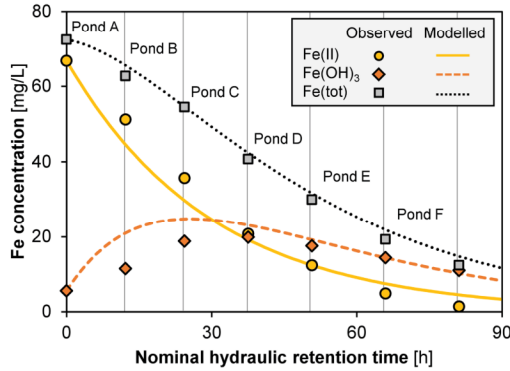


Fig. 7. Development of Fe concentration throughout the Marchand settling ponds A to F as a function of nominal HRT with symbols as Fe concentrations reported by Hedín (2013) and modelled lines.

García-Ríos et al., 2021; Yazbek et al., 2021). As noted above, in-depth evaluation of passive Fe removal in full-scale treatment systems regarding the underlying kinetics is, however, generally limited because only inflow and outflow datapoints are available.

Having said that, the Marchand system in Pennsylvania listed in Tab. S2 is one of the largest and best-characterised passive mine water treatment systems worldwide, consisting of six consecutive settling ponds (A to F) with a combined surface area of ≈ 2.5 ha followed by a ≈ 2.9 ha wetland (Hedín, 2008). According to long-term monitoring data from 2007 to 2012, the circumneutral and highly ferruginous discharge from the abandoned Marchand coal mine is estimated at an average $426 \text{ m}^3/\text{h}$ with an inflow Fe concentration of 72.4 mg/L that is successfully lowered below the discharge limit of 3 mg/L (Hedín, 2013). The intermediate sampling points of the consecutive settling ponds provide a rare opportunity to model the underlying Fe removal kinetics by relative least-square fitting of the concentration development along the flow path (Fig. 7).

Based on nominal HRT of the settling ponds and assuming $\geq 80\%$ oxygen saturation as well as a moderate (average) temperature of $\approx 10^\circ\text{C}$, k'_{ox} was fitted at $3.3 \times 10^{-2} \text{ h}^{-1}$, which corresponds to a pH of ≈ 6.7 . This accords well with the pH (range 6.3 to 7.1) and temperature (annual average 13 to 14°C) reported by Hedín (2008). The first-order coefficient k'_{sed} was fitted at $3.8 \times 10^{-2} \text{ h}^{-1}$, exceeding estimates from this study and thus substantiating the general impression from Fig. 6a as further discussed below. Altogether, the kinetics-based model approach works quite well to reproduce the observed Fe concentration levels, especially considering the fluctuation of critical parameters (flow rate, inflow Fe, HRT, etc.) as reported by Hedín (2008, 2013).

4. Implications

4.1. Rate-determining iron removal processes

As noted in the introduction, research on Fe removal in passive mine water treatment systems initially focussed on Fe(II) oxidation as the (assumed) rate-determining step (e.g., Kirby et al., 1999; Tarutis et al., 1999). While this is certainly applicable in acidic mine drainage, Fe(II) oxidation in circumneutral mine water occurs demonstrably rapid Dietz and Dempsey, 2017). Therefore, it is assumed that Fe(II) oxidation is only rate-determining for unfavourable conditions such as acidic pH, suboxic conditions, or low temperatures (e.g., Flanagan et al., 1994; Hedín, 2008; Sapsford, 2013). Based on the results of this study, we are now able to approximatively delineate the rate-determining Fe removal process at moderate Fe levels. To that end, overall Fe removal via

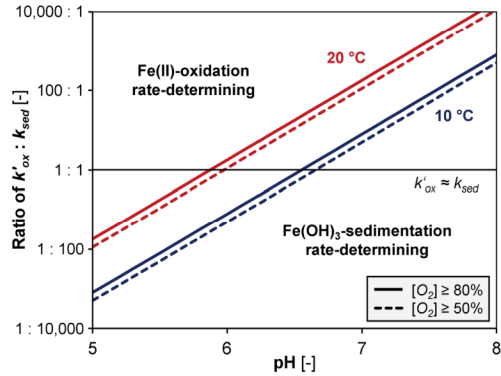


Fig. 8. Ratio of (pseudo) first-order Fe(II)-oxidation and Fe(OH)₃-sedimentation coefficients k'_{ox} and k'_{sed} as a semi-logarithmic function of pH at different temperature and oxygen saturation levels.

consecutive Fe(II) oxidation and Fe(OH)₃ sedimentation is analytically described by coupled integration of Eqs. (2) and (3) with:

$$[Fe]_{out} = [Fe(II)]_{in} \times e^{-k'_{ox} \times t} + \frac{k'_{ox} \times [Fe(II)]_{in} \times (e^{-k'_{ox} \times t} - e^{-k'_{sed} \times t})}{k'_{sed} - k'_{ox}} + [Fe(OH)_3]_{in} \times e^{-k'_{sed} \times t}. \quad (15)$$

For two consecutive processes of first order, the process with the smaller reaction constant is considered rate limiting (Capellos and Bielski, 1980). As k'_{ox} increases hundredfold with a pH-increase by one unit, the pH is ultimately the critical parameter (Stumm and Morgan, 1996). As illustrated in Fig. 8, Fe(II) oxidation is rate-determining for overall Fe removal under acidic conditions (pH < 6) whereas Fe(OH)₃ sedimentation becomes rate-determining under neutral or alkaline conditions (pH > 7) as previously suggested by Sapsford (2013). The two processes are roughly equally paced at weakly acidic conditions (pH 6 to 7) where k'_{ox} and k'_{sed} converge, and where variations in pH, temperature, or oxygenation may play a critical role.

4.2. Transferability

The model approaches developed in this study were derived from and tailored to the site-specific challenges and boundary conditions of the Westfield site – i.e. a fully oxygenated, moderately ferruginous seepage water subject to a strict Fe discharge limit. This starting situation differs from “classic” coal mine discharges that often exhibit high (ferrous) Fe levels and moderate Fe discharge limits. Therefore, the model approaches developed in this study explicitly provide a conservative basis for sizing of settling ponds and wetlands in integrated passive systems, focussing on low to moderate Fe levels and aiming at utmost operational reliability in due consideration of strict discharge permit criteria.

In this context, it is important to note that the kinetics-based model approach for settling ponds (oxidation and/or sedimentation) as combined in Eq. (15) disregards any catalytic effects such as heterogeneous Fe(II)-oxidation (Dietz and Dempsey, 2017), aggregation-driven Fe(OH)₃ sedimentation (Chikanda et al., 2021), or biogeochemical processes (Kappler et al., 2021; Melton et al., 2014). Therefore, the simplified model is expected to underestimate overall Fe removal at higher Fe levels. By way of example, the elevated k'_{sed} fitted in Fig. 7 is likely attributable to the much higher Fe level throughout the Marchand system where Fe(OH)₃ is expected to peak at $\approx 25 \text{ mg/L}$ after $\approx 24 \text{ h}$ in settling ponds B and C, providing sufficient dispersed solids for aggregation-driven sedimentation.

The tendency of the model approaches developed in this study to underestimate overall Fe removal dynamics by either disregarding or simplifying catalytic effects is – to a certain extent – intentional and imperative, not only for the sake of simplification but also because engineering model approaches are expected to intrinsically err on the conservative side to avoid operational failure and resultant pollution of receiving surface waters. This is particularly important in light of the complex interrelation of Fe(II) oxidation dynamics with gas transfer processes (O₂ diffusion and CO₂ degassing), aggregation-driven Fe(OH)₃ sedimentation, and actual RTD in passive systems as demonstrated by Dempsey et al. (2001). These aspects could not be investigated at the Westfield site due to the seepage water chemistry and should thus be the focus of future studies on full-scale systems to optimise the model approaches developed in this study.

5. Conclusions and outlook

In light of the contemporary spreading of passive technologies whilst also tightening of environmental regulations worldwide, it is inalienable to advance the sizing of passive mine water treatment systems. The insights and (quantitative) results from the Westfield pilot plant provide a novel scientific and technical basis for customised sizing of settling ponds and wetlands in due consideration of Fe removal kinetics. For settling ponds, we propose utilising a kinetics-based model approach for approximation of sedimentation-driven Fe(OH)₃ removal:

$$A = \frac{Q \times (\ln[Fe]_{out} - \ln[Fe]_{in})}{-k_{sed} \times z} \quad (16)$$

The first-order sedimentation coefficient k_{sed} from the pilot-scale settling ponds of $2.1(\pm 0.7) \times 10^{-2} \text{ h}^{-1}$ corresponds well with previous laboratory reports. The approach may be extended to further consider the preceding Fe(II) oxidation step according to Eq. (15), with only a small set of standard input parameters (Fe concentration, flow rate, pH) and simplifying assumptions (e.g. moderate temperature, steady pH) as well as technical pre-conditions (e.g. pre-aeration, sound hydraulic design) required to estimate the necessary HRT and thus pond size for overall Fe removal. The kinetics-based model approach provides a more realistic sizing foundation compared to assignment of a flat HRT or areal Fe removal rate, especially at low to moderate Fe levels that are ultimately relevant for strict discharge criteria.

For wetlands, we propose to advance the established area-adjusted sizing approach in Eq. (1) by incorporating the concentration-dependency parameterised in this study. Such practical simplification of complex, natural mitigation processes is common in the field of (waste)water treatment where sizing of engineered systems is typically achieved by conservative, empirical criteria:

$$A = \frac{Q \times ([Fe]_{in} - [Fe]_{out})}{m \times [Fe]_{in}^n} \quad (17)$$

The coefficients m and n were empirically determined as 0.2 and 1.4, respectively, for reliable polishing of finely dispersed, colloidal Fe in dense reed stands following pre-treatment in settling ponds. Under these conditions, the extended areal approach provides a more realistic approximation of the complex sedimentation and filtration mechanisms compared to the established, linear approach.

Finally, Eqs. (16) and (17) show that the pond or wetland size is expected to be linearly correlated with flow rate, whereas Fe removal per unit area exponentially increases with increasing Fe concentration. Therefore, dilution or blending of mine discharges should generally be avoided to minimise not only pollutant dispersion, but also the overall effort (and land consumption) of passive mine water treatment.

Funding

The study was conducted as part of a research project funded by the

German Federal Environmental Foundation (project no. 33,012/01–23).

Disclosures

The study was supported by Uniper Kraftwerke GmbH by providing administrative support and access to the study site. Uniper had no role in the study design or research.

Declaration of Competing Interest

The authors declare the following financial interests/personal relationships which may be considered as potential competing interests: Joscha Opitz, Martin Bauer, and Matthias Alte report administrative support was provided by Uniper Kraftwerke GmbH. Joscha Opitz, Martin Bauer, and Matthias Alte report a relationship with Uniper Kraftwerke GmbH that includes: consulting or advisory.

Data availability

Data will be made available on request.

Acknowledgement

The study was conducted as part of a research project funded by the German Federal Environmental Foundation (project no. 33012/01–23). We owe special thanks to Jutta Eckert for her tireless dedication and assistance during field and laboratory work.

Supplementary materials

Supplementary material associated with this article can be found in the online version, at doi:10.1016/j.watres.2023.119770.

References

- Baken, S., Salaets, P., Desmet, N., Seuntjens, P., Vanlierde, E., Smolders, E., 2015. Oxidation of iron causes removal of phosphorus and arsenic from stream water in groundwater-fed lowland catchments. *Environ. Sci. Technol.* 49, 2886–2894. <https://doi.org/10.1021/es505834y>.
- Banks, S., 2003. The UK Coal Authority minewater treatment scheme programme: performance of operational systems. *Water Environ. J.* 17, 117–122. <https://doi.org/10.1111/j.1747-6593.2003.tb00444.x>.
- Bodin, H., Mietto, A., Ehde, P., Persson, J., Weisner, S., 2012. Tracer behaviour and analysis of hydraulics in experimental free water surface wetlands. *Ecol. Eng.* 49, 201–211. <https://doi.org/10.1016/j.ecoleng.2012.07.009>.
- Braskerud, B., 2001. The influence of vegetation on sedimentation and resuspension of soil particles in small constructed wetlands. *J. Environ. Qual.* 30, 1447–1457. <https://doi.org/10.2134/jeq2001.3041447x>.
- Capellos, C., Bielski, B., 1980. *Kinetic Systems: Mathematical Description of Chemical Kinetics in Solution*. Robert Krieger Publishing.
- Chang, T., Chang, Y., Lee, W., Shih, S., 2016. Flow uniformity and hydraulic efficiency improvement of deep-water constructed wetlands. *Ecol. Eng.* 92, 28–36. <https://doi.org/10.1016/j.ecoleng.2016.03.028>.
- Chikanda, F., Otake, T., Koide, A., Ito, A., Sato, T., 2021. The formation of Fe colloids and layered double hydroxides as sequestration agents in the natural remediation of mine drainage. *Sci. Total Environ.* 774, 145183 <https://doi.org/10.1016/j.scitotenv.2021.145183>.
- Cravotta, C., 2021. Interactive PHREEQ-N AMDTreat water-quality modeling tools to evaluate performance and design of treatment systems for acid mine drainage. *Appl. Geochem.* 126, 104845 <https://doi.org/10.1016/j.apgeochem.2020.104845>.
- Cravotta, C., Brady, K., 2015. Priority pollutants and associated constituents in untreated and treated discharges from coal mining or processing facilities in Pennsylvania. *USA. Appl. Geochem.* 62, 108–130. <https://doi.org/10.1016/j.apgeochem.2015.03.001>.
- Dempsey, B., Roscoe, H., Ames, R., Hedin, R., Jeon, B., 2001. Ferrous oxidation chemistry in passive abiotic systems for the treatment of mine drainage. *Geochem. Explor. Environ. Anal.* 1, 81–88. <https://doi.org/10.1144/geochem.1.1.81>.
- Dietz, J., Dempsey, B., 2017. Heterogeneous oxidation of Fe(II) in AMD. *Appl. Geochem.* 81, 90–97. <https://doi.org/10.1016/j.apgeochem.2017.04.003>.
- Flanagan, N., Mitsch, W., Beach, K., 1994. Predicting metal retention in a constructed mine drainage wetland. *Ecol. Eng.* 3, 135–159. [https://doi.org/10.1016/0925-8574\(94\)90042-6](https://doi.org/10.1016/0925-8574(94)90042-6).
- García-Ríos, M., de Windt, L., Lugot, L., Cadiot, C., 2021. Modeling of microbial kinetics and mass transfer in bioreactors simulating the natural attenuation of arsenic and

- iron in acid mine drainage. *J. Hazard. Mater.* 405, 124133 <https://doi.org/10.1016/j.jhazmat.2020.124133>.
- Guo, C., Cui, Y., 2021. Improved solute transport and pollutant degradation model of free water surface constructed wetlands considering significant linear correlation between model parameters. *Bioresour. Technol.* 327, 124817 <https://doi.org/10.1016/j.biortech.2021.124817>.
- Headley, T., Kadlec, R., 2007. Conducting hydraulic tracer studies of constructed wetlands: a practical guide. *Ecol. Hydrobiol.* 7, 269–282. [https://doi.org/10.1016/S1642-3593\(07\)70110-6](https://doi.org/10.1016/S1642-3593(07)70110-6).
- Hedin, R., 2008. Iron removal by a passive system treating alkaline coal mine drainage. *Mine Water Environ.* 27, 200–209. <https://doi.org/10.1007/s10230-008-0041-9>.
- Hedin, R., 2013. Temperature independent removal of iron in a passive mine water system. In: *Proc. IMWA Conf.*, pp. 599–604.
- Hedin, R., Nairn, R., Kleinmann, R., 1994. *Passive Treatment of Coal Mine Drainage*. US Bureau of Mines. Information Circular 9389.
- Hove, M., van Hille, R., Lewis, A., 2008. Mechanisms of formation of iron precipitates from ferrous solutions at high and low pH. *Chem. Eng. Sci.* 63, 1626–1635. <https://doi.org/10.1016/j.ces.2007.11.016>.
- Johnson, D., Hallberg, K., 2002. Pitfalls of passive mine water treatment. *Rev. Environ. Sci. Biotechnol.* 1, 335–343. [https://doi.org/10.1016/0925-8574\(94\)90042-6](https://doi.org/10.1016/0925-8574(94)90042-6).
- Kadlec, R., Wallace, S., 2009. *Treatment Wetlands*, 2nd Ed. CRC Press.
- Kappler, A., Bryce, C., Mansor, M., Lueder, U., Byrne, J., Swanner, E., 2021. An evolving view on biogeochemical cycling of iron. *Nat. Rev. Microbiol.* 19, 360–374. <https://doi.org/10.1038/s41579-020-00502-7>.
- Kirby, C., Thomas, H., Southam, G., Donald, R., 1999. Relative contributions of abiotic and biological factors in Fe(II) oxidation in mine drainage. *Appl. Geochem.* 14, 511–530. [https://doi.org/10.1016/S0883-2927\(98\)00071-7](https://doi.org/10.1016/S0883-2927(98)00071-7).
- Kruse, N., Gozzard, E., Jarvis, A., 2009. Determination of hydraulic residence times in several UK mine water treatment systems and their relationship to iron removal. *Mine Water Environ.* 28, 115–123. <https://doi.org/10.1007/s10230-009-0068-6>.
- Lin, A., Debroux, J., Cunningham, J., Reinhard, M., 2003. Comparison of Rhodamine WT and bromide in the determination of hydraulic characteristics of constructed wetlands. *Ecol. Eng.* 20, 75–88. [https://doi.org/10.1016/S0925-8574\(03\)00005-3](https://doi.org/10.1016/S0925-8574(03)00005-3).
- Mayes, W., Batty, L., Younger, P., Jarvis, A., Koiv, M., Vohla, C., Mander, U., 2009. Wetland treatment at extremes of pH. *Sci. Total Environ.* 407, 3944–3957. <https://doi.org/10.1016/j.scitotenv.2008.06.045>.
- Melton, E., Swanner, E., Behrens, S., Schmidt, C., Kappler, A., 2014. The interplay of microbially mediated and abiotic reactions in the biogeochemical Fe cycle. *Nat. Rev. Microbiol.* 12, 797–808. <https://doi.org/10.1038/nrmicro3347>.
- Millero, F., Sorolongo, S., Izaguirre, M., 1987. The oxidation kinetics of Fe(II) in seawater. *Geochim. Cosmochim. Acta* 51, 793–801. [https://doi.org/10.1016/0016-7037\(87\)90993-7](https://doi.org/10.1016/0016-7037(87)90993-7).
- National Coal Board, 1982. *Technical Management of Water in the Coal Mining Industry*. Westminster Press.
- Opitz, J., Alte, M., Bauer, M., Peiffer, S., 2020. Quantifying iron removal efficiency of a passive mine water treatment system using turbidity as a proxy for (particulate) iron. *Appl. Geochem.* 122, 104731. <https://doi.org/10.1016/j.apgeochem.2020.104731>.
- Opitz, J., Alte, M., Bauer, M., Peiffer, S., 2021. The role of macrophytes in constructed surface flow wetlands for mine water treatment: a review. *Mine Water Environ.* 40, 587–605. <https://doi.org/10.1007/s10230-021-00779-x>.
- Opitz, J., Bauer, M., Alte, M., Schmidtmann, J., Peiffer, S., 2022a. Sedimentation kinetics of hydrous ferric oxides in ferruginous, circumneutral mine water. *Environ. Sci. Technol.* 56, 6360–6368. <https://doi.org/10.1021/acs.est.1c07640>.
- Opitz, J., Bauer, M., Eckert, J., Peiffer, S., Alte, M., 2022b. Optimising operational reliability and performance in aerobic passive mine water treatment: the multistage Westfield pilot plant. *Water Air Soil Pollut.* 233, 66. <https://doi.org/10.1007/s11270-022-05538-4>.
- Parker, K., 2003. Mine water management on a national scale – experiences from the coal authority. *Land Contam. Reclam.* 11, 181–190. <https://doi.org/10.2462/09670513.813>.
- Persson, J., Somes, N., Wong, T., 1999. Hydraulic efficiency of constructed wetlands and ponds. *Water Sci. Technol.* 40, 291–300. [https://doi.org/10.1016/S0273-1223\(99\)00448-5](https://doi.org/10.1016/S0273-1223(99)00448-5).
- Philips, N., Heyvaerts, S., Lammens, K., van Impe, J., 2005. Mathematical modelling of small wastewater treatment plants: power and limitations. *Water Sci. Technol.* 51, 47–54. <https://doi.org/10.2166/wst.2005.0350>.
- PIRAMID Consortium, 2003. *Engineering Guidelines For the Passive Remediation of Acidic And/Or Metalliferous Mine Drainage and Similar Wastewaters*. EC research project EVK1-CT-1999-000021.
- Sapsford, D., 2013. New perspectives on the passive treatment of ferruginous circumneutral mine waters in the UK. *Environ. Sci. Pollut. Res.* 20, 7827–7836. <https://doi.org/10.1007/s11356-013-1737-3>.
- Sapsford, D., Watson, I., 2011. A process-oriented design and performance assessment methodology for passive mine water treatment systems. *Ecol. Eng.* 37, 970–975. <https://doi.org/10.1016/j.ecoleng.2010.12.010>.
- Sheridan, C., Glasser, D., Hildebrandt, D., 2014. Estimating rate constants of contaminant removal in constructed wetlands treating winery effluent: a comparison of three different methods. *Process Saf. Environ. Prot.* 92, 903–916. <https://doi.org/10.1016/j.psep.2013.09.004>.
- Shih, S., Wang, H., 2020. Flow uniformity metrics for quantifying the hydraulic and treatment performance of constructed wetlands. *Ecol. Eng.* 155, 105942 <https://doi.org/10.1016/j.ecoleng.2020.105942>.
- Shih, S., Kuo, P., Fang, W., LePage, B., 2013. A correction coefficient for pollutant removal in free water surface wetlands using first-order modelling. *Ecol. Eng.* 61, 200–206. <https://doi.org/10.1016/j.ecoleng.2013.09.054>.
- Skousen, J., Rose, A., Geidel, G., Foreman, J., Evans, R., Hellier, W., 1998. *A handbook of technologies for avoidance and remediation of acid mine drainage*. Acid Mine Drainage Initiative.
- Skousen, J., Zipper, C., Rose, A., Ziemkiewicz, P., Nairn, R., McDonald, L., Kleinmann, R., 2017. Review of passive systems for acid mine drainage treatment. *Mine Water Environ.* 36, 133–153. <https://doi.org/10.1007/s10230-016-0417-1>.
- Smart, P., Laidlaw, I., 1977. An evaluation of some fluorescent dyes for water tracing. *Water Resour. Res.* 13, 15–33. <https://doi.org/10.1029/WR013001p00015>.
- von Sperling, M., 2002. Relationship between first-order decay coefficients in ponds, for plug flow, CSTR and dispersed flow regimes. *Water Sci. Technol.* 45, 17–24. <https://doi.org/10.2166/wst.2002.0003>.
- Stark, L., Williams, F., 1995. Assessing the performance indices and design parameters of treatment wetlands for H⁺, Fe, and Mn retention. *Ecol. Eng.* 5, 433–444. [https://doi.org/10.1016/0925-8574\(95\)00008-9](https://doi.org/10.1016/0925-8574(95)00008-9).
- Stephenson, R., Sheridan, C., 2021. Review of experimental procedures and modelling techniques for flow behaviour and their relation to residence time in constructed wetlands. *J. Water Process. Eng.* 41, 102044 <https://doi.org/10.1016/j.jwpe.2021.102044>.
- Stumm, W., Morgan, J., 1996. *Aquatic Chemistry: Chemical Equilibria and Rates in Natural Waters*, 3rd Ed. Wiley Interscience.
- Sutton, A., Sapsford, D., Moorhouse, A., 2015. *Mine water treatability studies for passive treatment of coal mine drainage*. In: *Proc. 10th ICARD & IMWA Annual Conf.*
- Tarulis, W., Stark, L., Williams, F., 1999. Sizing and performance estimation of coal mine drainage wetlands. *Ecol. Eng.* 12, 353–372. [https://doi.org/10.1016/S0925-8574\(98\)00114-1](https://doi.org/10.1016/S0925-8574(98)00114-1).
- Verschoren, V., Schoelnyck, J., Cox, T., Schoutens, K., Temmerman, S., Meire, P., 2017. Opposing effects of aquatic vegetation on hydraulic functioning and transport of dissolved and organic particulate matter in lowland river: a field experiment. *Ecol. Eng.* 105, 221–230. <https://doi.org/10.1016/j.ecoleng.2017.04.064>.
- Wahl, M., Brown, L., Soboyajo, A., Martin, J., Dong, B., 2010. Quantifying the hydraulic performance of treatment wetlands using the moment index. *Ecol. Eng.* 36, 1691–1699. <https://doi.org/10.1016/j.ecoleng.2010.07.014>.
- Watzlaf, G., Schroeder, K., Kleinmann, R., Kairies, C., Nairn, R., 2004. *The Passive Treatment of Coal Mine Drainage*. DOE/NETL-2004/1202.
- Wieder, R., 1989. A survey of constructed wetlands for acid coal mine drainage treatment in the eastern United States. *Wetlands* 9, 299–315. <https://doi.org/10.1007/BF03160750>.
- Yazbek, L., Cole, K., Sheddleski, A., Singer, D., Herndon, E., 2021. Hydrogeochemical processes limiting aqueous and colloidal Fe export in a headwater stream impaired by acid mine drainage. *ACS ES&T Water* 1, 68–78. <https://doi.org/10.1021/acsestwater.0c00002>.
- Younger, P., 2000. The adoption and adaptation of passive treatment technologies for mine waters in the United Kingdom. *Mine Water Environ.* 19, 84–97. <https://doi.org/10.1007/BF02687257>.

SUPPORTING INFORMATION

Development of a novel sizing approach for passive mine water treatment systems based on ferric iron sedimentation kinetics

Joscha Opitz^{a,b,*}, Martin Bauer^b, Matthias Alte^b, Stefan Peiffer^a

^a Department of Hydrology, University of Bayreuth, Bayreuth Center for Ecology and Environmental Research (BayCEER), Universitätsstraße 30, D-95447 Bayreuth, Germany

^b BASE Technologies GmbH, D-81241 Munich, Germany

* Corresponding author: joscha.opitz@uni-bayreuth.de

Published: Water Research
DOI: <https://doi.org/10.1016/j.watres.2023.119770>
Article Number: 119770

Received: October 20, 2022
Revised: February 13, 2023
Accepted: February 21, 2023

Number of Pages: 8
Supporting Figures: 2
Supporting Tables: 3

SUPPORTING FIGURES

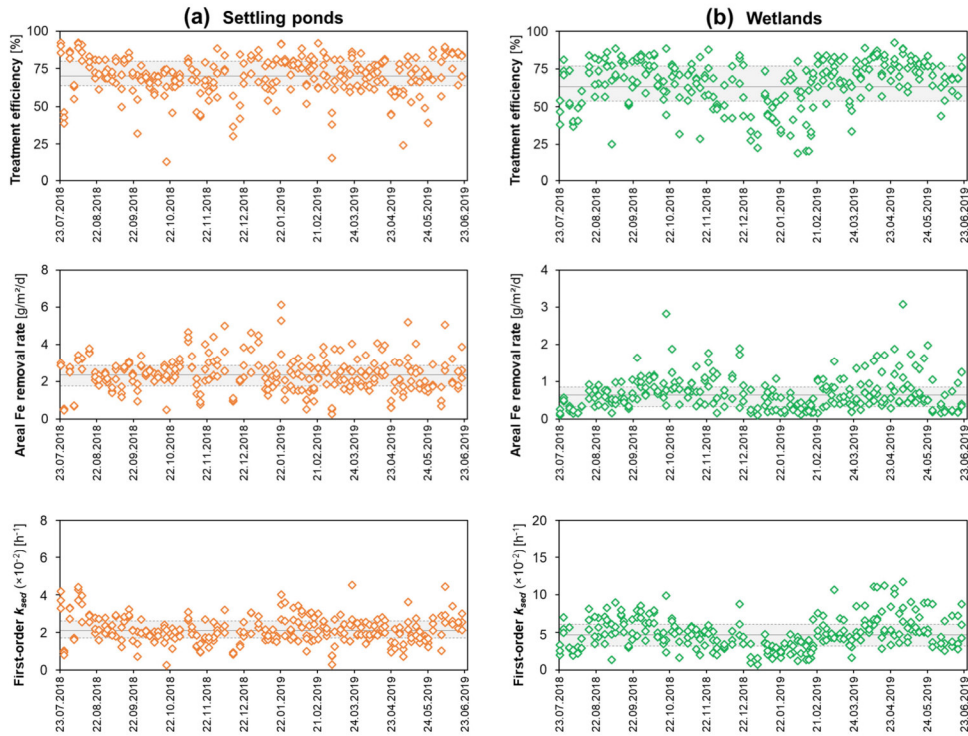


Figure S1. Temporal development of treatment efficiency, area-adjusted Fe removal (R_A) and first-order Fe removal coefficients (k_{sec}) in (a) settling ponds and (b) wetlands, with solid lines as averages and dashed lines as first and third quartiles ($n=270$).

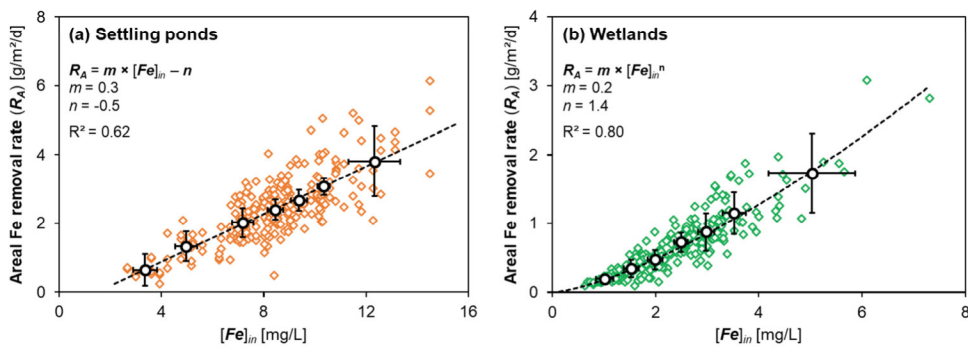


Figure S2. Correlation of area-adjusted Fe removal rates (R_A) with inflow Fe concentration in (a) settling ponds and (b) wetlands, with overall regression as dashed lines. To illustrate clustering effects, the data is aggregated in inflow Fe intervals with similar numbers of datapoints as black circles with standard deviation as error bars.

SUPPORTING TABLES

Table S1. Compilation of the most common sizing approaches for (a) settling ponds and (b) constructed surface-flow wetlands.

Approach	Sizing equation*	Sizing criteria	References
(a) Settling ponds			
Hydraulic loading	$A = Q \times R_A$	With $R_A = 100 \text{ m}^2/\text{L/s} \approx 1.2 \text{ m}^2/\text{m}^3/\text{d}$ (overflow rate of $1 \times 10^5 \text{ m/s}$)	[27]
Areal removal	$A = \frac{Q \times [\text{Fe}]_{\text{in}}}{R_A}$	With $R_A = 10\text{-}20 \text{ g/m}^2/\text{d}$ (analogous to wetlands)	[15]
Concentration-dependent	$A = \frac{Q \times \tau \times (1 + R_A)}{z}$	With $\tau = 1 \text{ d}$ and $R_A = 1$ per every 30 mg/L of Fe(II)	[27],[29]
Hydraulic retention time	$A = \frac{Q \times \tau}{z}$	With $\tau = 8\text{-}48 \text{ h} \approx 0.3\text{-}2 \text{ d}$	[22],[30],[37],[41]
(b) Constructed surface-flow wetlands			
Hydraulic loading	$A = Q \times R_A$	With $R_A \approx 300 \text{ m}^2/\text{L/s} \approx 3.4 \text{ m}^2/\text{m}^3/\text{d}$ at $Q \approx 27\text{-}55 \text{ m}^3/\text{d}$, $\text{pH} > 4$, $[\text{Fe}]_{\text{in}} < 50 \text{ mg/L}$	[18],[19]
Hydraulic retention time	$A = \frac{Q \times \tau}{z}$	With $\tau \geq 1 \text{ d}$ at $z \leq 0.3 \text{ m}$	[8]
Hydraulic loading	$A = Q \times \tau$	Acidic pH: With $\tau = 1 \text{ d}$ (max. flow velocity 0.4 m/d) Alkaline pH: With $\tau = 0.3 \text{ d}$ (max. flow velocity 1.0 m/d)	[8]
Hydraulic loading	$A = Q \times R_A$	With $R_A = 20 \text{ m}^2/\text{m}^3/\text{d}$	[8],[16]
Areal removal	$A = \frac{Q \times [\text{Fe}]_{\text{in}}}{R_A}$	Acidic pH: With $R_A = 4 \text{ g/m}^2/\text{d}$ at $\text{pH} 3$ and $10 \text{ g/m}^2/\text{d}$ at $\text{pH} 4$ Acidic/neutral pH: With $R_A = 2\text{-}4 \text{ g/m}^2/\text{d}$ for $\text{pH} < 5$ and $5\text{-}11 \text{ g/m}^2/\text{d}$ for $\text{pH} > 5$ Acidic/neutral pH: With $R_A \approx 5 \text{ g/m}^2/\text{d}$ at $\text{pH} < 5.5$ and $\approx 2 \text{ g/m}^2/\text{d}$ at $\text{pH} > 5.5$ Acidic/neutral pH: With $R_A = 5 \text{ g/m}^2/\text{d}$ at $\text{pH} < 6.5$ and $20 \text{ g/m}^2/\text{d}$ at $\text{pH} > 6.5$ Acidic/neutral pH: With $R_A = 2 \text{ g/m}^2/\text{d}$ for acidic and $11 \text{ g/m}^2/\text{d}$ for alkaline pH Neutral pH: With $R_A = 10\text{-}20 \text{ g/m}^2/\text{d}$	[13] [23] [4],[8] [17] [3],[38] [15]
Areal / percental removal	$A = \frac{Q \times [\text{Fe}]_{\text{in}}}{R_A}$	With $R_A = 20\text{-}40$ and $2\text{-}10 \text{ g/m}^2/\text{d}$ for 50 and 90% Fe-removal, respectively	[8]
Areal or volumetric removal (subsurface flow)	$A = \frac{Q \times [\text{Fe}]_{\text{in}}}{R_A}$	With $R_A = 2.55 \text{ g/m}^2/\text{d}$ at $\text{pH} 3.7$ to achieve $[\text{Fe}]_{\text{out}} = 3.5 \text{ mg/L}^{-1}$	[24]
First-order removal	$A = \frac{Q \times (\ln[\text{Fe}]_{\text{in}} - \ln[\text{Fe}]_{\text{out}})}{R_A}$	With $R_A = 0.18 \text{ m/d}$ as first order Fe removal constant	[36]

* All approaches were (re)arranged for surface area (A) in [m²] with flow rate (Q) in [m³/d], Fe concentration [Fe] in [g/m³], water depth (z) in [m], retention time (τ) in [d] and criteria (R_A) in [g/m²/d]

Table S2. Range of area-adjusted Fe removal rates in (a) settling ponds and (b) constructed surface-flow wetlands. Missing information or parameters were calculated from provided data. Passive systems with artificial aeration, chemical amendment (lime, NaOH, H₂O₂, flocculants, flocculant aids, etc.) or hybrid wetlands (combined surface and subsurface flow) were excluded. Note that averaged or aggregated data is listed that is often characterised by a considerable spatiotemporal spread. Only passive systems with inflow and/or outflow pH between 5.5 and 8.5 were considered.

System name	Country	Surface area A [m ²]	Flow rate Q [m ³ /h]	Nom. HRT <i>t_n</i> [d]	[Fe] _{in} [mg/L]	[Fe] _{out} [mg/L]	pH (in / out) [-]	Areal removal <i>R_A</i> [g/m ² /d]	Ref.
(a) Settling ponds									
Whittle lagoons	UK	800	92	0.68	34.6	15.0	6.8 / n/a	11.5	[2]
Otto Discharge	US	3050	287	0.71	11.3	10.4	6.2 / 6.5	2.03	[6]
Howe Bridge (P2)	US	460	7.8	n/a	211	170	6.3 / 6.0	17.5	[7]
Glyncastle (L1+L2)	UK	2771	74	n/a	24.5	14.1	6.2 / n/a	6.61	[10]
Morlais (L2)	UK	5680	432	n/a	21.5	1.3	6.4 / n/a	22.0	[10]
Marchand (ponds A+B)	US	6378	363	0.88	74.4	51.2	6.2 / 6.5	32.9	[11]
Marchand (ponds C+D)	US	6888	363	0.95	51.2	26.2	6.5 / 6.7	32.8	[11]
Marchand (ponds E+F)	US	7949	363	1.1	26.2	12.1	6.7 / 7.0	16.0	[11]
Marchand (pond A)	US	3189	426	0.37	72.4	62.7	6.3 / 6.5	31.1	[12]
Marchand (pond B)	US	3189	426	0.37	62.7	54.5	6.5 / 6.6	26.3	[12]
Marchand (pond C)	US	3444	426	0.40	54.5	40.7	6.6 / 6.7	41.0	[12]
Marchand (pond D)	US	3444	426	0.40	40.7	30.0	6.7 / 6.8	31.8	[12]
Marchand (pond E)	US	3975	426	0.47	30.0	19.3	6.8 / 6.9	2785	[12]
Marchand (pond F)	US	3975	426	0.47	19.3	12.4	6.9 / 7.1	17.8	[12]
Keystone Ditch	US	4200	516	0.3	37.0	32.0	6.3 / 6.4	20.7	[15]
Acomb East	UK	375	23	2.0	34.1	9.65	n/a	35.2	[20]
Acomb West	UK	375	21	2.1	34.1	5.05	n/a	39.1	[20]
Whittle	UK	800	90	0.93	16.8	21.6	n/a	18.9	[20]
Whittle	UK	800	92	0.91	40.3	22.6	n/a	48.9	[28],[29]
Taff Merthyr (L1)	UK	1300	65	n/a	6.73	4.41	n/a	2.79	[32]
Taff Merthyr (L1)	UK	1300	166	n/a	6.99	5.62	n/a	4.19	[32]
Taff Merthyr (L2)	UK	1300	92	n/a	6.90	4.24	n/a	4.53	[32]
Taff Merthyr (L3)	UK	1150	53	n/a	7.16	3.01	n/a	4.56	[32]
Taff Merthyr (L3)	UK	1150	45	n/a	9.26	3.06	n/a	5.94	[32]
Taff Merthyr (L4)	UK	1200	61	n/a	6.84	3.64	n/a	3.86	[32]
Taff Merthyr (L4)	UK	1200	51	n/a	6.54	3.82	n/a	2.78	[32]
Lindsay (L1)	UK	1200	41	n/a	19.2	8.17	n/a	9.10	[32]
Lindsay (L1)	UK	1200	36	n/a	17.7	7.33	n/a	7.39	[32]
Lindsay (L1+L2)	UK	2400	71	n/a	18.8	7.32	n/a	8.21	[32]

System name	Country	Surface area A [m ²]	Flow rate Q [m ³ /h]	Nom. HRT t _n [d]	[Fe] _{in} [mg/L]	[Fe] _{out} [mg/L]	pH (in/ out) [-]	Areal removal R _A [g/m ² /d]	Ref.
WW-2g	US	591	0.4	n/a	n/a	n/a	6.8/7.1	2.90	[33]
WW-2f	US	591	8.3	n/a	n/a	n/a	6.3/6.5	0.80	[33]
WW-30i	US	1930	1.1	n/a	n/a	n/a	4.7/6.0	3.20	[33]
WW-le	US	4091	2.2	n/a	n/a	n/a	6.3/6.6	0.20	[33]
WW-30h	US	1150	0.4	n/a	n/a	n/a	6.3/6.4	0.40	[33]
WW10c	US	305	2.9	n/a	n/a	n/a	5.5/5.9	0.80	[33]
Garth Tommawr (Cell 1)	UK	2480	86	n/a	30.1	8.60	5.8/4.1	17.98	[39]
Gwenffwd	UK	850	100	1.1	1.40	1.20	7.2/7.2	0.56	[31],[39]
Neville Street	CAN	11,000	480	2.0	7.30	3.10	6.2/6.9	4.40	[40]
(b) Surface-flow constructed wetlands									
Edmondsley	UK	3600	1.5	n/a	15.2	0.10	n/a	1.55	[1]
Fender	UK	6000	90	n/a	8.79	1.21	n/a	2.86	[1]
Gwynfi	UK	800	27	n/a	4.60	0.45	n/a	3.40	[1]
Kames	UK	3200	41	n/a	11.3	0.16	n/a	3.45	[1]
Minto	UK	7200	43	n/a	11.8	3.76	n/a	5.38	[1]
Old Meadows	UK	1600	8.3	n/a	2.30	0.80	n/a	4.03	[1]
Polkemmet	UK	2000	6.2	n/a	1.71	0.31	n/a	5.46	[1]
Woolley	UK	14,000	10.7	n/a	2.96	0.21	n/a	2.51	[1]
Whittle (Reedbed 1)	UK	3000	72	0.52	26.8	2.02	n/a	14.3	[2]
Whittle (Reedbed 2+3)	UK	6000	68	1.1	2.02	0.55	n/a	0.40	[2]
TVA 950 Coal Mine	US	3400	5.0	n/a	12.0	1.10	5.7/6.5	0.38	[3],[4]
TVA Widows Creek	US	4800	4.2	n/a	150	6.4	5.6/6.4	3.02	[3],[4]
TVA Impoundment 1	US	5700	4.4	n/a	69.0	0.90	6.1/6.7	1.26	[3],[4]
TVA Impoundment 3	US	1200	3.5	n/a	15.8	0.50	6.3/7.0	1.06	[3],[4]
TVA Impoundment 4	US	2000	7.9	n/a	65.0	0.40	6.3/6.3	6.09	[3],[4]
TVA 950 Coal Mine NE	US	2500	23	n/a	11.0	0.60	6.0/6.9	2.31	[3],[4]
TVA Colbert 013	US	9200	17	n/a	0.70	0.70	5.7/6.7	0.00	[3],[4]
TVA OLL	US	7550	23	n/a	10.0	2.10	6.2/6.4	0.58	[3],[4]
TVA Rocky Top 2	US	7300	17	n/a	45.2	0.60	5.7/6.8	2.44	[3],[4]
Otto Discharge (W1)	US	1860	287	0.05	10.4	9.98	6.5/6.5	1.55	[6]
Otto Discharge (W2)	US	1760	287	0.05	9.98	9.31	6.5/6.5	2.62	[6]
Coshocton	US	2174	23	0.7	198	6.52	6.5/6.5	49.2	[8]
Cedar	US	1360	34	n/a	95.0	n/a	6.3/n/a	24.2	[9]
Marchand (treatment)	US	23,424	363	n/a	12.1	1.80	7.0/7.5	4.00	[11]

System name	Country	Surface area A [m ²]	Flow rate Q [m ³ /h]	Nom. HRT t_n [d]	[Fe] _{in} [mg/L]	[Fe] _{out} [mg/L]	pH (in / out) [-]	Areal removal R_A [g/m ² /d]	Ref.
Marchand (mitigation)	US	5206	363	n/a	1.80	0.80	7.5/7.5	1.70	[11]
Marchand (combined)	US	28.630	426	n/a	12.4	1.00	7.1/7.8	4.07	[12]
Cedar	US	1360	9.4	1.7	198	6.52	6.3/6.4	2.2	[15]
Howe (lower)	US	3000	7.8	8.0	185	68	6.0/5.6	8.10	[15]
Howe (upper)	US	4388	302	0.28	272	185	6.0/6.2	42.7	[15]
Lambley	UK	4388	90	n/a	3.80	1.6	n/a	3.64	[20]
Whittle (Reedbed 1)	UK	2400	229	0.37	20.8	1.7	n/a	17.2	[20]
Lambley	UK	4388	720	n/a	5.83	1.16	6.6/6.7	5.83	[21]
Woolley	UK	14,000	8.0	1.5	10.0	1.0	n/a	11.1	[22]
Bowden	UK	990	2.7	n/a	58.2	5.90	n/a	10.1	[25]
TVA Impoundment 1	US	5700	6.2	n/a	44.0	0.90	6.3/7.2	0.49	[26]
TVA Widows Creek	US	4700	47	n/a	205	6.30	6.3/3.6	6.01	[26]
Taff Merthyr (A1)	UK	1567	47	n/a	4.44	0.23	7.0/7.2	3.04	[32]
Taff Merthyr (A1)	UK	1564	47	n/a	5.69	0.45	7.1/7.5	3.59	[32]
Taff Merthyr (B1)	UK	1080	58	n/a	4.27	0.10	7.3/7.4	5.37	[32]
Taff Merthyr (B1)	UK	1078	48	n/a	5.88	0.19	7.2/7.6	6.11	[32]
Taff Merthyr (C1)	UK	1949	66	n/a	4.54	0.04	7.5/7.5	3.65	[32]
Taff Merthyr (C1)	UK	1951	71	n/a	6.08	0.02	7.3/7.6	5.26	[32]
Taff Merthyr (D1)	UK	1200	49	n/a	3.01	1.08	7.4/7.6	1.89	[32]
Taff Merthyr (D1)	UK	1195	52	n/a	3.06	0.77	7.5/7.9	2.40	[32]
Taff Merthyr (E1)	UK	1120	61	n/a	3.64	1.48	6.9/7.1	2.80	[32]
Taff Merthyr (E1)	UK	1118	51	n/a	3.82	0.44	7.9/7.7	3.71	[32]
Lindsay (R1)	UK	1308	72	n/a	8.10	1.02	8.0/7.9	9.35	[32]
Lindsay (R1)	UK	1313	67	n/a	6.21	0.95	8.1/8.1	6.44	[32]
WV-2a	US	n/a	8.3	n/a	n/a	n/a	6.7/7.2	14.8	[33]
WV-2b	US	n/a	0.4	n/a	n/a	n/a	7.2/7.5	0.80	[33]
WV-7a	US	n/a	93	n/a	n/a	n/a	6.5/6.7	48.8	[33]
WV-7b	US	n/a	89	n/a	n/a	n/a	6.8/6.8	23.4	[33]
WV-7c	US	n/a	2.5	n/a	n/a	n/a	6.6/6.7	0.20	[33]
Simco #4	US	2623	20	n/a	111	42.0	6.5/6.4	12.4	[34]
Simco #4	US	4138	27	n/a	89	22.6	6.6/6.6	10.5	[35]
Whitworth No 1 (Cell 1)	UK	900	5.3	n/a	23.3	3.9	6.3/6.7	2.75	[39]
Whitworth No 1 (Cell 3)	UK	900	5.3	n/a	23.3	4.2	6.3/6.6	2.70	[39]
Whitworth A	UK	4500	27	3.8	7.40	2.00	7.0/7.3	0.78	[31],[39]

Table S3. Inflow water chemistry of the Westfield pilot plant (2018-2019) as average (\pm SD) with number of samples n=64 unless specified otherwise.

Parameter	Unit	Inflow concentration
pH (n=60)	-	7.5 (\pm 0.2)
Electrical conductivity (n=60)	μ S/cm	3240 (\pm 146)
Oxygen saturation (n=60)	%	89 (\pm 5)
Turbidity (n=338)*	NTU	76.1 (\pm 17.2)
Fe(tot) (n=90)	mg/L	8.33 (\pm 2.18)
Mn	μ g/L	1508 (\pm 268)
As (n=18)	μ g/L	6.37 (\pm 2.58)
Ca	mg/L	578 (\pm 45)
Mg	mg/L	112 (\pm 8.7)
F	mg/L	1.57 (\pm 0.16)
Cl	mg/L	95.9 (\pm 17.6)
Br	mg/L	0.84 (\pm 0.17)
SO ₄	mg/L	1601 (\pm 139)
NH ₄	mg/L	0.74 (\pm 0.15)
NO ₃	mg/L	1.06 (\pm 0.46)

* Daily averages of in-situ turbidity sensor measurements (WTW VisoTurb 700 IQ).

REFERENCES

- [1] Banks, S., 2003. The UK Coal Authority minewater treatment programme: Performance of operational systems. *Water Environ. J.* 17, 117-122. <https://doi.org/10.1111/J.1747-6593.2003.TB00444.X>.
- [2] Batty, L., Hooley, D., Younger, P., 2008. Iron and manganese removal in wetland treatment systems: Rates, processes and implications for management. *Sci. Total Environ.* 394, 1-8. <https://doi.org/10.1016/j.scitotenv.2008.01.002>.
- [3] Brodie, G., 1991. Achieving compliance with staged, aerobic, constructed wetlands to treat acid drainage. *Proc. ASMR*, 151-174. <https://doi.org/10.21000/JASMR91010151>.
- [4] Brodie, G., Hammer, D., Tomljanovich, D., 1988. Constructed wetlands for AMD control in Tennessee valley. *Proc. ASMR*, 325-331. <https://doi.org/10.21000/JASMR88010325>.
- [5] Brown, M., Barley, R., Wood, H., 2002. *Minewater Treatment: Technology Application and Policy*. IWA Publishing.
- [6] Cravotta, C., 2007. Passive aerobic treatment of net-alkaline, iron-laden drainage from a flooded underground anthracite mine, Pennsylvania, USA. *Mine Water Environ.* 26, 128-149. <https://doi.org/10.1007/s10230-007-0002-8>.
- [7] Dempsey, B., Roscoe, H., Ames, R., Hedin, R., Jeon, B., 2001. Ferrous oxidation chemistry in passive abiotic systems for treatment of mine drainage. *Geochem.: Explor. Environ. Anal.* 1, 81-88. <https://doi.org/10.1144/geochem.1.1.81>.
- [8] Fennessy, M., Mitsch, W., 1989. Treating coal mine drainage with an artificial wetland. *Res. J. Water Pollut. Control Fed.* 61, 1691-1701.
- [9] Flanagan, N., Mitsch, W., Beach, K., 1994. Predicting metal retention in a constructed mine drainage wetland. *Ecol. Eng.* 3, 135-139. [https://doi.org/10.1016/0925-8574\(94\)90042-6](https://doi.org/10.1016/0925-8574(94)90042-6).
- [10] Geroni, J., Sapsford, D., Bames, A., Watson, I., Williams, K., 2009. Current performance of passive treatment systems in South Wales, UK. *Proc. IMWA Conf.*, 486-494.
- [11] Hedin, R., 2008. Iron removal by a passive system treating alkaline coal mine drainage. *Mine Water Environ.* 27, 200-209. <https://doi.org/10.1007/s10230-008-0041-9>.
- [12] Hedin, R., 2013. Temperature independent removal of iron in a passive mine water system. *Proc. IMWA Conf.*, 599-604.
- [13] Hedin, R., Nairn, R., 1990. Sizing and performance of constructed wetlands: Case studies. *Proc. Mining and Reclamation Conf.*, Charleston.
- [14] Hedin, R., Nairn, R., 1992. Designing and sizing passive mine drainage treatment systems. *Proc. 30th West Virginia Surface Mine Drainage Task Force Symp.*, Morgantown.
- [15] Hedin, R., Nairn, R., Kleinmann, R. 1994. Passive treatment of coal mine drainage. *US Bureau of Mines, Information Circular 9389*.
- [16] Hellier, W., 1989. Constructed wetlands in Pennsylvania: An overview. *Proc. Int. Symp. on Biohydrometallurgy*, 599-611.
- [17] Hellier, W., Giovannitti, E., Slack, P., 1994. Best professional judgement analysis for constructed wetlands as a best available technology for the treatment of post-mining groundwater seeps. *Proc. Int. Land Reclamation and Mine Drainage Conf.*, 24-29.
- [18] Kleinmann, R., Tiernan, T., Solch, J., Harris, R., 1983. A low-cost, low-maintenance treatment system for acid mine drainage using Sphagnum moss and limestone. *Proc. Symp. on Surface Mining, Hydrology, Sedimentology and Reclamation*, Lexington, 241-245.
- [19] Kleinmann, R., Brooks, R., Huntsman, B., Pesavento, B., 1986. Constructed wetlands for the treatment of mine water. *Proc. Symp. on Mining, Hydrology, Sedimentology and Reclamation*, Lexington. Short Course Notes.
- [20] Kruse, N., Gozzard, E., Jarvis, A., 2009. Determination of hydraulic residence times in several UK mine water treatment systems and their relationship to iron removal. *Mine Water Environ.* 28, 115-123. <https://doi.org/10.1007/s10230-009-0068-6>.

- [21] Kusin, F., Jarvis, A., Gandy, C., 2010. Hydraulic residence time and iron removal in a wetland receiving ferruginous mine water over a 4 year period from commissioning. *Water Sci. Technol.* 62, 1937-1946. <https://doi.org/10.2166/wst.2010.495>.
- [22] Laine, D., Jarvis, A., 2003. Engineering design aspects of passive in-situ remediation of mining effluents. *Land Contam. Reclamat.* 11, 113-125. <https://doi.org/10.2462/09670513.805>
- [23] Lamb, H., Dodds-Smith, M., Gusek, J., 1998. Development of a long-term strategy for the treatment of acid mine drainage at Wheal Jane. In: *Acidic Mining Lakes: Acid Mine Drainage, Limnology and Reclamation* (Eds. Geller, W., Klapper, H., Salomons, W.), 335-346. Springer.
- [24] Manyin, T., Williams, F., Stark, L., 1997. Effects of iron concentration and flow rate on treatment of coal mine drainage in wetland mesocosms: An experimental approach to sizing of constructed wetlands. *Ecol. Eng.* 9, 171-185. [https://doi.org/10.1016/S0925-8574\(97\)10005-2](https://doi.org/10.1016/S0925-8574(97)10005-2).
- [25] Matthies, R., Aplin, A., Jarvis, A., 2010. Performance of a passive treatment system for net-acidic coal mine drainage over five years of operation. *Sci. Total Environ.* 408, 4877-4885. <https://doi.org/10.1016/j.scitotenv.2010.06.009>.
- [26] Mays, P., Edwards, G., 2001. Comparison of heavy metal accumulation in a natural wetland and constructed wetlands receiving acid mine drainage. *Ecol. Eng.* 16, 487-500. [https://doi.org/10.1016/S0925-8574\(00\)00112-9](https://doi.org/10.1016/S0925-8574(00)00112-9).
- [27] National Coal Board, 1982. *Technical management of water in the coal mining industry*. Westminster Press.
- [28] Nuttal, C., 2003. Testing and performance of a newly constructed full-scale passive treatment system at Whittle Colliery, Northumberland. *Land Contam. Reclamat.* 11, 105-112. <https://doi.org/10.2462/09670513.804>.
- [29] Paker, K., 2003. Mine water management on a national scale – Experiences from the Coal Authority. *Land Contam. Reclamat.* 11, 181-190. <https://doi.org/10.2462/09670513.813>.
- [30] PIRAMID Consortium, 2003. *Engineering guidelines for the passive remediation of acidic and/or metalliferous mine drainage and similar wastewaters*. EC 5th Framework RTD Project EVK1-CT-1999-000021.
- [31] Rees, B., Connelly, R., 2003. Review of design and performance of the Pelenna wetland systems. *Land Contam. Reclamat.* 11, 293-300. <https://doi.org/10.2462/09670513.828>.
- [32] Sapsford, D., Watson, I., 2011. A process-oriented design and performance assessment methodology for passive mine water treatment systems. *Ecol. Eng.* 37, 970-975. <https://doi.org/10.1016/j.ecoleng.2010.12.010>.
- [33] Skousen, J., Ziemkiewicz, P., 2005. Performance of 116 passive treatment systems for acid mine drainage. *Proc. ASMR*, 1100-1133. <https://doi.org/10.21000/JASMR05011100>.
- [34] Stark, L., Stevens, S., Webster, H., Wenerick, W., 1990. Iron loading, efficiency and sizing in a constructed wetland receiving mine drainage. *Proc. ASMR*, 393-402. <https://doi.org/10.21000/JASMR9000393>.
- [35] Stark, L., Williams, F., Stevens, S., Eddy, D., 1994. Iron retention and vegetative cover at the Simco constructed wetland: An appraisal through year eight of operation. *Proc. Int. Land Reclamation and Mine Drainage Conf.*, 89-98.
- [36] Tarutis, W., Stark, L., Williams, F., 1999. Sizing and performance estimation of coal mine drainage wetlands. *Ecol. Eng.* 12, 353-372. [https://doi.org/10.1016/S0925-8574\(98\)00114-1](https://doi.org/10.1016/S0925-8574(98)00114-1).
- [37] Watzlaf, G., Schroeder, K., Kleinmann, R., Kairies, C., Nairn, R., 2004. *The passive treatment of coal mine drainage*. DOE/NETL-2004/1202.
- [38] Wildemann, T., Brodie, G., Gusek, J., 1993. *Wetland Design for Mining Operations*. BiTech Publishers.
- [39] Wiseman, I., 2002. *Constructed Wetlands for Minewater Treatment*. Environment Agency, R&D Technical Report P2-181/TR.
- [40] Wolkersdorfer, C., 2011. Tracer test in a settling pond: The passive mine water treatment plant of the 1B mine pool, Nova Scotia, Canada. *Mine Water Environ.* 30, 105-112. <https://doi.org/10.1007/s10230-011-0147-3>.
- [41] Younger, P., Banwart, S., Hedin, R., 2002. *Mine Water: Hydrology, Pollution, Remediation*. Springer Science.

Statutory declarations and affirmations

(Eidesstattliche) Versicherungen und Erklärungen

(§ 9 Satz 2 Nr. 3 PromO BayNAT)

Hiermit versichere ich eidesstattlich, dass ich die Arbeit selbstständig verfasst und keine anderen als die von mir angegebenen Quellen und Hilfsmittel benutzt habe (vgl. Art. 64 Abs. 1 Satz 6 BayHSchG).

(§ 9 Satz 2 Nr. 3 PromO BayNAT)

Hiermit erkläre ich, dass ich die Dissertation nicht bereits zur Erlangung eines akademischen Grades eingereicht habe und dass ich nicht bereits diese oder eine gleichartige Doktorprüfung endgültig nicht bestanden habe.

(§ 9 Satz 2 Nr. 4 PromO BayNAT)

Hiermit erkläre ich, dass ich Hilfe von gewerblichen Promotionsberatern bzw. -vermittlern oder ähnlichen Dienstleistern weder bisher in Anspruch genommen habe noch künftig in Anspruch nehmen werde.

(§ 9 Satz 2 Nr. 7 PromO BayNAT)

Hiermit erkläre ich mein Einverständnis, dass die elektronische Fassung meiner Dissertation unter Wahrung meiner Urheberrechte und des Datenschutzes einer gesonderten Überprüfung unterzogen werden kann.

(§ 9 Satz 2 Nr. 8 PromO BayNAT)

Hiermit erkläre ich mein Einverständnis, dass bei Verdacht wissenschaftlichen Fehlverhaltens Ermittlungen durch universitätsinterne Organe der wissenschaftlichen Selbstkontrolle stattfinden können.

.....
Ort, Datum, Unterschrift